Université de Montréal

Données nouvelles sur l'innervation à dopamine du striatum et son co-phénotype glutamatergique

par
Noémie Bérubé-Carrière

Département de physiologie
Faculté de médecine

Thèse présentée à la Faculté des études supérieures et postdoctorales
en vue de l'obtention du grade de docteur en sciences neurologiques

Avril 2012

Université de Montréal
Faculté des études supérieures et postdoctorales

Cette thèse intitulée :

Données nouvelles sur l'innervation à dopamine du striatum et son co-phénotype glutamatergique

Présentée par :
Noémie Bérubé-Carrière

a été évaluée par un jury composé des personnes suivantes :

Pierre Blanchet, président-rapporteur
Laurent Descarries, directeur de recherche
Louis-Éric Trudeau, co-directeur
Barbara E. Jones, membre du jury
André Parent, examinateur externe
Thérèse Cabana, représentante du doyen de la FES

Résumé

Une sous-population des neurones à dopamine (DA) du mésencéphale ventral du rat et de la souris étant connue pour exprimer l'ARN messager du transporteur vésiculaire 2 du glutamate (VGLUT2), nous avons eu recours à l'immunocytochimie en microscopie électronique, après simple ou double marquage de l'enzyme de synthèse tyrosine hydroxylase (TH) et de VGLUT2, pour déterminer la présence de l'une et/ou l'autre protéine dans les terminaisons (varicosités) axonales de ces neurones et caractériser leur morphologie ultrastructurale dans diverses conditions expérimentales.

Dans un premier temps, des rats jeunes (P15) ou adultes (P90), ainsi que des rats des deux âges soumis à l'administration intraventriculaire cérébrale de la cytotoxine 6-hydroxydopamine (6-OHDA) dans les jours suivant la naissance, ont été examinés, afin d'étayer l'hypothèse d'un rôle de VGLUT2 au sein des neurones DA, au cours du développement normal ou pathologique de ces neurones. Chez le jeune rat, ces études ont montré: i) la présence de VGLUT2 dans une fraction importante des varicosités axonales TH immunoréactives du cœur du noyau accumbens ainsi que du néostriatum; ii) une augmentation de la proportion de ces terminaisons doublement marquées dans le noyau accumbens par suite de la lésion 6-OHDA néonatale; iii) le double marquage fréquent des varicosités axonales appartenant à l'innervation DA aberrante (néoinnervation), qui se développe dans la substance noire, par suite de la lésion 6-OHDA néonatale. Des différences significatives ont aussi été notées quant à la dimension des terminaisons axonales marquées pour la TH seulement, VGLUT2 seulement ou TH et VGLUT2. Enfin, à cet âge (P15), toutes les terminaisons doublement marquées sont apparues dotées d'une spécialisation membranaire synaptique, contrairement aux terminaisons marquées pour la TH ou pour VGLUT2 seulement.

Dans un deuxième temps, nous avons voulu déterminer le devenir du double phénotype chez le rat adulte (P90) soumis ou non à la lésion 6-OHDA néonatale. Contrairement aux observations recueillies chez le jeune rat, nous avons alors constaté: i) l'absence complète de terminaisons doublement marquées dans le cœur du noyau accumbens et le néostriatum d'animaux intacts, de même que dans les restes de la substance noire des animaux 6-OHDA lésés; ii) une très forte baisse de leur

nombre dans le cœur du noyau accumbens des animaux 6-OHDA lésés. Ces observations, suggérant une régression du double phénotype TH/VGLUT2 avec l'âge, sont venues renforcer l'hypothèse d'un rôle particulier d'une co-libération de glutamate par les neurones mésencéphaliques DA au cours du développement.

Dans ces conditions, il est apparu des plus intéressants d'examiner l'innervation DA méso-striatale chez deux lignées de souris dont le gène *Vglut2* avait été sélectivement invalidé dans les neurones DA du cerveau, ainsi que leurs témoins et des souris sauvages. D'autant que malgré l'utilisation croissante de la souris en neurobiologie, cette innervation DA n'avait jamais fait l'objet d'une caractérisation systématique en microscopie électronique. En raison de possibles différences entre le cœur et la coque du noyau accumbens, l'étude a donc porté sur les deux parties de ce noyau ainsi que le néostriatum et des souris jeunes (P15) et adultes (P70-90) de chaque lignée, préparées pour l'immunocytochimie de la TH, mais aussi pour le double marquage TH et VGLUT2, selon le protocole précédemment utilisé chez le rat.

Les résultats ont surpris. Aux deux âges et quel que soit le génotype, les terminaisons axonales TH immunoréactives des trois régions sont apparues comparables quant à leur taille, leur contenu vésiculaire, le pourcentage contenant une mitochondrie et une très faible incidence synaptique (5% des varicosités, en moyenne). Ainsi, chez la souris, la régression du double phénotype pourrait être encore plus précoce que chez le rat, à moins que les deux protéines ne soient très tôt ségréguées dans des varicosités axonales distinctes des mêmes neurones DA. Ces données renforcent aussi l'hypothèse d'une transmission diffuse (volumique) et d'un niveau ambiant de DA comme élément déterminant du fonctionnement du système mésostriatal DA chez la souris comme chez le rat.

Mots clés : dopamine, glutamate, transporteur vésiculaire du glutamate de type 2, noyau accumbens, néostriatum, substance noire, terminaisons (varicosités) axonales, co-localisation, développement, transmission diffuse, immunocytochimie, double marquage.

Summary

Knowing that a subset of rat and mouse mesencephalic dopamine (DA) neurons expresses the mRNA of the vesicular glutamate transporter type 2 (VGLUT2), we used electron microscopic immunocytochemistry, after single or double labeling of the biosynthetic enzyme tyrosine hydroxylase (TH) and of VGLUT2, to determine the presence of one and/or both proteins in axon terminals (varicosities) of these neurons and characterize their ultrastructural morphology under various experimental conditions.

At first, young (P15) or adult (P90) rats, subjected or not to cerebro-ventricular administration of the cytotoxin 6-hydroxydopamine (6-OHDA) a few days after birth, were examined in order to investigate the role of VGLUT2 in DA neurons during normal and pathological development of these neurons. In the young rats, these studies revealed: i) the presence of VGLUT2 in a significant fraction of TH immunoreactive varicosities in the core of the nucleus accumbens and the neostriatum; ii) an increase in the proportion of dually labeled terminals in the nucleus accumbens following neonatal 6-OHDA lesion; iii) frequent double labeling of TH varicosities belonging to the aberrant DA innervation (neoinnervation) which develops in the substantia nigra following neonatal 6-OHDA lesion. Significant differences were also noted in the size of the axon terminals labeled for TH only, VGLUT2 only, or TH and VGLUT2. Finally, at this age (P15), all the dually labeled terminals appeared equipped with a synaptic membrane specialization, unlike the terminals labeled for TH or for VGLUT2 only.

In a second step, we sought to determine the fate of the dual phenotype in adult rats (P90) subjected or not to the neonatal 6-OHDA lesion. In contrast with the observations made in young rats, we found: i) a complete absence of dually labeled terminals in the core of the nucleus accumbens and striatum of intact animals, as well as in the remains of the substantia nigra after neonatal 6-OHDA lesion; ii) a sharp decline of their number in the core of the nucleus accumbens of 6-OHDA-lesioned animals. These findings, suggesting a regression of the dual TH/VGLUT2 phenotype with age, reinforced the hypothesis of a specific role of the co-release of glutamate from midbrain DA neurons during development.

Under these conditions, it was of considerable interest to examine the DA meso-striatal innervation in two strains of mice whose *Vglut2* gene has been selectively invalidated in DA neurons, as well as in their control littermates and wild-type mice. This issue was particularly relevant with the increasing use of genetically modified mice in neurobiology; indeed, this DA innervation had never been systematically characterized by electron microscopy. Because of possible differences between the core and shell of the nucleus accumbens, the study included both parts of this nucleux as well as the striatum of young (P15) and adult (P70-90) mice of each strain, prepared for TH immunocytochemistry, and also for double labeling of TH and VGLUT2, according to the protocol previously used in rats.

The results were surprising. At both ages, regardless of the genotype, the TH immunoreactive axon terminals of the three regions appeared comparable in size, vesicle content, percent with mitochondria, and exceeding low frequency of synaptic membrane specialization (5% of varicosities, on average). Thus, in mice, the regression of the dual phenotype might be even more precocious than in rats, unless the two proteins are segregated very early in different axon terminals of the same DA neurons. These data also strenghten the hypothesis of a diffuse (volume) transmission and of an ambient level of DA as determinant elements in the functioning of the meso-striatal DA system in mice as well as rats.

Key words: dopamine, glutamate, vesicular glutamate transporter type 2, nucleus accumbens, neostriatum, substantia nigra, axon terminals (varicosities), co-localisation, development, diffuse transmission, immunocytochemistry, dual labeling.

Table des matières

Remerciements

Tout d'abord, je tiens à exprimer ma gratitude au Dr Laurent Descarries, qui m'a accueillie dans son laboratoire pour mes études graduées. Sa compétence et sa grande disponibilité ont forgé la scientifique que je suis. Je tiens aussi à remercier mon co-directeur, le Dr Louis-Éric Trudeau, pour son appui et sa rigueur scientifique, dont j'ai bénéficié tout au long de ma formation. Il me faut aussi souligner jusqu'à quel point l'expertise du Dr Mustapha Riad, généreusement partagée sur une base quotidienne, a facilité la réalisation de mes travaux.

Je remercie également le personnel des départements de Pathologie et biologie cellulaire et de Physiologie, ainsi que le Groupe de recherche sur le système nerveux central (GRSNC), pour leur soutien, et plus particulièrement Diane Gingras, Ginette Guay et Michel Lauzon, pour leur aide technique dans la préparation et l'examen du matériel de microscopie électronique. Merci aussi à plusieurs étudiants passés et présents du laboratoire pour tant de bons moments partagés. Ce fut notamment un vif plaisir de collaborer avec Grégory Dal Bo et Guillaume Fortin du laboratoire Trudeau.

Je souhaite aussi remercier les membres externes de mon comité de parrainage, les Drs Adriana Di Polo et Guy Doucet, pour leurs précieux conseils et leurs encouragements, ainsi que chacun des membres de mon jury de thèse pour leur lecture et leur évaluation de cet ouvrage.

Ma gratitude va aussi au GRSNC, au FRSQ et à la FESP de l'Université de Montréal pour l'appui financier accordé à un moment ou un autre de ma formation.

L'accomplissement d'une thèse de doctorat ne peut se faire sans le support de la famille et des amis, auxquels je tiens à exprimer ici toute ma reconnaissance. Finalement, je remercie tout particulièrement mon mari Gabriel de son soutien, sa confiance et sa patience, qui m'ont permis de persévérer dans cette grande entreprise qu'a été le doctorat. Et une pensée particulière pour ma petite Éléonore, qui malgré son jeune âge a déjà une grande influence sur sa maman…

Liste des tableaux

Introduction générale :

Premier article :

Deuxième article :

Liste des figures

Introduction générale :

Premier article :

Deuxième article :

Liste des abréviations

6-OHDA : 6-hydroxydopamine
5-HT : 5-hydroxytryptamine (sérotonine)
A : adrénaline
ACh : acétylcholine
AMPc : adénosine monophosphate cyclique
AMPA : *α-amino-3-hydroxy-5-methyl-4-isoxazole propionic acid*
ARNm : acide ribonucléique messager
ATV : aire tegmentaire ventrale
BNPI : *Brain Na^+-Dependent Inorganic Phosphate Co-transporter*
Ca^{2+} : calcium
CAMK : protéine kinase Ca^{2+}/calmoduline dépendante
cKO : knockout conditionnel
COMT : catéchol-O-méthyltransférase
DA : dopamine
DAT : transporteur de la dopamine
DNPI : *Differentiation-Associated Na^+-Dependent Inorganic Phosphate Transporter*
KO : knockout
L-DOPA : L-3,4-dihydroxyphénylalanine
MAO : monoamine-oxydase
MAPK : *Mitogen-Activated Protein Kinase*
Mg^+ : magnésium
NA : noradrénaline
NA^+ : sodium
NAC : *Nucleus Accumbens Core*
NAS : *Nucleus Accumbens Shell*
NS : néostriatum
NMDA : *N-methyl-D-aspartate*
PKC : protéine kinase C
PLT : potentialisation à long terme
PPSE : potentiel post-synaptique excitateur
SNc : substance noire, pars compacta
SNC : système nerveux central
SNr : substance noire, pars reticulata
TH : tyrosine hydroxylase
VAChT : transporteur vésiculaire de l'acétylcholine
VGLUT1 : transporteur vésiculaire du glutamate de type 1
VGLUT2 : transporteur vésiculaire du glutamate de type 2
VGLUT3 : transporteur vésiculaire du glutamate de type 3
VMAT2 : transporteur vésiculaire des monoamines de type 2

Chapitre 1 – Introduction générale

1 Dopamine

1.1 Bref rappel historique

Avant les années 1950, la dopamine (DA) était considérée comme un simple précurseur de la biosynthèse des catécholamines, noradrénaline (NA) et adrénaline (A). Dans son article rétrospectif sur la découverte de la neurotransmission à monoamine dans le système nerveux central (SNC), Carlsson (1987) explique que c'est l'étude d'un nouvel agent antipsychotique, la réserpine, qui lui a permis de conclure avec Hillarp que l'action de ce médicament n'était pas exclusive au neurotransmetteur sérotonine, mais impliquait aussi les catécholamines : DA, NA et A. Étant donné que les quantités de DA retrouvées dans le SNC étaient comparables à celles de la NA, et compte tenu de la disparition de la DA par suite de l'administration de réserpine, Carlsson et ses collègues ont suggéré que la DA soit davantage qu'un précurseur des catécholamines. Mais la reconnaissance de la DA comme véritable neurotransmetteur fut un long processus. La démonstration des faibles niveaux de DA dans le cerveau de patients parkinsoniens et celle de l'action thérapeutique de la L-3,4-dihydroxyphénylalanine (L-DOPA) n'y furent certes pas étrangères. Mais ce furent surtout la visualisation des groupes neuronaux dopaminergiques dans le cerveau du rat (Carlsson et coll., 1964; Dahlström et Fuxe, 1964) et l'étude des conséquences fonctionnelles de leur disparation par suite de lésions expérimentales (Andén et coll., 1964; Bertler et coll., 1964) qui ont été déterminantes. C'est d'ailleurs pour l'ensemble de ces travaux sur la DA que Carlsson a été récompensé du prix Nobel de physiologie, en 2000. Depuis la mise en évidence systèmes neuronaux DA dans le SNC, d'innombrables travaux ont laissé comprendre que la DA jouait un rôle crucial dans la régulation de la motricité et des comportements de récompense.

1.2 Utilisation neuronale du neurotransmetteur dopamine

Il est reconnu depuis longtemps que toutes les catécholamines sont dérivées de l'acide aminé essentiel L-tyrosine, par une voie de biosynthèse commune. L'étape limitante de cette biosynthèse est l'hydroxylation, par l'enzyme tyrosine hydroxylase (TH) de la tyrosine en L-DOPA (Nagatsu et coll., 1964). Étant donné que la DA ne transverse pas la barrière hémato-encéphalique, sa synthèse a lieu dans le SNC. Ainsi, l'enzyme de synthèse TH est-elle souvent utilisée comme marqueur des neurones DA, et

particulièrement de leurs corps cellulaires de la substance noire, pars compacta (SNc) et de l'aire tegmentaire ventrale (ATV), et voies de projection et varicosités ou terminaisons axonales du striatum, toutes régions anatomiques par ailleurs pratiquement dépourvues de neurones noradrénergiques ou adrénergiques (Moore et Card, 1984). La dernière étape de synthèse est la décarboxylation de la L-DOPA en DA par la DOPA décarboxylase, qui, pour sa part, n'est pas spécifique des neurones DA. Une fois synthétisée, on sait maintenant que c'est le transporteur vésiculaire des monoamines de type 2 (VMAT2), une autre protéine commune aux divers types de neurones à monoamine, qui emmagasine (stock) la DA dans les vésicules synaptiques des terminaisons axonales (Weihe et coll., 1994; Peter et coll., 1995; Erickson et coll., 1996), la mettant ainsi à l'abri de la dégradation enzymatique. Le consensus actuel veut aussi que ce soit l'arrivée d'un potentiel d'action et l'entrée massive de calcium qui s'ensuit qui provoque la fusion des vésicules synaptiques avec la membrane cellulaire et permettre ainsi la libération de la DA dans l'espace extracellulaire (exocytose), où celle-ci sera libre d'agir sur des récepteurs situés soit sur les terminaisons DA elles-mêmes (autorécepteurs) ou celles de leurs neurones cibles (hétérorécepteurs).

Comme dans le cas des autres catécholamines, c'est un mécanisme de recapture membranaire qui constitue le principal mode d'inactivation de la DA. On sait aujourd'hui que cette recapture est assurée par un transporteur membranaire spécifique de la DA, siglé DAT (DA transporter). Ce transporteur utilise le gradient sodique créé par la pompe NA^+/K^- adénosine triphosphate (NA^+/K^- ATPase) pour recapter la DA. Ce transport de la DA contre son gradient de concentration est saturable, stéréospécifique et de forte affinité. Il s'agit du mécanisme le plus efficace et rapide d'élimination de la DA extracellulaire (Jaber et coll., 1997; voir aussi Ramamoorthy et coll., 2011). Le DAT est réparti de façon plutôt uniforme tout au long de la membrane plasmique des neurones DA, incluant les segments inter-variqueux ainsi que les varicosités axonales (Nirenberg et coll., 1997).

La dégradation métabolique de la DA dépend principalement des enzymes monoamine-oxydase (MAO) et catéchol-O-méthyltransférase (COMT). La MAO est une enzyme mitochondriale qui dégrade la DA en acide dihydroxyphénylacétique (DOPAC). Ce métabolite est lui-même dégradé en acide homovanillique (HVA) par la COMT de l'espace extracellulaire. Les deux métabolites se retrouvent à la fois dans le plasma sanguin et l'urine. Dans l'espace extracellulaire, la COMPT peut aussi

transformer directement la DA en 3-methoxytyramine (3-MT), qui est cependant présente en plus petite quantité dans le plasma et dans l'urine.

1.3 Les récepteurs de la dopamine

Dans les années 1970, il est devenu clair que la DA pouvait activer des récepteurs induisant la production d'adénosine monophosphate cyclique (AMPc) (Kebabian et Greengard, 1971; Greengard, 2001) via la phosphorylation de protéines G, et donc qu'il s'agissait de récepteurs métabotropes. Au cours des années quatre-vingt, cinq sous-types de ces récepteurs (D1 à D5) ont été reconnus et classés en deux groupes selon leur couplage aux protéines G : la famille des récepteurs D1 (D1 et D5), et la famille des récepteurs D2 (D2, D3 et D4) (Kebabian et coll., 1984). L'ARNm du récepteur D1 est le plus abondant (Dearry et coll., 1990). Ces récepteurs stimulent l'activité de l'adénylate cyclase et par conséquent induisent une augmentation de l'AMPc (Monsma et coll., 1990; Herve et coll., 1993; Tiberi et coll., 1996). On les retrouve notamment dans le néostriatum (NS), le noyau accumbens et les tubercules olfactifs, ainsi que dans le système limbique, l'hypothalamus et le thalamus (Gerfen et coll., 1990). Dans le striatum, les récepteurs D1 sont préférentiellement localisés sur les neurones épineux de taille moyenne à l'origine de la voie striato-thalamo-corticale directe, alors que les récepteurs D2 se retrouvent surtout sur ceux de ces neurones qui sont à l'origine de la voie indirecte passant par le globus pallidus et le noyau sous-thalamique (Groenewegen et coll., 1993). Les récepteurs de la famille D2 étant couplés à une protéine Gi/Go, ils entraînent une inhibition de la production d'AMPc par l'adénylate cyclase (Kebabian et Calne, 1979). Ces récepteurs se retrouvent aussi sur les terminaisons axonales DA, où ils agissent comme autorécepteurs (Congar et coll., 2002).

1.4 Organisation générale du système à dopamine

Dans le SNC du rat, au moins six sous-systèmes de projection à la DA ont été décrits : mésostriatal, mésolimbocortical, diencéphalospinal, périventriculaire, incerto-hypothalamique et tubéro-hypophysaire, de même que deux populations d'interneurones DA, dans le bulbe olfactif et la rétine (voir Tableau 1). Les regroupements anatomiques de corps cellulaires dopaminergiques ont été initialement identifiés chez le rat par Dahlström et Fuxe (1964), qui ont utilisé une nomenclature alpha-numérique pour leur dénomination, du fait qu'aucun d'entre eux ne constituait l'ensemble de la population neuronale de la région anatomique en question. Selon Hökfelt (1984a), les corps cellulaires des groupes A8, A9 et A10 sont situés dans le mésencéphale (voir Figure 1), et ceux des groupes A11, A12, A13, A14 et A15 dans différentes régions du diencéphale. Les groupes A8, A9 et A10 sont respectivement retrouvés dans l'aire rétrorubrale, la SNc et l'ATV, et sont à l'origine des voies mésotriatale et mésolimbocorticale. Les axones du groupe A11, le plus caudal, se projettent vers la moelle épinière, alors que les autres groupes du diencéphale sont à l'origine d'innervations locales ou se projettent vers des aires de l'hypothalamus et l'hypophyse. Le groupe A16 du bulbe olfactif est un sous-ensemble d'interneurones périglomérulaires, et le groupe A17 de la rétine est une sous-population de cellules amacrines retrouvées dans la couche nucléaire interne. Ainsi, le système à dopamine se caractérise-t-il par sa forte compartimentation.

Figure 1 – Organisation générale du sous-système méso-striatal à dopamine de la souris. Immunocytochimie de la TH sur une coupe sagittale de cerveau de souris normale adulte. Abbréviations : NAC, cœur du noyau accumbens; NAS, coquille du noyau accumbens; NS, néostriatum; SN, substance noire.

A- Les groupes de corps cellulaires neuronaux à dopamine

Région	Dénomination	Localisation anatomique
Mésencéphale	A8	Substance noire, pars lateralis
	A9	Substance noire, pars compacta
	A10	Aire tegmentaire ventrale
Diencéphale	A11	Hypothalamus et thalamus périventriculaire
	A12	Noyaux arqué et périventriculaire
	A13	Zona incerta
	A14	Hypothalamus antérieur et aire préoptique
	A15	Hypothalamus rétrochiasmatique
Bulbe olfactif	A16	Cellules périglomérulaires
Rétine	A17	Cellules amacrines

B- Les sous-systèmes à dopamine

Sous-système	Dénomination	Origine anatomique
Mésostriatal	A9	Substance noire, pars compacta
	A10	Aire tegmentaire ventrale
Mésolimbocortical	A8	Substance noire, pars lateralis
	A9	Substance noire, pars compacta
	A10	Aire tegmentaire ventrale
Diencéphalospinal	A11	Sous-thalamus
Périventriculaire	Cellules dispersées	Substance grise périventriculaire (II et III) et périaqueducale
Incerto-hypothalamique	A11	Sous-thalamus
	A13	Hypothalamus périventriculaire
	A14	Région préoptique
Tubéro-hypophysaire	A12	Noyaux arqué et périventriculaire
Périglomérulaire olfactif	A16	Glomérules olfactifs
Rétinien	A17	Couche nucléaire interne

Tableau 1 – Les neurones à dopamine du système nerveux central. Tiré de Björklund et Lindvall (1984).

1.5 Le système à dopamine méso-striatal

1.5.1 Origine de l'innervation à dopamine du striatum

Chez le rat, et probablement les autres espèces de mammifères, l'origine de l'innervation DA du striatum dorsal et du striatum ventral est en bonne partie distincte. Les neurones DA de la SNc sont préférentiellement à l'origine des terminaisons axonales DA du striatum dorsal ou néostriatum des rongeurs ainsi que du caudé-putamen des primates (Andén et coll., 1966b; Moore et coll., 1971; Ungerstedt, 1971b; Lindvall et Bjorklund, 1974; Nauta et coll., 1974; Hökfelt et coll., 1976; Usunoff et coll., 1976), alors que les neurones DA de l'ATV se projettent majoritairement vers les deux sections du noyau accumbens, le cœur (*Nucleus Accumbens Core*, NAC) et la coquille (*Nucleus Accumbens Shell*, NAS) (Ungerstedt, 1971a), ainsi que le tubercule olfactif. L'ensemble de ces structures constitue le striatum, dont la dense innervation DA peut être visualisée par histochimie de fluorescence et par marquage immunohistochimique (Dahlström et Fuxe, 1964; Hökfelt et coll., 1984b).

Fallon et Moore (1978) ont démontré que les portions médianes et rostrales du néostriatum sont innervées par les neurones DA latéraux de l'ATV, qui innervent également le noyau accumbens. Les neurones DA latéraux de la SNc se projetteraient vers des aires plus latérales du néostriatum, alors que les portions caudales et ventrales du néostriatum seraient innervées par les neurones DA meso-télencéphaliques caudaux. L'orientation rostro-caudale des neurones DA de l'ATV et SNc est maintenue par leur projection au néostriatum, dont la topographie est également rostro-caudale, alors que dans l'axe dorso-ventral, la topographie des projections est inverse par rapport à celle des neurones DA de l'ATV et SNc. Il est à noter qu'un petit groupe de neurones dopaminergiques situé dans la tête du noyau raphé dorsalis, innerve aussi le néostriatum médian (Descarries et coll., 1986).

Nous avons vu que le groupe A9 fait partie de la substance noire, pars compacta (SNc), et le groupe A10 de l'aire tegmentaire ventrale (ATV) du mésencéphale ventral. Chez le rat, ces deux groupes contiendraient 15 000 à 20 000 corps cellulaires dans chaque hémisphère du cerveau (Hedreen et Chalmers, 1972; Guyenet et Crane, 1981; Swanson, 1982). Le nombre de corps cellulaires DA serait de 11 500 dans la SNc et de 9 000 dans l'ATV (Swanson, 1982), ce qui représente respectivement environ 70% et 40% de la population neuronale totale de ces deux régions (90% et 50%, respectivement,

selon Margolis et coll., 2006). Cependant, les données divergent sur le nombre de neurones DA mésencéphalique qui se projetteraient au néostriatum, évalué à 3 500 de chaque côté selon Andén et coll. (1966a) ou 7 000 selon Björklund et Lindvall (1984).

Chez la souris, le nombre des neurones DA mésencéphaliques varie selon la souche examinée. Les souris de souche BALB/cJ présenteraient 20 à 50% plus de neurones DA que les souris de souche CBA/cJ (Ross et coll., 1976; Baker et coll., 1980). Les groupes A9 et A10 seraient composés de 7 800 neurones DA chez la souris BALB/cJ et 6 200 neurones chez la souris CBA/cJ (Baker et coll., 1980). D'autres souches de souris ont aussi fait l'objet d'étude du nombre des neurones DA : 8 200 et 10 600 peupleraient respectivement la SNc et l'ATV chez la souche C57/BL/6 (total de 21 000 neurones DA dans le mésencéphale selon Nelson et coll., 1996) et la souche FVB/N présenterait quant à elle 31 000 neurones mésencéphaliques DA, dont environ 11 200 dans la SNc et 15 800 dans l'ATV (Nelson et coll., 1996). Au cours d'une étude récente, Fortin et coll. ont produit les chiffres de 5 500 neurones DA pour la SNc et 4 400 pour l'ATV chez la souris de souche mixte 129/Sv/J et C57Bl/6 (Fortin et coll.).

1.5.2 L'arborisation axonale terminale

L'étude de l'arborisation axonale de neurones DA mésencéphaliques par suite de l'incorporation unitaire d'un traceur hautement diffusible dans le corps cellulaire de neurones de la SNc et l'ATV a révélé l'existence de plusieurs patrons de projection de ces neurones vers le striatum (Gauthier et coll., 1999; Prensa et Parent, 2001). Les neurones DA de la SNc peuvent être regroupés en trois types selon les caractéristiques de leur arborisation axonale, alors que ceux de l'ATV sont de deux types. Les axones des neurones de la SNc du type 1 sont les plus nombreux. Ces neurones sont principalement situés dans la portion dorsale de la SNc et innervent directement le striatum. Les corps cellulaires des neurones de type 2 sont situés dans une portion plus médiane de la SNc et émettent deux collatérales avant de quitter la région, lesquelles se divisent en plusieurs segments minces et variqueux qui se répartissent dans la portion ventral de la SNc et la portion dorsale de la substance noire pars reticulata (SNr). Les corps cellulaires des neurones de type 3 sont situés dans la même région que ceux de type 1. Leurs axones, quant à eux, passent par l'aire hypothalamique latérale et donnent des collatérales courtes et variqueuses qui gagnent le noyau entopédonculaire. Les

axones de neurones de type 1 de l'ATV innervent le fundus striati alors que ceux des neurones de type 2 se projettent vers la matrice caudo-ventrale du striatum dorsal.

Plus récemment, en utilisant une méthode de visualisation fondée sur la surexpression d'une protéine fluorescente virale dans des neurones DA individuels, Matsuda et coll. (2009) ont décrit les caractéristiques morphométriques des arborisations axonales terminales de ces neurones dans le néostriatum du rat. À l'intérieur du néostriatum, les axones DA de la projection nigrostriatale forment des touffes, buissons ou écheveaux très denses, constitués de fines branches terminales, dont chacune est munie de nombreuses varicosités. Le volume moyen d'une arborisation terminale individuelle est de 0.54 mm^3, mais l'étude de Matsuda et coll. souligne les différences individuelles d'une arborisation terminale à l'autre, que ces auteurs attribuent à l'organisation compartimentée de la distribution de l'innervation DA striatale, particulièrement évidente au cours du développement, mais qui persiste chez l'adulte (Olson et coll., 1972; Graybiel et coll., 1987). Ainsi, dans la matrice, le volume moyen de l'arborisation DA serait de 0.47 mm^3 alors qu'il occuperait 0.07 mm^3 dans les îlots (striosomes).

1.5.3 Densité de l'innervation à dopamine de striatum

Chez le rat, il avait été initialement estimé en histochimie de fluorescence que l'axone d'un neurone DA innervant le néostriatum mesurait entre 55 et 77 cm de longueur et formait environ 500 000 varicosités (Andén et coll., 1966a). Ces varicosités axonales avaient été décrites comme petites (0.5 - 0.7 µm de diamètre) et situées à proximité des branches dendritiques des petits neurones majoritaires du néostriatum (Hökfelt et Ungerstedt, 1969; Hattori et coll., 1973; Ibata et coll., 1973). Toujours chez le rat, en utilisant l'autoradiographie après capture et stockage de DA tritiée dans des tranches de tissu, Doucet et coll. (1986) ont estimé la densité de l'innervation DA du néostriatum à 1.0 x 10^8 varicosités axonales par mm^3 de tissu dans la matrice et 1.7 x 10^8 dans les striosomes (Doucet et coll., 1986), démontrant ainsi que la compartimentation striatale de l'innervation DA, particulièrement évidente au cours du développement, persiste chez l'adulte. Ces densités correspondent grossièrement à une sur dix de toutes les varicosités axonales du striatum. Il s'agit d'une densité d'innervation exceptionnellement élevée, presque cent fois supérieure à celle de l'innervation 5-HT, par exemple (Soghomonian et coll., 1987). La seule qui lui est comparable, est celle de

l'innervation cholinergique, dont la densité n'a cependant jamais été chiffrée. Étant donné que le volume du néostriatum du rat est d'environ 45 mm^3, le nombre total de terminaisons DA du néostriatum s'élèverait à 4.5×10^9 de chaque côté du cerveau. Aucune donnée analogue n'est disponible au sujet de l'innervation DA du striatum ventral. Cependant, compte tenu de la densité comparable qu'on y observe lors des immunomarquages TH pour la microscopie optique ou la microscopie électronique, on peut supposer que le nombre des varicosités axonales DA y est équivalent. De même, il est probablement du même ordre dans le striatum de la souris (voir le chapitre 3 de cette thèse).

1.5.4 Ultrastructure de l'innervation striatale à dopamine

Les premières descriptions obtenues en microscopie électronique après marquage spécifique des terminaisons DA du striatum divergent à propos de leurs propriétés ultrastructurales. Les premières données, cytochimiques, ne donnent aucune indication de la présence de spécialisations membranaires associées à l'établissement de contacts synaptiques par les varicosités monoaminergique (DA et sérotonine) du néostriatum, dans du tissu fixé avec le permanganate de potassium (Hökfelt, 1968; voir aussi Tennyson et coll., 1974). Plus tard, une étude immunocytochimique vient confirmer que les terminaisons DA ne présentent pas de complexe de jonction synaptique dans du tissu fixé par aldéhyde et immunomarqué avec l'enzyme de biosynthèse tyrosine hydroxylase (TH) (Pickel et coll., 1976). Par contre, en 1980, une étude autoradiographique préliminaire, réalisée par Descarries et coll. (1980) après marquage *in vivo* avec la DA tritiée administrée par voie intraventriculaire cérébrale, démontre qu'une proportion significative des terminaisons (varicosités) axonales marquées dans la région paraventriculaire du néostriatum présentent des complexes de jonction synaptique, de type symétrique, c'est-à-dire sans épaississement prononcé de la membrane sur le versant post-synaptique.

Des études cytochimiques ou immunocytochimiques subséquentes en viennent à suggérer l'existence de deux catégories de terminaisons néostriatales DA : une catégorie restreinte, composée de larges varicosités dépourvues de spécialisations synaptiques membranaires, une deuxième plus abondante composée de varicosités plus petites caractérisées par la présence de complexe de jonction symétrique (Kaiya et Namba, 1981; Pickel et coll., 1981; Arluison et coll., 1984). À la suite d'une étude

immunocytochimique en coupes fines sériées, Freund et coll. (1984) rapportent que 411 terminaisons axonales TH immunopositives étaient synaptiques dans le néostriatum du rat adulte (Freund et coll., 1984). Une étude similaire, consacrée au striatum ventral, évalue à 69% la proportion des terminaisons axonales immunopositives établissant des contacts synaptiques : 42% avec des dendrites, 23% avec des terminaisons axonales non-marquées et 4% avec des corps cellulaires. Les autres terminaisons DA (31%) seraient dépourvues de spécialisations membranaires synaptiques (Bouyer et coll., 1984). Une étude subséquente de Voorn et coll. (1986), ayant recours à l'immunocytochimie avec un anticorps dirigé contre la DA elle-même, indique simplement que les varicosités DA du striatum ventral du rat adulte sont généralement pourvues de contacts synaptiques symétriques (Voorn et coll., 1986).

Pour clarifier la situation, à la suite d'une quinzaine d'années d'études des varicosités DA du néostriatum, d'abord marquées en autoradiographie avec la [^{3}H]DA puis en immunocytochimie avec des anticorps dirigés contre la TH ou encore contre la DA elle-même, Descarries et coll. (1996) ont utilisé cette dernière approche non seulement en coupes fines isolées mais aussi en coupes fines sériées. Indépendamment de l'approche utilisée, c'est-à-dire l'examen de l'entièreté des varicosités en coupes fines sériées (immunocytochimie DA) ou l'extrapolation stéréologique de l'incidence synaptique des varicosités entières à partir de la fréquence observée en coupes isolées (autoradiographie et immunocytochimie DA), le résultat s'est avéré le même : 30 à 40% des terminaisons examinées de la portion paraventriculaire (autoradioagraphie), ainsi que d'une région centrale (immunocytochimie) du néostriatum du rat adulte présentent une spécialisation membranaire synaptique, le plus souvent symétrique. Des valeurs du même ordre de grandeur ont été rapportées par la suite chez le rat de 21 jours : 35% des terminaisons DA de la matrice ont été alors considérés comme synaptiques, et 63% de celles des îlots (Antonopoulos et coll., 2002). Ces auteurs ont aussi examiné le striatum ventral, où ils ont rapporté des pourcentages de terminaisons synaptique de 47% et 71% pour le NAC et la NAS, respectivement. Par contre, des fréquences synaptiques beaucoup plus faibles ont été rapportées par Zahm (1992) dans un vaste échantillon de terminaisons TH immunoréactives examinées en coupes fines isolées chez le rat adulte (Zahm, 1992). Selon cet auteur, les fréquences synaptiques observées étaient alors de 2.3% dans le néostriatum, de 2.9% dans le NAC et de 2.4% dans la NAS. Dans ces deux études cependant, les résultats doivent être considérés avec prudence. L'examen a été

effectué en coupes fines isolées seulement et, dans les deux cas, la préservation morphologique des tissus laissait beaucoup à désirer si l'on en juge par la qualité des illustrations, rendant difficilement applicables les critères d'identification des jonctions synaptiques. De plus, si l'on en juge par la dimension moyenne des varicosités examinées par Antonopoulos et coll. (2002), rapportée comme supérieure à 0.8 µm, l'échantillon souffrait alors d'un biais évident en faveur des varicosités les plus volumineuses, faussant ainsi l'extrapolation stéréologique à la hausse. Enfin, signalons que plusieurs des études antérieures avaient noté une préférence des contacts synaptiques formés par les varicosités DA striatales pour les branches dendritiques et le cou des épines dendritiques, tant dans le NAS (Voorn et coll., 1986) que le néostriatum, et que ni l'une ni l'autre de ces localisations préférentielles ne semble avoir été détectée dans l'échantillon de Zahm (1992).

L'incidence synaptique des varicosités DA striatales n'ayant jamais été systématiquement évaluée chez le singe, presque toutes les données quantitatives sur la synaptologie de ces terminaisons ont donc été obtenues jusqu'à maintenant chez le rat (voir Tableau 2). Les seuls résultats rapportés pour la souris l'ont été dans le cadre de l'étude d'une souche mutante (Triarhou et coll., 1988b; Triarhou et coll., 1988a), où la comparaison a été effectuée sur un petit échantillon en provenance du néostriatum dorsal de deux souris normales. Il a alors été rapporté que 27% des terminaisons TH immunoréactives présentaient une jonction synaptique en coupe fine isolée.

Espèce	Région	Méthode	Incidence synaptique	Références
Rat	Néostriatum	Immuno TH coupe unique	Type 1 : 100 % Type 2 : nil	(Pickel et coll., 1981)
		Immuno TH coupe sériée	100%	(Freund et coll., 1984)
		Immuno TH coupe unique	2%	(Zahm, 1992)
		Autoradio [^{3}H]DA coupe unique	10%	(Descarries et coll., 1996)
		extrapolée	39%	
		Immuno DA coupe unique	12%	
		extrapolée	40%	
		coupe sériée	35%	
		Immuno DA extrapolée	Ilots : 62%, Matrice : 36%	(Antonopoulos et coll., 2002)
	N. accumbens	Immuno TH coupe unique	69%	(Bouyer et coll., 1984)
		Immuno DA coupe unique	38%	(Voorn et coll., 1986)
		Immuno TH coupe unique	Cœur : 3% Coque : 2%	(Zahm, 1992)
		Immuno DA extrapolée extrapolée	Cœur : 47%, Coque : 71%	(Antonopoulos et coll., 2002)
Souris	Néostriatum (dorso-latéral)	Immuno TH coupe unique extrapolée	27% 85%	(Triarhou et coll., 1988a)

Tableau 2 – Incidence synaptique des terminaisons à dopamine du striatum. Sont ici répertoriées les études qui rapportent une fréquence (%) avec laquelle les terminaisons examinées apparaissaient munies d'un complexe de jonction synaptique. Sous Méthode, « extrapolée » signifie que la fréquence pour le volume entier des varicosités a été calculée à partir du pourcentage observé en coupes uniques, grâce à la formule de Beaudet et Sotelo (1981).

1.5.5 Développement de l'innervation à dopamine du striatum

Chez le rat, deux groupes de neurones DA peuvent être identifiés dès le 14^{e} jour prénatal (Voorn et coll., 1988). À partir du 18^{e} jour prénatal, des fibres dopaminergiques en provenance du mésencéphale ventral commencent à innerver le striatum ventral, ainsi que le septum et le cortex. L'innervation striatale est alors caractérisée par des fibres minces ou épaisses qui envahissent d'abord le striatum dorsal, latéral et médian. Dès le 19^{e} jour prénatal, la SNc et l'ATV apparaissent distinctes et, à partir du 20^{e} jour, des fibres DA se retrouvent dans l'ensemble du striatum, dorsal et ventral. Pendant le développement prénatal, aucune varicosité ou terminaison axonale n'est observée. Ce n'est que durant la première semaine postnatale que la morphologie des fibres DA change, avec la prolifération de fibres minces et le développement de varicosités dont la distribution en îlots de densité relativement forte et en matrice de moindre densité est frappante. Le nombre de varicosités augmente ensuite, pour atteindre l'extrême densité caractéristique de l'adulte vers la fin de la 3^{e} semaine postnatale.

L'étude d'Antonopoulos et coll. (2002) a également rapporté des données sur l'incidence synaptique des varicosités DA du striatum à divers âge du développement postnatal chez le rat (Antonopoulos et coll., 2002). Ainsi, à la naissance, environ 75% de ces terminaisons présenteraient une spécialisation synaptique tant dans les îlots que la matrice du néostriatum, ainsi que dans le NAC et la NAS. Cette prédominance de varicosités axonales synaptiques se maintiendrait durant le développement post-natal; chez les ratons de 14 jours, 92% des varicosités TH immunoréactives des îlots et et 72% de celles de la matrice du néostriatum seraient alors synaptiques, ainsi que 76% dans le NAC et 100% dans la NAS. Toutes ces varicosités formeraient alors des contacts de type symétrique. Nous avons expliqué plus haut pourquoi les résultats obtenus par ces auteurs doivent être considérés avec circonspection.

De même, nous avons déjà mentionné que la présence d'îlots d'innervation DA de forte densité, au sein d'une matrice de moindre densité, est particulièrement frappante au cours du développement prénatal du striatum (Olson et coll., 1972; Voorn et coll., 1988). Ce même type de compartimentation en cours de maturation du système DA se retrouve chez le lapin (Tennyson et coll., 1972), la souris (Busceti et coll., 2008) et le singe (Lavoie et coll., 1989; Smith et coll., 1994).

1.6 La neurotransmission dopaminergique striatale

1.6.1 Propriétés fonctionnelles

Les neurones dopaminergiques présentent deux modes d'activité électrophysiologiques, sous formes de décharges toniques ou phasiques. Les décharges toniques sont des événements spontanés, qui sont sous le contrôle de courants membranaires de type générateur de rythme (Grace et Bunney, 1984; Grace et Onn, 1989). Ainsi, la teneur en DA du striatum est normalement maintenue par des décharges toniques (Keefe et coll., 1993) et la quantité de DA libérée dépend du nombre de neurones DA actifs (Grace, 1991; Floresco et coll., 2003). Quant à l'activation phasique du système mésostriatal DA, sous forme de décharge en bouffées, elle est sous l'influence des afférences glutamatergiques du noyau pédonculopontin (Futami et coll., 1995; Floresco et coll., 2003) et du noyau sous-thalamique (Smith et Grace, 1992).

1.6.2 Transmission synaptique et transmission diffuse

Le concept de transmission diffuse fut proposé sur la base d'observations en microscopie électronique montrant que les terminaisons (varicosités) axonales des neurones à sérotonine et noradrénaline du SNC n'étaient que partiellement synaptique chez le rat adulte (Descarries et coll., 1975; 1977). En effet, plusieurs de ces terminaisons axonales ou varicosités étaient dépourvues des spécialisations membranaires (complexes de jonctions) caractéristiques des synapses morphologiquement définies (Peters et Palay, 1996). Ces observations ont conduit à suggérer que, dans le cas de ces varicosités non synaptiques, la transmission chimique puisse avoir lieu à distance via l'activation de récepteurs extra-synaptiques (Beaudet et Descarries, 1976). De plus, en raison du fait que la présence de complexes de jonction impliquait une certaine fixité et permanence de la relation structuro-fonctionnelle entre les éléments pré- et post-synaptique, l'inverse a laissé supposer une certaine flexibilité et d'incessants mouvements de translocation, c'est-à dire de déplacement, des terminaisons axonales par rapport à leur environnement immédiat (Descarries et coll., 1975). Par la suite, ce concept de transmission diffuse, proposée comme complémentaire de la transmission synaptique, a été popularisé par de nombreux articles de synthèse, sous le vocable de "volume transmission" (transmission volumique) (Fuxe et Agnati, 1991).

Dans le cas des innervations majoritairement non jonctionnelles et hyperdenses, comme l'innervation cholinergique du striatum, mais aussi son innervation DA, Descarries et coll. ont aussi suggéré la possibilité qu'un faible niveau ambiant de transmetteur soit maintenu en permanence dans l'espace extracellulaire, auquel les événements de libération tonique ou phasique se superposeraient comme autant de fluctuations locales de la concentration de transmetteur. Les tenants d'une transmission dopaminergique exclusivement synaptique prétendent pour leur part que ce sont les décharges toniques qui maintiennent la concentration normale de DA dans le striatum par débordement de la DA hors des fentes synaptiques (Grace, 1991; Floresco et coll., 2003). Par contre, les quantités plus importantes de DA relâchées lors des décharges en bouffée (Grace, 1991; Floresco et coll., 2003) seraient rapidement recapturées par les transporteurs DAT situés sur les terminaisons axonales DA (Chergui et coll., 1994; Suaud-Chagny et coll., 1995), de telle sorte que les décharges phasiques agiraient de façon transitoire et uniquement à proximité des varicosités DA (Grace, 1991; Chergui et coll., 1994; Floresco et coll., 2003; Venton et coll., 2003). Cependant, lors de la libération tonique ou phasique simultanée par plusieurs terminaisons axonales, la concentration de DA dans le néostriatum pourrait rapidement augmenter.

Des études de microdialyse ont permis d'estimer le niveau ambiant de DA à 6.5 nM dans le néostriatum du rat adulte (Sam et Justice, 1996), une concentration de monoamine physiologiquement pertinente (Parsons et Justice, 1992). Ainsi, peut-on considérer que la relâche de DA augmente localement et temporairement le niveau ambiant de DA (Garris et coll., 1994; Zhang et coll., 2009), plutôt que de considérer la neurotransmission à DA striatale comme un phénomène de tout ou rien. La recapture de DA servirait à réguler ce niveau ambiant plutôt qu'a éliminer complètement la DA extracellulaire.

Descarries et coll. ont aussi suggéré que le niveau ambiant de DA puisse jouer un rôle important au plan physiologique, en contrôlant l'expression de divers récepteurs pour la DA elle-même ou d'autres transmetteurs (Descarries et coll., 1996). Le fait qu'il s'agisse d'une très faible concentration de DA pourrait expliquer son maintien malgré la disparition d'une forte proportion de ces terminaisons nerveuses au cours des processus lésionnels ou dégénératifs, et pourquoi les symptômes d'une dénervation DA striatale n'apparaissent qu'à la suite d'une perte d'au moins 80% de ces terminaisons.

1.7 Dérèglements pathologiques

La transmission dopaminergique apparait déréglée dans différentes maladies du SNC telles que la maladie de Parkinson, la schizophrénie, les dépendances aux drogues d'abus, le syndrome de Giles de la Tourette ainsi que le trouble d'attention/hyperactivité (revu par Kienast et Heinz, 2006). Dans le contexte du présent travail, nous nous contenterons d'évoquer quelques données générales concernant l'implication du système DA mésostriatal dans les trois premières conditions pathologiques.

- ***La maladie de Parkinson***

La maladie de Parkinson a été décrite par James Parkinson en 1817. Elle est caractérisée par un tremblement lent et persistent au repos, une rigidité musculaire et une akinésie. Alors que le lien entre la substance noire et la maladie fut établi au début du 20^{e} siècle (revu par Parent et Parent, 2010), ce n'est qu'après la démonstration d'une forte concentration de DA dans le striatum, principale région du cerveau impliquée dans le contrôle moteur, que Carlsson a proposé que la déplétion de DA puisse être à l'origine des symptômes moteurs de la maladie de Parkinson (Carlsson, 1959). La confirmation de cette hypothèse est venue l'année suivante, lorsqu'il fut constaté que les cerveaux post-mortem de patients parkinsoniens contenaient moins de DA que ceux de sujets témoins (Ehringer et Hornykiewicz, 1960), et que l'administration du précurseur de la DA, la L-DOPA, était bénéfique pour les patients parkinsoniens (Birkmayer et Hornykiewicz, 1961; Barbeau et coll., 1962). La maladie de Parkinson est aujourd'hui considérée comme plurifactorielle, résultant du vieillissement et d'une susceptibilité génétique et/ou de facteurs environnementaux (Surmeier et coll., 2010). Des mutations de quelques gènes, tel que Parkin, DJ-1, Pink-1 et *Leucine-Rich Repeat Kinase 2* (LLRK2), ont été rapportées dans les formes familiales de la maladie (Cookson, 2010; Gasser, 2010; Martin et coll., 2010). Il s'agit de protéines qui influencent directement ou indirectement la fonction mitochondriale, suggérant ainsi un rôle fondamental de cet organelle dans la physiopathologie de cette maladie.

Une caractéristique pathologique associée à la maladie est l'apparition des corps de Lewy, qui jalonne les stades d'évolution du Parkinson, tels que définis par Braak (Braak et coll., 2003); d'abord dans les noyaux ambigu et dorsal du vague, puis les noyaux olfactifs, la substance noire et finalement les aires associatives et préfrontales du néocortex. Ces large aggrégats protéiniques, détectés par histochimie en post-

mortem, se retrouvent fréquemment près des noyaux cellulaires et sont composés majoritairement d'α-synucléine (Spillantini et coll., 1997). Une hypothèse courante suppose que des mutations dans la protéine α-synucléine conduisent à l'augmentation de la formation d'oligomères et d'agrégats fibrillaires (Goedert et coll., 1998; Karpinar et coll., 2009). Également, l'accumulation d'α-synucléine à la synapse engendrerait une perte de protéines synaptiques et d'épines dendritiques (Kramer et Schulz-Schaeffer, 2007). Ce n'est que lorsque la dégénérescence des neurones de la SNc atteindrait 50% que les premiers symptômes parkinsoniens apparaitraient (Bernheimer et coll., 1973; Fearnley et Lees, 1991). À ce moment 80% de la DA du striatum serait déjà disparue. Tel que mentionné ci-dessus, l'hypothèse du niveau ambiant de transmetteur pourrait rendre compte de ce phénomène en apparence paradoxal.

Le traitement de première ligne de la maladie de Parkinson est l'administration de L-DOPA, le précurseur de la DA capable de traverser la barrière hémato-encéphalique, associée ou non à celle d'inhibiteurs des enzymes de dégradation de la DA et/ou d'agonistes des récepteurs DA. Cependant, la maladie continue de progresser et après 10 années de traitement, il y a généralement apparition de dyskinésies induites par L-DOPA (Voon et coll., 2009), lesquelles surviennent chez 90% des patients traités (Fabbrini et coll., 2007). Ces dyskinésies sont des mouvements involontaires, irréguliers, sans but et parfois répétitifs (Obeso et coll., 2007). Les mécanismes neurobiologiques à l'origine de cette complication thérapeutique majeure sont l'objet de recherches très actives.

- ***Schizophrénie***

L'hypothèse voulant qu'une libération excessive de DA dans le striatum ventral soit à l'origine de la schizophrénie vient d'études pharmacologiques (revu dans Kienast et Heinz, 2006). Elle repose en partie sur l'observation clinique de patients, qui ont présenté des manifestations schizoïdes, par suite de traitement à la L-DOPA pour la maladie de Parkinson. De même, la cocaïne et les amphétamines peuvent induire des épisodes schizoïdes qui ressemblent à la schizophrénie. Par ailleurs, les antagonistes des récepteurs dopaminergiques de type D2 sont les médicaments antipsychotiques les plus utilisés pour le traitement de la schizophrénie. La corrélation entre l'activité clinique des antipsychotiques et leur capacité à bloquer les récepteurs DA est très forte (Seeman et coll., 1976). Un raffinement de l'hypothèse est à l'effet que

deux systèmes dopaminergiques soient différentiellement perturbés dans la schizophrénie (Weinberger, 1987); les symptômes positifs, tel que délires et hallucinations seraient associés à une augmentation de l'activité du système mésolimbique, alors que les symptômes négatifs résulteraient d'une diminution d'activité du système DA mésocortical.

- ***La dépendance aux drogues d'abus***

Le système mésolimbique DA serait aussi préférentiellement impliqué dans la dépendance aux drogues d'abus. En effet, les neurones DA de l'ATV et leurs projections au noyau accumbens et au cortex préfrontal font partie des circuits de récompense du cerveau. Or, les drogues d'abus stimulent la relâche de DA dans le striatum ventral, créant une sensation initiale de plaisir et le renforcement de la consommation (Wise, 1988; Di Chiara, 1995). Dans le cortex préfrontal, la stimulation DA serait associée à l'anticipation d'une récompense (Merali et coll., 2004; Stark et coll., 2004).

Ainsi, chez le rat, l'alcool active les neurones DA de l'ATV et sa consommation chronique augmente la teneur en DA du NAS (Di Chiara et coll., 2004), ce qui entraîne une diminution de la densité mais non de l'affinité des récepteurs D2 dans le système limbique (Tupala et Tiihonen, 2004). Chez l'humain, l'alcool entraîne aussi une libération de DA dans le noyau accumbens (Boileau et coll., 2003) et des études en imagerie cérébrale démontrent aussi une corrélation entre l'augmentation de DA extracellulaire dans le striatum et la mesure de l'euphorie par les sujets (Di Chiara et coll., 2004). En post-mortem, une diminution de la densité des sites de liaison aux récepteurs D2 a également été constatée dans le noyau accumbens et l'amygdale, épargnant la substance noire (Tupala et Tiihonen, 2004).

1.8 Le modèle 6-hydroxydopamine

Les modèles animaux sont très utiles pour la compréhension de la maladie de Parkinson, notamment ceux qui résultent des lésions par des neurotoxines sélectives des neurones catécholaminergiques. Le plus ancien, qui repose sur l'utilisation de la 6-hydroxydopamine (6-OHDA) est encore l'un des plus utilisés (Schwarting et Huston, 1996b, a). Isolée à la fin des années 1950, la 6-OHDA fut rapidement employée chez le rat pour produire des lésions du système dopaminergique (Ungerstedt, 1968). La structure de la 6-OHDA est très similaire à celle de la DA, à l'exception d'un groupe

hydroxyle qui rend la molécule toxique pour les neurones dopaminergiques. La cytotoxine entre dans les neurones à catécholamine par leur transporteur membranaire et la toxicité de la 6-OHDA impliquerait un processus de stress oxydatif (Sachs et Jonsson, 1975). Pour protéger les neurones NA et léser sélectivement les neurones DA, la 6-OHDA peut être administrée à la suite d'un prétraitement avec un bloqueur du transporteur de la NA comme la désipramine. Étant donné que la 6-OHDA ne peut pas traverser la barrière hémato-encéphalique, la toxine doit être injectée directement dans le SNC. Des lésions bilatérales chez l'adulte entraînent la destruction du système nigrostriatal et des déficiences motrices et alimentaires létales (Ungerstedt, 1971c; Zigmond et Stricker, 1972; Marshall et coll., 1974). Pourtant, des lésions similaires chez le rat nouveau-né (Breese et Traylor, 1972), n'ont pas les mêmes conséquences. Malgré une destruction partielle du système dopaminergique et des changements structuraux et fonctionnels majeurs du striatum (Breese et coll., 1984; Stachowiak et coll., 1984; Berger et coll., 1985), les ratons survivent à la lésion sans déficit moteur apparent. On sait maintenant qu'ils développement une importante hyperinnervation sérotoninergique striatale (Breese et coll., 1984; Stachowiak et coll., 1984; Jackson et coll., 1988; Broaddus et Bennett, 1990; Castaneda et coll., 1990; Dewar et coll., 1990; Luthman et coll., 1990; Mrini et coll., 1995), dont les caractéristiques ultrastructurales sont comparable à celles de l'innervation à sérotonine du rat adulte normal (Descarries et coll., 1992). Par ailleurs, chez les rats lésés, la SNc, qui normalement ne reçoit pas d'innervation axonale DA (Wassef et coll., 1981), et apparaît alors dépeuplée de ses corps cellulaires et dendrites DA, est le siège d'une innervation aberrante DA, probablement issue de neurones de l'AVT épargnés par la lésion (Fernandes Xavier et coll., 1994). Ce phénomène a été qualifié de néoinnervation puisqu'il s'agit d'une innervation inexistante chez le rat normal. Au cours du premier travail décrit dans cette thèse, nous avons pu en déterminer les caractéristiques ultrastructurales qui n'avaient jamais été décrites auparavant (voir chapitre 2).

2 Glutamate

2.1 Le glutamate et ses récepteurs

2.1.1 Bref historique

Le glutamate est le neurotransmetteur excitateur majeur du SNC. Retrouvé en grande quantité dans le SNC, le glutamate est à l'origine d'une neurotransmission synaptique rapide nécessaire à toutes les fonctions du cerveau (Collingridge et Lester, 1989; Headley et Grillner, 1990). Le glutamate jouerait aussi un rôle dans le développement du SNC par l'induction et l'élimination des synapses (voir en autre Collingridge et coll., 2010). Même si les effets excitateurs du glutamate sont connus depuis les années 1950 (Hayashi, 1954; Curtis et Watkins, 1960), l'acceptation de son rôle en tant que neurotransmetteur est relativement récente. Dans les années 1970, le glutamate était encore un neurotransmetteur présumé (Johnson et Aprison, 1970; Hökfelt et Ljungdahl, 1972). C'est l'article de synthèse de Fonnum (1984) qui permettra la reconnaissance générale de son rôle de neurotransmetteur (Krnjevic, 1986; Watkins, 1986).

2.1.2 Utilisation neuronale du glutamate

Le glutamate est un acide aminé non-essentiel qui ne peut pas traverser la barrière hémato-encéphalique, mais se retrouve en forte concentration dans le SNC, entre 5 et 15 mmol par kg selon la région (Schousboe, 1981). La synthèse et la recapture du glutamate sont très fortement régulées, en autre par le cycle glutamate-glutamine (Nicholls, 1989; Shepherd, 1994). Le principal précurseur du glutamate est la glutamine, mais il peut aussi être synthétisé à partir de l'aspartate, par la transamination du cycle de Krebs dans les mitochondries. L'enzyme glutaminase phosphate dépendante (PAG, *Phosphate-Activated Glutaminase*) permet l'hydrolyse de la glutamine en glutamate dans les mitochondries des terminaisons axonales (Reijnierse et coll., 1975; Bradford et Ward, 1976). Il faut aussi noter que le glutamate est lui-même un précurseur dans la synthèse d'un autre neurotransmetteur, le GABA.

Aussitôt synthétisé, le glutamate est emmagasiné dans les vésicules synaptiques par l'un des trois transporteurs vésiculaires du glutamate (VGLUT1-3, *Vesicular Glutamate Transporter 1-3*). Après sa libération par exocytose dans la fente synaptique, le glutamate est rapidement recapturé non seulement pas les terminaisons axonales, mais aussi par les éléments post-synaptiques et les cellules gliales environnantes (Danbolt,

2001). Ces dernières utilisent l'enzyme glutamine synthétase pour convertir le glutamate en glutamine (Norenberg et Martinez-Hernandez, 1979). Alternativement, le glutamate peur aussi être dégradé en α-ketoglutamate par la déamination oxydative (Yu et coll., 1982; Westergaard et coll., 1996) ou par transamination (McKenna et coll., 1996). La glutamine peut par la suite être libérée par les astrocytes et recapturée par la terminaison axonale via des transporteurs à glutamine. Par suite de leur clonage et caractérisation, les transporteurs membranaires du glutamate peuvent être classés en cinq sous-types, GLT-1, GLAST, EAAC1, EAAT4 et EAAT5, en fonction de leur structure respective, (Sims et Robinson, 1999; Tanaka, 2000).

2.1.3 Les récepteurs du glutamate

Les récepteurs du glutamate forment deux groupes : ceux qui sont des canaux ioniques, les récepteurs ionotropes, et ceux qui sont couplés à différentes protéines G, les récepteurs métabotropes. Ainsi, trois familles de récepteurs ont été identifiées par clonage moléculaire. Deux familles sont constituées de récepteurs ionotropes activés soit par l'analogue du glutamate, le N-methyl-D-aspartate (NMDA), soit par le α-amino-3-hydroxy-5-methyl-4-isoxazole propionic acid (AMPA) ou le kaïnate. La troisième famille se compose des récepteurs métabotropes (Hollmann et Heinemann, 1994; Schoepfer et coll., 1994; Borges et Dingledine, 1998; Nakanishi et coll., 1998; Ozawa et coll., 1998; Dingledine et coll., 1999). Tous les récepteurs activés par le NMDA (NR1, NR2A, NR2B, NR2C et NR2D) ont une haute affinité pour le glutamate mais s'activent lentement (Patneau et Mayer, 1990). Les récepteurs AMPA/kaïnate (GluR1-9, KA1 et KA2) ont une moins grande affinité pour le glutamate, mais sont activés dès l'apparition de glutamate dans la fente synaptique et se désensibilisent rapidement (Tang et coll., 1989; Trussell et Fischbach, 1989). Les récepteurs métabotropes du glutamate peuvent être divisé en trois groupes selon leurs propriétés pharmacologiques : groupe I (mGluR1 et MGluR5), groupe II (mGluR2 et MGluR3) et groupe III (mGluR4, MGluR6, mGluR7 et MGluR8) (Krystal et coll., 2010). Les récepteurs des groupes I et II sont activés par l'acide (±)1-amino-cyclopentane-trans-1,3-dicarboxylic (trans-ACPD) alors que les récepteurs du groupe III sont activés par l'acide L(+)-2-amino-4-phosphonobutyric (L-AP4). De plus, les récepteurs du groupe I sont couplés à la phospholipase C et donc impliqués dans la production de l'inositol

triphosphate et du diacylglycérol, tandis que les récepteurs des groupes II et III sont couplés négativement à l'adénylate cyclase.

2.2 La neurotransmission glutamatergique

2.2.1 Propriétés de base

Le glutamate engendre une réponse excitatrice sous forme de potentiel post-synaptique excitateur (PPSE ou EPSP, *Excitatory Post-Synaptic Potential*). Toutefois, étant donné la variété des réponses engendrées par le glutamate, nous nous contenterons ici d'une description très succincte de ses propriétés électrophysiologiques de base.

Lors d'une transmission synaptique faible, ou à basse fréquence, le glutamate va se lier à la fois aux récepteurs AMPA/kaïnate et NMDA, mais ne pourra activer que les récepteurs AMPA/kaïnate, qui feront entrer des ions sodium (Na^+) dans le neurone post-synaptique. Les récepteurs NMDA ne sont activés que si le potentiel de membrane est suffisamment dépolarisé, car la présence d'un ion magnésium (Mg^{2+}) bloque leur canal transmembranaire. Lors d'une transmission synaptique à haute fréquence, les récepteurs AMPA/kaïnate sont recrutés en plus grand nombre et le potentiel de membrane se dépolarise. L'ion Mg^{2+} est alors expulsé du canal NMDA, ce qui permet au récepteur de s'activer, laissant maintenant passer les ions Na^+ et calcium (Ca^{2+}).

2.2.2 La potentialisation à long terme

L'entrée massive de calcium dans le neurone post-synaptique est à l'origine du phénomène décrit sous le vocable de potentialisation à long terme (PLT ou LTP, *Long Term Potentiation*). Ainsi, l'activité synaptique brève mais soutenue d'un neurone glutamatergique sur une dendrite peut provoquer un accroissement durable de l'efficacité synaptique de cette synapse. L'étude de la PTL débuta dans les années 1970, avec la découverte qu'une stimulation électrique à haute fréquence de l'hippocampe de lapin pouvait entraîner une augmentation de la transmission synaptique pendant quelques jours, voir des semaines (Bliss et Gardner-Medwin, 1973; Bliss et Lomo, 1973). Depuis, plusieurs mécanismes moléculaires ont été impliqués. Par exemple, l'activation des récepteurs NMDA et l'entrée de Ca^{2+} permettrait l'activation des protéines kinases Ca^{2+}/calmoduline dépendante (CaMK II et IV) et de la *Mitogen-Activated Protein Kinase* (MAPK) (Miyamoto, 2006). L'activation de la protéine kinase C (PKC) a aussi été impliquée dans la PLT (Angenstein et Staak, 1997; Van der Zee et coll., 1997).

L'activation des récepteurs NMDA, AMPA/kaïnate et métabotropes du glutamate semblerait nécessaire pour la formation d'un souvenir durable (Ng et coll., 1997). Plusieurs groupes ont en effet établis un lien entre la PLT et la mémoire, via la plasticité synaptique (Peng et coll., 2011). Ainsi, l'activation des récepteurs métabotropiques mGluR apparaît-elle essentielle pour l'induction et le maintien de la PLT de l'hippocampe à la fois dans des préparations *in vitro* et *in vivo* (Riedel et Reymann, 1996; Gravius et coll., 2010). La régulation du nombre et l'activité des récepteurs AMPA à la synapse glutamatergique sous-tend la PLT (Malinow et Malenka, 2002; Bredt et Nicoll, 2003; Collingridge et coll., 2004). Même si la plupart des études portent sur l'hippocampe, il faut souligner que la PLT est aussi présente dans diverses régions, dont le striatum (Lovinger, 2010). Dans l'amygdale, par exemple, la consolidation des apprentissages avec composantes émotionnelles nécessite la synthèse protéique engendrée par la PLT (Nader et coll., 2000).

2.2.3 Une dysfonction de la transmission glutamatergique : l'excitotoxicité

Étant donné la prédominance du glutamate dans le SNC, il n'est pas étonnant que ce neurotransmetteur soit mis en cause dans plusieurs pathologies. Dans le cadre du présent travail, cependant, nous nous contenterons de mentionner, à titre d'exemple, les accidents vasculaires cérébraux, où de nombreuses données renforcent l'hypothèse de l'excitotoxicité en tant que mécanisme pathophysiologique.

La concentration de glutamate peut être relativement élevée dans la fente synaptique, mais le glutamate est normalement éliminé très rapidement par des transporteurs à haute affinité. Par contre, lorsque les neurones sont fortement stimulés, le glutamate peut s'accumuler dans l'espace extracellulaire et activer de façon excessive ses récepteurs post-synaptiques. Ainsi, la transmission synaptique excitatrice est maintenue sur une longue durée, ce qui peut détruire les neurones par sur-stimulation, un concept nommé excitotoxicité. L'excitotoxicité du glutamate a été découverte par hasard, lorsque du glutamate de sodium a été ajouté à la nourriture de souriceaux entrainant une destruction des neurones de la rétine (Lucas et Newhouse, 1957). Quelques années plus tard, des études ont démontré que cette perte de neurones survenait non seulement dans la rétine, mais aussi dans de nombreuses autres régions du SNC (Olney, 1969, 1971). Lors d'accidents cérébrovasculaires, l'ischémie (arrêt ou diminution de l'apport sanguin) et l'hypoxie (réduction de la disponibilité en oxygène)

diminueraient l'apport d'énergie au SNC, ce qui entraînerait la dépolarisation neuronale et la libération excessive de glutamate. Un cercle vicieux serait ainsi engagé par la dépolarisation soutenue, la libération neuronale de glutamate, l'activation constante des récepteurs glutamatergiques et éventuellement la mort neuronale par excitotoxicité (Dreier, 2011).

2.2.4 Un rôle du glutamate au cours du développement?

Au cours des vingt dernières années, diverses données sont venues appuyer l'hypothèse d'un rôle possible du glutamate, sinon de la transmission glutamatergique, au cours du développement du SNC. Ainsi, des études *in vitro,* en cultures de neurones, ont démontré des effets du glutamate sur la croissance axonale. Tandis qu'une forte concentration de glutamate semble ralentir la croissance axonale dans des cultures de neurones hippocampiques (Mattson et coll., 1988; Brewer et Cotman, 1989; McKinney et coll., 1999), la formation de nouvelles neurites par les neurones embryonnaires spinaux de xénopes *in vivo* dépendrait d'un gradient de concentration croissante du glutamate (Zheng et coll., 1996). La stimulation locale des récepteurs AMPA/kaïnate pré-synaptique contribuerait à la motilité des terminaisons axonales et des cônes de croissance de neurones hippocampiques en culture ou en tranche (Chang et De Camilli, 2001; De Paola et coll., 2003; Tashiro et coll., 2003; Ibarretxe et coll., 2007). Lors de la croissance des axones, le glutamate pourrait être libéré aux site de pause des granules transportant des protéines impliquées dans la transmission synaptique, contribuant ainsi à la formation des complexes de jonction par son action inhibitrice sur la motilité des filopodes dendritiques (Sabo et coll., 2006). Le glutamate pourrait également favoriser la survie neuronale par la production rétrograde et la relâche de facteurs neurotrophiques, tel que le *Brain-Derived Neurotrophic Factor* (BDNF) (Lin et coll., 1993; Ho et coll., 1995; Hartmann et coll., 2001).

2.3 Les transporteurs vésiculaires du glutamate

2.3.1 Le problème de l'identification des neurones glutamatergiques

Contrairement aux neurones DA, les neurones glutamatergiques ne sont pas regroupés en noyaux, mais plutôt dispersés dans la plupart des régions du SNC. Pendant longtemps, la connaissance de ces neurones a reposé sur la mise en évidence de réponses excitatrices rapides détectées en électrophysiologie, ou l'effet de lésions cytotoxiques spécifiques. L'existence de neurones à glutamate locaux et de diverses voies de

projection glutamatergiques ont été ainsi reconnues (Broman et coll., 2003). Par contre, si l'on pouvait supposer que plusieurs populations neuronales utilisaient le glutamate comme neurotransmetteur, l'ubiquité même de leur distribution et les propriétés métaboliques du glutamate compliquaient l'identification spécifique de ces neurones (Fonnum, 1984; Broman et coll., 2003).

Les premiers travaux de visualisation immunocytochimique des neurones glutamatergiques ont eu recours à des anticorps dirigés contre le glutamate lui-même (Storm-Mathisen et coll., 1983; Ottersen et Storm-Mathisen, 1984; Storm-Mathisen et Ottersen, 1990; Sulzer et coll., 1998), ou contre la glutaminase dépendante du phosphate, une enzyme impliquée dans la biosynthèse du glutamate (Kaneko et coll., 1990). Étant donné que le glutamate est un acide aminé qui est présent dans toutes les cellules, il était difficile de distinguer son rôle en tant que métabolite de celui de neurotransmetteur, et risqué d'utiliser de tels anticorps pour identifier les neurones glutamatergiques.

On sait aussi depuis plus de 30 ans que le glutamate est enrichi dans les vésicules synaptiques (Disbrow et coll., 1982; Storm-Mathisen et coll., 1983), mais l'identification et la caractérisation des transporteurs vésiculaires qui y permettent son accumulation a été lente à venir. Nous verrons que grâce à la découverte récente de ces transporteurs (Ni et coll., 1994; Takamori et coll., 2000), le problème de l'identification des neurones glutamatergiques est maintenant essentiellement résolu, de nombreuses données antérieures ont pu être confirmées et nos connaissances du phénotype de ces neurones considérablement enrichies.

2.3.2 Identification et distribution des transporteurs vésiculaires du glutamate

Au départ identifié comme *Brain Na^+-Dependent Inorganic Phosphate Co-transporter* (BNPI) (Ni et coll., 1994), VGLUT1 est présent en grande concentration dans les vésicules synaptiques de neurones déjà connus comme glutamatergiques, de telle sorte qu'il a été renommé transporteur vésiculaire du glutamate (Bellocchio et coll., 1998; Bellocchio et coll., 2000; Takamori et coll., 2000). La distribution de l'expression (ARNm) de *Vglut1* semble cependant confinée à une sous-population de neurones du néocortex, de l'hippocampe et du cortex cérébelleux, si bien que l'absence de VGLUT1 dans les régions sous-corticales laissait supposer l'existence d'un second transporteur vésiculaire du glutamate (Ni et coll., 1995).

Par la suite, plusieurs groupes ont indépendamment identifié VGLUT2, initialement nommé *Differentiation-Associated Na^+-Dependent Inorganic Phosphate Transporter* (DNPI), en raison de son homologie (92%) avec la protéine humaine BNPI/VGLUT1 (Aihara et coll., 2000; Bai et coll., 2001; Fremeau et coll., 2001; Hayashi et coll., 2001; Herzog et coll., 2001; Takamori et coll., 2001; Varoqui et coll., 2002). L'expression de *Vglut2* est fortement enrichie dans les régions sous-corticales, notamment le diencéphale et autres noyaux sous-corticaux, les noyaux cérébelleux profonds et le tronc cérébral (Hisano et coll., 2000; Bai et coll., 2001; Fremeau et coll., 2001; Herzog et coll., 2001) et apparaît donc généralement complémentaire de celle de *Vglut1*.

Finalement, un troisième transporteur, VGLUT3, a été découvert en 2002 (Fremeau et coll., 2002; Gras et coll., 2002; Schafer et coll., 2002; Takamori et coll., 2002). Bien que VGLUT3 partage les mêmes caractéristiques structurales et fonctionnelles que VGLUT1 et VGLUT2, il diffère de ceux-ci par sa distribution en bonne partie restreinte à des populations neuronales n'ayant jamais été auparavant considérées comme glutamatergiques : les neurones à sérotonine du raphé dorsal, les neurones à acétylcholine (ACh) du striatum dorsal et ventral, ainsi qu'une sous-classe d'interneurones GABA du cortex cérébral et de l'hippocampe (Gras et coll., 2002; Schafer et coll., 2002; Herzog et coll., 2004a; Somogyi et coll., 2004). De plus, certains sous-groupes de neurones qu'on pourrait qualifier de principalement glutamatergiques expriment aussi *Vglut3* (et/ou contiennent la protéine), notamment dans le raphé, l'habenula, l'hypothalamus, les tubercules olfactifs et la cochlée (cellules ciliées internes) (Gras et coll., 2002; Herzog et coll., 2004a; Ruel et coll., 2008; Seal et coll., 2008; Commons, 2009; Jackson et coll., 2009).

Il est à noter que la surexpression de *Vglut1* dans des lignées cellulaires ou des cultures de neurones GABAergiques permet à ces cellules de libérer le glutamate, ce qui démontre bien que la présence du transporteur est nécessaire et suffisante pour que le glutamate soit accumulé dans les vésicules synaptiques et subséquemment libéré (Bellocchio et coll., 2000; Takamori et coll., 2000). De plus, les propriétés physiologiques des trois VGLUT correspondent à celles précédemment attribuées au premier transport vésiculaire du glutamate, soit : 1) une affinité pour le glutamate de l'ordre du millimolaire, 2) l'incapacité de reconnaître et transporter l'aspartate, la glutamine ou le GABA, 3) une dépendance au gradient de protons, 4) une dépendance à

la composante ΔΨ du gradient de pH (et non au ΔpH), et finalement 5) une dépendance biphasique au chlorure (Disbrow et coll., 1982; Naito et Ueda, 1985).

Dans ces conditions, on peut en conclure que la visualisation d'un transporteur vésiculaire du glutamate dans un neurone permet l'identification formelle de ce neurone comme glutamatergique, c'est-à-dire comme neurone utilisant le glutamate comme neurotransmetteur.

2.3.3 Les transporteurs vésiculaires du glutamate au cours du développement

Alors que *Vglut1* semble peu exprimé lors du développement prénatal du rat et de la souris, son expression augmente graduellement après la naissance pour éventuellement prédominer sur celle des deux autres transporteurs (Boulland et coll., 2004; Nakamura et coll., 2005). À l'inverse, l'expression de *Vglut2* est forte à la naissance (Boulland et coll., 2004), mais diminue avec l'âge, alors que l'expression de *Vglut3* augmente au cours du développement post-natal (Boulland et coll., 2004; Nakamura et coll., 2005). Dans certaines populations neuronales, il semble y avoir coexistence transitoire de *Vglut1* et *Vglut2* dans les mêmes terminaisons axonales lors du développement post-natal (Hioki et coll., 2003; Boulland et coll., 2004; Fremeau et coll., 2004; Wojcik et coll., 2004; Nakamura et coll., 2005).

2.3.4 L'invalidation génique des transporteurs vésiculaires du glutamate

La découverte des trois transporteurs vésiculaires du glutamate a non seulement permis l'identification formelle des neurones glutamatergiques dans le SNC, mais aussi d'étudier les conséquences de l'absence de chacun de ces transporteurs chez des souris dont le gène correspondant avait été invalidé dès la conception (knockout, KO). L'invalidation de *Vglut1* n'est pas fatale à la naissance, mais seulement après la période de sevrage (Fremeau et coll., 2004; Wojcik et coll., 2004). Comme nous l'avons déjà dit, la quantité d'ARNm de *Vglut1* est faible à la naissance et augmente par la suite, pour atteindre un plateau à 2 semaines de vie chez la souris (Boulland et coll., 2004). Par contre, dans le cas de *Vglut2,* dont l'expression est forte au cours du développement embryonnaire et de la période post-natale avant de diminuer par la suite (Boulland et coll., 2004; Nakamura et coll., 2005), les souris KO meurent à la naissance, en raison d'une incapacité respiratoire (Moechars et coll., 2006; Wallén-Mackenzie et coll., 2006). Les souris dont le gène *Vglut3* est invalidé ne présentent pas de dysfonctions motrices majeures (Gras et coll., 2008; Seal et coll., 2008), mais elles sont profondément sourdes

(Ruel et coll., 2008; Seal et coll., 2008) et sujettes à des crises d'épilepsies (Seal et coll., 2008).

3 Co-transmission glutamatergique

Dale avait postulé, en 1935, que les neurones fonctionnent comme une entité unique, et donc que tous les compartiments de la cellule ne formaient qu'un seul tout (Strata et Harvey, 1999). Ce principe qui porte son nom, a été reformulé par la suite pour signifier que les neurones ne synthétisent et libèrent qu'un même neurotransmetteur par toutes leurs terminaisons axonales. De nos jours, il semblerait que ce principe soit devenu l'exception plutôt que la règle, compte-tenu de l'identification d'innombrables peptides, mais aussi de plusieurs transmetteurs classiques comme co-transmetteurs. De nombreuses données permettent en effet d'affirmer que la co-localisation des transmetteurs est un phénomène extrêmement répandu dans le SNC (revu en autre par Trudeau, 2004; Gundersen, 2008; El Mestikawy et coll., 2011).

3.1 Co-expression et co-localisation des VGLUT dans le SNC

La disponibilité de marqueurs spécifiques des neurones qui utilisent le glutamate comme neurotransmetteur a permis d'approfondir l'étude et la signification du phénomène de co-localisation/co-transmission dans le cas de plusieurs espèces de neurones déjà caractérisés par un autre transmetteur primaire (voir El Mestikawy et coll., 2011). Ainsi, il est désormais établi que certains neurones à acétylcholine (ACh) ou GABA contiennent aussi VGLUT1, que VGLUT2 se retrouve dans les neurones à dopamine, noradrénaline ou adrénaline, et que VGLUT3 est présent dans de nombreux neurones à sérotonine (voir Tableau 3). Voyons brièvement où se situent ces divers co-phénotypes, à l'exclusion de VGLUT2 dans les neurones DA, la thématique centrale du présent ouvrage, que nous aborderons séparément plus loin (section 3.4).

L'ARNm de *Vglut1* et *Vglut2* sont tous deux retrouvés dans certains neurones ACh de la moelle épinière (Herzog et coll., 2004b; Nishimaru et coll., 2005). Certains neurones ACh de la partie basolatérale du complexe amygdalien expriment *Vglut3* (Nickerson Poulin et coll., 2006), ainsi que tous les interneurones ACh du striatum dorsal et ventral (Gras et coll., 2002; Schafer et coll., 2002). Les corps cellulaires et dendrites proximales (Fremeau et coll., 2002; Boulland et coll., 2004) de ces interneurones contiennent la protéine VGLUT3, de même que la majorité de leurs

terminaisons axonales (Gras et coll., 2002; Schafer et coll., 2002; Boulland et coll., 2004).

La plupart des neurones à sérotonine (5-HT) du raphé médian et dorsal expriment aussi l'ARNm de *Vglut3* (Schafer et coll., 2002; Hioki et coll., 2010), alors que la protéine est aussi présente, mais peu abondante, dans les corps cellulaires et dendrites de ces neurones. Si l'on en juge par les données d'immunofluorecence actuellement disponibles, il semblerait qu'une proportion relativement faible des terminaisons axonales issues de ces neurones 5-HT contiendrait aussi VGLUT3, particulièrement dans le cortex cérébral (Hioki et coll., 2004; Shutoh et coll., 2008; Amilhon et coll., 2010) et l'hippocampe (Schafer et coll., 2002; Shutoh et coll., 2008; Varga et coll., 2009; Amilhon et coll., 2010). Tout se passe comme si la 5-HT (et/ou son transporteur membranaire), ainsi que VGLUT3, pouvaient faire l'objet de ségrégation dans des terminaisons axonales différentes d'un même neurone. Ainsi, un même neurone 5-HT pourrait établir trois types de terminaisons : certaines purement glutamatergiques ou sérotoninergiques, et d'autres qui libéreraient les deux transmetteurs. Un même neurone pourrait ainsi transmettre à la fois un signal rapide excitateur et un autre plus lent (Lavin et coll., 2005). En accord avec cette hypothèse, une étude optogénétique récente a montré que la stimulation d'un neurone 5-HT du raphé peut déclencher une réponse rapide, médiée par les récepteurs AMPA de neurones GABAergiques de l'hippocampe, et une réponse plus lente médiée par un des récepteurs 5-HT (Varga et coll., 2009).

Il faut également souligner qu'un neurotransmetteur excitateur comme le glutamate co-existe dans certaines terminaisons axonales de neurones reconnus comme GABAergiques. Ainsi, VGLUT3 se retrouve dans des terminaisons par ailleurs identifiées comme GABAergiques au cours du développement du cortex cérébral et de l'hippocampe (Boulland et coll., 2004), et, à l'âge adulte, les trois transporteurs, VGLUT1, VGLUT2 ou VGLUT3 ont été identifiés dans des terminaisons axonales GABAergiques de ces régions (Herzog et coll., 2004a; Hioki et coll., 2004; Boulland et coll., 2009; Fattorini et coll., 2009; Soussi et coll., 2010; Zander et coll., 2010). De même, au cours du développement post-natal, l'ARNm de *Vglut3* est exprimé par les cellules de Purkinje et la protéine est présente dans des terminaisons axonales autour de ces cellules (Gras et coll., 2005).

3.2 Le concept de synergie vésiculaire

La présence du glutamate dans les terminaisons axonales de neurones définis par un autre neurotransmetteur laisse présager qu'un potentiel d'action puisse entrainer la libération des deux neurotransmetteurs, indépendamment ou conjointement. Mais la question se pose à savoir quel pourrait être le rôle du transporteur vésiculaire du glutamate, s'il se retrouve sur les mêmes vésicules synaptiques munies du transporteur vésiculaire de l'autre transmetteur, par exemple, le transporteur vésiculaire de l'ACh, VAChT, ou celui des monoamines, VMAT2.

Tel qu'illustré dans l'article récent de El Mestikawy et coll. (2011), le transport des neurotransmetteurs à l'intérieur des vésicules synaptiques est dépendant d'un gradient électrochimique établi par un transporteur ATPase (Maycox et coll., 1988). Par exemple, le transport de l'ACh ou des monoamines par leurs transporteurs vésiculaires respectifs dépend du gradient de pH (ΔpH). À l'inverse, le transport vésiculaire du glutamate repose sur le potentiel transmembranaire vésiculaire (ΔΨ) (Edwards, 2007). Le transport d'un neurotransmetteur à cations, tel l'ACh ou les monoamines, requiert la sortie de deux ions H^+, exerçant une forte demande sur le gradient ΔpH. Il a été proposé que la présence d'un VGLUT acidifierait les vésicules et permettrait une accumulation plus grande de l'autre neurotransmetteur, par exemple l'ACh, d'où une concentration plus forte de celui-ci dans la vésicule, et sa libération en plus forte concentration lors de l'exocytose. Ce concept a été nommé synergie vésiculaire (Gras et coll., 2008), et nous verrons plus loin qu'il pourrait trouver aussi à s'appliquer dans le cas des neurones à DA ayant fait l'objet de nos travaux (section 3.4.3).

3.3 Pathophysiologie

L'étude de l'implication du système glutamatergique dans diverses pathologies, tel que l'excitotoxicité (voir section 2.2.3), a connu des développements intéressants avec la découverte des VGLUT. Ainsi, une forme de surdité a pu être attribuée à la dysfonction du gène qui encode la protéine VGLUT3 chez l'humain (Ruel et coll., 2008). Nous avons vu que *Vglut3* est présent dans les cellules sensorielles ciliées internes de l'oreille et que son invalidation chez la souris entraine la surdité (Seal et coll., 2008). L'étude de l'expression des divers *Vglut* dans le cerveau post-mortem de patients parkinsoniens a permis d'y constater une augmentation des ARNm de *Vglut1* et *Vglut2*, de 24 et 29% respectivement, au sein du putamen (Kashani et coll., 2007). Par

ailleurs, en raison d'une diminution drastique de l'expression de *Vglut1* et *Vglut2* dans les cerveaux de patients souffrant de la maladie d'Alzheimer, et d'une corrélation hautement significative entre le degré de déficience cognitive et la réduction de *Vglut1* (Kashani et coll., 2008), l'expression de *Vglut1* dans le cortex préfrontal pourrait devenir un marqueur neurochimique précoce de cette maladie.

3.3.1 Le co-phénotype glutamatergique des neurones à dopamine

Les premiers travaux liant les monoamines (dont la DA) et le glutamate ont été ceux de Ottersen et Storm-Mathisen (1984). En raison d'une distribution régionale comparable après marquage immunocytochimique du glutamate ou de son enzyme de synthèse, ces auteurs ont suggéré que certains neurones à monoamine du mésencéphale et du tronc cérébral soient aussi glutamatergiques, tant chez le rat que la souris. Des travaux plus poussés en microscopie électronique chez le rat, ont confirmé que des neurones à monoamine exprimaient l'enzyme de synthèse du glutamate chez le rat adulte (Kaneko et coll., 1990). Une étude subséquente a montré que la plupart des neurones à dopamine (DA) du mésencéphale ventral pouvaient être immunomarqués pour le glutamate, tant chez le singe que chez le rat (Sulzer et coll., 1998). Dans le striatum, les terminaisons axonales marquées pour la tyrosine hydroxylase (TH, enzyme de synthèse de la dopamine) présentaient des jonctions synaptiques symétriques, alors que celles qui contenaient des vésicules marquées pour le glutamate formaient des jonctions synaptiques asymétriques (Sulzer et coll., 1998). Peu après l'identification de VGLUT2, un examen approfondi du tronc cérébral a révélé que son ARNm était présent dans la majorité des neurones à noradrénaline du groupe A2 (Stornetta et coll., 2002a) et la plupart des neurones adrénergique des groupes C1, C2 et C3 (Stornetta et coll., 2002b), laissant présager une co-transmission glutamatergique par ces neurones à monoamine.

	ARNm	Protéine	
		Corps cellulaire	Terminaisons
***Vglut1* ou VGLUT1**			
Acétylcholine	motoneurones spinaux [13]		n. interpedunculaire [25]
GABA		rétine [17]	cortex cérébral [7]
			cervelet [34]
			hippocampe [34]
			rétine [17]
***Vglut2* ou VGLUT2**			
Noradrénaline	A1, A2 [30]		
	area postrema [30]		
Adrénaline	C1 [30,31]		
	C2, C3 [30]		
Dopamine	A9, A10 [5,18,19,33]		n. accumbens [5,6]
	A11 [18]		néostriatum [5,6]
Acétylcholine	motoneurones spinaux [13,22]		moelle épinière [22]
GABA	nPAV [24]		APOR [24]
			hippocampe [2,29,34]
***Vglut3* ou VGLUT3**			
Sérotonine	NRD, NRM [15,26]	NRD [1,4,10,16,20,27]	amygdale [27]
		NRM [1,10,16,20,27]	ATV [35]
			bulbe olfactif [27]
			cortex cérébral [1,14,27]
			hippocampe [1,27,28,32]
			moelle épinière (CIM) [23]
			plexus supra-épendymaire [1]
Acétylcholine	prosencéphale basal [21]	prosencéphale basal [21]	amygdale [21]
	striatum [10,26]	striatum [3,8]	striatum [3,10,26]
GABA	hippocampe [13]	cortex cérébral [14]	cortex cérébral [14]
		cellules de Purkinje [11]	cellules de Purkinje [11]
		hippocampe [8,28]	hippocampe [3,12]
		n. corps trapézoïde [9]	olive supérieure [9]

Tableau 3 – Colocalisation d'un VGLUT dans les neurones « non glutamatergiques » du système nerveux central. Par neurones « non glutamatergiques », on entend ici que ces neurones ont été précédemment définis par leur contenu en transmetteur autre que le glutamate. La présence de glutamate comme co-transmetteur dans ces neurones est suggérée par leur contenu en transporteur vésiculaire du glutamate, tel que révélé par double marquage d'un l'ARNm *Vglut* (hybridation *in situ*) ou de la protéine VGLUT (immunocytochimie). Abbréviations : nPAV, noyau périventriculaire antéro-ventral; NRD, noyau du raphé dorsal; CIM, corne intermedio-latérale; NRM, noyau du raphé médian; APOR, aire pré-optique rostrale; ATV, aire tegmentaire ventrale. Données obtenues majoritairement chez le rat et la souris. Modifié de El Mestikawy et coll. (2011).

Bibliographie du tableau : 1, Amilhon et coll. (2010); 2, Boulland et coll. (2009); 3, Boulland et coll. (2004); 4, Commons (2009); 5, Dal Bo et coll. (2008a); 6, Descarries et coll. (2008); 7, Fattorini et coll. (2009); 8, Fremeau et coll. (2002); 9, Gillespie et coll. (2005); 10, Gras et coll. (2002); 11, Gras et coll. (2005); 12, Herzog et coll. (2004a); 13, Hezog et coll. (2004b); 14, Hioki et coll. (2004); 15, Hioki et coll. (2010); 16, Jackson et coll. (2009); 17, Kao et coll. (2004); 18, Kawano et coll. (2006); 19, Mendez et coll. (2008); 20, Mintz et Scott (2006); 21, Nickerson Poulin et coll. (2006); 22, Nishimaru et coll. (2005); 23, Oliveira et coll. (2003); 24, Ottem et coll. (2004); 25, Ren et coll. (2011); 26, Schafer et coll. (2002); 27, Shutoh et coll. (2008); 28, Somogyi et coll. (2004); 29, Soussi et coll. (2010); 30, Stornetta et coll. (2002a); 31, Stornetta et coll. (2002b); 32, Varga et coll. (2009); 33, Yamaguchi et coll. (2007); 34, Zander et coll. (2010); 35, Zhang et Morales (2010).

3.3.2 Études *in vitro*

En 1996, Plenz et Kitai ont rapporté que la stimulation du mésencéphale dans des cultures organotypiques de cortex, striatum et mésencéphale entraînait une réponse excitatrice rapide dans les neurones épineux moyens du striatum (Plenz et Kitai, 1996). Cette réponse pouvait être glutamatergique, du fait qu'il a été ensuite montré que les terminaisons de neurones dopaminergiques en co-culture et microculture co-libéraient du glutamate en plus de la DA (Sulzer et coll., 1998; Bourque et Trudeau, 2000), tout comme les terminaisons établies sur des neurones du noyau accumbens par des neurones DA en culture (Joyce et Rayport, 2000).

La première démonstration cytochimique de la présence de VGLUT2 dans les neurones DA est venue de travaux combinant l'immunocytochimie de la TH et de VGLUT2, ainsi que la RT-PCR, sur des cellules isolées de cerveau de rat en microculture (Dal Bo et coll., 2004). En effet, 80% des neurones DA en microculture, c'est-à-dire établissant leurs terminaisons axonales sur eux-mêmes (autapses), étaient à la fois immunopositifs pour la TH et pour VGLUT2. Fait intéressant, dans ces conditions, la plupart des varicosités qui étaient immunopositives pour VGLUT2 l'étaient aussi pour la TH. Néanmoins, plusieurs neurones avaient des arborisations axonales TH immunopositives dépourvues de VGLUT2, identifiée comme terminaisons axonales par des triples marquages avec SV2, une protéine associée aux vésicules synaptiques. Ces résultats sont compatibles avec l'hypothèse voulant que les neurones DA puissent établir divers types varicosités, dont certaines capables de co-libérer le glutamate (Sulzer et coll., 1998).

3.3.3 Études *in vivo*

Également à l'appui d'une transmission glutamatergique par les neurones DA, il a été montré que la stimulation électrique de la substance noire (SNc) évoque des potentiels post-synaptiques excitateurs dans les neurones épineux de taille moyenne du néostriatum (Kitai et coll., 1976). Plus récemment, plusieurs auteurs ont constaté que la stimulation de neurones DA présumés pouvait générer des potentiels post-synaptiques glutamatergiques, tant dans des tranches de cerveaux de souris que chez le rat anesthésié (Chuhma et coll., 2004; Lavin et coll., 2005; Chuhma et coll., 2009).

Des travaux subséquents ont démontré que, chez le rat, l'ARNm de *Vglut2* est présent dans les régions des corps cellulaires dopaminergiques dès la naissance (P0), mais diminue à l'âge adulte (Dal Bo et coll., 2008a). Au cours de cette même étude, nous avons démontré après double marquage immunocytochimique pour la microscopie électronique qu'une proportion significative (28%) des terminaisons axonales du noyau accumbens (cœur) du raton de 15 jours contenait les deux marqueurs, TH et VGLUT2. De plus, il s'est avéré que l'injection préalable de la toxine 6-hydroxydopamine (6-OHDA) dans les jours suivant la naissance entrainait une régulation à la haute de l'expression de *Vglut2* dans les corps cellulaires des neurones DA résiduels, ainsi qu'une augmentation significative (37%) de la proportion des terminaisons axonales doublement marquées à P15 dans le noyau accumbens (voir Annexe 2). Enfin, les varicosités axonales contenant à la fois TH et VGLUT2 sont toutes apparues munies de complexes de jonction membranaire synaptique, contrairement à celles qui étaient marquées pour la TH seulement, ou pour VGLUT2 seulement chez le raton de cet âge. Une autre étude du même laboratoire, réalisée la même année, a aussi montré, à la fois en culture et *in vivo*, que le contact avec les neurones GABA réduisait l'expression de *Vglut2* par les neurones DA (Mendez et coll., 2008). À l'inverse, la proportion de neurones DA qui expriment *Vglut2* se trouvait augmentée par suite de lésion de l'innervation GABAergique à la substance noire.

D'importantes différences sont rapportées quant à la proportion des neurones DA du mésencéphale qui exprime *Vglut2*. Kawano et coll. (2006) ont trouvé que 19% des neurones de l'aire tegmentaire ventrale (ATV) immunomarqués pour la TH exprimaient *Vglut2* (Kawano et coll., 2006) alors que Yamagushi et coll., 2007) affirment que 0.1% de ces mêmes neurones DA expriment à la fois l'ARNm de *TH* et celui de *Vglut2,* tel que démontré après double hybridation *in situ* (Yamaguchi et coll., 2007). L'écart entre les deux études reflète probablement une différence de sensibilité méthodologique, la combinaison de l'immunocytochimie et de l'hybridation apparaissant la plus sensible.

Soulignons enfin que, dans des tranches de cerveau de souris adulte (30 jours), l'activation sélective des neurones DA du mésencéphale par optogénétique génère

des événements synaptiques glutamatergiques dans la coquille du noyau accumbens, mais non au cœur de ce noyau ou dans le striatum dorsal (néostriatum) (Stuber et coll., 2010; Tecuapetla et coll., 2010), suggérant aussi qu'une sous-population des neurones DA du mésencéphale ventral puisse libérer le glutamate.

3.3.4 Les knockout conditionnels et le rôle présumé du glutamate dans les neurones à dopamine

Nous avons vu plus haut que la présence de glutamate dans les neurones DA du mésencéphale au cours du développement suggère un rôle de cette cotransmission au cours de la croissance de l'arborisation axonale de ces neurones et de leur synaptogénèse. Il a été proposé également que le concept de synergie vésiculaire, précédemment évoqué (section 3.1.3) pour expliquer l'accumulation accrue d'ACh dans les vésicules synaptiques qui possèdent à la fois VAChT et VGLUT3, s'applique aussi à l'accumulation de monoamines par les vésicules synaptiques contenant VMAT2 et VGLUT2 (Hnasko et coll., 2010).

Des travaux récents chez la souris dont le gène *Vglut2* est sélectivement invalidé dans les neurones DA favorisent plutôt la première hypothèse (Fortin et coll.). En culture de neurones DA du mésencéphale provenant de ces souris, une diminution de la croissance et de la survie neuronale est observée. *In vivo*, on constate une réduction du nombre des neurones DA dans le mésencéphale, de même que de la densité d'innervation DA et de la libération de DA dans le noyau accumbens. Reste à savoir comment ces défauts du système DA méso-striatal pourraient être responsables du phénotype comportemental anormal documenté chez ces souris et qui inclut une réduction considérable de la réponse locomotrice à l'amphétamine (Birgner et coll., 2010), une augmentation de l'auto-administration de sucrose et de cocaïne ainsi que de la prise de cocaïne induite par une stimulation pairée (Alsiö et coll., 2011), et divers déficits lors d'épreuves de motricité et du test de la nage forcée (Fortin et coll., soumis).

4 Objectifs généraux de l'étude

Même si, au cours des 10 dernières années, plusieurs études ont montré que les neurones DA du SNC peuvent utiliser le glutamate comme co-transmetteur chimique, la démonstration de la présence du transporteur vésiculaire du glutamate, VGLUT2 dans les terminaisons axonales dopaminergiques restait à venir. Le sujet était d'autant plus intéressant que l'innervation DA du striatum est connue pour être faiblement synaptique, alors que ce type de communication interneuronale est une caractéristique fondamentale de la transmission glutamatergique. Il apparaissait donc nécessaire de réexaminer l'organisation du système dopaminergique meso-striatal dans le contexte nouveau des études de co-localisation et de co-transmission DA-glutamate en cours, tant chez le rat que la souris, ainsi qu'en conditions normales et pathologiques.

4.1 Co-localisation TH/VGLUT2 chez le rat

Dans un premier temps, nous avons cherché à mettre en évidence la présence de VGLUT2 dans les terminaisons axonales à DA du striatum chez le rat. À cette fin, nous avons entrepris de conjuguer l'immunocytochimie de la TH à celle du VGLUT2, en microscopie photonique et surtout électronique. Au cours de cette étude, nous avons aussi voulu examiner l'hypothèse d'une plasticité développementale du double phénotype DA-glutamate, par comparaison de données obtenues chez le raton âgé de 15 jours (P15) et chez le rat adulte (P90). De plus, nous avons considéré la possibilité d'une plasticité post-lésionnelle de ce double phénotype, à la suite d'une destruction partielle du système DA par la cytotoxine 6-OHDA administrée peu après la naissance.

Après avoir étudié la distribution de l'ARNm de la *TH* et *Vglut2* dans la SNc et l'ATV par double hybridation *in situ* chez des rats P15 et P90 lésés ou non avec la 6-OHDA, nous avons entrepris une série d'expériences visant à caractériser le double phénotype des terminaisons axonales DA, par suite de simple marquage immunocytochimique pour la microscopie optique (TH) et double marquage (TH/VGLUT2) pour la microscopie électronique. Nous avons ainsi examiné le cœur du noyau accumbens aux deux âges et chez le rat normal et le rat lésé; le néostriatum chez le rat P15 et le rat adulte normaux, ainsi que la néoinnervation DA de la SNc

chez le rat P15 et le rat adulte lésés. La distribution des marquages (TH seul, VGLUT2 seul et TH/VGLUT2) a été quantifiée en microscopie électronique, de même que les caractéristiques morphologiques respectives des terminaisons axonales de chaque catégorie, incluant la fréquence synaptique.

4.2 L'innervation à dopamine du striatum chez la souris

Étant donné l'utilisation croissante de la souris, génétiquement modifiée ou non, pour l'étude du système dopaminergique, et tenant compte des données sur la co-localisation DA-glutamate dans les neurones DA méso-striataux du rat, nous avons ensuite entrepris une vaste analyse ultrastructurale de l'innervation DA du striatum ventral (NAC et NAS) et dorsal (NS), chez cette espèce, incluant deux modèles de souris dont le gène de VGLUT2 avait été sélectivement invalidé dans les neurones DA du mésencéphale (KO conditionnel). Cette stratégie visait à tester l'hypothèse voulant que la présence de glutamate dans les terminaisons DA contribue à l'établissement et au maintien de jonctions synaptiques par ces terminaisons axonales. Les données de microscopie électronique ont été principalement obtenues après marquage simple avec un anticorps primaire dirigé contre la TH, ainsi qu'après double marquage TH/VGLUT2. De nouveau, des animaux de 15 jours ou adultes (P70-90) ont été examinées, de manière à détecter tout changement phénotypique associé à la maturation.

Chapitre 2 – Premier article

The Dual Dopamine-Glutamate Phenotype of Growing Mesencephalic Neurons Regresses in Mature Rat Brain

Publié en 2009
dans:

The Journal of Comparative Neurology
517 : 873-891

Noémie Bérubé-Carrière, Mustapha Riad, Grégory Dal Bo,
Daniel Lévesque, Louis-Éric Trudeau, Laurent Descarries

L'article qui suit est le résultat d'expériences accomplies durant la première partie de mon doctorat. En tant qu'auteur principal, j'ai personnellement effectué tous les marquages immunocytochimiques sur les rats juvéniles et adultes, préparé le matériel, et recueilli et analysé les résultats de microscopie électronique. Avec l'aide d'un étudiant du laboratoire Trudeau, Grégory Dal Bo, j'ai réalisé les lésions à la 6-OHDA. Cet étudiant a effectué l'hybridation *in situ* des ARNm de *TH* et *Vglut2*, ainsi que leur visualisation et analyse. Les Drs Descarries, Trudeau et Riad ont conjointement supervisé mes travaux, de même que la rédaction de l'article.

THE DUAL DOPAMINE-GLUTAMATE PHENOTYPE OF GROWING MESENCEPHALIC NEURONS REGRESSES IN MATURE RAT BRAIN

Noémie BÉRUBÉ-CARRIÈRE [1], Mustapha RIAD [1], Grégory DAL BO [2],
Daniel LÉVESQUE [4], Louis-Eric TRUDEAU [2,5], and Laurent DESCARRIES [1,3,5]

Departments of [1] Pathology and Cell Biology, [2] Pharmacology, and [3] Physiology,
Faculty of Medicine; [4] Faculty of Pharmacy;
[5] Groupe de Recherche sur le Système Nerveux Central;
Université de Montréal, Montréal, QC, Canada

Running title: **Dual TH/VGLUT2 phenotype**

Corresponding author: Laurent Descarries m.d. [1]

Abbreviations: 6-OHDA, 6-hydroxydopamine; DA, dopamine; DAB, 3,3'-diaminobenzidine tetrahydrochloride; i.c.v., intra-cerebroventricular; nAcb, nucleus accumbens; NStr, neostriatum; SN, substantia nigra; SNc, substantia nigra, pars compacta; TH, tyrosine hydroxylase; VGLUT2, vesicular glutamate transporter 2; VTA, ventral tegmental area.

[1] This work was funded in part by CIHR grants MOP-3544 to L.D. and MOP-49951 to L.-É. T, and a grant from NARSAD to L.-É. T. It was also supported by an infrastructure grant from the FRSQ to the GRSNC (Groupe de Recherche sur le Système Nerveux Central).

ABSTRACT

Co-expression of tyrosine hydroxylase (TH) and the vesicular glutamate transporter 2 (VGLUT2) mRNAs in the ventral tegmental area (VTA), and colocalization of these proteins in axon terminals of the nucleus accumbens (nAcb) have been recently demonstrated in immature (15 day-old) rat. After neonatal 6-hydroxydopamine (6-OHDA) lesion, the proportion of VTA neurons expressing both mRNAs, and of nAcb terminals displaying the two proteins was enhanced. To determine the fate of this dual phenotype in adults, double *in situ* hybridization and dual immunolabeling for TH and VGLUT2 were performed in 90 day-old rats subjected or not to the neonatal 6-OHDA lesion. Very few neurons expressed both mRNAs in the VTA and substantia nigra (SN) of P90 rats, even after neonatal 6-OHDA. Dually immunolabeled terminals were no longer found in the nAcb of normal P90 rats, and exceedingly rare in the nAcb of 6-OHDA-lesioned rats, whereas they had represented 28% and 37% of all TH terminals at P15. Similarly, 17% of all TH terminals in normal neostriatum, and 46% in the dopamine neoinnervation of SN in 6-OHDA-lesioned rats, were also immunoreactive for VGLUT2 at P15, but none at P90. In these three regions, all dually labeled terminals made synapse, in contradistinction with those immunolabeled for only TH or VGLUT2 at P15. These results suggest a regression of the VGLUT2 phenotype of dopamine neurons with age, following normal development, lesion or sprouting after injury, and a role for glutamate in the establishment of synapses by these neurons.

Keywords (not in title): neoinnervation, neostriatum, nucleus accumbens, substantia nigra, tyrosine hydroxylase, ventral tegmental area, vesicular glutamate transporter 2

INTRODUCTION

Since the first demonstration that a an inorganic phosphate carrier was able to concentrate glutamate in synaptic vesicles (Ni et coll., 1994), three proteins capable of playing that role have been identified in mammalian central nervous system, and were therefore given the name of vesicular glutamate transporter 1, 2 and 3 (VGLUT1-3) (reviewed in Fremeau et coll., 2004; Liguz-Lecznar and Skangiel-Kramska, 2007; Trudeau, 2004). In adult rat brain, the expression patterns of VGLUT1 and VGLUT2 are largely complementary, VGLUT1 mRNA being widely found in pyramidal neurons of the neocortex and hippocampus, and in cerebellar cortex, whereas VGLUT2 mRNA predominates in diencephalic and other subcortical nuclei, deep cerebellar nuclei and the brainstem (Bai et coll., 2001; Fremeau et coll., 2001; Herzog et coll., 2001; Ni et coll., 1995). A third vesicular glutamate transporter has also been cloned, which shows a more restricted expression by neurons not classically considered to be glutamatergic, and notably serotonin neurons of the midbrain raphe and cholinergic neurons of the striatum and forebrain (Boulland et coll., 2004; Gras et coll., 2008; Gras et coll., 2002; Harkany et coll., 2003; Schafer et coll., 2002; Takamori et coll., 2002). There is also considerable *in situ* hybridization and immunocytochemical evidence for a colocalization of VGLUT2 in catecholaminergic neurons, notably in noradrenaline neurons of the A2 group and adrenaline neurons of the C1, C2 and C3 groups of the medulla (Stornetta et coll., 2002), and dopamine (DA) neurons of the mesencephalic groups A9 and A10 (Kawano et coll., 2006; Yamaguchi et coll., 2007).

Early evidence for the release of glutamate by mesencephalic DA neurons was obtained *in vitro*, in microcultures of isolated VTA neurons (Bourque and Trudeau, 2000; Sulzer et coll., 1998) and co-cultures of VTA DA neurons with GABAergic medium spiny neurons of the nucleus accumbens (nAcb) (Joyce and Rayport, 2000). In a subsequent study in primary cultures of postnatal rat mesencephalic neurons, as many as 80% of isolated neurons immunopositive for tyrosine hydroxylase (TH), the biosynthetic enzyme of DA, were shown to be VGLUT2 immunopositive (Dal Bo et coll., 2004). Different percentages were more recently reported in adult rat, in which 19% of TH immunopositive neurons of the VTA were shown to express VGLUT2

mRNA (Kawano et coll., 2006), and 0.1% of neurons to express both TH and VGLUT2 mRNA by double *in situ* hybridization (Yamaguchi et coll., 2007). The discrepancy between the latter proportions probably reflected differences in experimental approach, but the large difference between *in vitro* and *in vivo* data was suggestive of a regulation of VGLUT2 expression in DA neurons during development and/or in response to injury.

In a recent study in late embryonic and postnatal rat, evidence was indeed obtained suggesting that the dual TH/VGLUT2 phenotype of mesencephalic DA neurons innervating the nAcb of rat was repressed at late embryonic stages and could be reactivated after neonatal 6-hydroxydopamine (6-OHDA) lesioning of these neurons (Dal Bo et coll., 2008). In tissue sections of embryonic mesencephalon processed for dual *in situ* hybridization, there was a striking overlap between the labeling for TH and VGLUT2 mRNA at embryonic stages E14-E16, which was no longer found at stages E18-E21 and postnatally. Moreover, whereas only 1.8% of VTA neurons exhibiting TH mRNA signal were also labeled for VGLUT2 mRNA in normal 15-day-old rats (P15), this proportion increased to 26% of the surviving DA neurons in VTA after neonatal lesioning by cerebroventricular injection of 6-OHDA at P4. Lastly, electron microscopic examination of the nAcb after dual immunolabeling for TH and VGLUT2 demonstrated the presence of VGLUT2 protein in 28% of TH axon terminals in normal P15 rats, and in an even greater proportion (37%) of residual TH terminals in P15 rats 6-OHDA-lesioned at P4.

The general goal of the present study was to determine the fate of this dual dopamine/glutamate (TH/VGLUT2) phenotype with maturation of the brain. In particular, an answer was sought to the following questions. What is the proportion of DA neurons in normal adult rat VTA that co-express TH/VGLUT2 mRNA, and the frequency of colocalization of the two proteins in their DA axon terminals in nAcb? Does the reactivation of this double phenotype observed at P15 in rats neonatally lesioned with 6-OHDA persist in the adult? Are there TH immunoreactive axon terminals colocalizing VGLUT2 in immature or mature rat neostriatum (NStr)? Does the aberrant DA neoinnervation which pervades the remnants of SN after a neonatal 6-OHDA lesion (Fernandes Xavier et coll., 1994) display the dual TH/VGLUT2

phenotype? Are there morphological correlates, particularly in terms of synaptic features, of the existence of VGLUT2 in DA axon under these various conditions?

To answer these questions, double *in situ* hybridization for TH and VGLUT2 mRNA, as well as dual immunolabeling of the two proteins at electron microscopic level were used in adult (P90) as well as immature (P15) rats subjected or not to the neonatal cerebroventricular administration of 6-OHDA at P4. As in our prior studies (Dal Bo et coll., 2008; Descarries et coll., 2008), we focused on the nAcb, in which axon terminals from surviving DA neurons of the VTA are still found after the neonatal

6-OHDA lesion. We also examined DA terminals in the NStr of normal rats, as well as the DA neoinnervation of the SN after neonatal 6-OHDA lesion. In all instances, quantitative data was obtained on the number of terminals singly (TH and VGLUT2) and dually (TH/VGLUT2) labeled in an equivalent area of thin section examined in each rat, as well as on their intrinsic and synaptic features. Some of the results obtained in immature rat have already been published (Dal Bo et coll., 2008; Descarries et coll., 2008), but are included in the Tables to facilitate comparison with the adult.

MATERIALS AND METHODS

Animals

All procedures involving animals and their care were conducted in strict accordance with the Guide to the Care and Use of Experimental Animals (Ed2) of the Canadian Council on Animal Care. The experimental protocols were approved by the Comité de Déontologie pour l'Expérimentation sur des Animaux (CDEA) of the Université de Montréal. Sprague-Dawley male rats and pregnant dams were purchased from Charles River (St Constant, QC, Canada). Housing was at a constant temperature (21 °C) and humidity (60%), under a fixed 12 h light/dark cycle and with free access to food and water.

6-OHDA lesions

Neonatal 6-OHDA lesions were produced as previously described (Fernandes Xavier et coll., 1994; Jackson et coll., 1988; Stachowiak et coll., 1984). In brief, 4

day-old pups (P4) received a subcutaneous injection of desipramine (25 mg/kg s.c.; Sigma Chemical, St. Louis, MO), 45 min before toxin injection to protect noradrenergic neurons. 6-OHDA hydrochloride (10 mg/ml; Sigma), was dissolved in artificial CSF containing 0.2% ascorbic acid to prevent oxidation. Pups were anesthetized on ice, immobilized on a cold body mould, and administered 5 µl of 6-OHDA solution (i.e., 50 µg of 6-OHDA), in each lateral brain ventricle. The intra-cerebroventricular injections were made with a 30-gauge needle attached to a 10 µl Hamilton syringe, at rate of approximately 1.5 µl/min. The injection site was 1.5 mm lateral to bregma and 3.3 mm below the dura. The syringe was left in place for 3 min after each injection. The pups were then warmed in a humidified box and returned to their mother two hours later. They were maintained with their mother if sacrificed at P15, or caged in group after weaning if sacrificed as adults.

***In situ* hybridization of TH/VGLUT2 mRNA**

The double *in situ* hybridization technique used for the visualization of TH and VGLUT2 mRNAs in P90 rats, normal (n = 4) or 6-OHDA-lesioned (n = 4), was the same as previously described in detail in the study of P15 rats (Dal Bo et coll., 2008). The rats were anesthetized with halothane and their brain was quickly dissected out, immersed in cold phosphate-buffered saline (PBS, 50 mM, pH 7.4), and cut in two parts at the level of the median eminence. The rostral part containing the striatum was fixed by immersion in 4% paraformaldehyde (PFA) solution for 48 h and processed for TH immunohistochemistry as described below. The caudal part containing the mesencephalon was immersed in frozen isopentane and stored at – 80 °C until processed for *in situ* hybridization.

[^{35}S]UTP-labeled VGLUT2 probes, and a nonradioactive digoxigenin (Dig)-labeled TH probe were prepared as already described (Dal Bo et coll., 2008). To generate the VGLUT2 probes, complementary RNA (cRNA) was synthesized from pCRII-Topo plasmids containing a 539 base pair fragment of VGLUT2 cDNA (from nucleotide 386 to 924; GenBank accession no. NM 053427). An antisense probe was produced by linearization of the plasmid using the *Not* I restriction enzyme and SP_6 polymerase, and synthesized with the Promega riboprobe kit (Promega, Madison, WI, USA) and [^{35}S]UTP (Perkin-Elmer, Missisauga, ON, Canada). To produce the sense

probe, the *Hind* III restriction enzyme was used to linearize the plasmid and the probe was synthesized with T_3 polymerase. These labeled probes were purified with mini QuickSpin RNA columns (Roche Diagnostics, Laval, QC, Canada). The Dig-labeled TH probe was generated as previously described (Cossette et coll., 2004), from a 300 base pair *Pst*I-*Eco*RI restriction fragment of rat TH cDNA (from nucleotide 1279 to 1518; GenBank accession no. M 10244.1) contained in the pSP65 vector and linearized with HindIII. This antisense probe was synthesized with a T7 RNA polymerase. The radiolabeled VGLUT2 (2×10^6 CPM) and the Dig-labeled TH (20 ng/ml) probes were included simultaneously in the hybridization solution.

Double *in situ* hybridization was carried out on cryosections of the mesencephalon (12 µm-thick) fixed in 4% PFA. The TH probe was visualized with anti-Dig antibody and a Dig detection kit (Roche Diagnostic), and the VGLUT2 probe by coating autoradiography with LM-1 photographic emulsion (Amersham, ON, Canada). Slides used to compare the dual labeling between normal and 6-OHDA-lesioned rats were systematically processed together. The sections were examined under bright-field illumination with an Olympus IX-50 microscope (Carsen Group, Markham, ON, Canada), at 400 X magnification. Background labeling was measured and found at 0.37 to 0.53 silver grains per 500 μm^2 of section. As in previous studies (Kawano et coll., 2006), TH-Dig positive cells (DA neurons) were considered to be labeled for VGLUT2 mRNA if displaying 3 times the background level, i.e., at least 6 silver grains per cell body (Gratto and Verge, 2003). Singly and doubly labeled cells were counted in 5 sections per rat, between stereotaxic planes - 5.28 mm and - 6.24 mm from bregma (Paxinos and Watson, 2005), within the VTA and SN, pars compacta (SNc). A total of 3894 neurons displaying TH mRNA were counted in the 4 normal rats: 1727 in VTA and 2167 in SNc; 493 were counted in the 4 lesioned rats: 342 in the VTA and 151 in SNc.

To verify the extent of the 6-OHDA lesion in these same rats, the rostral brain specimens containing the striatum were processed for TH immunohistochemistry. After 48 h of fixation in PFA, 24 µm-thick transverse sections were cut with a vibratome (Leica Microsystems, Nussloch, Germany), and sequentially incubated in 5% normal goat serum solution containing 10% BSA and 0.1% Triton X-100 for 1 h,

in mouse monoclonal TH antibody (Clone TH-2, Sigma) diluted 1:1000 in PBS overnight, and in biotinylated anti-mouse antibodies (Jackson Immunoresearch, West Grove, PA, USA) diluted 1:1000, followed by 1:1000 streptavidin-HRP (Jackson). The peroxidase reaction was revealed with 0.05% 3,3'-diaminobenzidine tetrahydrochloride (DAB; Sigma) and hydrogen peroxide (0.01%) in Tris-HCl buffer (50 mM; pH 7.4).

TH and VGLUT2 immunocytochemistry

Rats were deeply anesthetized with sodium pentobarbital (80 mg/kg, i.p.) and fixed by intra-cardiac perfusion of a solution of 3% acrolein (50 ml for P15 rats; 250 ml for P90 rats) in 0.1 M phosphate buffer (PB, pH 7.4), followed by 4% PFA in the same buffer (150 ml for P15 rats; 300 ml for P90 rats). The brain was removed, post-fixed by immersion in the PFA solution at 4 °C (2 h for P15 rats; 1 h for P90 rats), and washed in phosphate buffered saline (PBS: 0.9 % NaCl in 50 mM PB, pH 7.4). Fifty µm-thick transverse sections at the level of SN and nAcb were then cut in PBS with a vibratome (VT100S, Leica), immersed in 0.1% sodium borohydride (Sigma) in PBS for 30 min at room temperature, and washed in this buffer before further processing.

Antibodies characterization. Mouse anti-TH (Clone TH-2 # T1299, Sigma) and/or rabbit anti-VGLUT2 (# 135 403, Synaptic Systems, Goettingen, Germany) antibodies were used. As described by Sigma, this particular monoclonal anti-TH antibody is derived from an hybridoma produced by the fusion of mouse myeloma cells and splenocytes from a mouse immunized against whole rat TH protein (Haycock, 1993). It recognizes a single epitope (~60 kDa, amino acids 9-16) present in the N-terminal region of both rodent and human TH, and has previously been used in combined immunocytochemical and *in situ* hybridization experiments to detect VGLUT2 mRNA in mesencephalic DA neurons (Kawano et coll., 2006). In the present study, the immunostaining specificity of this antibody towards DA neurons was evidenced not only by the topographic distribution of immunoreactive cell bodies and axon terminals in the different rat brain regions examined (see Hökfelt et coll., 1984), but also by their near total disappearance from the SN and NStr after neonatal 6-OHDA lesion.

As described by Synaptic Systems, the polyclonal anti-VGLUT2 antibody was raised in rabbit against a Strep-Tag® fusion protein from the C-terminal domain of the predicted sequence of rat vesicular glutamate transporter 2 (amino acids 510 - 582) (Takamori et coll., 2001). The immunocytochemical specificity of this particular antibody has been demonstrated by Western blot analysis of homogenized rat brains and/or crude synaptic vesicle fractions from rat brain, in which a single broad brand slightly above 60 kDa was found, and by pre-adsorption experiments with the GST fusion protein used as immunogen, in which the immunostaining of rat brain sections was completely eliminated (refs in Persson et coll., 2006; see also Takamori et coll., 2001; Zhou et coll., 2007).

TH immunolabeling for light microscopy. In order to ensure a successful visualization of mesencephalic DA neurons in these rats, and verify the extent of their lesioning and of the DA neoinnervation in SN after neonatal 6-OHDA, tissue to be processed for electron microscopy after dual TH and VGLUT2 labeling was first examined by light microscopy after immunolabeling for only TH. At room temperature, sections were preincubated for 1 h in a blocking solution containing 5% normal goat serum, 0.3% Triton X-100 and 0.5% gelatin in PBS, incubated overnight in a 1:1000 dilution of TH antibodies, and then, for 2 h, in a 1:1000 dilution of biotinylated goat anti-mouse (for TH) IgGs (Jackson Immunoresearch, West Grove, PA) in blocking solution. After rinses in PBS (3x10 min), they were incubated for 1 h in a 1:1000 dilution of horseradish peroxidase (HRP)-conjugated streptavidin (Jackson Immunoresearch), washed in PBS, incubated for 2 - 5 min in TBS containing 3,3'-diaminobenzidine tetrahydrochloride (0.05% DAB) and hydrogen peroxide (0.02%). The reaction was stopped by several washes in TBS followed by PB, and the sections mounted on microscope slides, dehydrated in ethanol, cleared in toluene and coverslipped with DPX. They were examined and photographed with a Leitz Diaplan optical microscope coupled to a Spot RT color digital camera, using Spot v4.0.5 for Windows (Diagnostic Instruments, Sterling Heights, MI). These images were adjusted for brightness, contrast and sharpness with the Adobe Photoshop software.

Double TH/VGLUT2 immunolabeling for electron microscopy. Sections were preincubated as above, except for omission of Triton X in the blocking solution, and then incubated 48 h, at room temperature, in a 1:500 dilution of both primary TH and VGLUT2 antibodies. After rinses in PBS, they were then placed overnight, at room temperature, in a 1:50 dilution of goat anti-rabbit IgGs conjugated to 1 nm colloidal gold particles (AuroProbe One, Amersham, Oakville, ON, Canada), and treated with IntenSE kit (Amersham) for 15 min, to increase the size of immunogold particles. The immunogold labeled sections were then processed for TH with the immunoperoxidase technique, as above.

Immunocytochemical controls included double immunocytochemical processing, but without either one or both primary antibodies. Only the expected single labeling was then observed after omitting one of the primary antibody, and no labeling whatsoever in the absence of both of them.

Further processing for electron microscopy was as previously described in detail (Riad et coll., 2000). In brief, sections were osmicated, dehydrated and flat-embedded in Durcupan resin (Sigma) between a glass slide and a plastic coverslip (Rinzl, Thomas Scientific, Swedesboro, NJ, USA). After 48 h of polymerization at 60 $^{\circ}$C, the coverslips were removed, and specimens from the regions of interest (nAcb, NStr and SN), were excised from the slides and glued at the tip of resin blocks. Ultrathin sections were then cut with an ultramicrotome (Reichert Ultracut S, Leica Canada, Montreal, QC, Canada), collected on bare square-meshed copper grids, stained with lead citrate and examined with an electron microscope (Philips CM100, Philips Electronics, St-Laurent, QC, Canada).

Quantitative analysis of electron microscopic data. Three brain regions were examined in P15 (n = 14) and P90 rats (n = 16) subjected or not to the neonatal 6-OHDA lesion at P4: the core of nAcb, at transverse levels corresponding to A 10.8 to 11.28 mm in the stereotaxic atlas of Paxinos and Watson (2005), a central portion of the dorsal striatum at this same transverse level, and a small piece of mesencephalic tissue located at mid-distance between the midline and the lateral border of the ventral tegmentum, in a location corresponding to the remnants of SN, pars compacta

and reticulata, at transverse levels corresponding to A 2.9 to 3.8 mm (Paxinos and Watson, 2005).

Doubly immunolabeled material from the nAcb was examined in seven normal and seven 6-OHDA-lesioned rats, aged 15 days (body weight: 15 - 20 g), and in eight normal and eight 6-OHDA-lesioned rats, aged 90 days (300 - 400 g). In each of these rat, a minimum of 50 electron micrographs were obtained from a narrow area of thin section less than 10 μm away from the tissue-resin border, at working magnifications ranging from 3,000 to 15,000 X. The film negatives were scanned (Epson Perfection 3200), converted into positive pictures, and adjusted for brightness and contrast with Photoshop (Adobe) before printing.

Most immunolabeled profiles could then be positively identified as axon varicosities, i.e. axon dilations (> 0.25 μm in transverse diameter) containing aggregated small vesicles, often one or more mitochondria, and displaying or not a synaptic membrane specialization (junctional complex). The immunoperoxidase labeling was in the form of a more or less dense, fine precipitate, often outlining the small vesicles or mitochondria and the plasma membrane of varicosities. Only axon varicosity profiles decorated with 3 or more silver-intensified gold particles were considered as immunogold labeled. Smaller immunolabeled profiles were assumed to represent intervaricose segments of unmyelinated axons.

Thirty micrographs per rat, printed at a uniform magnification of 30,000 X, were selected on the basis of optimal ultrastructural preservation. In this 50,000 μm^2 area of thin section in each rat, singly or dually immunolabeled profiles of axon varicosities were counted and categorized as immunopositive for only TH, only VGLUT2 or both TH and VGLUT2 (TH/VGLUT2). In normal rats, a total of 1699 axon terminals were thus examined at P15 and 1290 at P90. In rats neonatally lesioned with 6-OHDA, 1021 axon terminals were examined at P15 and 986 at P90. Since the same thin section surface was being examined in each rat, these counts could be expressed as means ± SEM per rat, for statistical comparison of the various types of labeling between normal and lesioned rats of the same age.

The varicosity profiles were then measured for long (L) and short (s) axes and mean diameter (L + s / 2), using the public domain, Image J processing software from

NIH, and classified as showing or not a synaptic junction, i.e., a localized straightening and thickening of apposed plasma membranes on either side of a slightly widened extracellular space. The length of junctional complexes was measured, and the synaptic frequency observed in single sections was extrapolated to the whole volume of varicosities by means of the stereological formula of Beaudet and Sotelo (1981; see also Umbriaco et coll., 1994).

A similar analysis was carried out on doubly labeled material from the NStr of 3 of the above 15 day-old and 3 of the above 90 day-old normal rats, and from the SN of 3 of the above 15 day-old and 3 of the above 90 day-old 6-OHDA-lesioned rats. 50,000 μm^2 of thin section were again examined in each rat, for a total of 468 immunolabeled terminals at P15 and 550 at P90 in the NStr of normal rats, and of 286 axon immunolabeled terminals at P15 and 201 at P90 in the SN of 6-OHDA-lesioned rats. In the SN, care was taken to restrict the analysis to axon terminals, excluding rare cell bodies or occasional TH, VGLUT2 or TH/VGLUT2 labeled dendrites, which were generally much larger, contained the typical array of microtubules, and were often contacted by synaptic terminals.

Statistics

All data were expressed as group mean ± SEM. Statistical analyses were performed with GraphPad Prism 4. Analyses of variance (one-way ANOVA) and unpaired Student's t-tests were used to determine statistical significance. P values below 0.05 were considered statistically significant. *In situ* hybridization being performed on frozen tissue sections, it was deemed meaningful to compare the number of cells singly or dually labeled for TH and VGLUT2 mRNA not only between normal and lesioned rats at each age, but also between P15 and P90 rats. However, fixed immature and mature rat brain tissue may not be equally permeable to immunoreagents. Therefore, the numbers of axon terminals in each category of immunolabeling were not compared between P15 and P90 rats.

RESULTS

Distribution of TH immunoreactivity in P15 and P90 rats, normal or subjected to neonatal 6-OHDA lesion

As visualized by light microscopy, the pattern of TH-immunostaining in normal rats was entirely consistent with earlier TH or DA immunocytochemical descriptions of the distribution of mesencephalic DA neuron soma-dendrites and axon terminals at both ages examined (Antonopoulos et coll., 2002; Hökfelt et coll., 1984; Voorn et coll., 1988). As previously reported (Hanaway et coll., 1971; Voorn et coll., 1988), at P15, all DA cell bodies were not yet tightly grouped in the pars compacta of SN, and many were still present in the pars reticulata (Fig. 1). However, in both NStr and nAcb, the DA innervation appeared to be already as dense at P15 than P90 (compare Figs 2 A and 2 C).

Also in keeping with earlier observations, after neonatal 6-OHDA lesion, there was an almost total disappearance of TH positive soma-dendrites in the pars compacta and reticulata of SN, and of TH axon terminals in the NStr, which appeared to be complete at P15. In contrast, even if some cell loss was also apparent in VTA, TH cell bodies were still visible in this region, as well as some TH axon terminals in both the core and shell of nAcb (Figs 2 B and 2 D). There were no indications of DA terminal sprouting in either NStr or nAcb at P90. However, as first reported by Fernandes Xavier et coll. (1994), in the lesioned rats, there was a striking DA neoinnervation of the remnants of SN, pars compacta and reticulata, by fine varicose, axon-like, TH immunoreactive processes, which were already numerous at P15, but even more abundant at P90 (Figs 1 B'-1 D').

Co-expression of TH and VGLUT2 mRNA in mesencephalic neurons of P15 and P90 rats, normal or subjected to neonatal 6-OHDA lesion

As previously observed in normal P15 rats, there were only few neurons expressing both TH and VGLUT2 mRNA in the VTA and SNc of normal P90 rats (Table 1), and these neurons were only weakly labeled for VGLUT2 mRNA, compared to presumptive glutamatergic neurons in neighboring anatomical regions such as the red nucleus (Supplementary Material). As also illustrated in

Supplementary Material, there was no cell labeling whatsoever in material processed with sense probes.

As had been seen at P15, the total number of neurons displaying only TH mRNA was markedly reduced in the VTA of adult (P90) 6-OHDA-lesioned rats ($p < 0.01$), and such neurons had almost totally disappeared from the SNc (Table 1 and Fig. 3). At P15, the proportion of VTA neurons co-expressing TH and VGLUT2 mRNA had been found to be significantly higher in 6-OHDA-lesioned compared to control rats, amounting to 26.3% compared to 1.8% of all TH mRNA positive neurons ($p < 0.001$). At P90, the proportion of dually labeled VTA neurons was also higher after the neonatal lesion than in controls ($p < 0.05$), but considerably lower than at P15 ($p < 0.001$), with only 7.2% of all TH mRNA positive neurons also labeled for VGLUT2 mRNA.

TH, VGLUT2 and TH/VGLUT2 immunoreactive axon terminals in the nAcb of P15 and P90 rats, normal or subjected to neonatal 6-OHDA lesion

As also reported previously in P15 rats, and illustrated here in Fig. 4 A,B, axon terminals labeled for TH or VGLUT2 were readily identified in the nAcb of both normal and 6-OHDA-lesioned rats at P90 (Fig. 4 C,D). Whereas a significant number of TH/VGLUT2 labeled terminals had been previously found in both normal and 6-OHDA-lesioned rats at P15 (e.g., Figs 5 A,B and 6 A-D), none were seen in the 8 normal P90 rats, and only 6 in the 8 neonatally lesioned P90 rats (Figs 5 C-E and 6 E-H).

As shown in Table 2, VGLUT2 was co-localized with TH in 28% of all TH labeled axon terminals in the nAcb of normal P15 rats. After the neonatal 6-OHDA lesion, the average number of all TH labeled terminals was markedly decreased ($p < 0.001$), but the proportion that were also labeled for VGLUT2 slightly but significantly increased (37%; $p < 0.05$). The apparent decrease in the mean number of terminals labeled for VGLUT2 only was not statistically significant ($p = 0.15$).

In P90 rats, the number of axon terminals labeled for TH only was also decreased after the neonatal 6-OHDA lesion ($p < 0.001$), without significant change in the number of terminals labeled for only VGLUT2. Only 6 TH/VGLUT2 labeled terminals were seen in the 8 rats neonatally lesioned with 6-OHDA.

Ultrastructural features of TH, VGLUT2 and TH/VGLUT2 immunoreactive axon terminals in the nAcb of P15 and P90 rats, normal or subjected to neonatal 6-OHDA lesion

The intrinsic and relational features of the singly or dually labeled terminals in the nAcb of normal and 6-OHDA-lesioned rats at P15 and P90 are summarized in Table 3 and illustrated in Figs. 4 - 6. There were no significant differences in size between axon terminals labeled for only TH in normal and 6-OHDA-lesioned rats at either age. In contrast, in both normal and 6-OHDA-lesioned rats, the size of terminals labeled for VGLUT2 only showed a significant and comparable increase between P15 and P90. In both normal and 6-OHDA-lesioned P15 rats, the terminals dually labeled for TH/VGLUT2 were comparable in size with those labeled for VGLUT2 only, and significantly larger than those labeled for TH only ($p < 0.05$). At P90, and in both normal and 6-OHDA-lesioned rats, the terminals labeled for VGLUT2 only were also significantly larger than those labeled for TH only. The length of synaptic junctions formed by terminals labeled for VGLUT2 only also showed a significant increase between P15 and P90 in both normal and 6-OHDA-lesioned rats.

As extrapolated stereologically from the observations in single thin sections, the synaptic incidence of nAcb axon terminals labeled for TH only was relatively low, but greater at P15 than P90, whether in normal (37% versus 7%) or in 6-OHDA-lesioned rats (70% versus 22%) (Table 3). The synaptic incidence of terminals labeled for VGLUT2 only was also relatively low in both normal (58%) and 6-OHDA-lesioned rats (71%) at P15, whereas, at P90, most if not all such varicosities appeared to be synaptic (96% and 106% in normal and 6-OHDA-lesioned rats, respectively). The synaptic incidence extrapolated for TH/VGLUT2 immunoreactive varicosities in normal and 6-OHDA-lesioned P15 rats was also greater than 100% (110% and 130%), suggesting that all these dually labeled terminals were synaptic, with a significant number making more than a single synaptic contact (e.g., Figs 5 C and 6 E). When the terminals labeled for only TH were pooled with those dually labeled for TH/VGLUT2, the synaptic incidence for all TH positive terminals at P15 was 57% in normal rats and 92% after the neonatal 6-OHDA lesion ($p > 0.001$).

TH, VGLUT2 and TH/VGLUT2 immunoreactive axon terminals in the NStr of normal P15 and P90 rats

In view of the near absence of DA terminals in the NStr after neonatal 6-OHDA lesion, the ultrastructural features of axon terminals labeled for TH, VGLUT2 or TH/VGLUT2 in this region were examined only in normal P15 and P90 rats (Table 3, Fig. 7). In the P15 rats, an average of 80 ± 12 terminals per rat were labeled for TH only, 58 ± 19 for VGLUT2 only, and 17 ± 6 for TH/VGLUT2 (17% of all TH terminals), whereas in P90 rats, 115 ± 5 terminals per rat were labeled for TH only, and 68 ± 8 for VGLUT2 only. Not a single dually labeled terminal was found in the NStr of P90 rats.

As in nAcb, the neostriatal axon terminals labeled for TH only were of the same size at P15 and P90, and significantly smaller than those labeled for TH/VGLUT2 at P15 ($p < 0.05$), or for VGLUT2 only at P90 ($p < 0.01$). In NStr, however, there was no apparent increase in size of the VGLUT2 terminals between P15 and P90, nor was the average length of junctions made by these terminals significantly different at the two ages.

The synaptic incidence of NStr terminals in the various categories of labeling is shown in Table 4. Again, terminals labeled for TH only were not often synaptic, but more frequently so at P15 (18%) than P90 (6%; $p < 0.01$). Terminals labeled for VGLUT2 only were much more frequently synaptic than the TH only ($p < 0.001$ at P15 and $p < 0.01$ at P90), but not all synaptic at P15 (70%) as opposed to P90 (99%). TH/VGLUT2 terminals at P15 also appeared to be mostly if not all synaptic (93%; $p < 0.01$ versus TH only), raising the synaptic incidence for all TH positive terminals (TH + TH/VGLUT2) to 31% at this age, compared to the 6% value at P90 ($p < 0.001$).

The DA neoinnervation in SN of P15 and P90 rats subjected to neonatal 6-OHDA lesion

As illustrated in Fig. 8, in both P15 and P90 rats, many of the TH as well as VGLUT2 immunoreactive profiles in the SN remnants after neonatal 6-OHDA lesion could be positively identified as axon varicosities (terminals), according to conventional morphological criteria (Peters and Palay, 1996; see also Materials and

Methods). In the three rats examined at each age, TH/VGLUT2 labeled varicosities were also found at P15, but not at P90. The average number of immunoreactive terminals per rat was 29 ± 12 for TH only, 44 ± 17 for VGLUT2 only, and 22 ± 6 for TH/VGLUT2 (46% of all TH terminals) at P15, whereas at P90, the corresponding numbers were 20 ± 3 for TH only and 47 ± 3 for VGLUT2 only.

Here again, terminals labeled for TH only or for VGLUT2 only did not differ in size between P15 and P90, but, at P90, the VGLUT2 terminals were significantly larger than the TH ($p < 0.05$) (Table 5). The synaptic incidence of terminals labeled for TH only was remarkably high at P15 (78%), and much lower at P90 (14%; $p < 0.01$). As in both nAcb and NStr, the terminals labeled for VGLUT2 only were not all synaptic at P15 (65%), as opposed to P90 (104%; $p < 0.05$). Again, the extrapolated synaptic incidence of the terminals dually labeled for TH/VGLUT2 at P15 was superior to 100% (120%), suggesting that many of these varicosities made more than a single synaptic contact. The synaptic incidence for all TH axon terminals at P15 was 97%, and therefore much higher than at P90 ($p < 0.001$).

DISCUSSION

This study demonstrates a regression of the dual TH/VGLUT2 phenotype of mesencephalic DA neurons with age in three conditions: normal maturation (in nAcb and NStr), after its reactivation by a lesion (in VTA and nAcb), and during the growth of a neoinnervation (in SN). Moreover, in all three conditions, the presence of VGLUT2 protein in DA axon terminals appeared to be associated with the formation of synaptic junctions by these terminals, which suggests a particular role for glutamate in the establishment of synaptic junctions by mesencephalic DA neurons.

Methodological considerations

Even though there were no reasons to doubt the specificity of the immunocytochemical signals observed in the present study, it could not be ascertained that all TH and/or VGLUT2 axon terminals were actually identified under the conditions of these double immunolabeling experiments. In tissue prepared for electron microscopy, the pre-embedding immunogold technique used to detect VGLUT2 is notoriously less sensitive that the immunoperoxidase-DAB technique,

and the penetration of immunoreagents limited. For these reasons, our quantitative evaluation of the number of axon terminals in the different categories of labeling was restricted to the superficial parts of embedded tissue sections and the number of axon terminals in each categories of immunolabeling had to be considered as relative estimates rather than true numbers. But even more importantly, when axon terminals failed to show TH and/or VGLUT2 immunoreactivity, this did not mean that the corresponding proteins were absent, but could merely indicate that they were present in insufficient concentration to be detected.

As the electron microscopic examination was carried out in single thin sections, the number of varicosities in each category of immunolabeling was an approximation of their real number in the tissue, because larger varicosities had a greater chance of being detected than smaller ones. For this reason, the percentages of TH/VGLUT2 terminals over all TH terminals, as provided in Table 2, were recalculated after applying Abercrombie's formula to the counts (Abercrombie, 1946). This formula, T / T + h, where T = section thickness and h = the mean diameter of the objects, yields a ratio of "real" versus observed number (Guillery, 2002), which was applied to the total number of varicosities in each category. When recalculated for "corrected" numbers, the percentages of TH/VGLUT2 over all TH terminals did not markedly differ, amounting to 25% and 35% instead of 28% and 37% in the nAcb of normal and 6-OHDA-lesioned P15 rats, respectively, 15% instead of 17% in the NStr of normal P15 rats, and 37% instead of 46% in the SN of the 6-OHDA-lesioned P15 rats.

Regression of the dual TH/VGLUT2 phenotype

In the three brain regions examined, there was an almost complete disappearance of TH immunopositive axon terminals labeled for VGLUT2 between P15 and P90. This was in keeping with the marked reduction in number of neurons observed by double *in situ* hybridization to contain both TH and VGLUT2 mRNA in the VTA of P15 and P90 rats neonatally lesioned with 6-OHDA. The fact that such a decrease was not apparent in normal rats was probably due to the relative insensitivity of the double *in situ* hybridization technique, also evidenced by the difference in number of doubly labeled neurons visualized in the adult VTA with this technique

(see also Yamaguchi et coll., 2007) compared to a combination of TH immunocytochemistry and VGLUT2 *in situ* hybridization (Kawano et coll., 2006) or to single-cell RT PCR (Mendez et coll., 2008). The difference between P15 and P90 would become apparent by double *in situ* hybridization when the amount of VGLUT2 mRNA would be increased in the DA neurons as a result of reactivation of the dual phenotype by the lesion (Dal Bo et coll., 2008).

In view of its previous demonstration in the SN of postnatal rat (Janec and Burke, 1993; Oo and Burke, 1997) developmental cell death of DA neurons had to be considered as a possible explanation for the disappearance of axon terminals dually labeled for TH and VGLUT2 between P15 and P90. However, this naturally occurring phenomenon involves very few SN cells after P15, and it has not been demonstrated to occur in the VTA. It could therefore hardly account for the selective loss of the relatively large number of axon terminals that ceased to display both proteins, as observed in the nAcb and NStr of mature rat. Two other theoretical possibilities had to be envisaged: an elimination of only those axon terminals containing both proteins or conversely, the addressing and progressive segregation of these proteins in different axonal branches of the same neurons. The former possibility was readily excluded, as it was clear from the light microscopic examination of TH-immunostained material that the density of TH labeling did not significantly decrease between P15 and P90 in any of the conditions and regions examined, including the SN after neonatal 6-OHDA lesion. As for the segregation hypothesis, already envisaged by Sulzer et al (1998) and Dal Bo et al (2004) on the basis of observations in tissue culture, it could not be formally excluded from our observations in nAcb or NStr. However, it was hardly compatible with our data on the size of terminals showing only TH versus those showing only VGLUT2 or TH/VGLUT2 in the DA-neoinnervation condition, unless postulating that, by addressing TH and VGLUT2 to separate axonal branches, an equal number of doubly labeled varicosities would be converted into only TH and only VGLUT2 varicosities. Indeed, one would have then expected a change in the proportion of smaller versus larger terminals between P15 and P90, which was not actually the case (43.0% at P15, 43.6% at P90).

Although speculative, a more likely explanation was an activation of the VGLUT2 gene in DA neurons during their growth, followed by a repression of its transcription in mature DA neurons. Several studies have already suggested that the dual phenotype of DA neurons is a transient phenomenon associated with growth, either during development (Dal Bo et coll., 2008; Kawano et coll., 2006; Yamaguchi et coll., 2007) or in response to injury (Dal Bo et coll., 2004; Mendez et coll., 2008). In the present study, this would explain why the DA neoinnervation in substantia nigra, which develops only postnatally, is the region displaying the greatest proportion of TH terminals colocalizing VGLUT2 at P15. It would also account for the fact that, in P15 rats, a greater proportion of doubly labeled axon terminals was found in nAcb than NStr, in which the maturation of the DA innervation appears to be more advanced than in nAcb at that age (Tarazi et coll., 1998).

Ultrastructural characteristics

In the present study, particular attention was paid to the frequency with which the axon terminals (varicosities) in the various categories of immunolabeling made a synapse. As the electron microscopic observations were made in single ultrathin sections, stereological extrapolation of the synaptic incidence for the whole volume of varicosities required a measurement of their average diameter and length of visible junctions. In so doing, novel information was acquired on the intrinsic as well as relational features of DA terminals during normal development, following 6-OHDA lesion and after aberrant sprouting, but also of glutamatergic terminals during normal development.

In all conditions and regions examined, including SN, the axon terminals labeled for TH were comparable in size and appearance at P15 and P90, even though the aberrant fibers in SN were still growing at P15, as evidenced by their much greater number at P90 than P15 (Fig. 2; see also Fernandes Xavier et coll., 1994). Thus, varicosities belonging to growing DA fibers look mature, and should be capable of transmitter release, including those doubly labeled for TH and VGLUT2. Another characteristic of the terminals labeled for TH was the relatively high frequency with which they made synapse at P15 compared to adult. This difference was already significant in the nAcb and NStr of normal rat, but even greater in the

case of the residual TH terminals of the nAcb after 6-OHDA lesioning, and of the neoinnervation in SN. A similar trend for higher synaptic incidence of DA varicosities during postnatal development had already been observed by Antonopoulos et coll. (2002), who reported that DA immunoreactive axon terminals from the dorsal and ventral striatum of P14 rat were much more frequently synaptic than at P21.

Our values for the nAcb and NStr of normal P15 rat were much lower than in that particular study, presumably due to differences in sampling, but also to an underestimation of the synaptic frequency in our heavily labeled TH material, in which dense DAB precipitate on the plasmalemma of immunopositive profiles could obscure the presence of small, symmetrical synaptic junctions, as expected from these terminals (e.g., Descarries et coll., 1996; Moss and Bolam, 2008). This was much less likely to occur in the case of the TH/VGLUT2 terminals, which always appeared to be less densely TH-immunostained and displayed prominent and relatively large synaptic junctions, much as the terminals labeled for VGLUT2 only. A similar explanation probably accounted for the 7% and 6% values of synaptic incidence for TH immunoreactive terminals in adult rat nAcb and NStr, which were considerably lower than previously found after radioautographic labeling of neostriatal DA terminals by [^{3}H]DA uptake radioautography or DA immunocytochemistry (Descarries et coll., 1996). As for the relatively high synaptic incidences of TH terminals here measured at both P15 and P90 in the nAcb and SN of neonatally 6-OHDA-lesioned rats, they were in keeping with the fact that many of these terminals were presumably those of growing axons, thus recapitulating the frequent synaptic relationships observed during normal development.

In contrast to the TH only terminals, the terminals labeled for VGLUT2 only appeared to be morphologically immature in the nAcb at P15, as they were significantly smaller and displayed shorter synaptic junctions at P15 than P90, in both normal and 6-OHDA-lesioned rats. This immaturity was also indicated by the fact that these VGLUT2 terminals were not yet all synaptic, as they would become in the adult (present study; see also Fujiyama et coll., 2006; Lacey et coll., 2005; Moss and Bolam, 2008). In this context, it was all the more striking to find that all dually

labeled TH/VGLUT2 terminals at P15, whether in the normal nAcb or NStr, or in the nAcb and the neoinnervation of SN after 6-OHDA lesioning, did make a synaptic junction. This suggested a link between the presence of VGLUT2 and the formation of synapses by these terminals.

The role of VGLUT2 in growing DA neurons

It is likely that glutamate may be released by axonal boutons that contain one of its vesicular transporters. Both in culture (Bourque and Trudeau, 2000; Joyce and Rayport, 2000; Sulzer et coll., 1998) and suggested *in vivo* (Chuhma et coll., 2004; Lavin et coll., 2005), strong physiological evidence has accumulated for the release of glutamate by axon terminals of mesencephalic DA neurons. Glutamate released from DA axon terminals could be implicated in developmental events such as proliferation, migration, differentiation and arbor size development (reviewed in Cline and Haas, 2008; Ruediger and Bolz, 2007). It could also act as a signal for the establishment of synaptic junctions by growing axons, as recently proposed on the basis of *in vivo* observations on the pausing of synaptic vesicle protein transport vesicles at predefined sites along growing axons (Sabo et coll., 2006). Moreover, during postnatal development or in response to injury, the presence of VGLUT2 in DA terminals could allow for a greater intravesicular accumulation and release of DA than at maturity, as recently demonstrated to be the case for VGLUT3 and acetylcholine in striatal cholinergic interneurons of adult rat (Gras et coll., 2008). Whether the regression of the dual glutamatergic phenotype would then have something to do with the loss of junctions by mature DA terminals is an intriguing possibility. In this regard, it would be of interest to determine whether the localization of VGLUT2 is more frequent or persistent in DA axon terminals of the anteromedial or the occipital cortex that appear to be mostly if not entirely synaptic in the adult, contrary to those in dorsal and ventral striatum.

Acknowledgments: This work was funded in part by CIHR grants MOP-3544 to L.D. and MOP-49951 to L.-É. T, and a grant from NARSAD to L.-É. T. It was also supported by an infrastructure grant from the FRSQ to the GRSNC (Groupe de Recherche sur le Système Nerveux Central). N. B.-C. was the recipient of a studentship from the GRSNC and FRSQ. The plasmids used to prepare VGLUT2

probe were kindly provided by Dr. S. El Mestikawy. The authors wish to thank Jérome Maheux for their help with the *in situ* hybridization experiments.

REFERENCES

Abercrombie M. 1946. Estimation of nuclear population from microtome sections. Anat Rec 94:239-247.

Antonopoulos J, Dori I, Dinopoulos A, Chiotelli M, Parnavelas JG. 2002. Postnatal development of the dopaminergic system of the striatum in the rat. Neuroscience 110:245-256.

Bai L, Xu H, Collins JF, Ghishan FK. 2001. Molecular and functional analysis of a novel neuronal vesicular glutamate transporter. J Biol Chem 276:36764-36769.

Beaudet A, Sotelo C. 1981. Synaptic remodeling of serotonin axon terminals in rat agranular cerebellum. Brain Res 206:305-329.

Boulland JL, Qureshi T, Seal RP, Rafiki A, Gundersen V, Bergersen LH, Fremeau RT, Jr., Edwards RH, Storm-Mathisen J, Chaudhry FA. 2004. Expression of the vesicular glutamate transporters during development indicates the widespread corelease of multiple neurotransmitters. J Comp Neurol 480:264-280.

Bourque MJ, Trudeau LE. 2000. GDNF enhances the synaptic efficacy of dopaminergic neurons in culture. Eur J Neurosci 12:3172-3180.

Chuhma N, Zhang H, Masson J, Zhuang X, Sulzer D, Hen R, Rayport S. 2004. Dopamine neurons mediate a fast excitatory signal via their glutamatergic synapses. J Neurosci 24:972-981.

Cline H, Haas K. 2008. The regulation of dendritic arbor development and plasticity by glutamatergic synaptic input: a review of the synaptotrophic hypothesis. J Physiol 586:1509-1517.

Cossette M, Parent A, Levesque D. 2004. Tyrosine hydroxylase-positive neurons intrinsic to the human striatum express the transcription factor Nurr1. Eur J Neurosci 20:2089-2095.

Dal Bo G, Berube-Carriere N, Mendez JA, Leo D, Riad M, Descarries L, Levesque D, Trudeau LE. 2008. Enhanced glutamatergic phenotype of mesencephalic dopamine neurons after neonatal 6-hydroxydopamine lesion. Neuroscience 156:59-70.

Dal Bo G, St-Gelais F, Danik M, Williams S, Cotton M, Trudeau LE. 2004. Dopamine neurons in culture express VGLUT2 explaining their capacity to release glutamate at synapses in addition to dopamine. J Neurochem 88:1398-1405.

Descarries L, Berube-Carriere N, Riad M, Bo GD, Mendez JA, Trudeau LE. 2008. Glutamate in dopamine neurons: synaptic versus diffuse transmission. Brain Res Rev 58:290-302.

Descarries L, Watkins KC, Garcia S, Bosler O, Doucet G. 1996. Dual character, asynaptic and synaptic, of the dopamine innervation in adult rat neostriatum: a quantitative autoradiographic and immunocytochemical analysis. J Comp Neurol 375:167-186.

Fernandes Xavier FG, Doucet G, Geffard M, Descarries L. 1994. Dopamine neoinnervation in the substantia nigra and hyperinnervation in the interpeduncular

nucleus of adult rat following neonatal cerebroventricular administration of 6-hydroxydopamine. Neuroscience 59:77-87.

Fremeau RT, Jr., Troyer MD, Pahner I, Nygaard GO, Tran CH, Reimer RJ, Bellocchio EE, Fortin D, Storm-Mathisen J, Edwards RH. 2001. The expression of vesicular glutamate transporters defines two classes of excitatory synapse. Neuron 31:247-260.

Fremeau RT, Jr., Voglmaier S, Seal RP, Edwards RH. 2004. VGLUTs define subsets of excitatory neurons and suggest novel roles for glutamate. Trends Neurosci 27:98-103.

Fujiyama F, Unzai T, Nakamura K, Nomura S, Kaneko T. 2006. Difference in organization of corticostriatal and thalamostriatal synapses between patch and matrix compartments of rat neostriatum. Eur J Neurosci 24:2813-2824.

Gras C, Amilhon B, Lepicard EM, Poirel O, Vinatier J, Herbin M, Dumas S, Tzavara ET, Wade MR, Nomikos GG, Hanoun N, Saurini F, Kemel ML, Gasnier B, Giros B, El Mestikawy S. 2008. The vesicular glutamate transporter VGLUT3 synergizes striatal acetylcholine tone. Nat Neurosci 11:292-300.

Gras C, Herzog E, Bellenchi GC, Bernard V, Ravassard P, Pohl M, Gasnier B, Giros B, El Mestikawy S. 2002. A third vesicular glutamate transporter expressed by cholinergic and serotoninergic neurons. J Neurosci 22:5442-5451.

Gratto KA, Verge VM. 2003. Neurotrophin-3 down-regulates trkA mRNA, NGF high-affinity binding sites, and associated phenotype in adult DRG neurons. Eur J Neurosci 18:1535-1548.

Hanaway J, McConnell JA, Netsky MG. 1971. Histogenesis of the substantia nigra, ventral tegmental area of Tsai and interpeduncular nucleus: an autoradiographic study of the mesencephalon in the rat. J Comp Neurol 142:59-73.

Harkany T, Hartig W, Berghuis P, Dobszay MB, Zilberter Y, Edwards RH, Mackie K, Ernfors P. 2003. Complementary distribution of type 1 cannabinoid receptors and vesicular glutamate transporter 3 in basal forebrain suggests input-specific retrograde signalling by cholinergic neurons. Eur J Neurosci 18:1979-1992.

Haycock JW. 1993. Multiple forms of tyrosine hydroxylase in human neuroblastoma cells: quantitation with isoform-specific antibodies. J Neurochem 60:493-502.

Herzog E, Bellenchi GC, Gras C, Bernard V, Ravassard P, Bedet C, Gasnier B, Giros B, El Mestikawy S. 2001. The existence of a second vesicular glutamate transporter specifies subpopulations of glutamatergic neurons. J Neurosci 21:RC181.

Hökfelt T, Märtensson R, Björklund A, Kleinau S, Goldstein M. 1984. Distributional maps of tyrosine-hydroxylase-immunoreactive neurons in the rat brain. In: Björklund A, Hokfelt T, editors. Handbook of chemical neuroanatomy, Vol 2. Amsterdam: Elsevier. p 277-379.

Jackson D, Bruno JP, Stachowiak MK, Zigmond MJ. 1988. Inhibition of striatal acetylcholine release by serotonin and dopamine after the intracerebral administration of 6-hydroxydopamine to neonatal rats. Brain Res 457:267-273.

Janec E, Burke RE. 1993. Naturally Occurring Cell Death during Postnatal Development of the Substantia Nigra Pars Compacta of Rat. Molecular and Cellular Neuroscience 4:30-35.

Joyce MP, Rayport S. 2000. Mesoaccumbens dopamine neuron synapses reconstructed *in vitro* are glutamatergic. Neuroscience 99:445-456.

Kawano M, Kawasaki A, Sakata-Haga H, Fukui Y, Kawano H, Nogami H, Hisano S. 2006. Particular subpopulations of midbrain and hypothalamic dopamine neurons express vesicular glutamate transporter 2 in the rat brain. J Comp Neurol 498:581-592.

Lacey CJ, Boyes J, Gerlach O, Chen L, Magill PJ, Bolam JP. 2005. GABA(B) receptors at glutamatergic synapses in the rat striatum. Neuroscience 136:1083-1095.

Lavin A, Nogueira L, Lapish CC, Wightman RM, Phillips PE, Seamans JK. 2005. Mesocortical dopamine neurons operate in distinct temporal domains using multimodal signaling. J Neurosci 25:5013-5023.

Liguz-Lecznar M, Skangiel-Kramska J. 2007. Vesicular glutamate transporters (VGLUTs): the three musketeers of glutamatergic system. Acta Neurobiol Exp (Wars) 67:207-218.

Mendez JA, Bourque MJ, Dal Bo G, Bourdeau ML, Danik M, Williams S, Lacaille JC, Trudeau LE. 2008. Developmental and target-dependent regulation of vesicular glutamate transporter expression by dopamine neurons. J Neurosci 28:6309-6318.

Moss J, Bolam JP. 2008. A dopaminergic axon lattice in the striatum and its relationship with cortical and thalamic terminals. J Neurosci 28:11221-11230.

Ni B, Rosteck PR, Jr., Nadi NS, Paul SM. 1994. Cloning and expression of a cDNA encoding a brain-specific Na(+)-dependent inorganic phosphate cotransporter. Proc Natl Acad Sci U S A 91:5607-5611.

Ni B, Wu X, Yan GM, Wang J, Paul SM. 1995. Regional expression and cellular localization of the Na(+)-dependent inorganic phosphate cotransporter of rat brain. J Neurosci 15:5789-5799.

Oo TF, Burke RE. 1997. The time course of developmental cell death in phenotypically defined dopaminergic neurons of the substantia nigra. Brain Res Dev Brain Res 98:191-196.

Paxinos G, Watson C. 2005. The Rat Brain in Stereotaxic Coordinates: Elsevier Academic Press.

Persson S, Boulland JL, Aspling M, Larsson M, Fremeau RT, Jr., Edwards RH, Storm-Mathisen J, Chaudhry FA, Broman J. 2006. Distribution of vesicular glutamate transporters 1 and 2 in the rat spinal cord, with a note on the spinocervical tract. J Comp Neurol 497:683-701.

Peters A, Palay SL. 1996. The morphology of synapses. J Neurocytol 25:687-700.

Riad M, Garcia S, Watkins KC, Jodoin N, Doucet E, Langlois X, el Mestikawy S, Hamon M, Descarries L. 2000. Somatodendritic localization of 5-HT1A and preterminal axonal localization of 5-HT1B serotonin receptors in adult rat brain. J Comp Neurol 417:181-194.

Ruediger T, Bolz J. 2007. Neurotransmitters and the development of neuronal circuits. Adv Exp Med Biol 621:104-115.

Sabo SL, Gomes RA, McAllister AK. 2006. Formation of presynaptic terminals at predefined sites along axons. J Neurosci 26:10813-10825.

Schafer MK, Varoqui H, Defamie N, Weihe E, Erickson JD. 2002. Molecular cloning and functional identification of mouse vesicular glutamate transporter 3 and its expression in subsets of novel excitatory neurons. J Biol Chem 277:50734-50748.

Stachowiak MK, Bruno JP, Snyder AM, Stricker EM, Zigmond MJ. 1984. Apparent sprouting of striatal serotonergic terminals after dopamine-depleting brain lesions in neonatal rats. Brain Res 291:164-167.

Stornetta RL, Sevigny CP, Schreihofer AM, Rosin DL, Guyenet PG. 2002. Vesicular glutamate transporter DNPI/VGLUT2 is expressed by both C1 adrenergic and nonaminergic presympathetic vasomotor neurons of the rat medulla. J Comp Neurol 444:207-220.

Sulzer D, Joyce MP, Lin L, Geldwert D, Haber SN, Hattori T, Rayport S. 1998. Dopamine neurons make glutamatergic synapses *in vitro*. J Neurosci 18:4588-4602.

Takamori S, Malherbe P, Broger C, Jahn R. 2002. Molecular cloning and functional characterization of human vesicular glutamate transporter 3. EMBO Rep 3:798-803.

Takamori S, Rhee JS, Rosenmund C, Jahn R. 2001. Identification of differentiation-associated brain-specific phosphate transporter as a second vesicular glutamate transporter (VGLUT2). J Neurosci 21:RC182.

Tarazi FI, Tomasini EC, Baldessarini RJ. 1998. Postnatal development of dopamine and serotonin transporters in rat caudate-putamen and nucleus accumbens septi. Neurosci Lett 254:21-24.

Trudeau LE. 2004. Glutamate co-transmission as an emerging concept in monoamine neuron function. J Psychiatry Neurosci 29:296-310.

Umbriaco D, Watkins KC, Descarries L, Cozzari C, Hartman BK. 1994. Ultrastructural and morphometric features of the acetylcholine innervation in adult rat parietal cortex: an electron microscopic study in serial sections. J Comp Neurol 348:351-373.

Voorn P, Kalsbeek A, Jorritsma-Byham B, Groenewegen HJ. 1988. The pre- and postnatal development of the dopaminergic cell groups in the ventral mesencephalon and the dopaminergic innervation of the striatum of the rat. Neuroscience 25:857-887.

Yamaguchi T, Sheen W, Morales M. 2007. Glutamatergic neurons are present in the rat ventral tegmental area. Eur J Neurosci 25:106-118.

Zhou J, Nannapaneni N, Shore S. 2007. Vesicular glutamate transporters 1 and 2 are differentially associated with auditory nerve and spinal trigeminal inputs to the cochlear nucleus. J Comp Neurol 500:777-787.

Table 1

Number and proportion of neurons co-expressing TH and VGLUT2 mRNA in the ventral tegmental area and substantia nigra of normal and 6-OHDA-lesioned immature (P15) and mature (P90) rats

	TH total		TH/VGLUT2		TH/VGLUT2 percent	
Normal	**P15**	**P90**	**P15**	**P90**	**P15**	**P90**
Total number	2775	3894	25	46		
VTA	102 ± 7	86 ± 9	1.8 ± 0.3	2 ± 0.3	1.8 ± 0.3 %	2.4 ± 0.5 %
SN	152 ± 12	109 ± 4	0.7 ± 0.4	0.3 ± 0.1	0.4 ± 0.2 %	0.3 ± 0.1 %
6-OHDA						
Total number	152	493	36	26		
VTA	39 ± 5 ***	17 ± 2 **	10.3 ± 1 ***	1.3 ± 0.4	26.3 ± 2.5 % ***	7.2 ± 1.5 % *†††
SN	4.6 ± 2.6 ***	8 ± 2 ***	0	0	0	0

Total number counted and mean ± SEM for the number of neurons per section (3 or 4 sections per rat at P15 and 5 sections per rat at P90) in four rats at each age. On the right, the number of dually labeled neurons (TH/VGLUT2) is expressed as a percentage of all neurons containing TH mRNA (TH total). The data at P15 are from Dal Bo et al (2008b). * $p < 0.05$, ** $p < 0.01$, *** $p < 0.001$ for 6-OHDA-lesioned versus normal rats of the same age. ††† $p < 0.001$ for P90 versus P15 rats.

Table 2

Mean number of immunoreactive axon terminals in the nucleus accumbens, neostriatum and substantia nigra of normal or 6-OHDA-lesioned immature (P15) and mature (P90) rats

	TH		VGLUT2		TH/VGLUT2	
	P15	**P90**	**P15**	**P90**	**P15**	**P90**
Normal						
nAcb	115 ± 6	64 ± 4	82 ± 21	97 ± 5	45 ± 5 (28%)	0
NStr	152 ± 12	109 ± 4	58 ± 19	68 ± 8	17 ± 6 (17%)	0
6-OHDA						
nAcb	63 ± 7 ***	15 ± 2 ***	46 ± 9	108 ± 13	37 ± 4 (37% *)	6/120
SN	29 ± 1	20 ± 3	44 ± 17	47 ± 3	22 ± 6 (46%)	0

An equivalent thin section surface of 1665 μm^2 was examined in each region and each rat, as explained in Materials and Methods. Mean ± SEM per rat, for the total number of rats and of axon terminals given in following Tables. In brackets, the number of dually labeled terminals (TH/VGLUT2) is expressed as a percentage of all terminals containing TH. * $p < 0.05$, *** $p < 0.001$ for 6-OHDA-lesioned versus normal rats of the same age.

Table 3

Structural features of immunoreactive axon terminals in the nucleus accumbens of normal or 6-OHDA-lesioned immature (P15) and mature (P90) rats

	TH		VGLUT2		TH/VGLUT2
	P15	**P90**	**P15**	**P90**	**P15**
Normal					
Total number	807	511	574	779	318
Mean diameter (µm)	0.49 ± 0.02	0.49 ± 0.02	0.54 ± 0.02	0.69 ± 0.02 §§§ †††	0.58 ± 0.04 §
% with synaptic junction	14 ± 2	3 ± 1 †††	21 ± 2	36 ± 2 †††	34 ± 3
Length of junction (µm)	0.17 ± 0.02	0.19 ± 0.02	0.19 ± 0.02	0.28 ± 0.01 ††	0.16 ± 0.03
Synaptic incidence (%)	37 ± 5	7 ± 1 †††	58 ± 6	96 ± 6 †††	110 ± 9
6-OHDA-lesioned					
Total number	440	120	325	860	256
Mean diameter (µm)	0.52 ± 0.03	0.53 ± 0.03	0.58 ± 0.03	0.70 ± 0.01 §§§ ††	0.64 ± 0.03 §
% with synaptic junction	25 ± 2 **	9 ± 2 * †††	21 ± 2	37 ± 2 †††	34 ± 5
Length of junction (µm)	0.16 ± 0.01	0.22 ± 0.04	0.14 ± 0.01	0.26 ± 0.01 †††	0.13 ± 0.03
Synaptic incidence (%)	70 ± 6 ***	22 ± 5 * †††	71 ± 8	106 ± 7 ††	130 ± 20

An equivalent thin section surface of 1665 μm^2 was examined in each rat, as explained in Materials and Methods. Mean ± SEM per rat, from 7 rats at P15 and 8 rats at P90, for the total number of terminals indicated in brackets. In view of their absence in normal rat and very small number after 6-OHDA lesion, no values are listed for TH/VGLUT2 immunopositive axon terminals in mature (P90) rats. See Results for description of differences between the three categories of labeled terminals at the same age (§ $p < 0.05$ versus TH; §§§ $p < 0.001$), between terminals in a given category in normal or 6-OHDA-lesioned rats of the same age (* $p < 0.05$, ** $p < 0.01$, *** $p < 0.001$), and between terminals of a given category in normal or 6-OHDA-lesioned rats according to age (†† $p < 0.01$, ††† $p < 0.001$).

Table 4

Structural features of immunoreactive axon terminals in the neostriatum of immature (P15) and mature (P90) normal rats

	TH		VGLUT2		TH/VGLUT2
	P15	**P90**	**P15**	**P90**	**P15**
Total number	242	345	174	205	52
Mean diameter (μm)	0.41 ± 0.01	0.43 ± 0.01	0.57 ± 0.07	0.60 ± 0.03 §§	0.53 ± 0.03 §
% with synaptic junction	9 ± 0.4	3 ± 1 ††	26 ± 1 §§§	36 ± 4 §§	38 ± 4 §§
Length of junction (μm)	0.19 ± 0.01	0.16 ± 0.01	0.19 ± 0.02	0.22 ± 0.02	0.20 ± 0.01
Synaptic incidence (%)	18 ± 1	6 ± 2 ††	70 ± 4 §§§	99 ± 12 §§	93 ± 11 §§

Means ± SEM per rat from 3 rats at each age, for the total number of terminals indicated in brackets. No TH/VGLUT2 immunopositive axon terminals were observed in mature (P90) rats. See Results for description of differences between categories of labeled terminals at the same age (§ $p < 0.05$, §§ $p < 0.01$, §§§ $p < 0.001$ versus TH), and between P15 and P90 normal rats (†† $p < 0.01$).

Table 5

Structural features of immunoreactive axon terminals in the substantia nigra of immature (P15) and mature (P90) 6-OHDA-lesioned rats

	TH		VGLUT2		TH/VGLUT2
	P15	**P90**	**P15**	**P90**	**P15**
Total number	86	61	133	140	67
Mean diameter (µm)	0.50 ± 0.06	0.50 ± 0.04	0.64 ± 0.04	0.75 ± 0.06 §	0.73 ± 0.09
% with synaptic junction	34 ± 4	5 ± 1 ††	25 ± 4	34 ± 1 §§§	39 ± 3
Length of junction (µm)	0.23 ± 0.02	0.17 ± 0.03	0.26 ± 0.02	0.25 ± 0.01 §	0.24 ± 0.01
Synaptic incidence (%)	78 ± 9	14 ± 3 ††	65 ± 11	104 ± 2 §§§ †	120 ± 10 *§*

Means ± SEM from 3 rats at each age, for the total number of terminals indicated in brackets. No TH/VGLUT2 immunopositive terminals were observed in mature (P90) rats. See Results for description of differences between categories of labeled terminals at the same age (§ $p < 0.05$ and §§§ $p < 0.001$ versus TH; *§* $p < 0.05$ versus TH and VGLUT2), and between P15 and P90 6-OHDA-lesioned rats († $p < 0.05$, †† $p < 0.01$).

FIGURE LEGENDS

Figure 1 - Low and higher magnification pictures from TH immunostained sections taken at the same transverse level across the ventral mesencephalon, in P15 (**A**, **A'**, **B**, **B'**) and P90 rats (**C**, **C'**, **D**, **D'**), normal (**A**, **A'**, **C**, **C'**) or neonatally lesioned with 6-OHDA (**B**, **B'**, **D**, **D'**). These micrographs and those of Fig. 2 illustrate the various conditions in which the mesencephalic TH neurons of adult rat (P90) were examined by comparison to immature rat (P15) for co-expression of VGLUT2 mRNA (Fig. 3) or colocalization of VGLUT2 protein in some of their axon terminals (varicosities) (Figs. 4-8). Note that, at both ages, TH immunostained cell bodies and dendrites were almost totally absent from the SN of 6-OHDA-lesioned rats, but still present in appreciable number in the VTA. Note how the pattern of TH immunostaining in the zona reticulata of SN (framed area) differs according to age and to normal and post-lesioned state. In normal rats at both ages, only dendrites (and at P15, a few cell bodies still migrating toward their final destination) are seen in this part of SN. In the 6-OHDA-lesioned rats, TH immunostained dendrites are no longer visible in the zona reticulata, but fine, varicose TH immunostained fibers may be observed to have pervaded this region at P15, and to have developed into a relatively dense axonal neoinnervation at P90 (for further description and illustration, see Fernandes Xavier et coll., 1994). Scale bars (1 mm in **D** and 200 μm in **D'**).

Figure 2 - Micrographs from TH-immunostained sections at a more rostral transverse level than in Fig. 1, illustrating the nAcb and NStr in P15 (**A, A', B, B'**) and P90 (**C**, **C'**, **D**, **D'**) rats, normal (**A**, **A'**, **C**, **C'**) or neonatally lesioned with 6-OHDA (**B**, **B'**, **D**, **D'**). The low magnification pictures illustrate the almost total disappearance of DA (TH immunostained) innervation in the NStr, but persistence of a significant number of TH immunostained terminals in the nAcb (as well as in the olfactory tubercle, ot) of 6-OHDA-lesioned rats (**B**, **D**). This is also apparent in the higher magnification views of the nAcb (**A'-D'**). Scale bar (in **D'**): 200 μm.

Figure 3 - Expression of TH and VGLUT2 mRNAs in SNc and VTA neurons of 90 day-old normal (**A-C**) or neonatally 6-OHDA-lesioned (**D-F**) rats. Double *in situ* hybridization with DIG-labeled and radiolabeled to detect TH mRNA (purple) and VGLUT2 mRNA (silver grains), respectively. **A** and **D**: Low power micrographs

from normal (**A**) and 6-OHDA-lesioned rat (**D**) illustrating the effects of the 6-OHDA lesion. At this low magnification, the silver grain labeling of VGLUT2 mRNA are barely visible, but there is an almost total disappearance of the TH mRNA labeling in the SNc, as well as a considerable reduction of this labeling in the VTA as a result of the 6-OHDA lesion. In **B** and **C**, co-expression of TH and VGLUT2 mRNA is observed in a few neurons of the SNc and VTA of normal rats (thick black arrows). In 6-OHDA-lesioned rats, there are no neurons expressing both TH and VGLUT2 mRNA in the remnants of the SNc (**E**), but some surviving DA neurons co-express VGLUT2 mRNA in the VTA (thick black arrow in **F**). Some neurons expressing only VGLUT2 are present in the SNc and VTA of both normal and 6-OHDA-lesioned rats, as exemplified in **E** (empty arrow). Scale bar (in **F**): 25 μm.

Figure 4 - Low magnification electron micrographs illustrating immunoreactive axon terminals (varicosities) in the nAcb of P15 (**A**, **B**) and P90 rats (**C**, **D**), normal (**A**, **C**) or neonatally lesioned with 6-OHDA (**B**, **D**), after dual immunolabeling for TH and VGLUT2. In this and the following figures, TH and VGLUT2 were respectively labeled with the immunoperoxidase technique (fine DAB precipitate) and the immunogold technique (silver intensified, immunogold particles), and varicosities labeled for only TH, only VGLUT2 and both TH/VGLUT2 designated by thin black arrows, empty arrows and thick black arrows, respectively. In the small area illustrated in **A** (P15, normal rat), only varicosities singly labeled for TH or VGLT2 are visible, whereas in **B** (P15, 6-OHDA-lesioned rat), several dually, TH/VGLUT2-labeled varicosities (thick black arrows), in addition to singly labeled ones, may be observed. Three of these four doubly labeled terminals are closely apposed to a neuronal cell body (N in nucleus). In adult rats (**C, D**), singly labeled TH and VGLUT2 varicosities are seen in both the normal and 6-OHDA-lesioned rat, but not dually labeled ones. Also note the reduced number of only TH varicosities in **B** and **D** (6-OHDA-lesioned rat) compared to **A** and **B** (normal rat). Scale bars: 1 μm.

Figure 5 - Higher magnification views of immunoreactive axon terminals in the nAcb of P15 and P90 normal rats, after dual immunolabeling for TH (immunoperoxidase-DAB) and VGLUT2 (immunogold). At P15 (**A**, **B**), but not P90 (**C-E**), dually immunolabeled terminals (thick black arrows) are seen in addition to

terminals singly labeled for TH (thin black arrows) or VGLUT2 (empty arrows). In **A**, a synaptic junction (between small arrows) is formed by the dually labeled terminal, which is also the case for the larger of the two dually labeled terminals in **B**. In **C**, note the two large asymmetrical synaptic contacts (between small arrows) onto dendritic spines (sp) formed by one of two nearby VGLUT2 terminals. The larger one of these contacts appears to be annular (see also Fig. 6 E). In **D**, a VGLUT2 varicosity is directly apposed to one of two TH terminals. In **E**, the left-sided VGLUT2 varicosity appears to make synapse (between small arrows) onto the dendritic profile to which the TH terminal is directly apposed. Also note the generally larger size of VGLUT2 compared to TH labeled terminals. Scale bars: 0.5 μm.

Figure 6 - Axon terminals from the nAcb of P15 (**A**-**D**) and P90 rats (**E**-**H**) neonatally lesioned with 6-OHDA, after dual immunolabeling for TH (immunoperoxidase-DAB) and VGLUT2 (immunogold). Dually immunolabeled terminals (thick black arrows) were numerous at P15, in addition to terminals singly labeled for TH (thin black arrows) or for VGLUT2 (empty arrows). In **A** and **B**, two of these terminals are seen in synaptic junction (between small arrows) with dendritic profiles (branch, db, in A; spine, sp, in B). In **C** and **D**, the dually labeled varicosities presumably make synapse in another plane of section. The three adjacent VGLUT2 varicosities in **C** are directly apposed to one another, and the elongated one displays an asymmetrical synaptic junction (between small arrows). In **D**, the dually labeled varicosity may be observed to emerge from its thin, unmyelinated parent axon. In **E** and **F**, note the larger size of VGLUT2 compared to TH varicosities (in **F**) as already observed at P15. The larger of the two VGLUT2 varicosities in **E** forms a wide annular, asymmetrical synaptic specialization (between small arrows) on a dendritic spine (sp), as already seen in Fig. 5 C. In **F**, the two VGLUT2 varicosities are directly apposed to one another, and also to a dendritic spine (sp) to which the lower of two TH varicosities is also juxtaposed. **G** and **H** illustrate in adjacent thin sections the very rare occurrence of a dually labeled terminal in the nAcb of adult rats neonatally lesioned with 6-OHDA. Scale bar (in **H**): 0.5 μm.

Figure 7 - Immunoreactive axon terminals from the NStr of normal P15 (**A**, **B**) and P90 rats (**C**, **D**) after dual immunolabeling for TH (immunoperoxidase-DAB)

and VGLUT2 (immunogold). In **A**, an axon terminal labeled for VGLUT2 (empty arrow) and two smaller varicosities labeled for **TH** (thin black arrows) are seen. In **B**, a dually labeled varicosity (thick black arrow) forms two asymmetrical synaptic contacts (between small arrows) onto small dendritic profiles. **C** and **D** demonstrate in adjacent thin sections the presence of VGLUT2 and TH axon terminals close to one another. Note the asymmetrical synapse (between small arrows) formed by the VGLUT2 terminal on the left. Scale bar (in **D**): 0.5 µm.

Figure 8 - Immunoreactive axon terminals of the DA neoinnervation in SN of 6-OHDA-lesioned P15 (**A**, **B**) and P90 rats (**C**, **D**), after dual immunolabeling for TH (immunoperoxidase-DAB) and VGLUT2 (immunogold). In **A,** the singly labeled TH terminals (thin black arrow) appears to be synaptic (between small arrows), as was often the case for these varicosities at P15. **B** is an example (thick black arrow) of the many dually labeled varicosities which were then found to be all synaptic (between small arrows) in the remnants of SN. This synaptic junction is made onto a large dendritic branch (db). **C** and **D** illustrate in adjacent thin sections the presence of TH (thin black arrows) as well as VGLUT2 axon varicosities (empty arrows) in the remnants of SN, at an age when its DA neoinnervation no longer displays doubly labeled varicosities. In **D**, note the small synaptic contact (between arrows) made by the VGLUT2 varicosity with the large dendritic branch (db) to which the TH varicosity is also juxtaposed. Scale bar (in **D**): 0.5 µm.

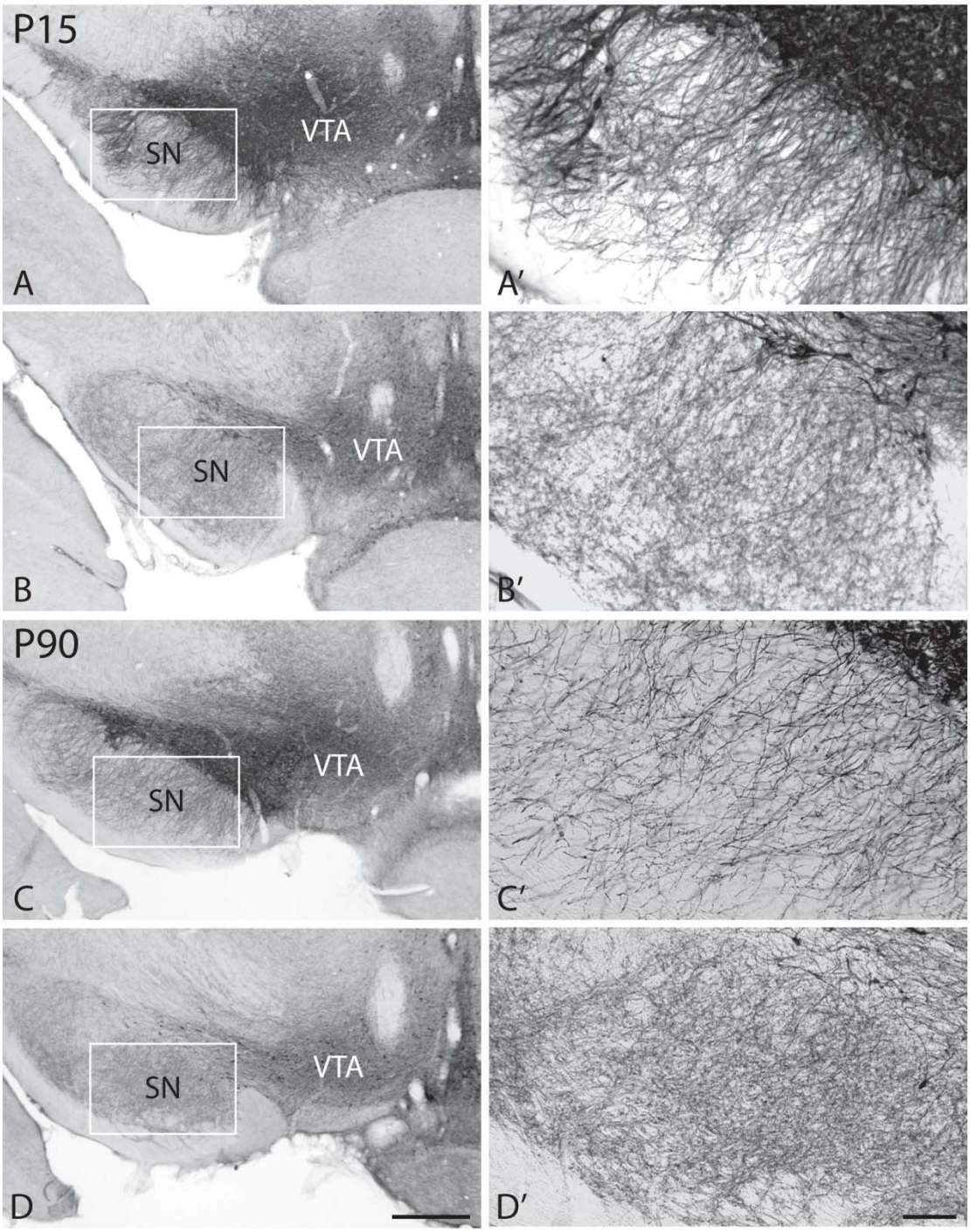

Figure 1 – Low-magnification and higher magnification pictures from Thimmunostained sections taken at the same transverse level across the ventral mesencephalon, in P15 and P90 rats, normal or neonatally lesioned with 6-OHDA

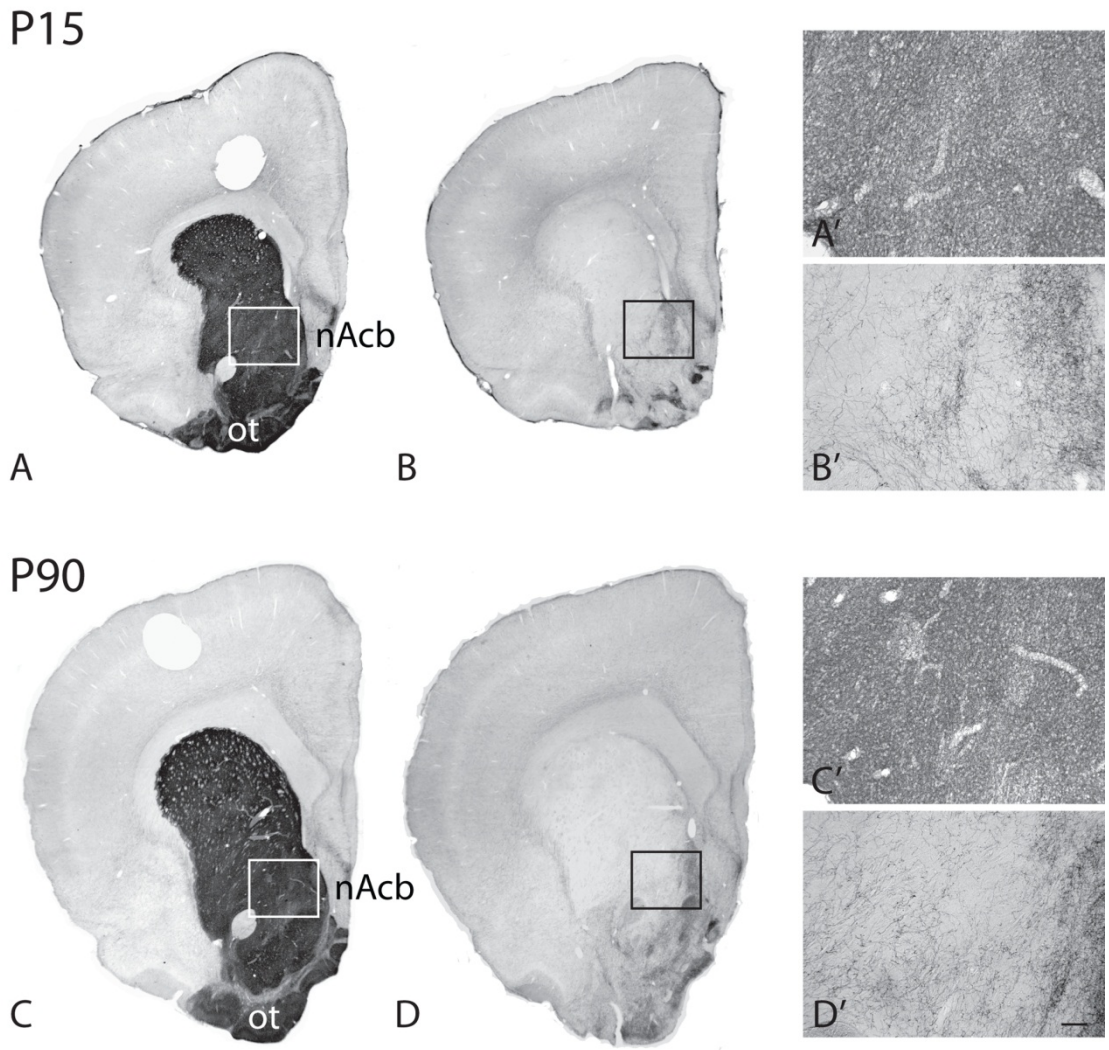

Figure 2 – Micrographs from TH-immunostained sections at a more rostral transverse level than in Figure 1, illustrating the nAcb and NStr in P15 and P90 rats, normal or neonatally lesioned with 6-OHDA

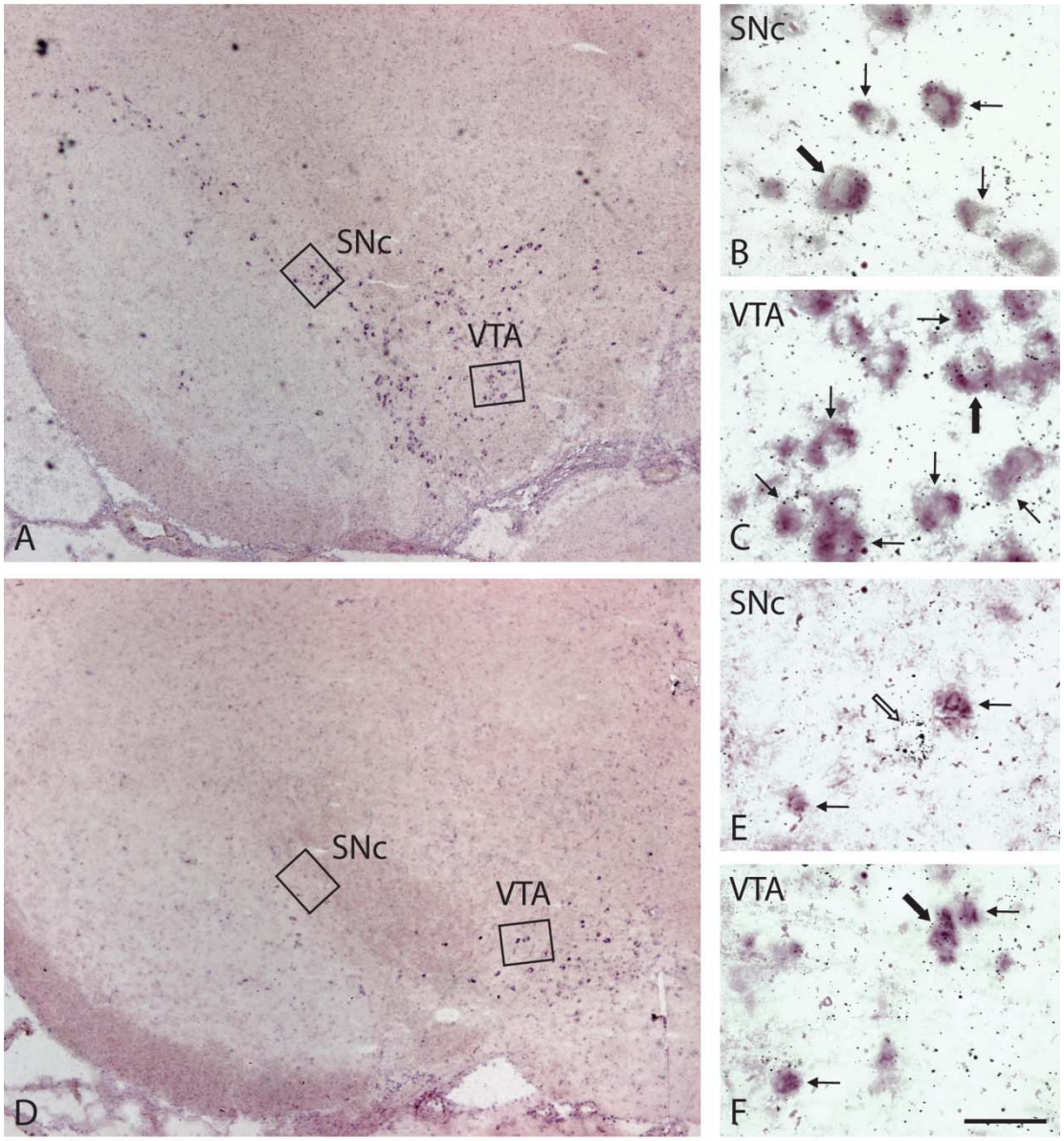

Figure 3 – Expression of TH and VGLUT2 mRNAs in SNc and VTA neurons of 90-day-old normal or neonatally 6-OHDA-lesioned rats

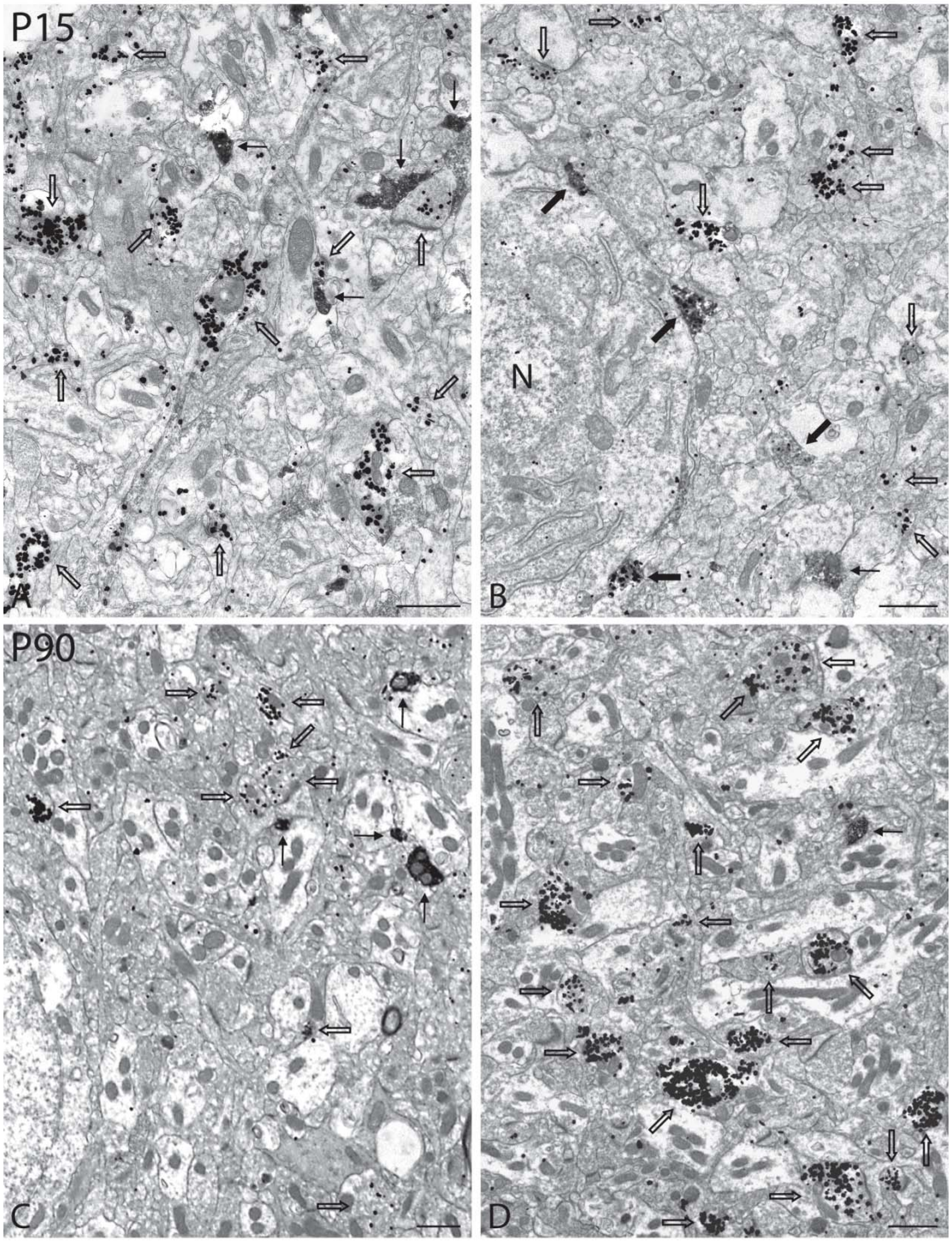

Figure 4 – Low-magnification electron micrographs illustrating immunoreactive axon terminals (varicosities) in the nAcb of P15 and P90 rats, normal or neonatally lesioned with 6-OHDA, after dual immunolabeling for TH and VGLUT2

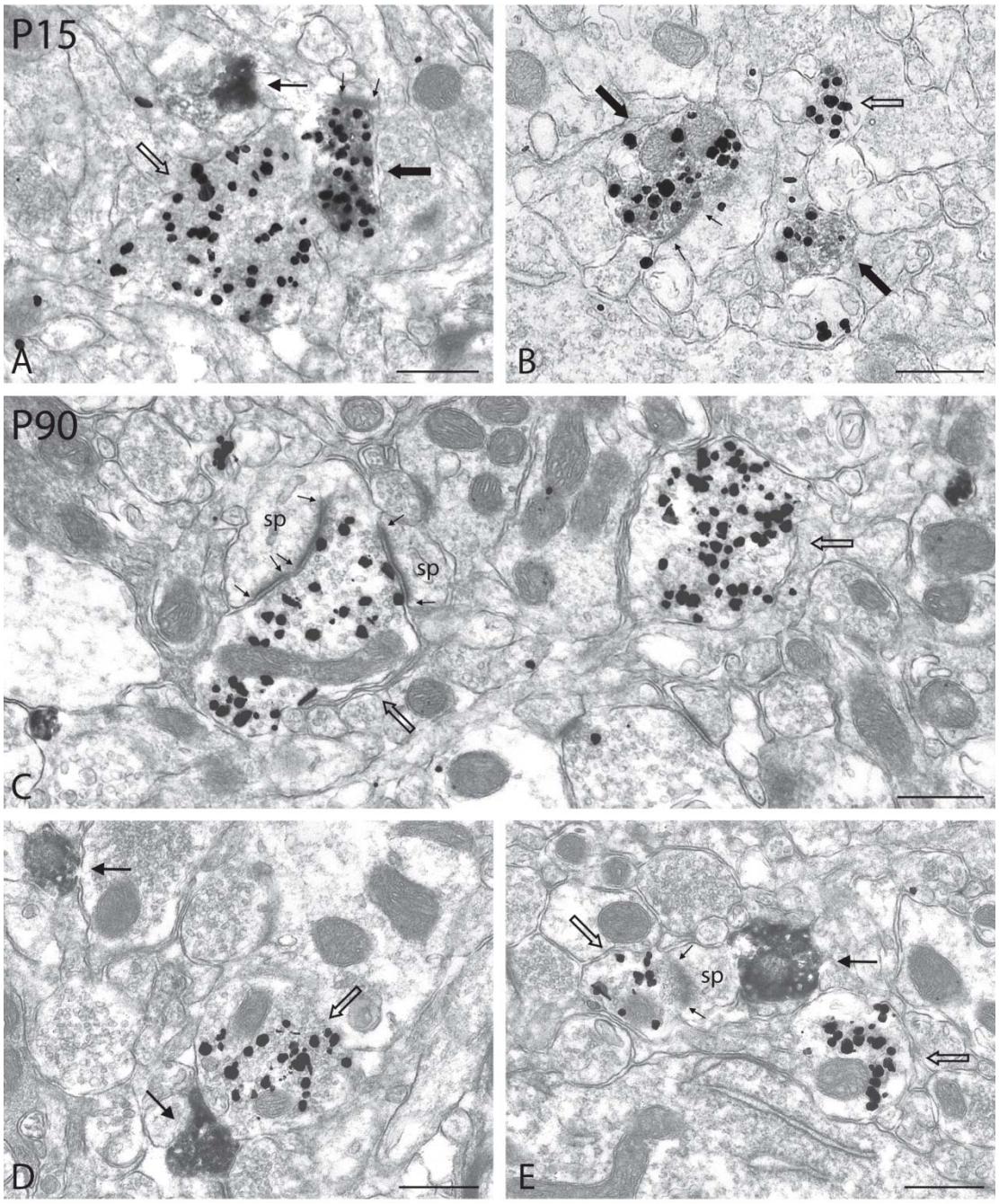

Figure 5 – Higher magnification views of immunoreactive axon terminals in the nAcb of P15 and P90 normal rats, after dual immunolabeling for TH (immunoperoxidase-DAB) and VGLUT2 (immunogold)

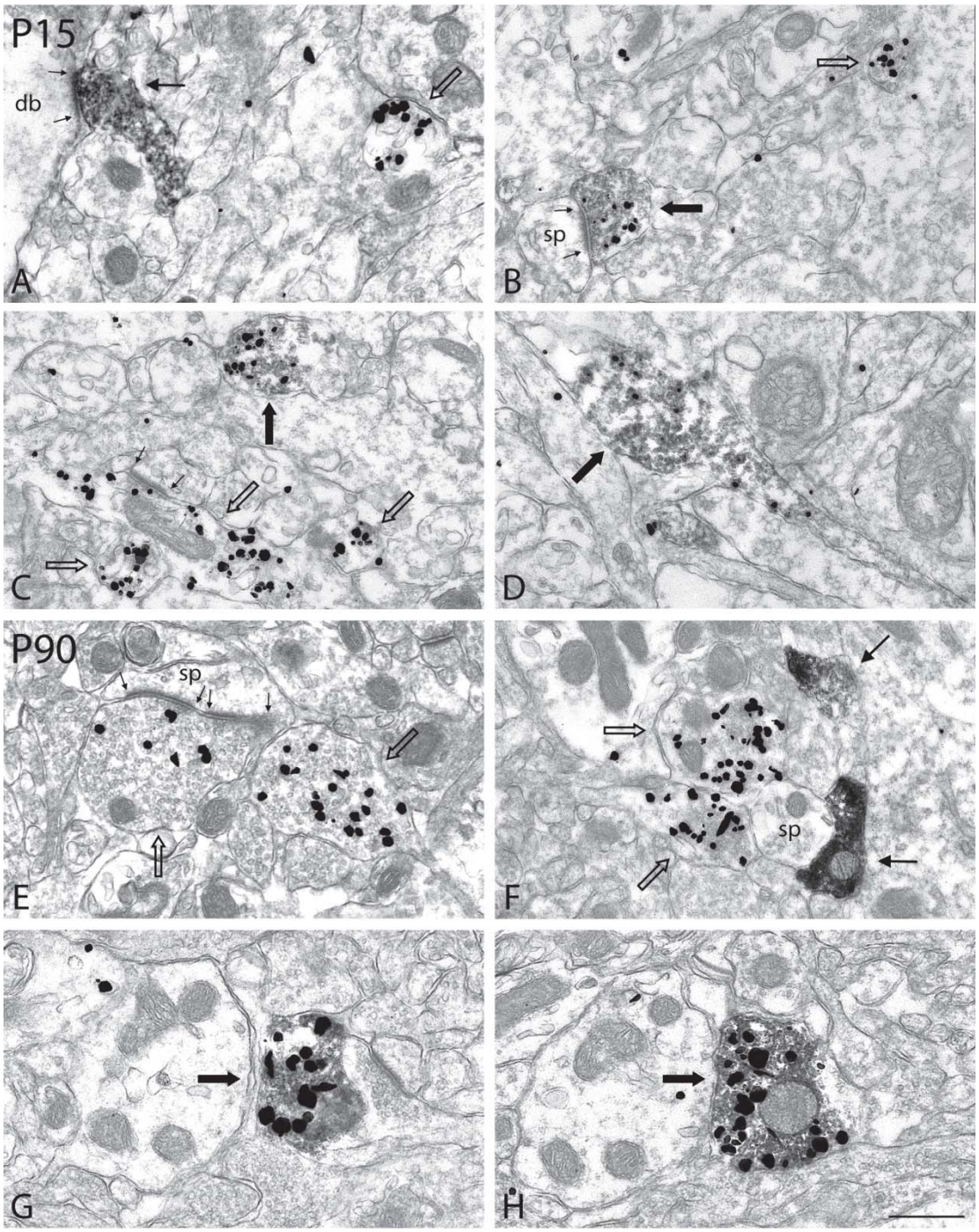

Figure 6 – Axon terminals from the nAcb of P15 and P90 rats neonatally lesioned with 6-OHDA, after dual immunolabeling for TH (immunoperoxidase-DAB) and VGLUT2 (immunogold)

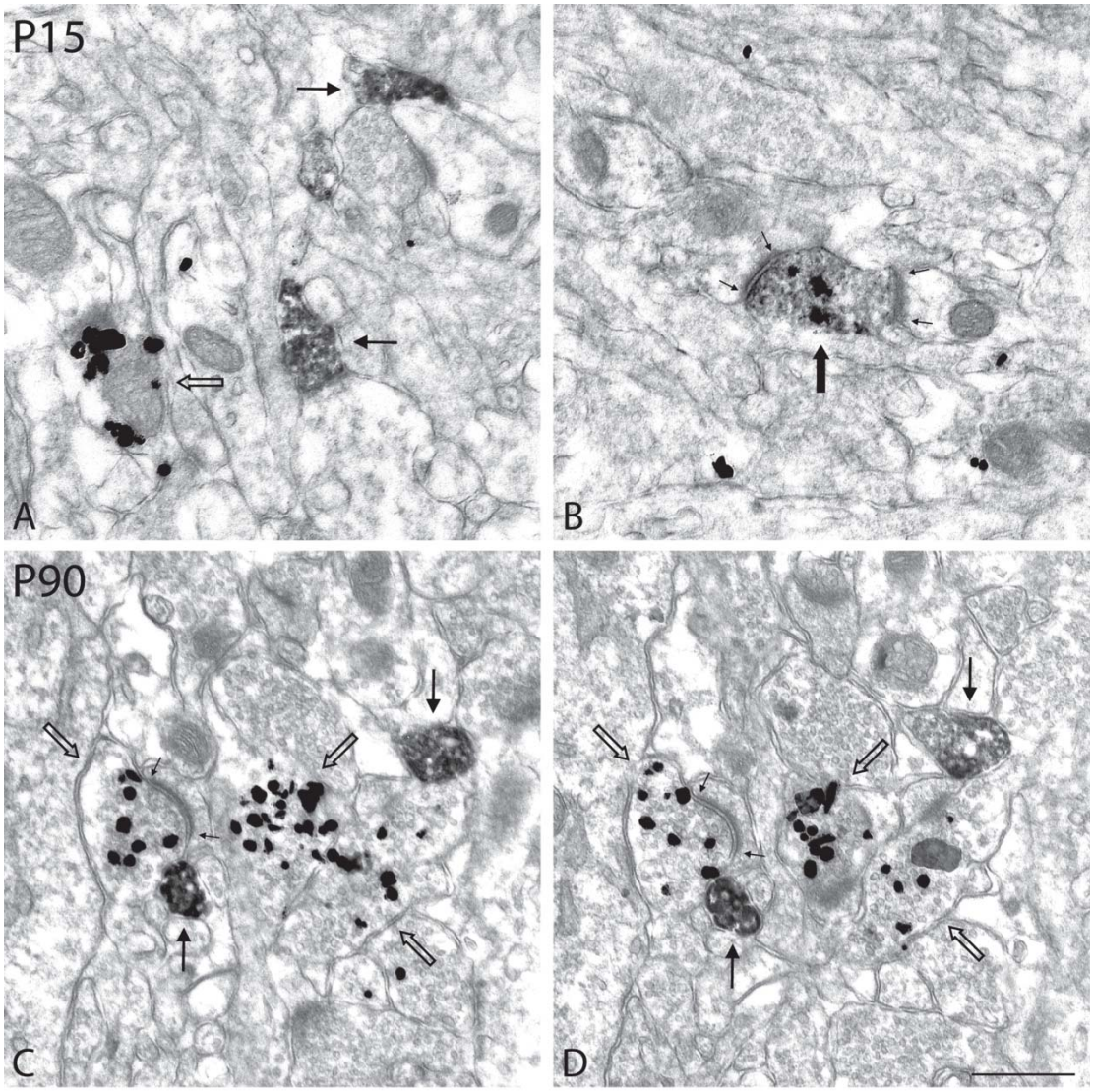

Figure 7 – Immunoreactive axon terminals from the NStr of normal P15 and P90 rats after dual immunolabeling for TH (immunoperoxidase-DAB) and VGLUT2 (immunogold)

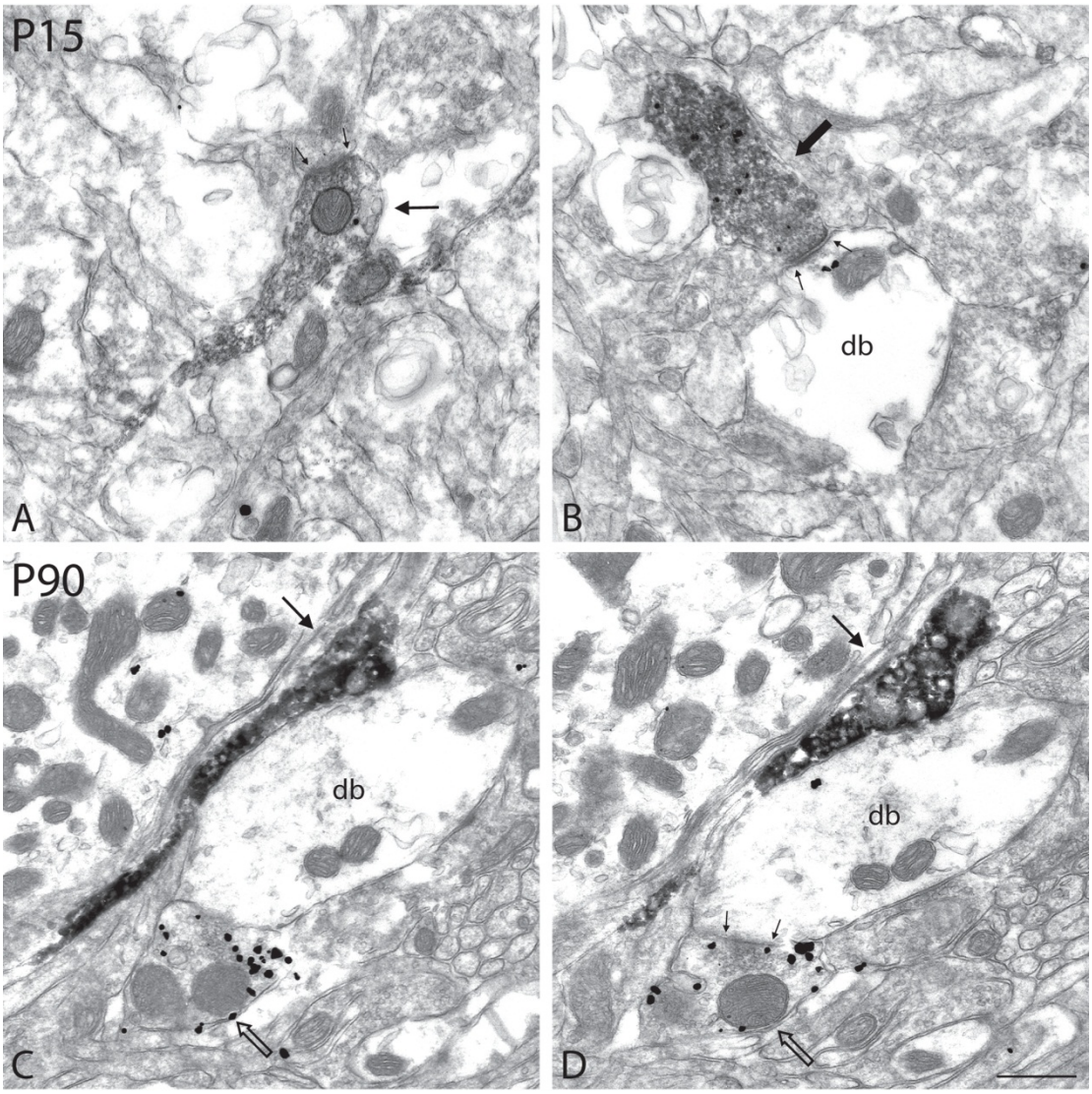

Figure 8 – Immunoreactive axon terminals of the DA neoinnervation in SN of 6-OHDA-lesioned P15 and P90 rats, after dual immunolabeling for TH (immunoperoxidase-DAB) and VGLUT2 (immunogold)

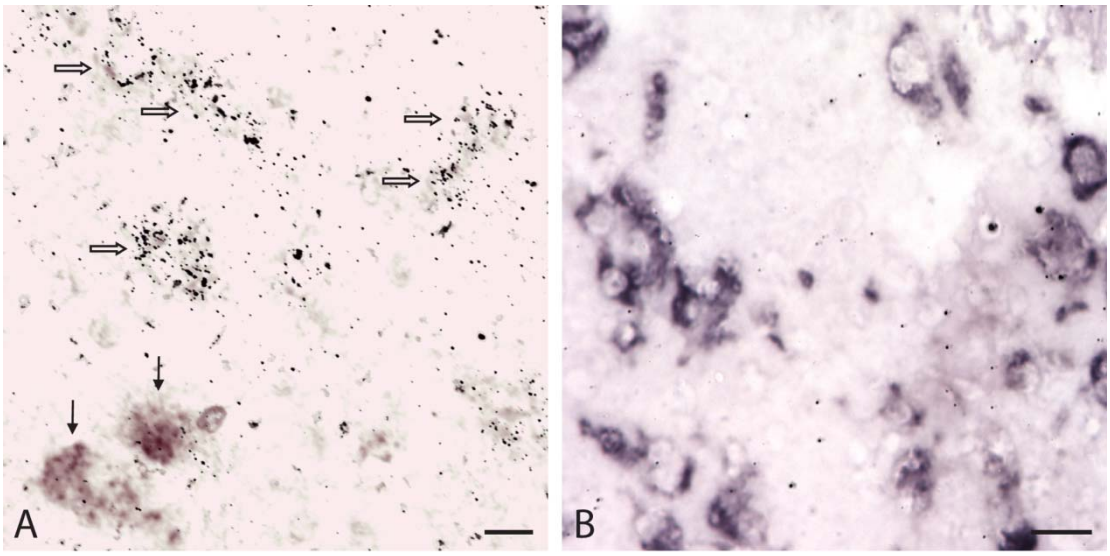

Supplementary Figures

A - After double *in situ* hybridization with a radiolabeled probe to detect VGLUT2 mRNA and DIG to detect TH mRNA, many neurons display strong VGLUT2 mRNA labeling (empty arrows) in a region of the red nucleus bordering the parabrachial pigmented nucleus (PBP) in a normal mature (P90) rat. Two neurons of the PBP, labeled for TH only (black arrows) are visible at lower left.

B –Section from the same region of the red nucleus in a 15 day-old normal rat, illustrating the lack of cellular VGLUT2 mRNA labeling after tissue processing for double *in situ* hybridization (DIG-labeling for TH mRNA; radiolabeling for VGLUT2 mRNA), but with a sense probe against VGLUT2 mRNA. Neurons labeled for TH ony are designated by black arrows. Scale bar (for A and B): 25 μm.

Chapitre 3 – Deuxième article

Ultrastructural Characterization of the Meso-striatal Dopamine Innervation in Mice, Including Two Mouse Lines of Conditional VGLUT2 Knockout in Dopamine Neurons

Publié en 2012

dans:

The European Journal of Neuroscience

35 : 527-538

Noémie Bérubé-Carrière, Ginette Guay, Guillaume Fortin, Klas Kullander, Lars Olson, Åsa Wallén-Mackenzie, Louis-Éric Trudeau, Laurent Descarries

Ce deuxième article est le résultat des expériences entreprises dans la seconde partie de mon doctorat. Lors d'un séjour en Suède dans le laboratoire de Dr Wallén-Mackenzie, j'ai effectué les marquages immunocytochimiques sur des souris normales et cKO, jeunes et adultes. Le même travail a été accompli sur des souris du laboratoire Trudeau. J'ai été assisté par Ginette Guay pour la préparation et la collecte du matériel pour la microscopie électronique. Les travaux ainsi que la rédaction de l'article ont été supervisés par les Drs Descarries et Trudeau.

ULTRASTRUCTURAL CHARACTERIZATION OF THE MESO-STRIATAL DOPAMINE INNERVATION IN MICE, INCLUDING TWO MOUSE LINES OF CONDITIONAL VGLUT2 KNOCKOUT IN DOPAMINE NEURONS

Noémie BÉRUBÉ-CARRIÈRE [1], Ginette GUAY [1], Guillaume M. FORTIN [2],
Klas KULLANDER [3], Lars OLSON [4], Åsa WALLÉN-MACKENZIE [3],
Louis-Eric TRUDEAU [2,6] and Laurent DESCARRIES [1,5,6]

Departments of [1] Pathology and Cell Biology, [2] Pharmacology, and [5] Physiology,
Faculty of Medicine; [6] Groupe de Recherche sur le Système Nerveux Central;
Université de Montréal, Montréal, QC, Canada;
[3] Department of Neuroscience, Unit of Developmental Genetics,
Uppsala University, Uppsala, and
[4] Department of Neuroscience, Karolinska Institutet, Stockholm, Sweden

Running title: **Dopamine innervation of mouse striatum**

Corresponding author: Laurent Descarries m.d.

Keywords: nucleus accumbens, neostriatum, conditional *Vglut2* KO, tyrosine hydroxylase immunocytochemistry, electron microscopy, diffuse transmission

Abstract

Despite the increasing use of genetically modified mice to investigate the dopamine (DA) system, little is known about the ultrastructural features of the striatal DA innervation in the mouse. This issue is particularly relevant in view of recent evidence for expression of the vesicular glutamate transporter 2 (VGLUT2) by a subset of mesencephalic DA neurons in mouse as well as rat. We used immuno-electron microscopy to characterize tyrosine hydroxylase (TH)-labeled terminals in the core and shell of nucleus accumbens and the neostriatum of two mouse lines in which the *Vglut2* gene was selectively disrupted in DA neurons (cKO), their control littermates, and C57BL/6/J wild-type mice, aged P15 or adult. The three regions were also examined in cKO mice and their controls of both ages after dual TH/VGLUT2 immunolabeling. Irrespective of the region, age and genotype, the TH immunoreactive varicosities appeared comparable in size, vesicular content, percent with mitochondria, and exceedingly low frequency of synaptic membrane specialization. No dually labeled axon terminals were found at either age in control as well as cKO mice. Unless TH and VGLUT2 are segregated in different axon terminals of the same neurons, these results favor the view that the glutamatergic cophenotype of mesencephalic DA neurons is more important during the early development of these neurons than for the establishment of their scarce synaptic connectivity. They also suggest that, in mouse even more than rat, the meso-striatal DA system operates mainly through non-targeted release of DA, diffuse transmission, and the maintenance of an ambient DA level.

Introduction

The word «synapse» was coined by Sherrington (1897) more than 50 years before synaptic junctions between CNS neurons were first seen. It was meant to designate sites of functional contact between distinct neuronal entities. When electron microscopy revealed the presence of small areas of plasma membrane differentiation between neuronal elements, against which storage-like vesicles accumulated on the side of presumed transmitter release (Robertson, 1953; Palade & Palay, 1954), these junctional complexes came to be recognized as the hallmark of synapses (Peters & Palay, 1996). For many years, they were actually considered as the only site of chemical communication between CNS neurons. Transmitter release would take place by exocytosis alongside presynaptic thickenings, and receptors for the transmitter would be confined to postsynaptic densities.

When CNS monoamine neurons were first demonstrated to be only partly synaptic, (Descarries *et coll.*, 1975; 1977), in the sense that many of their axon varicosities, terminals or boutons did not display a synaptic membrane specialization, it was logical to envisage the possibility that chemical transmission from these varicosities be widespread (diffuse or volume transmission) through activation of extrasynaptic transmitter receptors (Beaudet & Descarries, 1976). Moreover, because the presence of junctional complexes implied some fixity and permanence in the structural relationship between pre- and post-synaptic elements, the converse was suggestive of some flexibility and mobility of the releasing sites with respect to their immediate microenvironment (Descarries *et coll.*, 1975).

In this context, and in view of the increasing use of this species in contemporary neuroscience, the almost total lack of knowledge about the ultrastructural morphology of the meso-striatal innervation in mouse, and notably the junctional versus non junctional nature of its axon terminals, is surprising. The sole exception is the report of Triarhou et coll. (1988), describing the cytological relationships of TH-immunolabeled axon terminals in the laterodorsal neostriatum of two normal mice, as part of a broader group of investigations in heterozygous and homozygous Weaver mutants. Detailed information in the mouse is especially desired in view of the increasing use of genetically modified mice for studies of the DA

system (e.g., Birgner *et coll.*, 2009; Stuber *et coll.*, 2010), and notably the growing evidence that a subpopulation of mesencephalic DA neurons expresses the type 2 vesicular glutamate transporter (*Vglut2*) in both mouse and rat (Dal Bo *et coll.*, 2004; Kawano *et coll.*, 2006; Yamaguchi *et coll.*, 2007; Dal Bo *et coll.*, 2008; Mendez *et coll.*, 2008; Stuber *et coll.*, 2010). Moreover, recent optogenetic studies have shown that activation of mesencephalic DA neurons evokes glutamate-mediated synaptic events in the nucleus accumbens, but not the neostriatum of adult mice (Stuber *et coll.*, 2010; Tecuapetla *et coll.*, 2010), suggesting that the glutamatergic cophenotype of a subset of mesencephalic DA neurons might not regress with age in this species, contrary to the situation in rats (Bérubé-Carrière *et coll.*, 2009; see also Moss *et coll.*, 2011).

In this study, we used immuno-electron microscopy after TH immunolabeling, to analyze the fine structural characteristics of the meso-striatal DA innervation in the ventral and dorsal striatum of two lines of conditional KO mice (cKOs) in which the *Vglut2* gene was specifically disrupted in DA neurons, their respective controls and wild type mice. Mice aged P15 or adult were examined to detect morphological differences that might be associated with maturation. Doubly TH- and VGLUT2-immunolabeled material from control and cKO mice of both ages was also examined, to search for dually labeled terminals in the controls. Major differences were not observed between regions, ages and genotypes, and no dually labeled terminals were found. Nonetheless, the bulk of the observations provide new insights into the role of the glutamatergic co-phenotype of mesencephalic DA neurons, as well as the functional properties of the meso-striatal DA system.

Materials and Methods

Animals

All procedures involving animals and their care were conducted in strict accordance with the *Guide to care and use of experimental animals* (Ed. 2) of the Canadian Council on Animal Care, as well as the guidelines of Swedish regulation and European Union Legislation. The experimental protocols were approved by the Comité de déontologie pour l'expérimentation sur des animaux (CDEA) of the Université de Montréal, and by the Uppsala animal ethical committee. Housing was

at a constant temperature (21^0C) and humidity (60%), under a fixed 12 hours light/dark cycle and free access to food and water.

Two lines of *Vglut2*$^{f/f;DAT\text{-}cre}$ cKO mice and their littermate controls were used, in addition to wild-type mice (C57BL/6/J from Charles River, Saint-Constant, QC). The first line of cKOs (Upp) was generated in Uppsala (Sweden), according to Birgner et coll. (2009). In brief, transgenic mice in which *Cre* was specifically expressed in cells expressing the DA transporter DAT (*DAT-Cre* of mixed C57BL/6/J and Sv129 background) (Ekstrand *et coll.*, 2007) were mated with *Vglut2*$^{f/f}$ mice (mixed C57BL/6/J and Sv129 background) (Wallén-Mackenzie *et coll.*, 2006), and the colony maintained by breeding *Vglut2*$^{f/+;DAT\text{-}cre}$ with *Vglut2*$^{f/f}$ mice, to produce *Vglut2*$^{f/f;DAT\text{-}cre}$ cKO and *Vglut2*$^{f/f}$ control mice. The second line (Mtl) was produced in Montreal (Canada), as described in detail by Fortin et coll. (submitted). *DAT-Cre* transgenic mice (129/Sv/J background) (Zhuang *et coll.*, 2005) were mated with *Vglut2*$^{f/f}$ mice (mixed 129/Sv/J-C57BL/6/J background) (Tong *et coll.*, 2007), and the colony maintained by breeding *Vglut2*$^{f/+;DAT\text{-}cre}$ mice with *Vglut2*$^{f/f}$ mice, to produce *Vglut2*$^{f/f;DAT\text{-}cre}$ cKO and *Vglut2*$^{f/+;DAT\text{-}cre}$ control mice. In all experiments, only male mice were used to avoid potential confounding effects of gender.

Antibody characterization

As in our previous study (Bérubé-Carrière *et coll.*, 2009), the Clone TH-2 (T1299) from Sigma was used to detect tyrosine hydroxylase (TH). This monoclonal anti-TH antibody produced in mouse recognizes an epitope (amino acids 9-16) present in the N-terminal region of both rodent and human TH (Haycock, 1993). Its specificity for DA neurons was evidenced not only by the topographic distribution of immunoreactive TH cell bodies and axon terminals in the different brain regions examined (e.g., Fig.1), but also by their near total disappearance from mesencephalon and striatum after neonatal 6-OHDA lesion (Bérubé-Carrière *et coll.*, 2009). The polyclonal anti-VGLUT2 antibody (Synaptic Systems, Goettingen, Germany) was raised in rabbit against a Strep-Tag fusion protein from the C-terminal domain of the predicted sequence (amino acid 510-582) of rat vesicular glutamate transporter 2 (Takamori et coll., 2001). The immunocytochemical specificity of this particular antibody has been demonstrated by Western blot analysis of homogenized rat brains

and/or crude synaptic vesicle fractions from rat brain, in which a single broad brand slightly above 60 kDa was found, and by pre-adsorption experiments with the GST fusion protein used as immunogen, in which the immunostaining of rat brain sections was completely eliminated (Takamori *et coll.*, 2001; Persson *et coll.*, 2006; Zhou *et coll.*, 2007). This antibody has been previously used in combined immunocytochemical and *in situ* hybridization experiments to detect *Vglut2* mRNA in rat mesencephalic DA neurons (Kawano *et coll.*, 2006), as well as for double TH and VGLUT2 immunolabeling of axon terminals in rat striatum at the electron microscopic level (Dal Bo *et coll.*, 2008; Descarries *et coll.*, 2008; Bérubé-Carrière *et coll.*, 2009).

Single TH immunolabeling for light and electron microscopy

After deep anesthesia with sodium pentobarbital (80 mg/kg i.p.), immature (P15) and adult (70-90 day-old) mice were fixed by intra-cardiac perfusion of a solution of 3% acrolein in 0.1 M phosphate buffer (PB, pH 7.4) (50 ml for P15 mice; 100 ml for adult mice), followed by 4% PFA in the same buffer (100 ml for P15 mice; 150 ml for adult mice): 5 cKO (2 Upp and 3 Mtl) and 5 littermate controls (2 Upp and 3 Mtl) at P15, and 6 adult cKO (3 Upp and 3 Mtl) and their littermate controls (3 Upp and 3 Mtl). An additional experiment was also carried out in two adult, wild-type mice, in which 200 ml of 3% glutaraldehyde and 2.5% PFA in 0.1 M cacodylate buffer (pH 7.4) was perfused as primary fixative. In all cases, the brain was removed, post-fixed by immersion for 1 h in the PFA solution at 4°C, and washed in phosphate-buffered saline (PBS: 0.9% NaCl in 50 mM PB, pH 7.4). 50 um-thick transverse sections across the striatum (between stereotaxic levels 1.18 – 1.54 mm anterior to bregma in Franklin and Paxinos atlas (2008) were then cut in PBS with a vibrating microtome (VT100S; Leica Microsystems), immersed in 0.1% sodium borohydride (Sigma) in PBS for 30 min at room temperature, and washed in this buffer before immunocytochemical processing.

As already described in detail (Bérubé-Carrière *et coll.*, 2009), sections intended for light microscopy were sequentially incubated in blocking solution containing 0.1% Triton X-100 (1 h), mouse monoclonal anti-TH antibody diluted 1:1000 (24 h), biotinylated goat anti-mouse IgGs (Jackson Immunoresearch) diluted

1:1000 (1.5 h), a 1:1000 solution of horseradish peroxidase (HRP)-conjugated streptavidin (Jackson Immunoreseach) (1 h), and 3,3'-diaminobenzidine tetrahydrochloride (0.05% DAB, Vector) and 0.005% hydrogen peroxide (2-3 min).

Sections intended for electron microscopy were similarly processed except for the omission of Triton X-100 in the blocking solution. Once immunostained, they were osmicated for 1 h in 1% OsO_4, dehydrated in a graded series of ethanol, and flat embedded in Durcupan resin (Sigma) between two sheets of Aclar plastic (EMS/Cederlane). After polymerization, the areas of interest were excised from the Aclar sheets and glued at the tip of resin blocks. Ultrathin (silver-gold) sections were then cut from the surface of the blocks, stained with Reynold's lead citrate and examined by electron microscopy (Philips CM100).

Dual TH/VGLUT2 immunolabeling for electron microscopy

Sections were processed as above, except for incubation for 24 h at room temperature in a 1:500 dilution of both primary TH and VGLUT2 antibodies. After rinses in PBS, they were then placed overnight, at room temperature, in a 1:50 dilution of donkey anti-rabbit IgGs conjugated to 0.8 nm colloidal gold particles (Aurion, Netherlands), and treated with either IntenSE kit (Amersham, Oakville, ON, Canada) or the HQ Silver kit (Nanoprobes, NY, USA), to increase the size of immunogold particles. The immunogold-labeled sections were then processed for TH with the immunoperoxidase technique, as above.

Immunocytochemical controls included double immunocytochemical processing, but without either one or both primary antibodies. Only the expected single labeling was then observed after omitting one of the primary antibodies, and no labeling in the absence of both of them.

Quantitative analysis of TH-immunolabeled material

After single TH immunolabeling for electron microscopy, the nucleus accumbens core (NAC), nucleus accumbens shell (NAS) and neostriatum (NS) were examined in each of the 22 mice (P15: 5 cKO and 5 control; adult: 6 cKO and 6 control) fixed by primary fixation of acrolein, the NAS in 3 mice (Mtl) of each of these four groups, and the NAC only in the 2 wild-type, adult mice fixed with the

glutaraldehyde-formaldehyde mixture. In every region of each mouse, at least 25 electron micrographs were taken at a working magnification of 15 000 X, within a narrow area of a thin section less than 10 µm away from the tissue-resin border. The film negatives were scanned (Epson Perfection 3200), converted into positive pictures, and adjusted for brightness and contrast with Adobe Photoshop, before printing at a final magnification of 37 500 X.

Most immunolabeled profiles could then be positively identified as axon varicosities, i.e., axon dilations (> 0.25 µm in transverse diameter) containing aggregated small vesicles, often one or more mitochondria, and displaying or not a synaptic membrane specialization (junctional complex). Using the public-domain Image J processing software from NIH, all axon varicosity profiles showing a distinct contour were measured for area, long (L) and short (s) axes and mean diameter (L + s /2), and then classified as showing or not a synaptic junction, i.e. a localized straightening and thickening of apposed plasma membranes on either side of a slightly widened extracellular space. The length of junctional complexes was measured, the synaptic targets identified, and the synaptic frequency observed in single thin sections was extrapolated to the whole volume of varicosities by means of the stereological formula of Beaudet and Sotelo (1981), which takes into account the average size of varicosity profiles, the average length of visible junctions and the thickness of the sections to calculate the probability of seeing the junction if one is made by every varicosity.

In total, 1135 TH-immunolabeled axon terminals were thus examined in the P15 (550 in control; 585 in cKO), and 1451 in the adult mice (709 in control; 742 in cKO) (see Tables 1 and 2 for number examined in the different regions). In each control and cKO mice of both ages, the number of axon terminals examined in every region was almost the same. In the 2 wild-type adult mice fixed by perfusion of the glutaraldehyde-paraformaldehyde mixture, 115 terminals were examined.

Electron microscopic examination of TH/VGLUT2 immunolabeled material

After dual TH/VGLUT2 immunolabeling, the three areas of interest were examined in thin sections from the 12 cKO (Mtl) mice and their controls processed for single TH immunolabeling + one additional mouse in each group, for a total of 16

mice. In every region of each mouse, 10 to 26 electron micrographs were obtained as above, which allowed for the examination of a total of 969 electron micrographs and a thin section surface of 48 450 μm^2 (see Supplementary Table 1 for details and the number of labeled axon terminals visualized in each region and each group). In tissue areas closest to the tissue-resin border, there was obvious background labeling, in the form of dispersed silver-intensified gold particles. However, no attempt was made to subtract this non specific labeling for analysis of the results, because the VGLUT2 immunolabeling of axon varicosities was very strong, and no TH positive varicosities ever displayed 3 or more immunogold particles, except for a single profile of exceptionally large size, onto which 3 immunogold particles were seen (see Figure 6A).

Statistics

Statistical analyses were performed in Prism 5 (GraphPad, La Jolla, USA). One-way ANOVA and unpaired Student's *t*-test were used to assess statistical significance. Results are presented as mean values ± SEM. *P* values below 0.05 were considered statistically significant.

Results

Light microscopic visualization of striatal TH-immunostained innervation

In sections processed for light microscopic immunocytochemistry after TH-labeling with the immunoperoxidase-DAB technique, the expected very dense labeling of the DA innervation was observed throughout the ventral and dorsal striatum of control as well as cKO mice (Fig. 1). In such 50 µm-thick sections permeabilized with Triton X-100 and immunostained throughout their full thickness, this confluent labeling precluded any quantitative assessment of the number of axon varicosities in cKO versus control mice.

Ultrastructural features of TH immunoreactive varicosities

Immunoreactive axon varicosities (terminals) were readily identified as such in single thin sections for electron microscopy from material immunolabeled for TH only (Figs. 2-5). Irrespective of the region (NAC, NAS and NS) and experimental group examined, these axon terminals were relatively small, generally round or

oblong in shape but sometimes irregular in contour, and filled with small, round or ovoid synaptic vesicles, often accompanied by one or more mitochondria (Figs. 2-5). Larger varicosity profiles were also observed (e.g., Figs. 3D and 4E), but relatively uncommon. The immunoperoxidase-DAB labeling was in the form of a more or less dense, fine precipitate, often outlining the small vesicles or mitochondria and the plasma membrane of varicosities. In many instances, a varicosity profile could be seen emerging from its parent unmyelinated axon (Figs. 2B, 3C), in which case small vesicles were also present within the axon proper. It was not uncommon to find TH-labeled varicosities lying very close (Fig. 3F) or juxtaposed to one another (Fig. 5C), or almost in continuity along the same axon (Figs. 3A, 3D, 4E).

All morphological parameters of the TH-labeled varicosities in each region and both ages were initially analyzed separately for the two types of cKO mice and their respective littermate controls (see Supplementary Tables 2 and 3). However, because there were no statistically significant differences in dimensions, % with mitochondria or synaptic incidence between any of these subgroups, data from the two cKO lines were pooled for presentation, as well as the data from their respective controls (Tables 1 and 2).

Tables 1 and 2 give the results of this morphometric analysis for the three regions, P15 and adult and control or cKO mice. Overall, the diameter of TH-labeled varicosity profiles ranged between 0.39 and 0.49 μm, averaging 0.47 ± 0.01 μm. This corresponded to an area of 0.14 to 0.21 μm^2 (0.19 ± 0.01 μm^2 on average), as individually calculated by Image J. The proportion of labeled varicosities containing one or more mitochondria ranged from 27 - 48% (total average: 38 ± 2%). In contrast to unlabeled varicosity profiles in their immediate surrounding, only a very small proportion of the TH-labeled profiles from each region exhibited a morphologically defined area of synaptic membrane specialization in all experimental groups (P15 or adult mice, cKO mice and their controls, adult wild type mice). The few junctions that were observed (65 in total) were mostly symmetrical (e.g., Figs. 2A, 2C, 2D, 3A, 4A, 4C, 5A-A') and made either with dendritic branches (Fig. 2A, 2C, 2D, 3A, 4A, 5A-A'), or more rarely with spines (Fig. 4C). Although some labeled-varicosity

profiles were occasionally found in direct apposition with neuronal cell bodies, no morphologically defined axo-somatic synapses were seen.

Overall, the proportion of TH-labeled varicosities observed to form a synaptic junction in our single thin sections ranged from 0.5 - 5.1%, averaging 2.6 ± 0.5%. The mean length of junctions formed by these few synaptic varicosities ranged from 0.14 - 0.28 μm, averaging 0.20 ± 0.01 μm, again without significant difference between subgroups (Supplementary Table 4). According to the formula of Beaudet and Sotelo (1981), this would represent a synaptic incidence ranging from 1.1 - 11.8% and averaging 5.6 ± 1%, as extrapolated to the whole volume of varicosities. These percentages have to be regarded with caution, however, as they were calculated by means of a probabilistic formula applied to a very small number of occurrences.

Overall, there were more synapses made with dendritic branches than spines, but because the number of TH-labeled varicosities observed in synaptic junction was so small, it was not deemed proper to number their relative proportions. Both synaptic configurations were observed in each region, at both ages and in control as well as cKO mice, except in the NAC of adult control and cKO mice, two samples in which only a single varicosity was found to engage in a structurally identifiable synapse (with a dendritic branch). In neostriatum, two examples of synapses on the neck of spines were seen, including the one illustrated in Fig. 4A. This particular TH-labeled varicosity was most unusual in making two synapses with different dendritic branches.

As illustrated in Fig. 5, the 115 TH-labeled axon terminals examined in the NAC of adult wild-type mice perfused with a mixture of glutaraldehyde and formaldehyde did not differ in any way from those perfused with acrolein as primary fixative (average diameter: 0.46 ± 0.01 μm; area: 0.17 ± 0.01 μm^2; % with mitochondria: 34 ± 5%; average length of junctions: 0.19 ± 0.04 μm; frequency of synaptic junction in single thin sections: 3 ± 1%).

Lack of dually TH/VGLUT2 immunolabeled axon varicosities in mice ventral and dorsal striatum

As shown in Supplementary Table 3, and illustrated in Fig. 6, a large number of TH- or VGLUT2-immunolabeled axon terminals could be observed in the electron

microscopic material prepared for dual immunolabeling. Despite this extensive examination, however, not a single axon terminal was found to be convincingly dually labeled in either region of the control as well as cKO mice of both ages.

Discussion

The main finding of the present study is that DA (TH-labeled) axon varicosities in the ventral and dorsal mouse striatum are very rarely synaptic. This was observed in both immature and mature cKO and control animals, as well as in wild type adults.

Methodological considerations

The anatomical distribution of the immunocytochemical labeling obtained with the present TH antibody confirmed its specificity, as established in earlier studies (for example see Kawano *et coll.*, 2006). In theory, TH immunoreactivity should identify noradrenaline as well as DA axon terminals in the striatum, but the latter are known to be scarce in NS and only slightly more common in NAC and NAS (Carlsson, 1959; Moore & Card, 1984).

Because the present electron microscopic analysis was carried out in single rather than serial thin sections, there was a risk of underestimating the frequency with which the TH-labeled terminals made a synaptic membrane specialization, especially after labeling with the immunoperoxidase-DAB technique. This was the reason for keeping the density of DAB immunoprecipitate to a level ensuring clearcut detection, but which did not occlude eventual areas of synaptic membrane differentiation. However, all observed junctional complexes made by TH-labeled varicosities were relatively small, usually symmetrical, and often poorly differentiated. For this reason, and knowing how much synaptic junctions can vary in their amount of postsynaptic opacity (see Colonnier, 1968), mere localized straightenings of apposed membrane were accepted as evidence of a junction (e.g., Figs. 2D, 3A, 5A,A').

In the search for dually labeled terminals, there was no reason to doubt the double immunolabeling method used, since it had consistently provided positive results in the rat, and revealed the expected high number of varicosity profiles immunolabeled for either TH and VGLUT2 in the mouse. As in our previous studies,

VGLUT2 was detected with the immunogold and TH with the immunoperoxidase technique, to allow for comparison between double labeling and earlier or present single labeling data. The double immunolabeling was carried out in that order, because artefactual immunogold deposits over all TH positive terminals had been found in prior experiments carried out in the reverse order.

Intrinsic and relational features of striatal DA terminals

To our knowledge, this is the first extensive description of the ultrastructural characteristics of DA (TH-immunolabeled) axon terminal arborizations in ventral as well as dorsal striatum of the mouse. Triarhou et coll. (1988) provided some information about the relationships of TH-labeled varicosities in the dorsolateral striatum (but not the NAC or NAS), and it was not clear if the single section profiles of these varicosities had been systematically examined to estimate synaptic incidence. The relatively high synaptic frequency then reported for two wild type mice (27%) should therefore be regarded with caution.

The small average size of meso-striatal DA varicosities measured in the present study was consistent with earlier measurements made in rat by electron microscopic [^{3}H]DA uptake autoradiography (Descarries *et coll.*, 1996) or TH immunocytochemistry (Pickel *et coll.*, 1981; Freund *et coll.*, 1984; Voorn *et coll.*, 1986; Zahm, 1992; Descarries *et coll.*, 1996; Bérubé-Carrière *et coll.*, 2009). The sole exception was the study by Antonopoulos et coll. (2002) during postnatal rat development, in which an almost twice as large average size of TH-labeled varicosity profiles was reported (0.8-0.9 µm in diameter). This presumably reflected a sampling bias and could account for the exceedingly high values of synaptic incidence (80-100%) which were then extrapolated using the stereological formula of Beaudet and Sotelo (1981). The equivalent average size of striatal DA varicosities at P15 and in the adult had already been noted in our previous study in the rat (Bérubé-Carrière *et coll.*, 2009). If the size of axon terminals somehow relates to their physiological strength (Pierce & Lewin, 1994), this could indicate that these terminals are fully functional at P15. Likewise, the percentage of varicosity profiles exhibiting mitochondria was similar in all subgroups, suggesting comparable energetic demands.

The very low frequency of synaptic striatal DA varicosities observed in the NAC, NAS and NS of P15 and adult mice was suggestive of a species difference between mice and rats, in which previous measurements have yielded significantly higher proportions. Zahm (1992) had reported percentages of 2.3-2.9% in a large, systematic sample of TH-labeled varicosities from NAC, NAS and NS, but this was in single thin sections and not extrapolated to the whole volume of varicosities. In our own study after double TH and VGLUT2 immunolabeling, the values of synaptic incidence extrapolated to the whole volume of TH-labeled varicosities were 55% and 31% in the NAC and NS of P15 rats, and 7% and 6% in the NAC and NS of adult rats, respectively (Bérubé-Carrière *et coll.*, 2009). As repeatedly observed in rat, most of the rare junctional DA varicosities in mouse striatum made symmetrical synapses with dendritic branches. Strategic synaptic localizations such as the neck of spines (e.g., Freund *et coll.*, 1984; Descarries *et coll.*, 1996) were very rare in the mouse.

It was unexpected not to find a single axon terminal dually immunolabeled for both TH and VGLUT2 in neither the nucleus accumbens nor the neostriatum of P15 and P60 control mice. It is tempting to speculate that this finding is indicative of an earlier regression of the dual DA/glutamate phenotype with maturation in mice than rats. This results however needs to be reconciled with recent optogenetic findings, obtained in brain slices from adult mice, which demonstrate that selective stimulation of DA neurons of the VTA may evoke glutamatergic synaptic events in the NAs (Stuber *et coll.*, 2010; Tecuapetla *et coll.*, 2010). Several explanations have already been proposed for such a discrepancy (Moss *et coll.*, 2011), among which the most interesting could be an early segregation of TH and VGLUT2 in distinct axon terminals of meso-striatal DA neurons (Trudeau, 2004; El Mestikawy *et coll.*, 2011). Such a fundamental issue will obviously need to be addressed in future experiments.

Interestingly, the synaptic incidence of striatal DA varicosities as well as their size and the proportion containing mitochondria were similar in the two cKO mouse lines and their littermate controls. In another study carried out in parallel, a ~20% reduction in the number of DA neurons was recently documented in the ventral mesencephalon of the Mtl *Vglut2* cKO mice, accounting for a reduced density of DA innervation (~30%) and diminished DA release in the nucleus accumbens of these

mice (submitted). Furthermore, *in vitro*, the growth and survival of cultured DA neurons from these cKO mice was then shown to be impaired. Taken altogether, these observations suggest that the dual glutamate/dopamine phenotype of mesencephalic DA neurons, which is particularly prominent during development, could be more important for regulating the number and growth of these neurons than for their establishment and/or maintenance of a scarce synaptic connectivity.

A new image of the meso-striatal DA innervation

Even if a definitive description of the meso-striatal DA innervation in the mouse awaits its three dimensional reconstruction at the electron microscopic level, the present examination in single thin sections justifies a revision of pre-conceived notions on the morphological organization of this system. In rat, nigrostriatal DA axons have been shown to project directly to, and branch profusely within striatum (Gauthier *et coll.*, 1999; see also Prensa & Parent, 2001), giving rise to a very dense innervation, estimated at 1 x 10^8 varicosities per mm^3 in the striatal matrix and 1.7 x 10^8 in the striosomes and subcallosal streak (Doucet *et coll.*, 1986). As visualized with a viral vector expressing membrane-targeted green fluorescent protein, single meso-striatal DA axons form an extremely profuse, bush-like terminal arbour extending over a relatively large striatal volume (Matsuda *et coll.*, 2009). At the ultrastructural level, the frequent proximity and occasional juxtaposition of TH-labeled varicosity profiles reflects this density of innervation (e.g., Fig. 3 in Descarries *et coll.*, 1996). It is also apparent that, in all parts of striatum, many DA varicosities may be continuous along the same axon, and not spaced at intervals of a few microns, as is the case of its less dense serotonin innervation, for example (e.g., Soghomonian *et coll.*, 1987; 1989). Also meaningful is the presence of synaptic vesicle aggregates within narrow as well as enlarged segments of the DA axons (e.g., Freund *et coll.*, 1984; Voorn *et coll.*, 1986), which suggests that exocytotic DA release might occur along the whole extent of these axonal arborizations, and not only at their sites of varicose dilation.

Functional considerations

Because such a small proportion of striatal DA varicosities form differentiated synaptic junctions in the mouse, it may also be inferred that diffuse transmission

plays a particularly important role in the functioning of the meso-striatal system in this species. How this relates to specific functions and behaviors controlled by the DA system in mouse as opposed to other rodents and more phylogenetically distant species such as primates and humans remains to be determined. The extreme density of the meso-striatal DA innervation and the possible diffusion of DA in the extracellular space despite DA reuptake (Wightman & Zimmerman, 1990), has also led to us to postulate that spontaneous and evoked release from such a multitude of release sites permanently maintains a low, basal extracellular level of DA throughout the striatum (Descarries *et coll.*, 1996). Several studies have indeed demonstrated that there are physiologically relevant basal concentrations of DA in the rat striatal neuropil (Parsons & Justice, 1992), upon which DA efflux occuring in response to single action potentials or burst firing will be superimposed (Garris *et coll.*, 1994; Zhang *et coll.*, 2009). Among other functions, this ambient level of DA could allow for a sustained activation and regulation of the widely distributed, high-affinity receptors for DA and/or other transmitters in striatum. The fact that only a low level of DA would be needed to maintain such a control might in turn account for the notion that a large proportion of DA terminals must be lost before clinical manifestations result from lesions of the meso-striatal system, as well as for restoration of its functioning by grafts of DA neurons (Perlow *et coll.*, 1979) which do not reestablish the pre-existent synaptic circuitry.

Acknowledgements: N.B.-C. was recipient of a doctoral studentship from the Fonds de la Recherche en Santé du Québec (FRSQ). This work was funded in part by CIHR grants MOP-3544 and MOP-106562 to L.D., MOP-49951 to L.-É.T., and MOP-106556 to L.-É.T. and L.D., as well a grant from NARSAD to L.-É.T. L.-É.T. and L.D. also benefitted from an infrastructure grant of the FRSQ to the GRSNC (Groupe de Recherche sur le Système Nerveux Central), and L.-É.T. and Å.W.-M. from a joint grant of The Swedish Foundation for International Cooperation in Research and Higher Education. Research in Å.W.-M.'s laboratory is supported by the Swedish Research Council, the Swedish Brain Foundation, Swedish Brain Power, the Åhlén and Wiberg Foundations, the National Board of Health and Welfare and Uppsala

University. Karin Nordenankar and Diane Gingras provided technical assistance. The authors also thank Prof. Nils-Göran Larsson for sharing the DAT-Cre mouse line at the origin of the Uppsala *Vglut2*$^{f/f;DAT\text{-}cre}$ mouse, Drs. Xiaoxi Zhuang and Bradford Lowell for having produced and provided the mice at the origin of the Montreal *Vglut2*$^{f/f;DAT\text{-}cre}$ mouse.

Abbreviations: cKO, conditional knockout; DA, dopamine; DAB, 3,3'-diaminobenzidine tetrahydrochloride; NAC, nucleus accumbens, core; NAS, nucleus accumbens, shell; NS, neostriatum; TH, tyrosine hydroxylase; VGLUT2, vesicular glutamate transporter 2

References

Antonopoulos, J., Dori, I., Dinopoulos, A., Chiotelli, M. & Parnavelas, J.G. (2002) Postnatal development of the dopaminergic system of the striatum in the rat. *Neuroscience*, **110**, 245-256.

Beaudet, A. & Descarries, L. (1976) Quantitative data on serotonin nerve terminals in adult rat neocortex. *Brain Res*, **111**, 301-309.

Beaudet, A. & Sotelo, C. (1981) Synaptic remodeling of serotonin axon terminals in rat agranular cerebellum. *Brain Res*, **206**, 305-329.

Bérubé-Carrière, N., Riad, M., Dal Bo, G., Lévesque, D., Trudeau, L.-É. & Descarries, L. (2009) The dual dopamine-glutamate phenotype of growing mesencephalic neurons regresses in mature rat brain. *J Comp Neurol*, **517**, 873-891.

Birgner, C., Nordenankar, K., Lundblad, M., Mendez, J.A., Smith, C., le Greves, M., Galter, D., Olson, L., Fredriksson, A., Trudeau, L.-É., Kullander, K. & Wallén-Mackenzie, Å. (2009) VGLUT2 in dopamine neurons is required for psychostimulant-induced behavioral activation. *Proc Natl Acad Sci U S A*, **107**, 389-394.

Carlsson, A. (1959) The occurrence, distribution and physiological role of catecholamines in the nervous system. *Pharmacol Rev*, **11**, 490-493.

Colonnier, M. (1968) Synaptic patterns on different cell types in the different laminae of the cat visual cortex. An electron microscope study. *Brain Res*, **9**, 268-287.

Dal Bo, G., Bérubé-Carrière, N., Mendez, J.A., Leo, D., Riad, M., Descarries, L., Lévesque, D. & Trudeau, L.-É. (2008) Enhanced glutamatergic phenotype of mesencephalic dopamine neurons after neonatal 6-hydroxydopamine lesion. *Neuroscience*, **156**, 59-70.

Dal Bo, G., St-Gelais, F., Danik, M., Williams, S., Cotton, M. & Trudeau, L.-É. (2004) Dopamine neurons in culture express VGLUT2 explaining their capacity to release glutamate at synapses in addition to dopamine. *J Neurochem*, **88**, 1398-1405.

Descarries, L., Beaudet, A. & Watkins, K.C. (1975) Serotonin nerve terminals in adult rat neocortex. *Brain Res*, **100**, 563-588.

Descarries, L., Bérubé-Carrière, N., Riad, M., Bo, G.D., Mendez, J.A. & Trudeau, L.-É. (2008) Glutamate in dopamine neurons: synaptic versus diffuse transmission. *Brain Res Rev*, **58**, 290-302.

Descarries, L., Watkins, K.C., Garcia, S., Bosler, O. & Doucet, G. (1996) Dual character, asynaptic and synaptic, of the dopamine innervation in adult rat neostriatum: a quantitative autoradiographic and immunocytochemical analysis. *J Comp Neurol*, **375**, 167-186.

Descarries, L., Watkins, K.C. & Lapierre, Y. (1977) Noradrenergic axon terminals in the cerebral cortex of rat. III. Topometric ultrastructural analysis. *Brain Res*, **133**, 197-222.

Doucet, G., Descarries, L. & Garcia, S. (1986) Quantification of the dopamine innervation in adult rat neostriatum. *Neuroscience*, **19**, 427-445.

Ekstrand, M.I., Terzioglu, M., Galter, D., Zhu, S., Hofstetter, C., Lindqvist, E., Thams, S., Bergstrand, A., Hansson, F.S., Trifunovic, A., Hoffer, B., Cullheim, S., Mohammed, A.H., Olson, L. & Larsson, N.G. (2007) Progressive parkinsonism in mice with respiratory-chain-deficient dopamine neurons. *Proc Natl Acad Sci U S A*, **104**, 1325-1330.

El Mestikawy, S., Wallén-Mackenzie, A., Fortin, G.M., Descarries, L. & Trudeau, L.-É. (2011) From glutamate co-release to vesicular synergy: vesicular glutamate transporters. *Nat Rev Neurosci*, **12**, 204-216.

Fortin, G.M., Bourque, M.J., Mendez, J.A., Leo, D., Nordenankar, K., Birgner, C., Arvidsson, E., Rymar, V.V., Bérubé-Carrière, N., Descarries, L., Sadikot, A.F., Wallén-Mackenzie, Å. & Trudeau, L.-É. (2011) Glutamate corelease promotes growth and survival of a subset of midbrain dopamine neurons. Submitted.

Franklin, K.B.J. & Paxinos, G. (2008) *The Mouse Brain in Stereotaxic Coordinates*. Elsevier Academic Press, New York.

Freund, T.F., Powell, J.F. & Smith, A.D. (1984) Tyrosine hydroxylase-immunoreactive boutons in synaptic contact with identified striatonigral neurons, with particular reference to dendritic spines. *Neuroscience*, **13**, 1189-1215.

Garris, P.A., Ciolkowski, E.L., Pastore, P. & Wightman, R.M. (1994) Efflux of dopamine from the synaptic cleft in the nucleus accumbens of the rat brain. *J Neurosci*, **14**, 6084-6093.

Gauthier, J., Parent, M., Lévesque, M. & Parent, A. (1999) The axonal arborization of single nigrostriatal neurons in rats. *Brain Res*, **834**, 228-232.

Haycock, J.W. (1993) Multiple forms of tyrosine hydroxylase in human neuroblastoma cells: quantitation with isoform-specific antibodies. *J Neurochem*, **60**, 493-502.

Kawano, M., Kawasaki, A., Sakata-Haga, H., Fukui, Y., Kawano, H., Nogami, H. & Hisano, S. (2006) Particular subpopulations of midbrain and hypothalamic dopamine neurons express vesicular glutamate transporter 2 in the rat brain. *J Comp Neurol*, **498**, 581-592.

Matsuda, W., Furuta, T., Nakamura, K.C., Hioki, H., Fujiyama, F., Arai, R. & Kaneko, T. (2009) Single nigrostriatal dopaminergic neurons form widely spread and highly dense axonal arborizations in the neostriatum. *J Neurosci*, **29**, 444-453.

Mendez, J.A., Bourque, M.J., Dal Bo, G., Bourdeau, M.L., Danik, M., Williams, S., Lacaille, J.C. & Trudeau, L.-É. (2008) Developmental and target-

dependent regulation of vesicular glutamate transporter expression by dopamine neurons. *J Neurosci*, **28**, 6309-6318.

Moore, R.Y. & Card, J.P. (1984) Noradrenaline-containing neuron systems. In Björklund, A., Hökfelt, T. (eds) *Handbook of Chemical Neuroanatomy*. Elsevier, Amsterdam, pp. 123-156.

Moss, J., Ungless, M.A. & Bolam, J.P. (2011) Dopaminergic axons in different divisions of the adult rat striatal complex do not express vesicular glutamate transporters. *Eur J Neurosci*, **33**, 1205-1211.

Palade, G.E. & Palay, S.L. (1954) Electron microscope observations of interneuronal and neuromuscular synapses. *Anat Rec*, **118**, 335-336.

Parsons, L.H. & Justice, J.B., Jr. (1992) Extracellular concentration and *in vivo* recovery of dopamine in the nucleus accumbens using microdialysis. *J Neurochem*, **58**, 212-218.

Perlow, M.J., Freed, W.J., Hoffer, B.J., Seiger, A., Olson, L. & Wyatt, R.J. (1979) Brain grafts reduce motor abnormalities produced by destruction of nigrostriatal dopamine system. *Science*, **204**, 643-647.

Persson, S., Boulland, J.L., Aspling, M., Larsson, M., Fremeau, R.T., Jr., Edwards, R.H., Storm-Mathisen, J., Chaudhry, F.A. & Broman, J. (2006) Distribution of vesicular glutamate transporters 1 and 2 in the rat spinal cord, with a note on the spinocervical tract. *J Comp Neurol*, **497**, 683-701.

Peters, A. & Palay, S.L. (1996) The morphology of synapses. *J Neurocytol*, **25**, 687-700.

Pickel, V.M., Beckley, S.C., Joh, T.H. & Reis, D.J. (1981) Ultrastructural immunocytochemical localization of tyrosine hydroxylase in the neostriatum. *Brain Res*, **225**, 373-385.

Pierce, J.P. & Lewin, G.R. (1994) An ultrastructural size principle. *Neuroscience*, **58**, 441-446.

Prensa, L. & Parent, A. (2001) The nigrostriatal pathway in the rat: A single-axon study of the relationship between dorsal and ventral tier nigral neurons and the striosome/matrix striatal compartments. *J Neurosci*, **21**, 7247-7260.

Robertson, J.D. (1953) Ultrastructure of two invertebrate synapses. *Proc Soc Exp Biol Med*, **82**, 219-223.

Sherrington, C.S. (1897) The central nervous system. In Foster, M., Sherrington, C.S. (eds) *A Textbook of Physiology*. Macmillan, London, pp. 915-1000.

Soghomonian, J.J., Descarries, L. & Watkins, K.C. (1989) Serotonin innervation in adult rat neostriatum. II. Ultrastructural features: a radioautographic and immunocytochemical study. *Brain Res*, **481**, 67-86.

Soghomonian, J.J., Doucet, G. & Descarries, L. (1987) Serotonin innervation in adult rat neostriatum. I. Quantified regional distribution. *Brain Res*, **425**, 85-100.

Stuber, G.D., Hnasko, T.S., Britt, J.P., Edwards, R.H. & Bonci, A. (2010) Dopaminergic terminals in the nucleus accumbens but not the dorsal striatum corelease glutamate. *J Neurosci*, **30**, 8229-8233.

Takamori, S., Rhee, J.S., Rosenmund, C. & Jahn, R. (2001) Identification of differentiation-associated brain-specific phosphate transporter as a second vesicular glutamate transporter (VGLUT2). *J Neurosci*, **21**, RC182.

Tecuapetla, F., Patel, J.C., Xenias, H., English, D., Tadros, I., Shah, F., Berlin, J., Deisseroth, K., Rice, M.E., Tepper, J.M. & Koos, T. (2010) Glutamatergic

signaling by mesolimbic dopamine neurons in the nucleus accumbens. *J Neurosci*, **30**, 7105-7110.

Tong, Q., Ye, C., McCrimmon, R.J., Dhillon, H., Choi, B., Kramer, M.D., Yu, J., Yang, Z., Christiansen, L.M., Lee, C.E., Choi, C.S., Zigman, J.M., Shulman, G.I., Sherwin, R.S., Elmquist, J.K. & Lowell, B.B. (2007) Synaptic glutamate release by ventromedial hypothalamic neurons is part of the neurocircuitry that prevents hypoglycemia. *Cell Metab*, **5**, 383-393.

Triarhou, L.C., Norton, J. & Ghetti, B. (1988) Synaptic connectivity of tyrosine hydroxylase immunoreactive nerve terminals in the striatum of normal, heterozygous and homozygous weaver mutant mice. *J Neurocytol*, **17**, 221-232.

Trudeau, L.-É. (2004) Glutamate co-transmission as an emerging concept in monoamine neuron function. *J Psychiatry Neurosci*, **29**, 296-310.

Voorn, P., Jorritsma-Byham, B., Van Dijk, C. & Buijs, R.M. (1986) The dopaminergic innervation of the ventral striatum in the rat: a light- and electron-microscopical study with antibodies against dopamine. *J Comp Neurol*, **251**, 84-99.

Wallén-Mackenzie, Å., Gezelius, H., Thoby-Brisson, M., Nygard, A., Enjin, A., Fujiyama, F., Fortin, G. & Kullander, K. (2006) Vesicular glutamate transporter 2 is required for central respiratory rhythm generation but not for locomotor central pattern generation. *J Neurosci*, **26**, 12294-12307.

Wightman, R.M. & Zimmerman, J.B. (1990) Control of dopamine extracellular concentration in rat striatum by impulse flow and uptake. *Brain Res Brain Res Rev*, **15**, 135-144.

Yamaguchi, T., Sheen, W. & Morales, M. (2007) Glutamatergic neurons are present in the rat ventral tegmental area. *Eur J Neurosci*, **25**, 106-118.

Zahm, D.S. (1992) An electron microscopic morphometric comparison of tyrosine hydroxylase immunoreactive innervation in the neostriatum and the nucleus accumbens core and shell. *Brain Res*, **575**, 341-346.

Zhang, L., Doyon, W.M., Clark, J.J., Phillips, P.E. & Dani, J.A. (2009) Controls of tonic and phasic dopamine transmission in the dorsal and ventral striatum. *Mol Pharmacol*, **76**, 396-404.

Zhou, J., Nannapaneni, N. & Shore, S. (2007) Vessicular glutamate transporters 1 and 2 are differentially associated with auditory nerve and spinal trigeminal inputs to the cochlear nucleus. *J Comp Neurol*, **500**, 777-787.

Zhuang, X., Masson, J., Gingrich, J.A., Rayport, S. & Hen, R. (2005) Targeted gene expression in dopamine and serotonin neurons of the mouse brain. *J Neurosci Methods*, **143**, 27-32.

Table 1

DA axon terminals in the nucleus accumbens core and shell of immature (P15) and mature (P70-90), control and *Vglut2* cKO mice

	Nucleus accumbens core				Nucleus accumbens shell			
	P15		P70-90		P15		P70-90	
	Control (n = 5)	**cKO** (n = 5)	**Control** (n = 6)	**cKO** (n = 6)	**Control** (n = 3)	**cKO** (n = 3)	**Control** (n = 3)	**cKO** (n = 3)
Number examined	182	210	268	235	115	122	162	190
Dimensions								
mean diameter (μm)	0.47 ± 0.02	0.47 ±0.03	0.48 ± 0.01	0.48 ± 0.01	0.44 ± 0.02	0.48 ± 0.04	0.45 ± 0.04	0.39 ± 0.02
area (μm^2)	0.19 ± 0.02	0.18 ± 0.02	0.20 ± 0.01	0.20 ± 0.01	0.16 ± 0.02	0.21 ± 0.03	0.17 ± 0.02	0.14 ± 0.01
Mitochondria (%)	27 ± 2	36 ± 2	37 ± 3	34 ± 4	37 ± 9	46 ± 2	48 ± 2	43 ± 5
Synaptic incidence								
single section (%)	5 ± 2	3 ± 1	3 ± 1	4 ± 1	3 ± 1	2 ± 1	1 ± 1	1 ± 1
junction length (μm)	0.20 ± 0.01	0.22 ± 0.01	0.26 ± 0.03	0.20 ± 0.01	0.24 ± 0.05	0.28 ± 0.03	0.16	0.18
whole varicosity (%)	11 ± 3	7 ± 2	6 ± 2	8 ± 2	5 ± 1	5 ± 3	2 ± 2	2 ± 1

Mean ± SEM from the number of mice indicated in brackets. In this and the following table, the stereological formula of Beaudet & Sotelo (1981) was used to extrapolate the synaptic incidence for whole varicosities from the percentage of varicosity profiles showing a junction in single sections (details in Materials and Methods).

Table 2

DA axon terminals in the neostriatum of immature (P15) and mature (P70-90), control and *Vglut2* cKO mice

	P15		P70-90	
	Control (n = 5)	**cKO** (n = 5)	**Control** (n = 6)	**cKO** (n = 6)
Number examined	253	253	279	317
Dimensions				
mean diameter (µm)	0.48 ± 0.02	0.45 ± 0.02	0.48 ± 0.01	0.49 ± 0.01
area (μm^2)	0.20 ± 0.02	0.19 ± 0.01	0.19 ± 0.01	0.20 ± 0.01
Mitochondria (%)	35 ± 2	31 ± 6	42 ± 3	43 ± 3
Synaptic incidence				
single section (%)	5 ± 1	3 ± 1	1 ± 1	1 ± 1
junction length (µm)	0.20 ± 0.01	0.22 ± 0.04	0.14	0.16 ± 0.02
whole varicosity (%)	12 ± 2	7 ± 2	3 ± 3	2 ± 1

Mean ± SEM from the number of mice indicated in brackets.

Supplementary Table 1

Surface of thin section examined and number of TH and VGLUT2 terminals visualized after dual TH/VGLUT2 immunolabeling

	P15 (n = 4)						**P60** (n = 4)					
	NAC		**NAS**		**NS**		**NAC**		**NAS**		**NS**	
	Control	Mtl cKO	Control	Mtl cKO	Control	Mtl cKO	Control	Mtl cKO	Control	Mtl cKO	Control	Mtl cKO
Surface (μm^2)	5100	3500	5300	2050	5300	2800	4950	4350	5100	3500	5150	2500
TH	219	148	257	113	273	133	197	230	233	158	290	124
VGLUT2	229	116	334	138	241	113	349	196	283	101	268	52

Supplementary Table 2

DA axon terminals in the nucleus accumbens (core and shell) and neostriatum of immature (P15) and mature (P70-90) mice of the two lines of *Vglut2* cKO (Upp and Mtl)

	P15					P70-90				
	NAC		NAS	NS		NAC		NAS	NS	
	Upp (n = 2)	Mtl (n = 3)	Mtl (n = 3)	Upp (n = 2)	Mtl (n = 3)	Upp (n = 3)	Mtl (n = 3)	Mtl (n = 3)	Upp (n = 3)	Mtl (n = 3)
lumber examined	91	119	122	95	158	102	133	190	160	157
imensions										
mean diameter (µm)	0.45 ± 0.03	0.48 ± 0.05	0.48 ± 0.02	0.47 ± 0.01	0.44 ± 0.03	0.50 ± 0.01	0.47 ± 0.02	0.40 ± 0.02	0.49 ± 0.01	0.49 ± 0.03
area (μm^2)	0.18 ± 0.01	0.18 ± 0.03	0.21 ± 0.04	0.21 ± 0.01	0.18 ± 0.02	0.23 ± 0.01	0.18 ± 0.01	0.14 ± 0.01	0.22 ± 0.01	0.19 ± 0.02
Mitochondria (%)	31 ± 1	40 ±1	46 ± 2	19 ±5	40 ± 5	29 ± 8	38 ± 3	43 ± 2	37 ± 2	49 ± 3
ynaptic incidence										
single section (%)	5 ± 1	6 ± 2	2 ± 1	5 ± 1	2 ± 1	3 ± 1	4 ± 1	1 ± 1	1 ± 1	0
junction length (µm)	0.23 ± 0.01	0.21 ± 0.03	0.28 ±0.03	0.29 ± 0.03	0.15 ± 0.01	0.19 ± 0.01	0.22 ± 0.01	0.18	0.17 ± 0.02	-
whole varicosity (%)	9 ± 1	5 ± 3	5 ± 3	9 ± 1	5 ± 3	7 ± 4	10 ± 3	1 ± 1	3 ± 3	0

Mean ± SEM from the number of mice indicated in brackets. In this and the following table, the stereological formula of Beaudet & Sotelo (1981) was used to extrapolate the synaptic incidence for whole varicosities from the percentage of varicosity profiles showing a junction in single sections (details in Materials and Methods).

Supplementary Table 3

DA axon terminals in the nucleus accumbens (core and shell) and neostriatum of immature (P15) and mature (P70-90) littermate control mice for the two lines of *Vglut2* cKO (Upp and Mtl)

	P15					P70-90				
	NAC		NAS	NS		NAC		NAS	NS	
	Upp (n = 2)	Mtl (n = 3)	Mtl (n = 3)	Upp (n = 2)	Mtl (n = 3)	Upp (n = 3)	Mtl (n = 3)	Mtl (n = 3)	Upp (n = 3)	Mtl (n = 3)
Number examined	85	97	115	93	160	123	145	162	138	141
Dimensions										
mean diameter (µm)	0.50 ± 0.03	0.45 ± 0.03	0.44 ± 0.02	0.52 ± 0.01	0.46 ± 0.03	0.47 ± 0.02	0.50 ± 0.01	0.45 ± 0.04	0.50 ± 0.02	0.47 ± 0.02
area (μm^2)	0.22 ± 0.03	0.17 ± 0.02	0.16 ± 0.02	0.24 ± 0.01	0.18 ± 0.02	0.21 ± 0.02	0.19 ± 0.01	0.17 ± 0.02	0.22 ± 0.02	0.17 ± 0.01
Mitochondria (%)	25 ± 1	29 ± 3	37 ± 9	36 ± 4	34 ± 2	33 ± 3	41 ± 3	48 ± 2	40 ± 3	43 ± 5
Synaptic incidence										
single section (%)	2 ± 1	7 ± 2	3 ± 1	6 ± 3	5 ± 1	3 ± 2	3 ± 1	1 ± 1	2 ± 2	0
junction length (µm)	0.20 ± 0.04	0.21 ± 0.01	0.24 ±0.05	0.22 ± 0.02	0.19 ± 0.01	0.31 ± 0.02	0.21 ± 0.02	0.16	0.14	-
whole varicosity (%)	6 ± 1	14 ± 4	5 ± 1	14 ± 5	12 ± 2	5 ± 3	7 ± 2	2 ± 2	5 ± 5	0

Mean ± SEM from the number of mice indicated in brackets.

Figure legends

Figure 1- Regions of neostriatum (NS) and nucleus accumbens, core (NAC) and shell (NAS) sampled for electron microscopy. These sections across the striatum of P15 (**A,B**) and adult (**C,D**) control (**A,C**) and cKO (**B,D**) mice (Mtl) were processed for TH immunocytochemistry with the peroxidase-DAB technique.

Figure 2- Dopamine terminals from the core of nucleus accumbens in P15 or adult control and *Vglut2* cKO mice. As illustrated in this and the following figures, the TH-immunolabeled terminals (varicosities) in NAC (Figs. 2 and 5) and NAS (Fig. 3), as well as in NS (Fig. 4), share similar ultrastructural features, whether in control or *Vglut2* cKO mice of both ages (see also Tables 1 and 2). These varicosities are relatively small, generally round or ovoid in shape, filled with small vesicles, associated or not with mitochondria, and a vast majority is without apparent synaptic membrane specialization (junctional complex). **A**, **C** and **D** are rare examples of TH-labeled synaptic varicosities, most of which form small, symmetrical junctions (between small arrows) with dendritic branches (db). **B** and **E,E'** are more typical examples of asynaptic terminals. In **B**, the labeled varicosity is seen emerging from its parent, thin, unmyelinated axon (empty arrow), and it is directly apposed to several other, unlabeled varicosities (av). **E** and **E'** are two sections across the same labeled terminal, neither of which displays a synaptic membrane specialization. **A** and **D** are from $Vglut2^{f/+;DAT\text{-}cre}$ and $Vglut2^{f/f}$ controls, respectively, whereas **C** is from a cKO (Mtl) and **B**,**E**,**E'** from cKO (Upp) mice. Tissue primarily fixed by perfusion of acrolein. Scale bar (in **E'**): 1 μm.

Figure 3- Dopamine terminals from the shell of nucleus accumbens in P15 or adult control and *Vglut2* cKO mice. These electron micrographs from the NAS (control or *Vglut2* cKO generated in Montreal) further illustrate ultrastructural characteristics of meso-striatal DA terminals in the mouse. In **A**, two varicosities, along the same axon, are juxtaposed to a dendritic branch (db), with which the upper one forms a relatively wide symmetrical synapse (between small arrows). In **B-F,** all labeled terminals appear to be asynaptic. In **A**, **B**, **C**, and **E**, intervaricose axon segments are designated by empty arrows. In **D**, the varicosity appears to be larger than average and its parent axon (empty arrow) contains small vesicles in its narrow as well as dilated portion. Tissue primarily fixed by perfusion of acrolein. Scale bar (in **F**): 1 μm.

Figure 4- Dopamine terminals from the neostriatum in P15 or adult control and *Vglut2* cKO mice. The TH labeled varicosity in **A** is truly exceptional, as it displays not only one but two synaptic junctions (between small arrows) made with distinct dendritic branches (db). The synapse on the right is on the neck of a spine (sp) which arises from the upper dendritic branch. This spine is contacted synaptically on its head by another axon varicosity (av), unlabeled. **C** illustrates the rare occurrence of a labeled varicosity in synaptic contact (between small arrows) with a dendritic spine (sp). In this case, the junction looks rather asymmetrical. Note that this synaptic labeled varicosity is itself juxtaposed to another labeled varicosity profile, which is not entirely uncommon. **B**, **D, E** and **F** are representative of the large majority of asynaptic labeled terminals. In **B**, the presence of three varicosity profiles within the same field reflects the high density of innervation. In **E**, the two elongated profiles presumably belong to the same axon, again illustrating the very short interval between such varicosities. **F** is another example of a relatively large TH-labeled varicosity. **A,E** and **D** are from *Vglut2*$^{f/+;DAT\text{-}cre}$ and *Vglut2*$^{f/f}$ controls, respectively, whereas **B** is from a cKO (Mtl) and **C,F** from cKO mice. Tissue primarily fixed by perfusion of acrolein. Scale bar (in **F**): 1 μm.

Figure 5- Dopamine terminals from the core of nucleus accumbens in adult wild type mice fixed by perfusion of a glutaraldehyde–paraformaldehyde mixture. There was no apparent difference in the ultrastructural features of TH-labeled varicosities from these mice, by comparison with those from control and cKO mice perfused with acrolein as primary fixative (see Results for morphometric data). **A** and **A'** are two sections across the same labeled varicosity, which forms a relatively wide, symmetrical synaptic contact (between small arrows) with a dendritic branch (db). In **B**, two labeled varicosity profiles appear more typically asynaptic. Scale bar (in **B**): 1 μm.

Figure 6- Low-magnification electron micrographs illustrating the lack of dually, TH/VGLUT2-labeled axon terminals in control as well as cKO mice. **A** and **B** are from the NAC and NAS of P15 mice, and **C** and **D** from the NS of adult mice. TH and VGLUT2 were respectively labeled with the immunoperoxidase technique (fine diaminobenzidine precipitate) and the immunogold technique (silver-intensified immunogold particles). TH terminals are designated by black arrows and VGLUT2 terminals by empty arrows. Scale bar (in **D**): 1 μm.

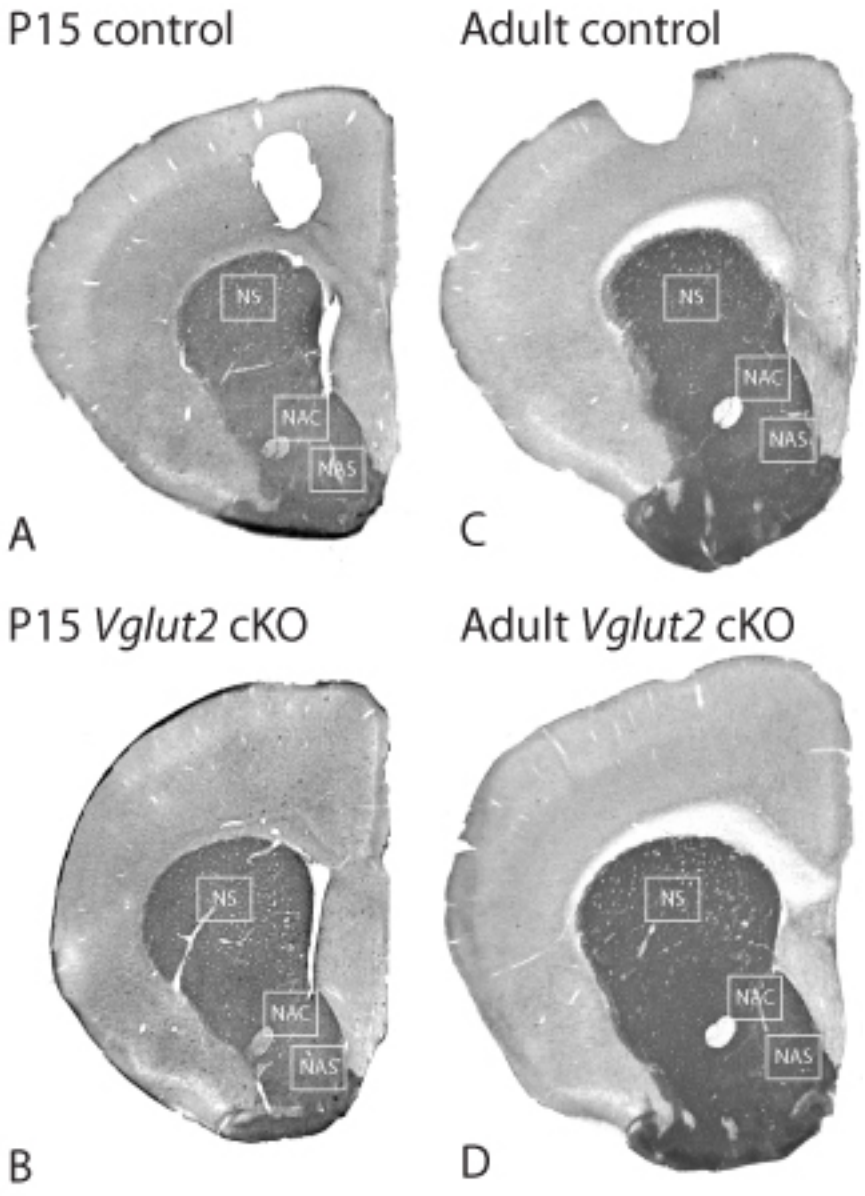

Figure 1 – Regions of neostriatum (NS) and nucleus accumbens core (NAC) and shell (NAS) sampled for electron microscopy

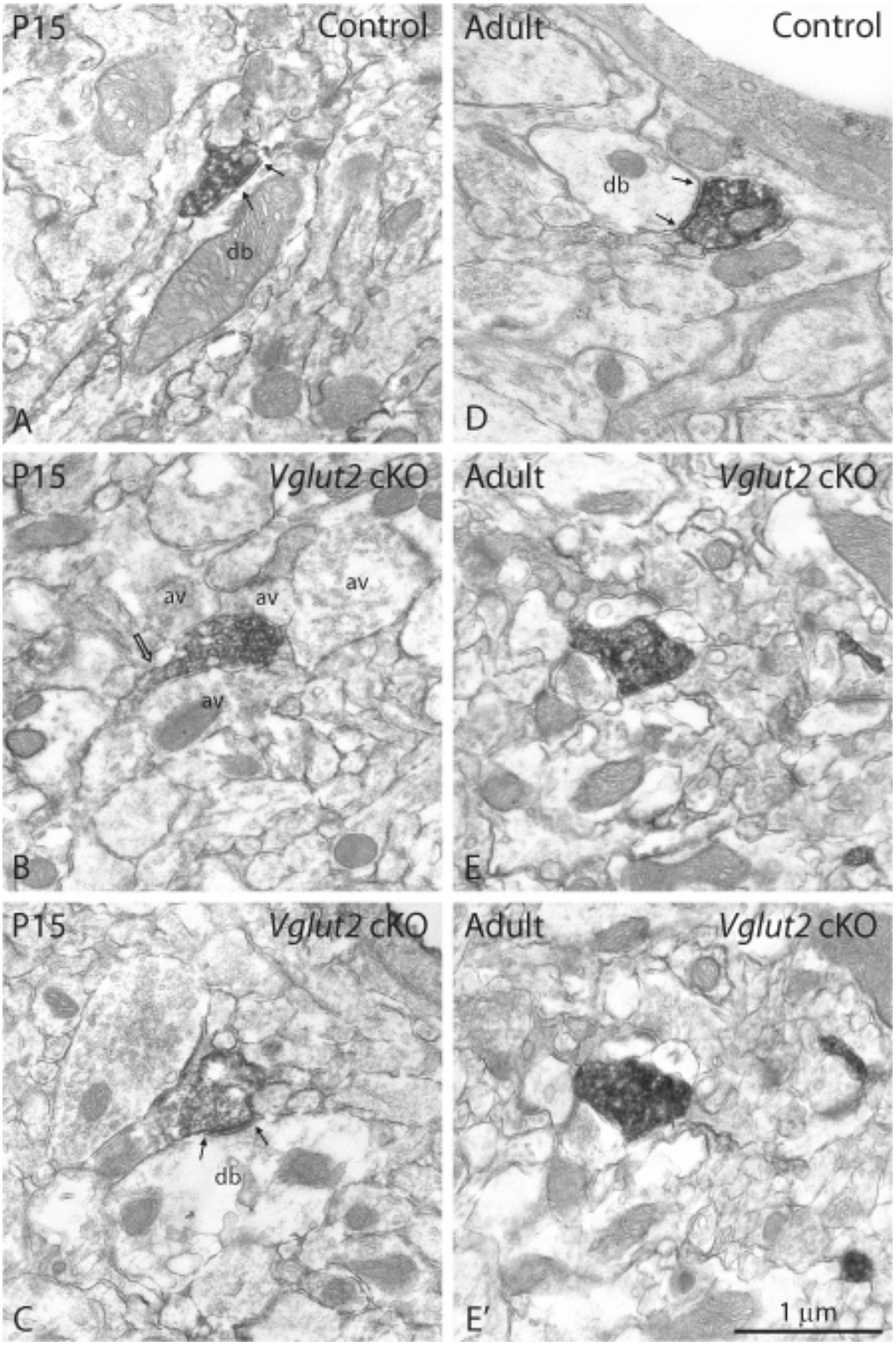

Figure 2 – DA terminals from the NAC in P15 or adult control and *Vglut2* cKO mice

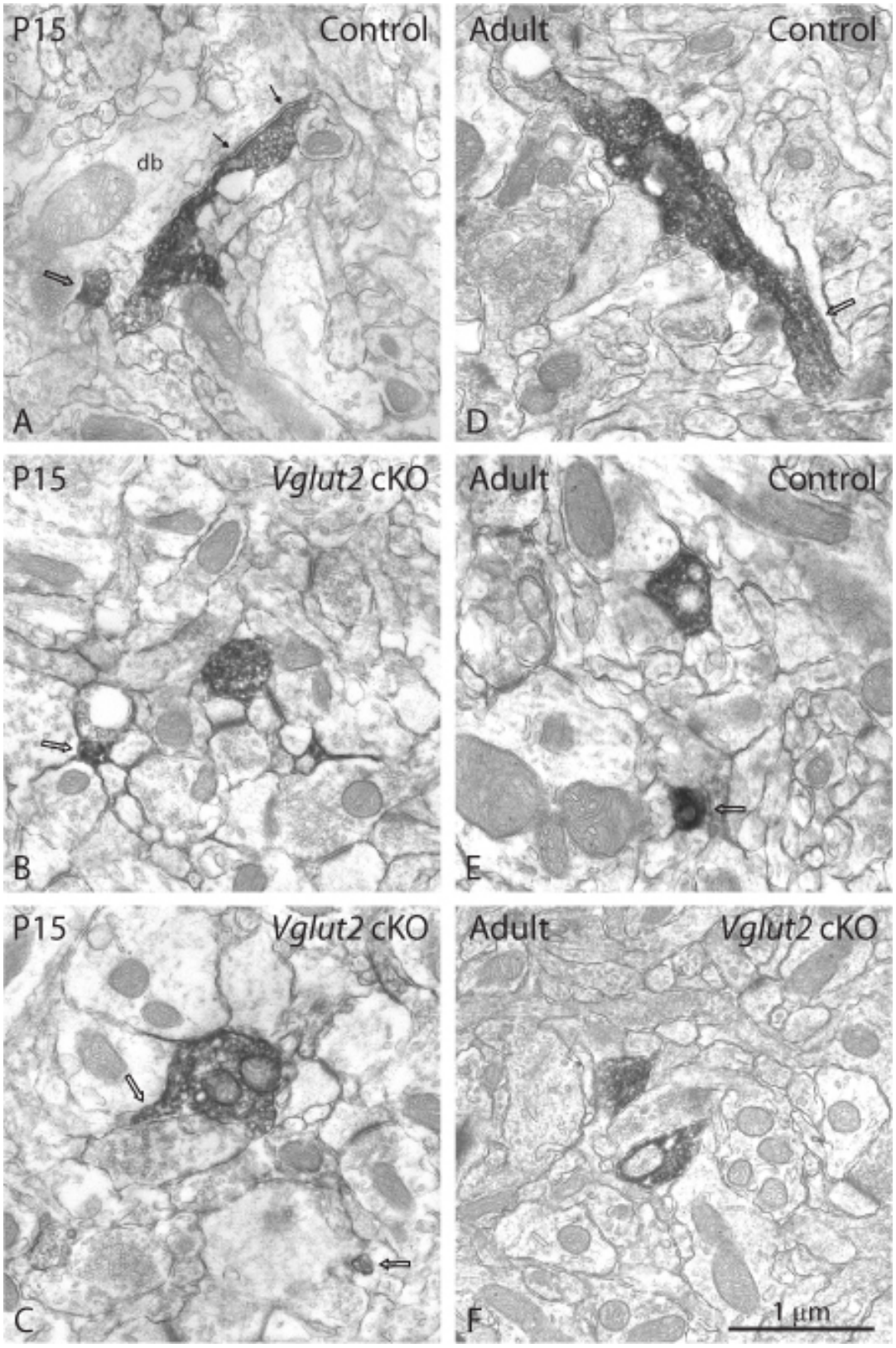

Figure 3 – DA terminals from the NAS in P15 or adult control and *Vglut2* cKO mice

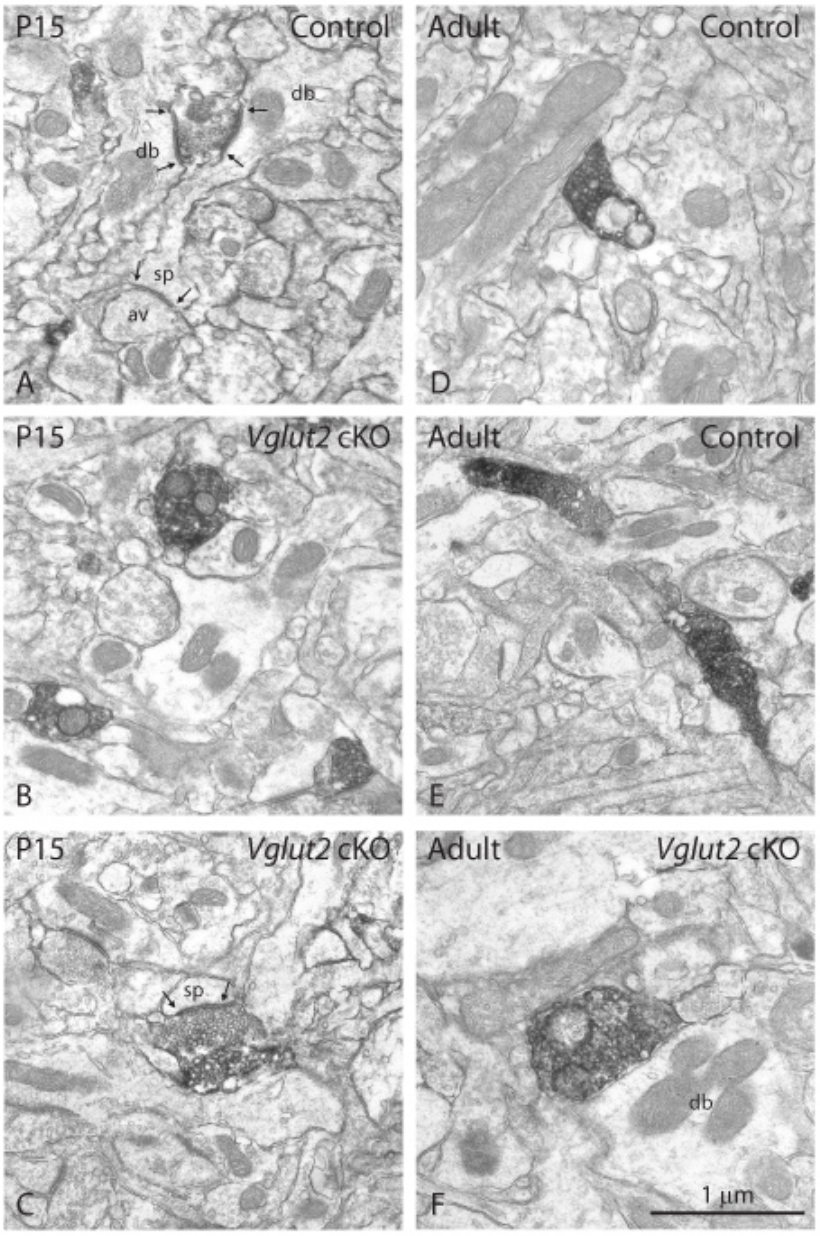

Figure 4 – DA terminals from the neostriatum in P15 or adult control and *Vglut2* cKO mice

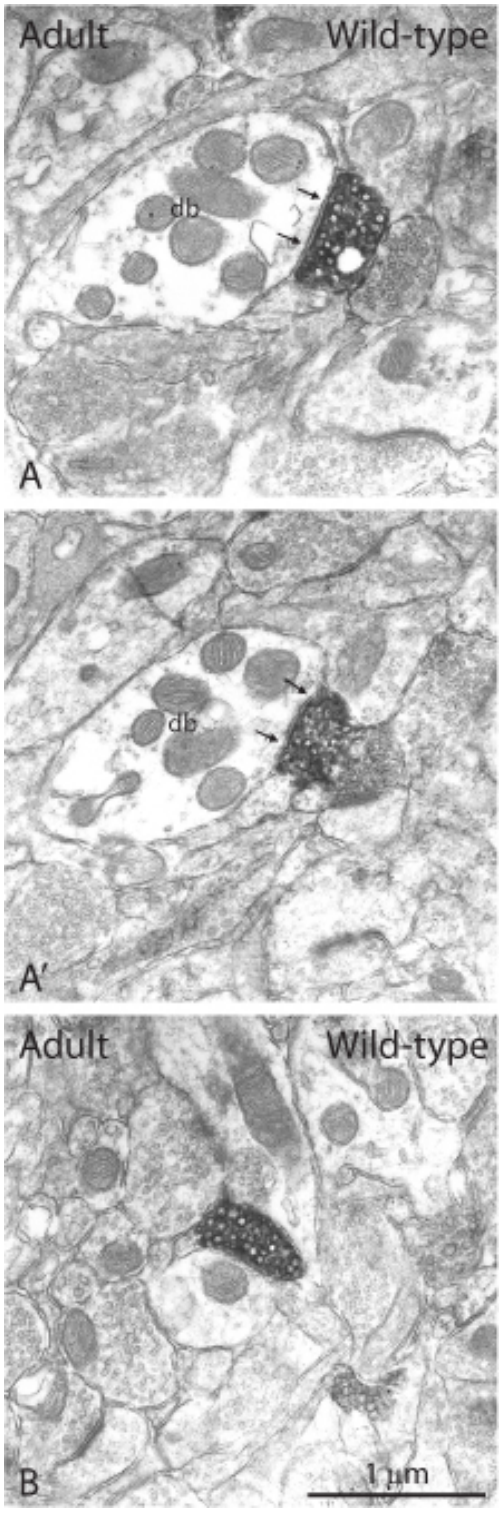

Figure 5 – DA terminals from the core of nucleus accumbens in adult wild-type mice fixed by perfusion with a glutaraldehyde-paraformaldehyde mixture

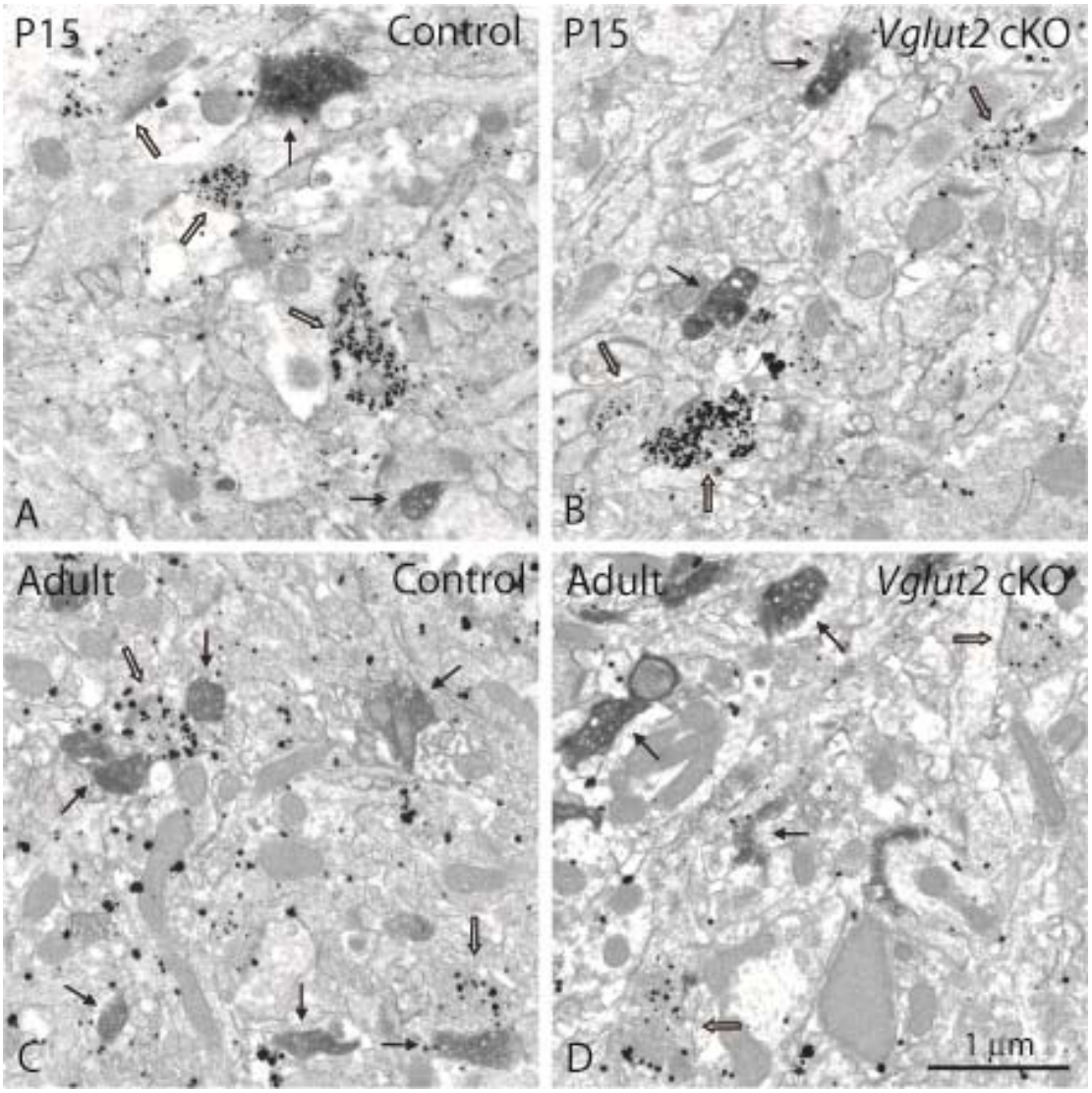

Figure 6 – Low-magnification electron micrographs illustrating the lack of dually TH-VGLUT2-labeled axon terminals in control as well as cKO mice

Chapitre 4 – Discussion générale

Les deux volets de cette thèse présentent une nouvelle image du système DA mésostriatal, tant chez le rat que chez la souris. Chez le rat, ils démontrent la présence du transporteur vésiculaire du glutamate VGLUT2 au sein d'une fraction significative des terminaisons (varicosités) axonales du système DA mésostriatal à l'âge de 15 jours, suivie d'une régression de ce double phénotype à l'âge adulte. Chez la souris, la régression du double phénotype pourrait être plus précoce, à moins que, chez les deux espèces, l'absence de colocalisation de VGLUT2 dans les terminaisons immunopositives pour la TH ne résulte d'une ségrégation des deux protéines dans des varicosités axonales distinctes des mêmes neurones. L'ensemble des résultats actuellement disponibles suggère toutefois un rôle important de la co-libération de glutamate par les terminaisons axonales DA au cours du développement de ces neurones.

Par ailleurs, notre caractérisation ultrastructurale des terminaisons axonales TH immunoréactives du noyau accumbens et du néostriatum de la souris renforce l'hypothèse d'une transmission diffuse (volumique) et d'un niveau ambiant de transmetteur comme élément déterminant du fonctionnement du système mésostriatal DA. Étant donné la faible fréquence des contacts synaptiques formés par ces varicosités axonales, tant chez la jeune souris que la souris adulte, il faut également envisager la possibilité qu'à l'échelon moléculaire, les mécanismes et modalités de libération de DA à partir de telles varicosités, de même que les lieux d'ancrage de ses récepteurs, soient fondamentalement différents de ceux que l'on connait pour d'autres systèmes neuronaux entièrement synaptiques.

1 La stratégie expérimentale

1.1 Les anticorps

Il n'y a aucune raison de douter de la spécificité des anticorps utilisés au cours des deux volets de cette thèse. Par contre, il est impossible d'affirmer que toutes les terminaisons TH et/ou VGLUT2 ont été identifiées au cours de nos travaux. L'absence de réactivité en immunocytochimie de fluorescence, ainsi qu'en microscopie photonique ou électronique, ne permet pas de conclure à une absence totale d'antigène au sein des éléments examinés. En microcopie électronique, notamment, les problèmes de

pénétration des anticorps et des immunoréactifs compliquent la situation. De plus, le marquage à l'or en pré-enrobage, utilisé pour la visualisation du VGLUT2 lors des doubles marquages est notoirement moins sensible que celui à l'immunoperoxydase-DAB (utilisé pour visualiser la TH).

En théorie, l'immunomarquage TH devrait détecter non seulement les terminaisons axonales DA, mais aussi les terminaisons à noradrénaline (NA) des différentes régions du cerveau. Cependant, ces dernières échappent au marquage lors de l'utilisation des protocoles conventionnels d'immunocytochimie TH, même si les raisons de cet état de fait restent à élucider. De plus, comparativement à leurs homologues DA, les terminaisons NA sont très rares sinon inexistantes dans le NS et peu nombreuses dans le NAC et NAS des rongeurs (Carlsson, 1959; Moore et Card, 1984).

1.2 Les doubles marquages immunocytochimiques

Comme nous l'avons dit ci-dessus, le fait qu'une varicosité axonale ne présente pas d'immunomarquage TH et/ou VGLUT2 n'implique pas nécessairement une absence totale de la protéine en question, car celle-ci pourrait simplement ne pas l'être en quantité suffisante pour être détectée. En revanche, nous avons validé la signification des résultats positifs en double marquage, en montrant que le deuxième marquage est absent lors de l'omission des anticorps primaires ou secondaires correspondants.

En tant qu'élément d'interprétation, il faut aussi tenir compte du fait que le striatum reçoit une forte innervation glutamatergique du thalamus ainsi que du cortex (Hisano et coll., 2000; Bai et coll., 2001; Fremeau et coll., 2001; Herzog et coll., 2001). Ainsi, dans le matériel doublement marqué pour la TH et VGLUT2, devient-il impossible de savoir si les terminaisons striatales immunomarquées seulement pour VGLUT2 sont celles de neurones essentiellement glutamatergiques se projetant à partir du thalamus ou celles de neurones DA du mésencéphale qui ne contiendraient pas du tout ou insuffisamment de TH pour permettre sa détection.

1.3 La quantification des données

À cause des aléas de la fixation chimique et de la pénétration des anticorps dans le tissu préparé pour la microcopie électronique, il est peu probable que toutes les terminaisons TH et/ou VGLUT2 aient été détectées dans l'ensemble du matériel examiné en microscopie électronique. Pour cette raison, dans le premier volet de cette

thèse, nous avons volontairement omis de comparer le nombre de terminaisons appartenant aux diverses catégories de marquage (TH, VGLUT2 et TH/VGLUT2) entre des rats d'âge différent (les jeunes et les adultes). Lors de ces études, cependant, il était possible de comparer le nombre de terminaisons marquées aux deux âges chez les rats lésés à la 6-OHDA durant la période néonatale comparativement aux témoins, en respectant les règles suivantes : confiner l'examen aux régions des coupes fines proches de l'interface tissu-résine; identifier tous les profils de varicosité marqués présents dans ces régions; examiner une surface comparable de coupe fine d'un animal à l'autre; effectuer le dénombrement des différents types de varicosités chez un nombre suffisant d'animaux pour justifier une validation statistique des résultats.

Malgré tout, en coupes fines isolées, les terminaisons axonales les plus volumineuses avaient plus de chance d'être détectées que les plus petites, ce qui était le cas des terminaisons TH/VGLUT2, significativement plus grosses que les terminaisons marquées pour la TH seule. Aussi, en réponse à la demande d'un arbitre lors de la publication de nos premiers résultats, avons-nous appliqué la formule d'Abercrombie (Abercrombie, 1946) au calcul de cette proportion. Cette formule prend en compte l'épaisseur des coupes ainsi que le diamètre moyen des objets observés; elle produit un facteur de correction qui permet d'arriver au « nombre véritable » plutôt qu'au « nombre observé » des objets étudiés (Guillery, 2002). Ainsi, la proportion « corrigée » des terminaisons TH/VGLUT2 est-elle passé de 25% à 28% et de 35% à 37% dans le NAC du raton normal ou 6-OHDA lésé, respectivement, de 17% à 15% dans le NS du raton témoin, et de 46% à 37% dans la SNc du raton 6-OHDA lésé, ce qui, somme toute, ne représente pas une grande différence.

Par contre, lors du deuxième volet de la thèse, nous n'avons pas cherché à comparer le nombre de terminaisons TH, VGLUT2 et TH/VGLUT2 entre les souris VGLUT2 cKO et leurs témoins, jeunes ou adultes. L'objectif était plutôt d'examiner un grand nombre de terminaisons marquées pour la TH seulement dans plusieurs régions du striatum (NAC, NAS, NS), afin de savoir si le knockout conditionnel de VGLUT2 dans les neurones DA entrainait des changements significatif de la morphologie de ces terminaisons. Ici, nous nous sommes donc contentés de photographier un nombre suffisant de terminaisons marquées (environ 30 par région et par souris) pour constituer un échantillon représentatif, quelle que soit la condition expérimentale examinée. Quant

aux expériences de double marquage, elles visaient essentiellement à trouver des terminaisons axonales contenant TH et VGLUT2 chez la souris, pour déterminer si celles-ci seraient toutes synaptiques, tel que précédemment observé chez le raton.

1.4 Morphométrie et extrapolation de l'incidence synaptique

Au cours de ce travail, nous avons pris soin d'obtenir une image de tous les profils de varicosités marqués pour la TH et/ou VGLUT2, c'est-à-dire de tout profil axonal mesurant plus de 0.25 µm de diamètre et contenant un agrégat de vésicules synaptiques, avec ou sans mitochondrie et spécialisation membranaire synaptique.

Les varicosités axonales ont été mesurées pour le diamètre long (L), court (c) et moyen (L + c / 2) à l'aide du logiciel Image J du NIH. Par la suite, nous avons noté la présence et la longueur des jonctions synaptiques, définies par une apposition des membranes plasmiques parallèles et leur épaississement de part et d'autre d'un espace extracellulaire légèrement élargi. La fréquence synaptique observée en coupe fine isolée a été extrapolée au volume entier de la varicosité selon la formule stéréologique de Beaudet et Sotelo (1981), telle que validée par Umbriaco et coll. (Umbriaco et coll., 1994).

Étant donné que les données ont été obtenues en coupes fines isolées, il fallait être conscient du risque de sous-estimer l'incidence synaptique des terminaisons axonales marquées, surtout dans le cas du marquage à l'immunoperoxidase-DAB, qui obscurcit le contenu de la varicosité et peut ainsi rendre difficile la visualisation d'un complexe de jonction synaptique. Aussi, dans le deuxième volet de la thèse où les terminaisons synaptiques sont apparues particulièrement rares, nous avons tenu compte de la diversité d'apparence que peuvent revêtir les complexes de jonction, des plus petits et symétriques aux plus larges et asymétriques (Colonnier, 1968), et retenues comme synaptiques certaines varicosités dont le seul signe de différenciation membranaire synaptique était une petite zone de rectitude et d'apposition parallèle des membranes.

2 Régression du co-phénotype glutamatergique des neurones à dopamine chez le rat adulte

2.1 Rappel des principaux résultats

Ayant initialement observé une régression de la co-expression de l'ARNm de la *TH* et du *Vglut2* dans le mésencéphale ventral du raton aux stades embryonnaires tardifs et durant la période néonatale, puis démontré la co-localisation de ces deux protéines dans les terminaisons axonales du NAC chez le raton de 15 jours, il nous est apparu nécessaire de déterminer le devenir du double phénotype à l'âge adulte. À cette fin, des doubles hybridations *in situ*, ainsi que des doubles marquages immunocytochimiques pour la TH et VGLUT2 ont été effectués chez des rats adultes soumis ou non à la lésion 6-OHDA néonatale. Chez l'adulte témoin ou 6-OHDA lésé, très peu de neurones exprimant à la fois l'ARNm de *TH* et celui de*Vglut2* dans l'ATV et la SNc ont été détectés. Aucune terminaison axonale doublement marquée pour la TH et VGLUT2 n'a été détectée dans le NAC du rat adulte normal, alors que celles-ci représentaient 28% de toutes les varicosités TH de ce noyau à P15. Chez le rat adulte lésé à la 6-OHDA, nous n'avons trouvé qu'un très petit nombre de terminaisons doublement marquées dans le NAC, contrairement au 37% des terminaisons résiduelles TH précédemment trouvé dans ce noyau à P15. De la même façon, alors que 17% des terminaisons TH du NS du rat témoin et 46% de celles de la néoinnervation DA de la SN du rat 6-OHDA lésé étaient aussi immunomarquées pour le VGLUT2 à l'âge de 15 jours, aucune terminaison doublement marquée n'a été retrouvée dans ces deux régions à l'âge adulte. Dans chaque région, il a été aussi noté que toutes les terminaisons doublement marquées étaient munies de complexes de jonction membranaire synaptique, contrairement à celles marquées pour la TH seule chez le raton et l'adulte ou pour VGLUT2 seul chez le raton de 15 jours.

2.2 Implications fonctionnelles

Étant donné l'expression précoce de l'ARNm de *Vglut2* dans les neurones mésencéphaliques DA au cours de la période embryonnaire, la répression de cette expression juste avant la naissance puis durant la période postnatale, ainsi que la régression du double phénotype TH/VGLUT2 dans les terminaisons axonales des neurones DA chez le rat adulte, il semble des plus probables que la libération de

glutamate par les neurones DA joue un rôle déterminant au cours du développement de ces neurones. Sans avoir tout compris des signaux moléculaires qui activent le double phénotype lors du développement post-natal (ou par suite d'une lésion) et l'inactivent chez adulte, on sait déjà que l'expression de *Vglut2* est inhibée *in vitro* lorsque les neurones DA en culture entrent en contact avec des neurones GABA (Mendez et coll., 2008). De plus, des études en cours montrent que l'application d'antagonistes des récepteurs NMDA réduit de façon significative la survie de neurones DA mis en culture alors que le knockout conditionnel du gène *Vglut2* chez la souris s'accompagne d'une réduction de la croissance et la survie des neurones DA mésencéphaliques tant en culture que chez l'animal, diminue la densité des innervations DA et glutamatergique ainsi que la libération de DA dans le noyau accumbens de la souris adulte, et affecte le comportement moteur de l'animal (Fortin et coll., soumis).

L'observation montrant que les neurones DA du mésencéphale du rat adulte soient pourvus de terminaisons axonales pour un tiers synaptiques et pour les deux tiers asynaptiques (Descarries et coll., 1996) soulève la question de ce qui distingue fonctionnellement les deux types de varicosités. Trudeau avait déjà formulé l'hypothèse voulant que le glutamate libéré par les neurones DA le soit à partir de leurs terminaisons pourvues de jonctions synaptiques (Trudeau, 2004). Le fait que toutes les varicosités présentant le double phénotype TH/VGLUT2 soient munies d'un complexe de jonction synaptique chez le rat de 15 jours semble favoriser cette hypothèse. Par contre, le double phénotype régresse avec l'âge, tandis qu'une spécialisation membranaire synaptique persiste sur le tiers des terminaisons DA du striatum. Serait-ce que le double phénotype soit d'une importance particulière lors de la formation de ces varicosités synaptiques, plutôt que du maintien de cette caractéristique morphologique? À moins que ces neurones DA ne soient progressivement le siège d'une ségrégation de la TH et de VGLUT2 dans des branches ou des varicosités différentes de leur arborisation axonale. En microculture d'un seul neurone DA, la majorité des varicosités TH apparait aussi immunofluorescente pour VGLUT2, mais certaines varicosités TH immunonégatives pour VGLUT2 sont observées près du corps cellulaire (Dal Bo et coll., 2004). La question est cruciale, en raison des conséquences fonctionnelles que pourraient signifier l'une ou l'autre configuration. Il faudra bien trouver le moyen d'y répondre expérimentalement, même si cela s'avère difficile.

La présence des VGLUT dans des terminaisons axonales traditionnellement associées à la libération d'un autre neurotransmetteur amène aussi son lot de questions au plan neurobiologique (voir en autres Marder, 1999; El Mestikawy et coll., 2011). Lorsque les deux transmetteurs coexistent dans une même terminaison, sont-ils présents dans les mêmes vésicules synaptiques ou dans des vésicules synaptiques différentes? La résolution présentement obtenue en microscopie électronique limite la capacité de répondre à cette question. Dans le cas de la colocalisation de VGLUT3 dans les interneurones cholinergiques du néostriatum, un rôle de synergie vésiculaire a été proposé à l'effet que la présence du transporteur glutamatergique permette le stockage (et donc la libération) d'une quantité accrue d'acétylcholine dans les vésicules synaptiques de ces neurones (Gras et coll., 2008). Une étude récente a déjà suggéré qu'il puisse en être de même dans le cas de la coexistence de VGLUT2 dans les neurones DA (Hnasko et coll., 2010). Cependant, il faut noter que notre observation d'une absence de colocalisation de la TH et de VGLUT2 dans les terminaisons axonales dopaminergiques chez l'adulte n'est pas compatible avec l'idée d'une synergie vésiculaire via VGLUT2 dans ces terminaisons.

Advenant que le glutamate et la DA soient libérés à partir des mêmes varicosités, on peut aussi se demander si les deux transmetteurs sont co-libérés lors de l'arrivée d'un même potentiel d'action ou si certains mécanismes régulent la libération de l'un plutôt que l'autre transmetteur. En Introduction, nous avons déjà mentionné la possibilité que le double phénotype des neurones DA rende compte de l'émission d'un signal rapide (glutamatergique) suivie d'un signal modulateur plus lent (dopaminergique) (Lapish et coll., 2006; Lapish et coll., 2007). De plus, la double nature de la neurotransmission DA, tonique ou phasique, pourrait être à l'origine d'une régulation différentielle de la libération de glutamate et de celle de la DA par les terminaisons axonales de ces neurones (Trudeau, 2004). Ainsi, lors de décharges toniques à basse fréquence, alors que la libération de DA est réduite, le glutamate pourrait être prédominant. À l'inverse, lors des décharges en bouffée, de plus haute fréquence, la transmission dopaminergique serait favorisée. On conçoit que ces propriétés fonctionnelles prendraient une toute autre signification s'il fallait que le VGLUT2 et la TH se trouvent séquestrés dans des terminaisons axonales différentes des mêmes neurones. Les mécanismes du ciblage différentiel des deux protéines devraient alors être étudiés.

3 Caractérisation de l'innervation à dopamine striatale de la souris

3.1 Rappel des principaux résultats

L'étude de l'innervation mésostriatale DA de la souris nous est apparue d'autant plus justifiée qu'on ignorait presque tout des caractéristiques ultrastructurales de cette innervation, malgré l'utilisation croissante des souris génétiquement modifiées pour l'étude du système dopaminergique. L'étude s'avérait également pertinente du fait de l'identification récente d'une sous-population de neurones mésencéphaliques DA exprimant *Vglut2,* aussi bien chez la souris que chez le rat. Nous avons donc utilisé l'immunocytochimie TH en microscopie électronique pour caractériser la morphologie ultrastructurale des terminaisons DA du NAC, NAS et du néostriatum (NS) dans deux lignées de souris dont le gène *Vglut2* avait été sélectivement invalidé dans les neurones DA (cKO) ainsi et leurs témoins, de même que chez quelques souris C57BL/6/J sauvages. Comme précédemment chez le rat, l'examen a été effectué chez des souris jeunes (P15) et adultes (P70-90). Les trois régions ont aussi été examinées chez des souris cKO et témoins des deux âges par suite d'un immunomarquage double TH/VGLUT2. Dans chacune des trois régions, quel que soit l'âge et le génotype des souris, les terminaisons immunomarquées pour la TH se sont avérées comparables en terme de taille, de contenu vésiculaire, de pourcentage contenant une mitochondrie et de leur incidence synaptique très faible (5% des varicosités, en moyenne). Du fait qu'aucune terminaison doublement immunomarquée pour TH et VGLUT2 n'ait été observée chez les souris témoins des deux âges suggère que la régression du double phénotype glutamate-dopamine est plus précoce chez la souris que chez le rat, étayant l'hypothèse d'une importance particulière du double phénotype au cours du développement précoce des neurones DA.

3.2 Implication fonctionnelles

À moins qu'ici encore, la TH et le VGLUT2 ne soient ségrégués dans des branches ou des terminaisons axonales différentes d'un même neurone DA, il faut croire que chez la souris, tel que et peut-être davantage que chez le rat, l'innervation mésostriatale DA fonctionne principalement par libération diffuse et non non-ciblée de DA, et, probablement, grâce au maintien en permanence d'un faible niveau ambiant de DA dans l'espace extracellulaire.

Étant donné l'innervation DA extrêmement dense du striatum et la diffusion possible de la DA dans l'espace extracellulaire malgré sa recapture (Wightman et Zimmerman, 1990), cette hypothèse avait déjà émise dans le cas de l'innervation DA du néostriatum chez le rat (Descarries et coll., 1996). Plusieurs études ont en effet suggéré l'existence d'un niveau basal de DA dans le neuropile du striatum de rat (Parsons et Justice, 1992) lequel apparaît suffisant pour mettre en jeu des récepteurs à haute affinité. Selon cette hypothèse, la relâche de DA en réponse à un potentiel d'action unique ou une décharge en bouffée viendrait se superposer localement à ce niveau de base, comme des gouttes de pluie tombant à la surface d'une mare. En autres fonctions, ce niveau ambiant de DA pourrait permettre un contrôle durable de l'expression de récepteurs à haute affinité, largement distribués sur les éléments du striatum, pour y contrôler l'expression de divers gènes et réguler la libération d'autres transmetteurs. Dans ces conditions, le phénomène de recapture servirait surtout à restreindre la sphère d'influence du transmetteur localement libéré, ainsi qu'à contrôler le niveau de base. Le fait que ce niveau ambiant de DA soit faible pourrait expliquer le fait que les déficits fonctionnels résultants d'une dénervation DA striatale n'apparaissent qu'à la suite de la disparition d'une très forte proportion des terminaisons axonales DA. Son existence pourrait aussi rendre compte des récupérations fonctionnelles, quoique limitées, observées après greffe (Perlow et coll., 1979), sans rétablissement des circuits synaptiques préexistants.

En l'absence de complexes de jonction membranaire sur une si grande majorité des terminaisons mésostriatales DA de la souris, il faut aussi s'interroger sur les mécanismes de libération et le mode d'action du transmetteur issu de telles varicosités, en tenant compte des connaissances actuelles de la machinerie moléculaire responsable de l'exocytose du transmetteur et de l'ancrage des récepteurs dans le cas des terminaisons axonales synaptiquement différenciées.

Lorsque les varicosités sont asynaptiques, on peut supposer que les molécules connues pour être enrichies au niveau des densités présynaptiques et qui assurent l'arrimage et l'exocytose des vésicules (Schoch et Gundelfinger, 2006) sont dispersées de façon plutôt uniforme sur toute la surface des varicosités, ce qui devrait permettre la libération de DA à divers endroits de leur pourtour, plutôt que dans une zone restreinte, préétablie et relativement fixe de leur surface. Une telle dispersion des sites de relâche

rappelle le mécanisme évoqué pour la libération dendritique de la DA, qui, sans être complètement caractérisé, ne semble pas requérir la présence d'une zone active, ni le même contingent de protéines d'exocytose retrouvé dans les terminaisons synaptiques typiques, libérant le glutamate ou le GABA (Nirenberg et coll., 1996; Witkovsky et coll., 2009; Mendez et coll., 2011). Dans ce cas de figure, on peut envisager que la libération du transmetteur soit en quelque sorte aléatoire, non ciblée, par rapport aux éléments du microenvironnement immédiat des varicosités.

Quant aux molécules d'échafaudage et d'adhésion identifiées aux sites de jonction post-synaptique (revu par Zhai et Bellen, 2004), on peut leur supposer deux rôles fondamentaux. D'une part, assurer l'agrégation et l'ancrage des récepteurs dans une zone particulière (la densité postsynaptique) des éléments synaptiquement contactés; d'autre part, assurer une certaine stabilité de la relation spatiale entre les éléments pré- et post-synaptiques. A contrario, la rareté des jonctions postsynaptiques formées par les varicosités DA striatales suggère une dispersion des récepteurs sur les éléments dopaminoceptifs, en accord avec les rares données actuelles sur la distribution subcellulaire des récepteurs DA, qui n'ont jamais été visualisés au sein même des interfaces synaptiques et toujours sur des portions "extra-synaptiques" des éléments dopaminoceptifs (Smiley et coll., 1994; Bergson et coll., 1995; Missale et coll., 1998).

Pour ce qui est d'une relation durable avec des partenaires particuliers du microenvironnement immédiat des varicosités DA, il faut se rappeler qu'une autre caractéristique morphologique de ces terminaisons axonales est l'hétérogénéité de leur forme, laquelle pourrait aussi traduire une certaine instabilité structurelle, à la fois de leur configuration générale et de leur contenu. Il est bien connu que tous les constituants internes des varicosités sont mobiles dans les axones. Ainsi, les rares reconstructions tridimensionnelles de varicosités axonales du cerveau qui ont été effectuées à partir de coupes ultrafines sériées pour la microscopie électronique (ex., Umbriaco et coll., 1994) montrent des bosses et des creux de leur surface, qui correspondent à la présence d'organites internes, et notamment de mitochondries. Quant aux complexes (ou granules) de transport des protéines dites pré-synaptiques, où ceux des protéines retrouvées dans les "zones actives" comme Bassoon et Piccolo, ils ont été qualifiés d'extrêmement mobiles dans les axones de neurones en culture (Ahmari et coll., 2000; Shapira et coll., 2003). Des observations similaires ont été rapportées au sujet de la

protéine constitutive du transporteur membranaire de la DA (DAT), et ce tant dans les varicosités axonales que les extensions dendritiques de neurones DA mésencéphaliques en culture (Eriksen et coll., 2009). Dans ce contexte, on peut imaginer une certaine mobilité ou translocation des varicosités elles-mêmes le long de leur axone, et que la libération par exocytose de DA, induite ou spontanée, puisse survenir dans une myriade de lieux qui changent constamment de microlocalisation précise en regard du microenvironnement tissulaire.

4 Perspectives d'avenir

En l'absence de terminaison axonales présentant le co-phénotype TH/VGLUT2, chez la jeune souris, on peut se demander si le co-phénotype dopamine-glutamate régresse plus précocement chez cette espèce que chez le rat. Sans doute cette question mériterait-elle une étude en double hybridation *in situ* de la co-expression de TH et VGLUT2 dans le mésencéphale de la souris au cours de la période embryonnaire tardive et de la période néonatale, étude qui pourrait également être effectuée en conjuguant l'immunocytochimie de la TH à l'hybridation *in situ* de VGUT2. On peut également s'interroger sur la possibilité que la co-localisation TH/VGLUT2 observée chez le raton mais absente chez l'adulte se retrouve de nouveau dans certaines pathologies neurologiques adultes dans un but compensateur?

Une explication alternative que nous avons déjà envisagée est celle d'une ségrégation particulièrement précoce de la TH et VGLUT2 dans certaines branches et/ou varicosités des neurones DA de la souris. En théorie, trois cas de figure sont possibles : des branches ou varicosités axonales des neurones DA contenant la TH seulement (DA), d'autres VGLUT2 seulement (glutamate) et d'autres encore contenant TH et VGLUT2 et donc capables de libérer les deux transmetteurs. La ségrégation de TH et de VGLUT2 dans des branches différentes du même neurone permettrait de réconcilier nos résultats avec des données récentes d'optogénétique démontrant une libération de glutamate après stimulation sélective des neurones DA du mésencéphale dans des tranches du prosencéphale de souris adulte (Stuber et coll., 2010; Tecuapetla et coll., 2010).

Régler la question de la ségrégation est un défi de taille, qui représente aussi une perspective d'avenir des plus intéressantes par suite de nos travaux. La solution pourrait venir d'une étude en microscopie électronique combinant l'immunocytochimie de la TH et de VGLUT2 à celle d'une molécule hautement diffusible introduite par marquage

juxtacellulaire ou transfection virale d'un neurone DA mésencéphalique. Ainsi, chez le rat de 15 jours, on pourrait marquer l'arborisation axonale d'un seul neurone DA, vérifier la nature DA de ce neurone par immunocytochimie TH du mésencéphale ventral, puis examiner le ou les territoires de distribution de l'arborisation axonale (ex. noyau accumbens) en microscopie électronique, à la recherche de varicosités axonales immunoréactives pour l'un et/ou l'autre marqueur après double marquage du marqueur diffusible et de la TH ou VGLUT2. Une histoire à suivre…

Enfin, sans doute y aurait-il lieu de mieux caractériser, à l'échelon moléculaire, les terminaisons axonales DA dépourvues de jonctions synaptiques, pour savoir dans quelle mesure leurs mécanismes et leur mode de libération, ainsi que leurs propriétés fonctionnelles, sont comparables ou diffèrents de ceux des terminaisons typiquement synaptiques.

Bibliographie (Introduction et discussion générales)

Abercrombie, M. (1946). "Estimation of nuclear population from microtome sections." Anat Rec **94**: 239-247.

Ahmari, S. E., J. Buchanan and S. J. Smith (2000). "Assembly of presynaptic active zones from cytoplasmic transport packets." Nat Neurosci **3**(5): 445-451.

Aihara, Y., H. Mashima, H. Onda, S. Hisano, H. Kasuya, T. Hori, S. Yamada, H. Tomura, Y. Yamada, I. Inoue, I. Kojima and J. Takeda (2000). "Molecular cloning of a novel brain-type Na(+)-dependent inorganic phosphate cotransporter." J Neurochem **74**(6): 2622-2625.

Alsiö, J., K. Nordenankar, E. Arvidsson, C. Birgner, S. Mahmoudi, B. Halbout, C. Smith, G. M. Fortin, L. Olson, L. Descarries, L.-É. Trudeau, K. Kullander, D. Lévesque and Å. Wallén-Mackenzie (2011). "Enhanced sucrose and cocaine self-administration and cue-induced drug seeking after loss of VGLUT2 in midbrain dopamine neurons in mice." J Neurosci **31**(35): 12593-12603.

Amilhon, B., E. Lepicard, T. Renoir, R. Mongeau, D. Popa, O. Poirel, S. Miot, C. Gras, A. M. Gardier, J. Gallego, M. Hamon, L. Lanfumey, B. Gasnier, B. Giros and S. El Mestikawy (2010). "VGLUT3 (vesicular glutamate transporter type 3) contribution to the regulation of serotonergic transmission and anxiety." J Neurosci **30**(6): 2198-2210.

Andén, N. E., A. Carlsson, A. Dahlström, K. Fuxe, N. A. Hillarp and K. Larsson (1964). "Demonstration and mapping out of nigro-neostriatal dopamine neurons." Life Sci **3**: 523-530.

Andén, N. E., K. Fuxe, B. Hamberger and T. Hökfelt (1966a). "A quantitative study on the nigro-neostriatal dopamine neuron system in the rat." Acta Physiol. Scand. **67**(3): 306-312.

Andén, N. E., A. Dahlström, F. Fuxe, K. Larsson, L. Olson and U. Ungerstedt (1966b). "Ascending monoamine neurons to the telecephalon and diencephalon." Acta Physiol. Scand. **67**: 313-326.

Angenstein, F. and S. Staak (1997). "Receptor-mediated activation of protein kinase C in hippocampal long-term potentiation: facts, problems and implications." Prog Neuropsychopharmacol Biol Psychiatry **21**(3): 427-454.

Antonopoulos, J., I. Dori, A. Dinopoulos, M. Chiotelli and J. G. Parnavelas (2002). "Postnatal development of the dopaminergic system of the striatum in the rat." Neuroscience **110**(2): 245-256.

Arluison, M., M. Dietl and J. Thibault (1984). "Ultrastructural morphology of dopaminergic nerve terminals and synapses in the striatum of the rat using tyrosine hydroxylase immunocytochemistry: a topographical study." Brain Res Bull **13**(2): 269-285.

Bai, L., H. Xu, J. F. Collins and F. K. Ghishan (2001). "Molecular and functional analysis of a novel neuronal vesicular glutamate transporter." J Biol Chem **276**(39): 36764-36769.

Baker, H., T. H. Joh and D. J. Reis (1980). "Genetic control of number of midbrain dopaminergic neurons in inbred strains of mice: relationship to size and neuronal density of the striatum." Proc Natl Acad Sci U S A **77**(7): 4369-4373.

Barbeau, A., T. L. Sourkes and G. F. Murphy (1962). Les catécholamines dans la maladie de Parkinson. Geneva, Georg & CO.

Beaudet, A. and L. Descarries (1976). "Quantitative data on serotonin nerve terminals in adult rat neocortex." Brain Res **111**(2): 301-309.

Beaudet, A. and C. Sotelo (1981). "Synaptic remodeling of serotonin axon terminals in rat agranular cerebellum." Brain Res **206**(2): 305-329.

Bellocchio, E. E., H. Hu, A. Pohorille, J. Chan, V. M. Pickel and R. H. Edwards (1998). "The localization of the brain-specific inorganic phosphate transporter suggests a specific presynaptic role in glutamatergic transmission." J Neurosci **18**(21): 8648-8659.

Bellocchio, E. E., R. J. Reimer, R. T. Fremeau, Jr. and R. H. Edwards (2000). "Uptake of glutamate into synaptic vesicles by an inorganic phosphate transporter." Science **289**(5481): 957-960.

Berger, T. W., S. Kaul, E. M. Stricker and M. J. Zigmond (1985). "Hyperinnervation of the striatum by dorsal raphe afferents after dopamine-depleting brain lesions in neonatal rats." Brain Res **336**(2): 354-358.

Bergson, C., L. Mrzljak, J. F. Smiley, M. Pappy, R. Levenson and P. S. Goldman-Rakic (1995). "Regional, cellular, and subcellular variations in the distribution of D1 and D5 dopamine receptors in primate brain." J Neurosci **15**(12): 7821-7836.

Bernheimer, H., W. Birkmayer, O. Hornykiewicz, K. Jellinger and F. Seitelberger (1973). "Brain dopamine and the syndromes of Parkinson and Huntington. Clinical, morphological and neurochemical correlations." J Neurol Sci **20**(4): 415-455.

Bertler, A., B. Falck, C. G. Gottfries, L. Ljunggren and E. Rosengren (1964). "Some observations on adrenergic connections between mesencephalon and cerebral hemispheres." Acta Pharmacol Toxicol (Copenh) **21**: 283-289.

Birgner, C., K. Nordenankar, M. Lundblad, J. A. Mendez, C. Smith, M. le Greves, D. Galter, L. Olsön, A. Fredriksson, L.-É. Trudeau, K. Kullander and Å. Wallén-Mackenzie (2010). "VGLUT2 in dopamine neurons is required for psychostimulant-induced behavioral activation." Proc Natl Acad Sci U S A **107**(1): 389-394.

Birkmayer, W. and O. Hornykiewicz (1961). "[The L-3,4-dioxyphenylalanine (DOPA)-effect in Parkinson-akinesia]." Wien Klin Wochenschr **73**: 787-788.

Björklund, A. and O. Lindvall (1984). Dopamine-containing systems in the CNS. Handbook of Chemical Neuroanatomy. Classical Transmitters in the CNS, Part 1. A. Björklund and T. Hökfelt. Eds. New York, Elsevier. **Vol. 2:** 55-122.

Bliss, T. V. and T. Lomo (1973). "Long-lasting potentiation of synaptic transmission in the dentate area of the anaesthetized rabbit following stimulation of the perforant path." J Physiol **232**(2): 331-356.

Bliss, T. V. and A. R. Gardner-Medwin (1973). "Long-lasting potentiation of synaptic transmission in the dentate area of the unanaestetized rabbit following stimulation of the perforant path." J Physiol **232**(2): 357-374.

Boileau, I., J. M. Assaad, R. O. Pihl, C. Benkelfat, M. Leyton, M. Diksic, R. E. Tremblay and A. Dagher (2003). "Alcohol promotes dopamine release in the human nucleus accumbens." Synapse **49**(4): 226-231.

Borges, K. and R. Dingledine (1998). "AMPA receptors: molecular and functional diversity." Prog Brain Res **116**: 153-170.

Boulland, J. L., T. Qureshi, R. P. Seal, A. Rafiki, V. Gundersen, L. H. Bergersen, R. T. Fremeau, Jr., R. H. Edwards, J. Storm-Mathisen and F. A. Chaudhry (2004). "Expression of the vesicular glutamate transporters during development indicates the widespread corelease of multiple neurotransmitters." J Comp Neurol **480**(3): 264-280.

Boulland, J. L., M. Jenstad, A. J. Boekel, F. G. Wouterlood, R. H. Edwards, J. Storm-Mathisen and F. A. Chaudhry (2009). "Vesicular glutamate and GABA transporters sort to distinct sets of vesicles in a population of presynaptic terminals." Cereb Cortex **19**(1): 241-248.

Bourque, M. J. and L.-É. Trudeau (2000). "GDNF enhances the synaptic efficacy of dopaminergic neurons in culture." Eur J Neurosci **12**(9): 3172-3180.

Bouyer, J. J., T. H. Joh and V. M. Pickel (1984). "Ultrastructural localization of tyrosine hydroxylase in rat nucleus accumbens." J Comp Neurol **227**(1): 92-103.

Braak, H., K. Del Tredici, U. Rub, R. A. de Vos, E. N. Jansen Steur and E. Braak (2003). "Staging of brain pathology related to sporadic Parkinson's disease." Neurobiol Aging **24**(2): 197-211.

Bradford, H. F. and H. K. Ward (1976). "On glutaminase activity in mammalian synaptosomes." Brain Res **110**(1): 115-125.

Bredt, D. S. and R. A. Nicoll (2003). "AMPA receptor trafficking at excitatory synapses." Neuron **40**(2): 361-379.

Breese, G. R. and T. D. Traylor (1972). "Developmental characteristics of brain catecholamines and tyrosine hydroxylase in the rat: effects of 6-hydroxydopamine." Br J Pharmacol **44**(2): 210-222.

Breese, G. R., A. A. Baumeister, T. J. McCown, S. G. Emerick, G. D. Frye, K. Crotty and R. A. Mueller (1984). "Behavioral differences between neonatal and adult 6-hydroxydopamine-treated rats to dopamine agonists: relevance to neurological symptoms in clinical syndromes with reduced brain dopamine." J Pharmacol Exp Ther **231**(2): 343-354.

Brewer, G. J. and C. W. Cotman (1989). "NMDA receptor regulation of neuronal morphology in cultured hippocampal neurons." Neurosci Lett **99**(3): 268-273.

Broaddus, W. C. and J. P. Bennett, Jr. (1990). "Postnatal development of striatal dopamine function. II. Effects of neonatal 6-hydroxydopamine treatments on D1 and D2 receptors, adenylate cyclase activity and presynaptic dopamine function." Brain Res Dev Brain Res **52**(1-2): 273-277.

Broman, J., E. Rinvik, M. Sassoe-Pognetto, H. Khalkhali Sandiz and O. P. Ottersen (2003). Glutamate. The Rat Nervous System, Third Edition. G. Paxinos. Eds. New York, Elsevier**:** 1269-1292.

Busceti, C. L., F. Biagioni, F. Mastroiacovo, D. Bucci, P. Lenzi, L. Pasquali, A. Trabucco, F. Nicoletti and F. Fornai (2008). "High number of striatal dopaminergic neurons during early postnatal development: correlation analysis with dopaminergic fibers." J Neural Transm **115**(10): 1375-1383.

Carlsson, A. (1959). "The occurrence, distribution and physiological role of catecholamines in the nervous system." Pharmacol Rev **11**(2, Part 2): 490-493.

Carlsson, A., B. Falck, K. Fuxe and N. A. Hillarp (1964). "Cellular Localization of Monoamines in the Spinal Cord." Acta Physiol Scand **60**: 112-119.

Carlsson, A. (1987). "Perspectives on the discovery of central monoaminergic neurotransmission." Annu Rev Neurosci **10**: 19-40.

Castaneda, E., I. Q. Whishaw, L. Lermer and T. E. Robinson (1990). "Dopamine depletion in neonatal rats: effects on behavior and striatal dopamine release assessed by intracerebral microdialysis during adulthood." Brain Res **508**(1): 30-39.

Chang, S. and P. De Camilli (2001). "Glutamate regulates actin-based motility in axonal filopodia." Nat Neurosci **4**(8): 787-793.

Chergui, K., M. F. Suaud-Chagny and F. Gonon (1994). "Nonlinear relationship between impulse flow, dopamine release and dopamine elimination in the rat brain in vivo." Neuroscience **62**(3): 641-645.

Chuhma, N., H. Zhang, J. Masson, X. Zhuang, D. Sulzer, R. Hen and S. Rayport (2004). "Dopamine neurons mediate a fast excitatory signal via their glutamatergic synapses." J Neurosci **24**(4): 972-981.

Chuhma, N., W. Y. Choi, S. Mingote and S. Rayport (2009). "Dopamine neuron glutamate cotransmission: frequency-dependent modulation in the mesoventromedial projection." Neuroscience **164**(3): 1068-1083.

Collingridge, G. L. and R. A. Lester (1989). "Excitatory amino acid receptors in the vertebrate central nervous system." Pharmacol Rev **41**(2): 143-210.

Collingridge, G. L., J. T. Isaac and Y. T. Wang (2004). "Receptor trafficking and synaptic plasticity." Nat Rev Neurosci **5**(12): 952-962.

Collingridge, G. L., S. Peineau, J. G. Howland and Y. T. Wang (2010). "Long-term depression in the CNS." Nat Rev Neurosci **11**(7): 459-473.

Colonnier, M. (1968). "Synaptic patterns on different cell types in the different laminae of the cat visual cortex. An electron microscope study." Brain Res **9**(2): 268-287.

Commons, K. G. (2009). "Locally collateralizing glutamate neurons in the dorsal raphe nucleus responsive to substance P contain vesicular glutamate transporter 3 (VGLUT3)." J Chem Neuroanat **38**(4): 273-281.

Congar, P., A. Bergevin and L.-É. Trudeau (2002). "D2 receptors inhibit the secretory process downstream from calcium influx in dopaminergic neurons: implication of K+ channels." J Neurophysiol **87**(2): 1046-1056.

Cookson, M. R. (2010). "Unravelling the role of defective genes." Prog Brain Res **183**: 43-57.

Curtis, D. R. and J. C. Watkins (1960). "The excitation and depression of spinal neurones by structurally related amino acids." J Neurochem **6**: 117-141.

Dahlström, A. and K. Fuxe (1964). "Evidence for the Existence of Monoamine-Containing Neurons in the Central Nervous System. I. Demonstration of Monoamines in the Cell Bodies of Brain Stem Neurons." Acta Physiol Scand: (Suppl. 232), 231-255.

Dal Bo, G., F. St-Gelais, M. Danik, S. Williams, M. Cotton and L.-É. Trudeau (2004). "Dopamine neurons in culture express VGLUT2 explaining their capacity to release glutamate at synapses in addition to dopamine." J Neurochem **88**(6): 1398-1405.

Dal Bo, G., N. Bérubé-Carrière, J. A. Mendez, D. Leo, M. Riad, L. Descarries, D. Lévesque and L.-É. Trudeau (2008a). "Enhanced glutamatergic phenotype of mesencephalic dopamine neurons after neonatal 6-hydroxydopamine lesion." Neuroscience **156**(1): 59-70.

Dal Bo, G., N. Berube-Carriere, J. A. Mendez, D. Leo, M. Riad, L. Descarries, D. Levesque and L. E. Trudeau (2008b). "Enhanced glutamatergic phenotype of mesencephalic dopamine neurons after neonatal 6-hydroxydopamine lesion." Neuroscience **156**(1): 59-70.

Danbolt, N. C. (2001). "Glutamate uptake." Prog Neurobiol **65**(1): 1-105.

De Paola, V., S. Arber and P. Caroni (2003). "AMPA receptors regulate dynamic equilibrium of presynaptic terminals in mature hippocampal networks." Nat Neurosci **6**(5): 491-500.

Dearry, A., J. A. Gingrich, P. Falardeau, R. T. Fremeau, Jr., M. D. Bates and M. G. Caron (1990). "Molecular cloning and expression of the gene for a human D1 dopamine receptor." Nature **347**(6288): 72-76.

Descarries, L., A. Beaudet and K. C. Watkins (1975). "Serotonin nerve terminals in adult rat neocortex." Brain Res **100**(3): 563-588.

Descarries, L., K. C. Watkins and Y. Lapierre (1977). "Noradrenergic axon terminals in the cerebral cortex of rat. III. Topometric ultrastructural analysis." Brain Res **133**(2): 197-222.

Descarries, L., O. Bosler, F. Berthelet and M. H. Des Rosiers (1980). "Dopaminergic nerve endings visualised by high-resolution autoradiography in adult rat neostriatum." Nature **284**(5757): 620-622.

Descarries, L., F. Berthelet, S. Garcia and A. Beaudet (1986). "Dopaminergic projection from nucleus raphe dorsalis to neostriatum in the rat." J Comp Neurol **249**(4): 511-520, 484-515.

Descarries, L., J. J. Soghomonian, S. Garcia, G. Doucet and J. P. Bruno (1992). "Ultrastructural analysis of the serotonin hyperinnervation in adult rat neostriatum following neonatal dopamine denervation with 6-hydroxydopamine." Brain Res **569**(1): 1-13.

Descarries, L., K. C. Watkins, S. Garcia, O. Bosler and G. Doucet (1996). "Dual character, asynaptic and synaptic, of the dopamine innervation in adult rat neostriatum: a quantitative autoradiographic and immunocytochemical analysis." J Comp Neurol **375**(2): 167-186.

Descarries, L., N. Bérubé-Carrière, M. Riad, G. D. Bo, J. A. Mendez and L.-É. Trudeau (2008). "Glutamate in dopamine neurons: synaptic versus diffuse transmission." Brain Res Rev **58**(2): 290-302.

Dewar, K. M., J. J. Soghomonian, J. P. Bruno, L. Descarries and T. A. Reader (1990). "Elevation of dopamine D2 but not D1 receptors in adult rat neostriatum after neonatal 6-hydroxydopamine denervation." Brain Res **536**(1-2): 287-296.

Di Chiara, G. (1995). "The role of dopamine in drug abuse viewed from the perspective of its role in motivation." Drug Alcohol Depend **38**(2): 95-137.

Di Chiara, G., V. Bassareo, S. Fenu, M. A. De Luca, L. Spina, C. Cadoni, E. Acquas, E. Carboni, V. Valentini and D. Lecca (2004). "Dopamine and drug addiction: the nucleus accumbens shell connection." Neuropharmacology **47 Suppl 1**: 227-241.

Dingledine, R., K. Borges, D. Bowie and S. F. Traynelis (1999). "The glutamate receptor ion channels." Pharmacol Rev **51**(1): 7-61.

Disbrow, J. K., M. J. Gershten and J. A. Ruth (1982). "Uptake of L-[3H] glutamic acid by crude and purified synaptic vesicles from rat brain." Biochem Biophys Res Commun **108**(3): 1221-1227.

Doucet, G., L. Descarries and S. Garcia (1986). "Quantification of the dopamine innervation in adult rat neostriatum." Neuroscience **19**(2): 427-445.

Dreier, J. P. (2011). "The role of spreading depression, spreading depolarization and spreading ischemia in neurological disease." Nat Med **17**(4): 439-447.

Edwards, R. H. (2007). "The neurotransmitter cycle and quantal size." Neuron **55**(6): 835-858.

Ehringer, H. and O. Hornykiewicz (1960). "[Distribution of noradrenaline and dopamine (3-hydroxytyramine) in the human brain and their behavior in diseases of the extrapyramidal system]." Klin Wochenschr **38**: 1236-1239.

El Mestikawy, S., Å. Wallén-Mackenzie, G. M. Fortin, L. Descarries and L.-É. Trudeau (2011). "From glutamate co-release to vesicular synergy: vesicular glutamate transporters." Nat Rev Neurosci **12**(4): 204-216.

Erickson, J. D., M. K. Schafer, T. I. Bonner, L. E. Eiden and E. Weihe (1996). "Distinct pharmacological properties and distribution in neurons and endocrine cells of two isoforms of the human vesicular monoamine transporter." Proc Natl Acad Sci U S A **93**(10): 5166-5171.

Eriksen, J., S. G. Rasmussen, T. N. Rasmussen, C. B. Vaegter, J. H. Cha, M. F. Zou, A. H. Newman and U. Gether (2009). "Visualization of dopamine transporter trafficking in live neurons by use of fluorescent cocaine analogs." J Neurosci **29**(21): 6794-6808.

Fabbrini, G., J. M. Brotchie, F. Grandas, M. Nomoto and C. G. Goetz (2007). "Levodopa-induced dyskinesias." Mov Disord **22**(10): 1379-1389; quiz 1523.

Fallon, J. H. and R. Y. Moore (1978). "Catecholamine innervation of the basal forebrain. IV. Topography of the dopamine projection to the basal forebrain and neostriatum." J Comp Neurol **180**(3): 545-580.

Fattorini, G., C. Verderio, M. Melone, S. Giovedi, F. Benfenati, M. Matteoli and F. Conti (2009). "VGLUT1 and VGAT are sorted to the same population of synaptic vesicles in subsets of cortical axon terminals." J Neurochem **110**(5): 1538-1546.

Fearnley, J. M. and A. J. Lees (1991). "Ageing and Parkinson's disease: substantia nigra regional selectivity." Brain **114 (Pt 5)**: 2283-2301.

Fernandes Xavier, F. G., G. Doucet, M. Geffard and L. Descarries (1994). "Dopamine neoinnervation in the substantia nigra and hyperinnervation in the interpeduncular nucleus of adult rat following neonatal cerebroventricular administration of 6-hydroxydopamine." Neuroscience **59**(1): 77-87.

Floresco, S. B., A. R. West, B. Ash, H. Moore and A. A. Grace (2003). "Afferent modulation of dopamine neuron firing differentially regulates tonic and phasic dopamine transmission." Nat Neurosci **6**(9): 968-973.

Fonnum, F. (1984). "Glutamate: a neurotransmitter in mammalian brain." J Neurochem **42**(1): 1-11.

Fortin, G. M., M. J. Bourque, J. A. Mendez, D. Leo, K. Nordenankar, C. Birgner, E. Arvidsson, V. V. Rymar, N. Bérubé-Carrière, A. M. Claveau, L. Descarries, A. F. Sadikot, Å. Wallén-Mackenzie and L.-É. Trudeau "Glutamate corelease promotes growth and survival of midbrain dopamine neurons ".

Fortin, G. M., M. J. Bourque, J. A. Mendez, D. Leo, K. Nordenankar, C. Birgner, E. Arvidsson, V. V. Rymar, N. Bérubé-Carrière, L. Descarries, A. F. Sadikot, Å. Wallén-Mackenzie and L.-É. Trudeau "Glutamate corelease promotes growth and survival of a subset of midbrain dopamine neurons." soumis.

Fremeau, R. T., Jr., M. D. Troyer, I. Pahner, G. O. Nygaard, C. H. Tran, R. J. Reimer, E. E. Bellocchio, D. Fortin, J. Storm-Mathisen and R. H. Edwards (2001). "The expression of vesicular glutamate transporters defines two classes of excitatory synapse." Neuron **31**(2): 247-260.

Fremeau, R. T., Jr., J. Burman, T. Qureshi, C. H. Tran, J. Proctor, J. Johnson, H. Zhang, D. Sulzer, D. R. Copenhagen, J. Storm-Mathisen, R. J. Reimer, F. A. Chaudhry and R. H. Edwards (2002). "The identification of vesicular glutamate transporter 3 suggests novel modes of signaling by glutamate." Proc Natl Acad Sci U S A **99**(22): 14488-14493.

Fremeau, R. T., Jr., K. Kam, T. Qureshi, J. Johnson, D. R. Copenhagen, J. Storm-Mathisen, F. A. Chaudhry, R. A. Nicoll and R. H. Edwards (2004). "Vesicular glutamate transporters 1 and 2 target to functionally distinct synaptic release sites." Science **304**(5678): 1815-1819.

Freund, T. F., J. F. Powell and A. D. Smith (1984). "Tyrosine hydroxylase-immunoreactive boutons in synaptic contact with identified striatonigral neurons, with particular reference to dendritic spines." Neuroscience **13**(4): 1189-1215.

Futami, T., K. Takakusaki and S. T. Kitai (1995). "Glutamatergic and cholinergic inputs from the pedunculopontine tegmental nucleus to dopamine neurons in the substantia nigra pars compacta." Neurosci Res **21**(4): 331-342.

Fuxe, K. and L. F. Agnati (1991). Two Principal Modes of Electrochemical Communication in the Brain: Volume versus Wiring Transmission. Volume Transmission in the Brain: Novel Mechanisms for Neural Transmission. K. Fuxe and L. F. Agnati. Eds. New York, Raven Press**:** 1-9.

Garris, P. A., E. L. Ciolkowski, P. Pastore and R. M. Wightman (1994). "Efflux of dopamine from the synaptic cleft in the nucleus accumbens of the rat brain." J Neurosci **14**(10): 6084-6093.

Gasser, T. (2010). "Identifying PD-causing genes and genetic susceptibility factors: current approaches and future prospects." Prog Brain Res **183**: 3-20.

Gauthier, J., M. Parent, M. Lévesque and A. Parent (1999). "The axonal arborization of single nigrostriatal neurons in rats." Brain Res **834**(1-2): 228-232.

Gerfen, C. R., T. M. Engber, L. C. Mahan, Z. Susel, T. N. Chase, F. J. Monsma, Jr. and D. R. Sibley (1990). "D1 and D2 dopamine receptor-regulated gene expression of striatonigral and striatopallidal neurons." Science **250**(4986): 1429-1432.

Gillespie, D. C., G. Kim and K. Kandler (2005). "Inhibitory synapses in the developing auditory system are glutamatergic." Nat Neurosci **8**(3): 332-338.

Goedert, M., M. G. Spillantini and S. W. Davies (1998). "Filamentous nerve cell inclusions in neurodegenerative diseases." Curr Opin Neurobiol **8**(5): 619-632.

Grace, A. A. and B. S. Bunney (1984). "The control of firing pattern in nigral dopamine neurons: single spike firing." J Neurosci **4**(11): 2866-2876.

Grace, A. A. and S. P. Onn (1989). "Morphology and electrophysiological properties of immunocytochemically identified rat dopamine neurons recorded in vitro." J Neurosci **9**(10): 3463-3481.

Grace, A. A. (1991). "Phasic versus tonic dopamine release and the modulation of dopamine system responsivity: a hypothesis for the etiology of schizophrenia." Neuroscience **41**(1): 1-24.

Gras, C., E. Herzog, G. C. Bellenchi, V. Bernard, P. Ravassard, M. Pohl, B. Gasnier, B. Giros and S. El Mestikawy (2002). "A third vesicular glutamate transporter expressed by cholinergic and serotoninergic neurons." J Neurosci **22**(13): 5442-5451.

Gras, C., J. Vinatier, B. Amilhon, A. Guerci, C. Christov, P. Ravassard, B. Giros and S. El Mestikawy (2005). "Developmentally regulated expression of VGLUT3 during early post-natal life." Neuropharmacology **49**(6): 901-911.

Gras, C., B. Amilhon, E. M. Lepicard, O. Poirel, J. Vinatier, M. Herbin, S. Dumas, E. T. Tzavara, M. R. Wade, G. G. Nomikos, N. Hanoun, F. Saurini, M. L. Kemel, B. Gasnier,

B. Giros and S. El Mestikawy (2008). "The vesicular glutamate transporter VGLUT3 synergizes striatal acetylcholine tone." Nat Neurosci **11**(3): 292-300.

Gravius, A., M. Pietraszek, A. Dekundy and W. Danysz (2010). "Metabotropic glutamate receptors as therapeutic targets for cognitive disorders." Curr Top Med Chem **10**(2): 187-206.

Graybiel, A. M., E. C. Hirsch and Y. A. Agid (1987). "Differences in tyrosine hydroxylase-like immunoreactivity characterize the mesostriatal innervation of striosomes and extrastriosomal matrix at maturity." Proc Natl Acad Sci U S A **84**(1): 303-307.

Greengard, P. (2001). "The neurobiology of slow synaptic transmission." Science **294**(5544): 1024-1030.

Groenewegen, H. J., H. W. Berendse and S. N. Haber (1993). "Organization of the output of the ventral striatopallidal system in the rat: ventral pallidal efferents." Neuroscience **57**(1): 113-142.

Guillery, R. W. (2002). "On counting and counting errors." J Comp Neurol **447**(1): 1-7.

Gundersen, V. (2008). "Co-localization of excitatory and inhibitory transmitters in the brain." Acta Neurol Scand Suppl **188**: 29-33.

Guyenet, P. G. and J. K. Crane (1981). "Non-dopaminergic nigrostriatal pathway." Brain Res **213**(2): 291-305.

Hartmann, M., R. Heumann and V. Lessmann (2001). "Synaptic secretion of BDNF after high-frequency stimulation of glutamatergic synapses." EMBO J **20**(21): 5887-5897.

Hattori, T., H. C. Fibiger, P. L. McGeer and L. Maler (1973). "Analysis of the fine structure of the dopaminergic nigrostriatal projection by electron microscopic autoradiography." Exp Neurol **41**(3): 599-611.

Hayashi, M., M. Otsuka, R. Morimoto, S. Hirota, S. Yatsushiro, J. Takeda, A. Yamamoto and Y. Moriyama (2001). "Differentiation-associated Na+-dependent inorganic phosphate cotransporter (DNPI) is a vesicular glutamate transporter in endocrine glutamatergic systems." J Biol Chem **276**(46): 43400-43406.

Hayashi, T. (1954). "Effects of sodium glutamate on the nervous system." Keio J. Med. **3**: 183-192.

Headley, P. M. and S. Grillner (1990). "Excitatory amino acids and synaptic transmission: the evidence for a physiological function." Trends Pharmacol Sci **11**(5): 205-211.

Hedreen, J. C. and J. P. Chalmers (1972). "Neuronal degeneration in rat brain induced by 6-hydroxydopamine; a histological and biochemical study." Brain Res **47**(1): 1-36.

Herve, D., M. Levi-Strauss, I. Marey-Semper, C. Verney, J. P. Tassin, J. Glowinski and J. A. Girault (1993). "G(olf) and Gs in rat basal ganglia: possible involvement of G(olf) in the coupling of dopamine D1 receptor with adenylyl cyclase." J Neurosci **13**(5): 2237-2248.

Herzog, E., G. C. Bellenchi, C. Gras, V. Bernard, P. Ravassard, C. Bedet, B. Gasnier, B. Giros and S. El Mestikawy (2001). "The existence of a second vesicular glutamate transporter specifies subpopulations of glutamatergic neurons." J Neurosci **21**(22): RC181.

Herzog, E., J. Gilchrist, C. Gras, A. Muzerelle, P. Ravassard, B. Giros, P. Gaspar and S. El Mestikawy (2004a). "Localization of VGLUT3, the vesicular glutamate transporter type 3, in the rat brain." Neuroscience **123**(4): 983-1002.

Herzog, E., M. Landry, E. Buhler, R. Bouali-Benazzouz, C. Legay, C. E. Henderson, F. Nagy, P. Dreyfus, B. Giros and S. El Mestikawy (2004b). "Expression of vesicular glutamate transporters, VGLUT1 and VGLUT2, in cholinergic spinal motoneurons." Eur J Neurosci **20**(7): 1752-1760.

Hioki, H., F. Fujiyama, K. Taki, R. Tomioka, T. Furuta, N. Tamamaki and T. Kaneko (2003). "Differential distribution of vesicular glutamate transporters in the rat cerebellar cortex." Neuroscience **117**(1): 1-6.

Hioki, H., F. Fujiyama, K. Nakamura, S. X. Wu, W. Matsuda and T. Kaneko (2004). "Chemically specific circuit composed of vesicular glutamate transporter 3- and preprotachykinin B-producing interneurons in the rat neocortex." Cereb Cortex **14**(11): 1266-1275.

Hioki, H., H. Nakamura, Y. F. Ma, M. Konno, T. Hayakawa, K. C. Nakamura, F. Fujiyama and T. Kaneko (2010). "Vesicular glutamate transporter 3-expressing nonserotonergic projection neurons constitute a subregion in the rat midbrain raphe nuclei." J Comp Neurol **518**(5): 668-686.

Hisano, S., K. Hoshi, Y. Ikeda, D. Maruyama, M. Kanemoto, H. Ichijo, I. Kojima, J. Takeda and H. Nogami (2000). "Regional expression of a gene encoding a neuron-specific Na(+)-dependent inorganic phosphate cotransporter (DNPI) in the rat forebrain." Brain Res Mol Brain Res **83**(1-2): 34-43.

Hnasko, T. S., N. Chuhma, H. Zhang, G. Y. Goh, D. Sulzer, R. D. Palmiter, S. Rayport and R. H. Edwards (2010). "Vesicular glutamate transport promotes dopamine storage and glutamate corelease in vivo." Neuron **65**(5): 643-656.

Ho, A., A. C. Gore, C. S. Weickert and M. Blum (1995). "Glutamate regulation of GDNF gene expression in the striatum and primary striatal astrocytes." NeuroReport **6**(10): 1454-1458.

Hökfelt, T. (1968). "In vitro studies on central and peripheral monoamine neurons at the ultrastructural level." Z Zellforsch Mikrosk Anat **91**(1): 1-74.

Hökfelt, T. and U. Ungerstedt (1969). "Electron and fluorescence microscopical studies on the nucleus caudatus putamen of the rat after unilateral lesions of ascending nigro-neostriatal dopamine neurons." Acta Physiol Scand **76**(4): 415-426.

Hökfelt, T. and A. Ljungdahl (1972). "Application of cytochemical techniques to the study of suspected transmitter substances in the nervous system." Adv Biochem Psychopharmacol **6**: 1-36.

Hökfelt, T., O. Johansson, K. Fuxe, M. Goldstein and D. Park (1976). "Immunohistochemical studies on the localization and distribution of monoamine neuron systems in the rat brain. I. Tyrosine hydroxylase in the mes- and diencephalon." Med Biol **54**(6): 427-453.

Hökfelt, T., R. Martensson, A. Björklund, K. S. and M. Goldstein (1984a). Distribution maps of tyrosine-hydroxylase-immunoreactive neurons in the rat brain. Handbook of Chemical Neuroanatomy. Classical Transmitters in the CNS, Part 1. A. Björklund and T. Hökfelt. Eds. New York, Elsevier. **Vol. 2:** 277-379.

Hökfelt, T., C. B. Smith, G. Norell, A. Peters, A. Crane, M. Goldstein, M. Brownstein and L. Sokoloff (1984b). "Attempts to combine 2-deoxyglucose autoradiography and tyrosine hydroxylase immunohistochemistry." Neuroscience **13**(2): 495-512.

Hollmann, M. and S. Heinemann (1994). "Cloned glutamate receptors." Annu Rev Neurosci **17**: 31-108.

Ibarretxe, G., D. Perrais, F. Jaskolski, A. Vimeney and C. Mulle (2007). "Fast regulation of axonal growth cone motility by electrical activity." J Neurosci **27**(29): 7684-7695.

Ibata, Y., Y. Nojyo, T. Matsuura and Y. Sano (1973). "Nigro-neostriatal projection. A correlative study with Fink-Heimer impregnation, fluorescence histochemistry and electron microscopy." Z Zellforsch Mikrosk Anat **138**(3): 333-344.

Jaber, M., S. Jones, B. Giros and M. G. Caron (1997). "The dopamine transporter: a crucial component regulating dopamine transmission." Mov Disord **12**(5): 629-633.

Jackson, D., J. P. Bruno, M. K. Stachowiak and M. J. Zigmond (1988). "Inhibition of striatal acetylcholine release by serotonin and dopamine after the intracerebral administration of 6-hydroxydopamine to neonatal rats." Brain Res **457**(2): 267-273.

Jackson, J., B. H. Bland and M. C. Antle (2009). "Nonserotonergic projection neurons in the midbrain raphe nuclei contain the vesicular glutamate transporter VGLUT3." Synapse **63**(1): 31-41.

Johnson, J. L. and M. H. Aprison (1970). "The distribution of glutamic acid, a transmitter candidate, and other amino acids in the dorsal sensory neuron of the cat." Brain Res **24**(2): 285-292.

Joyce, M. P. and S. Rayport (2000). "Mesoaccumbens dopamine neuron synapses reconstructed in vitro are glutamatergic." Neuroscience **99**(3): 445-456.

Kaiya, H. and M. Namba (1981). "Two types of dopaminergic nerve terminals in the rat neostriatum. An ultrastructural study." Neurosci Lett **25**(3): 251-256.

Kaneko, T., H. Akiyama, I. Nagatsu and N. Mizuno (1990). "Immunohistochemical demonstration of glutaminase in catecholaminergic and serotoninergic neurons of rat brain." Brain Res **507**(1): 151-154.

Kao, Y. H., L. Lassova, T. Bar-Yehuda, R. H. Edwards, P. Sterling and N. Vardi (2004). "Evidence that certain retinal bipolar cells use both glutamate and GABA." J Comp Neurol **478**(3): 207-218.

Karpinar, D. P., M. B. Balija, S. Kugler, F. Opazo, N. Rezaei-Ghaleh, N. Wender, H. Y. Kim, G. Taschenberger, B. H. Falkenburger, H. Heise, A. Kumar, D. Riedel, L. Fichtner, A. Voigt, G. H. Braus, K. Giller, S. Becker, A. Herzig, M. Baldus, H. Jackle, S. Eimer, J. B. Schulz, C. Griesinger and M. Zweckstetter (2009). "Pre-fibrillar alpha-synuclein variants with impaired beta-structure increase neurotoxicity in Parkinson's disease models." EMBO J **28**(20): 3256-3268.

Kashani, A., C. Betancur, B. Giros, E. Hirsch and S. El Mestikawy (2007). "Altered expression of vesicular glutamate transporters VGLUT1 and VGLUT2 in Parkinson disease." Neurobiol Aging **28**(4): 568-578.

Kashani, A., E. Lepicard, O. Poirel, C. Videau, J. P. David, C. Fallet-Bianco, A. Simon, A. Delacourte, B. Giros, J. Epelbaum, C. Betancur and S. El Mestikawy (2008). "Loss of VGLUT1 and VGLUT2 in the prefrontal cortex is correlated with cognitive decline in Alzheimer disease." Neurobiol Aging **29**(11): 1619-1630.

Kawano, M., A. Kawasaki, H. Sakata-Haga, Y. Fukui, H. Kawano, H. Nogami and S. Hisano (2006). "Particular subpopulations of midbrain and hypothalamic dopamine neurons express vesicular glutamate transporter 2 in the rat brain." J Comp Neurol **498**(5): 581-592.

Kebabian, J. W. and P. Greengard (1971). "Dopamine-sensitive adenyl cyclase: possible role in synaptic transmission." Science **174**(16): 1346-1349.

Kebabian, J. W. and D. B. Calne (1979). "Multiple receptors for dopamine." Nature **277**(5692): 93-96.

Kebabian, J. W., M. Beaulieu and Y. Itoh (1984). "Pharmacological and biochemical evidence for the existence of two categories of dopamine receptor." Can J Neurol Sci **11**(1 Suppl): 114-117.

Keefe, K. A., M. J. Zigmond and E. D. Abercrombie (1993). "In vivo regulation of extracellular dopamine in the neostriatum: influence of impulse activity and local excitatory amino acids." J Neural Transm Gen Sect **91**(2-3): 223-240.

Kienast, T. and A. Heinz (2006). "Dopamine and the diseased brain." CNS Neurol Disord Drug Targets **5**(1): 109-131.

Kitai, S. T., M. Sugimori and J. D. Kocsis (1976). "Excitatory nature of dopamine in the nigro-caudate pathway." Exp Brain Res **24**(4): 351-363.

Kramer, M. L. and W. J. Schulz-Schaeffer (2007). "Presynaptic alpha-synuclein aggregates, not Lewy bodies, cause neurodegeneration in dementia with Lewy bodies." J Neurosci **27**(6): 1405-1410.

Krnjevic, K. (1986). Amino Acid: 30 year's progress in research. Fast and Slow Signaling in the Nervous System. L. L. Iversen and E. Goodman. Eds. Oxford, Oxford University Press**:** 3-15.

Krystal, J. H., S. J. Mathew, D. C. D'Souza, A. Garakani, H. Gunduz-Bruce and D. S. Charney (2010). "Potential psychiatric applications of metabotropic glutamate receptor agonists and antagonists." CNS Drugs **24**(8): 669-693.

Lapish, C. C., J. K. Seamans and L. J. Chandler (2006). "Glutamate-dopamine cotransmission and reward processing in addiction." Alcohol Clin Exp Res **30**(9): 1451-1465.

Lapish, C. C., S. Kroener, D. Durstewitz, A. Lavin and J. K. Seamans (2007). "The ability of the mesocortical dopamine system to operate in distinct temporal modes." Psychopharmacology (Berl) **191**(3): 609-625.

Lavin, A., L. Nogueira, C. C. Lapish, R. M. Wightman, P. E. Phillips and J. K. Seamans (2005). "Mesocortical dopamine neurons operate in distinct temporal domains using multimodal signaling." J Neurosci **25**(20): 5013-5023.

Lavoie, B., Y. Smith and A. Parent (1989). "Dopaminergic innervation of the basal ganglia in the squirrel monkey as revealed by tyrosine hydroxylase immunohistochemistry." J Comp Neurol **289**(1): 36-52.

Lin, L. F., D. H. Doherty, J. D. Lile, S. Bektesh and F. Collins (1993). "GDNF: a glial cell line-derived neurotrophic factor for midbrain dopaminergic neurons." Science **260**(5111): 1130-1132.

Lindvall, O. and A. Bjorklund (1974). "The organization of the ascending catecholamine neuron systems in the rat brain as revealed by the glyoxylic acid fluorescence method." Acta Physiol. Scand. Suppl **412**: 1-48.

Lovinger, D. M. (2010). "Neurotransmitter roles in synaptic modulation, plasticity and learning in the dorsal striatum." Neuropharmacology **58**(7): 951-961.

Lucas, D. R. and J. P. Newhouse (1957). "The toxic effect of sodium L-glutamate on the inner layers of the retina." AMA Arch Ophthalmol **58**(2): 193-201.

Luthman, J., E. Brodin, E. Sundstrom and B. Wiehager (1990). "Studies on brain monoamine and neuropeptide systems after neonatal intracerebroventricular 6-hydroxydopamine treatment." Int J Dev Neurosci **8**(5): 549-560.

Malinow, R. and R. C. Malenka (2002). "AMPA receptor trafficking and synaptic plasticity." Annu Rev Neurosci **25**: 103-126.

Marder, E. (1999). "Neural signalling: Does colocalization imply cotransmission?" Curr Biol **9**(21): R809-811.

Margolis, E. B., H. Lock, G. O. Hjelmstad and H. L. Fields (2006). "The ventral tegmental area revisited: is there an electrophysiological marker for dopaminergic neurons?" J Physiol **577**(Pt 3): 907-924.

Marshall, J. F., J. S. Richardson and P. Teitelbaum (1974). "Nigrostriatal bundle damage and the lateral hypothalamic syndrome." J Comp Physiol Psychol **87**(5): 808-830.

Martin, I., V. L. Dawson and T. M. Dawson (2010). "The impact of genetic research on our understanding of Parkinson's disease." Prog Brain Res **183**: 21-41.

Matsuda, W., T. Furuta, K. C. Nakamura, H. Hioki, F. Fujiyama, R. Arai and T. Kaneko (2009). "Single nigrostriatal dopaminergic neurons form widely spread and highly dense axonal arborizations in the neostriatum." J Neurosci **29**(2): 444-453.

Mattson, M. P., P. Dou and S. B. Kater (1988). "Outgrowth-regulating actions of glutamate in isolated hippocampal pyramidal neurons." J Neurosci **8**(6): 2087-2100.

Maycox, P. R., T. Deckwerth, J. W. Hell and R. Jahn (1988). "Glutamate uptake by brain synaptic vesicles. Energy dependence of transport and functional reconstitution in proteoliposomes." J Biol Chem **263**(30): 15423-15428.

McKenna, M. C., U. Sonnewald, X. Huang, J. Stevenson and H. R. Zielke (1996). "Exogenous glutamate concentration regulates the metabolic fate of glutamate in astrocytes." J Neurochem **66**(1): 386-393.

McKinney, R. A., A. Luthi, C. E. Bandtlow, B. H. Gahwiler and S. M. Thompson (1999). "Selective glutamate receptor antagonists can induce or prevent axonal sprouting in rat hippocampal slice cultures." Proc Natl Acad Sci U S A **96**(20): 11631-11636.

Mendez, J. A., M. J. Bourque, G. Dal Bo, M. L. Bourdeau, M. Danik, S. Williams, J. C. Lacaille and L.-É. Trudeau (2008). "Developmental and target-dependent regulation of vesicular glutamate transporter expression by dopamine neurons." J Neurosci **28**(25): 6309-6318.

Mendez, J. A., M. J. Bourque, C. Fasano, C. Kortleven and L. E. Trudeau (2011). "Somatodendritic dopamine release requires synaptotagmin 4 and 7 and the participation of voltage-gated calcium channels." J Biol Chem **286**(27): 23928-23937.

Merali, Z., J. McIntosh and H. Anisman (2004). "Anticipatory cues differentially provoke in vivo peptidergic and monoaminergic release at the medial prefrontal cortex." Neuropsychopharmacology **29**(8): 1409-1418.

Mintz, E. M. and T. J. Scott (2006). "Colocalization of serotonin and vesicular glutamate transporter 3-like immunoreactivity in the midbrain raphe of Syrian hamsters (Mesocricetus auratus)." Neurosci Lett **394**(2): 97-100.

Missale, C., S. R. Nash, S. W. Robinson, M. Jaber and M. G. Caron (1998). "Dopamine receptors: from structure to function." Physiol Rev **78**(1): 189-225.

Miyamoto, E. (2006). "Molecular mechanism of neuronal plasticity: induction and maintenance of long-term potentiation in the hippocampus." J Pharmacol Sci **100**(5): 433-442.

Moechars, D., M. C. Weston, S. Leo, Z. Callaerts-Vegh, I. Goris, G. Daneels, A. Buist, M. Cik, P. van der Spek, S. Kass, T. Meert, R. D'Hooge, C. Rosenmund and R. M. Hampson (2006). "Vesicular glutamate transporter VGLUT2 expression levels control quantal size and neuropathic pain." J Neurosci **26**(46): 12055-12066.

Monsma, F. J., Jr., L. C. Mahan, L. D. McVittie, C. R. Gerfen and D. R. Sibley (1990). "Molecular cloning and expression of a D1 dopamine receptor linked to adenylyl cyclase activation." Proc Natl Acad Sci U S A **87**(17): 6723-6727.

Moore, R. Y., R. K. Bhatnagar and A. Heller (1971). "Anatomical and chemical studies of a nigro-neostriatal projection in the cat." Brain Res **30**(1): 119-135.

Moore, R. Y. and J. P. Card (1984). Noradrenaline-containing neuron system. Handbook of Chemical Neuroanatomy. Classical Transmitters in the CNS, Part 1. A. Björklund and T. Hökfelt. Eds. New York, Elsevier. **Vol. 2:** 123-156.

Mrini, A., J. P. Soucy, F. Lafaille, P. Lemoine and L. Descarries (1995). "Quantification of the serotonin hyperinnervation in adult rat neostriatum after neonatal 6-hydroxydopamine lesion of nigral dopamine neurons." Brain Res **669**(2): 303-308.

Nader, K., G. E. Schafe and J. E. Le Doux (2000). "Fear memories require protein synthesis in the amygdala for reconsolidation after retrieval." Nature **406**(6797): 722-726.

Nagatsu, T., M. Levitt and S. Udenfriend (1964). "Tyrosine hydroxylase. The initial step in norepinephrine biosynthesis." J Biol Chem **239**: 2910-2917.

Naito, S. and T. Ueda (1985). "Characterization of glutamate uptake into synaptic vesicles." J Neurochem **44**(1): 99-109.

Nakamura, K., H. Hioki, F. Fujiyama and T. Kaneko (2005). "Postnatal changes of vesicular glutamate transporter (VGluT)1 and VGluT2 immunoreactivities and their colocalization in the mouse forebrain." J Comp Neurol **492**(3): 263-288.

Nakanishi, S., Y. Nakajima, M. Masu, Y. Ueda, K. Nakahara, D. Watanabe, S. Yamaguchi, S. Kawabata and M. Okada (1998). "Glutamate receptors: brain function and signal transduction." Brain Res Brain Res Rev **26**(2-3): 230-235.

Nauta, H. J., M. B. Pritz and R. J. Lasek (1974). "Afferents to the rat caudoputamen studied with horseradish peroxidase. An evaluation of a retrograde neuroanatomical research method." Brain Res **67**(2): 219-238.

Nelson, E. L., C. L. Liang, C. M. Sinton and D. C. German (1996). "Midbrain dopaminergic neurons in the mouse: computer-assisted mapping." J Comp Neurol **369**(3): 361-371.

Ng, K. T., B. S. O'Dowd, N. S. Rickard, S. R. Robinson, M. E. Gibbs, C. Rainey, W. Q. Zhao, G. L. Sedman and L. Hertz (1997). "Complex roles of glutamate in the Gibbs-Ng model of one-trial aversive learning in the new-born chick." Neurosci Biobehav Rev **21**(1): 45-54.

Ni, B., P. R. Rosteck, Jr., N. S. Nadi and S. M. Paul (1994). "Cloning and expression of a cDNA encoding a brain-specific Na(+)-dependent inorganic phosphate cotransporter." Proc Natl Acad Sci U S A **91**(12): 5607-5611.

Ni, B., X. Wu, G. M. Yan, J. Wang and S. M. Paul (1995). "Regional expression and cellular localization of the Na(+)-dependent inorganic phosphate cotransporter of rat brain." J Neurosci **15**(8): 5789-5799.

Nicholls, D. G. (1989). "Release of glutamate, aspartate, and gamma-aminobutyric acid from isolated nerve terminals." J Neurochem **52**(2): 331-341.

Nickerson Poulin, A., A. Guerci, S. El Mestikawy and K. Semba (2006). "Vesicular glutamate transporter 3 immunoreactivity is present in cholinergic basal forebrain neurons projecting to the basolateral amygdala in rat." J Comp Neurol **498**(5): 690-711.

Nirenberg, M. J., R. A. Vaughan, G. R. Uhl, M. J. Kuhar and V. M. Pickel (1996). "The dopamine transporter is localized to dendritic and axonal plasma membranes of nigrostriatal dopaminergic neurons." J Neurosci **16**(2): 436-447.

Nirenberg, M. J., J. Chan, R. A. Vaughan, G. R. Uhl, M. J. Kuhar and V. M. Pickel (1997). "Immunogold localization of the dopamine transporter: an ultrastructural study of the rat ventral tegmental area." J Neurosci **17**(14): 5255-5262.

Nishimaru, H., C. E. Restrepo, J. Ryge, Y. Yanagawa and O. Kiehn (2005). "Mammalian motor neurons corelease glutamate and acetylcholine at central synapses." Proc Natl Acad Sci U S A **102**(14): 5245-5249.

Norenberg, M. D. and A. Martinez-Hernandez (1979). "Fine structural localization of glutamine synthetase in astrocytes of rat brain." Brain Res **161**(2): 303-310.

Obeso, J. A., M. Merello, M. C. Rodriguez-Oroz, C. Marin, J. Guridi and L. Alvarez (2007). "Levodopa-induced dyskinesias in Parkinson's disease." Handb Clin Neurol **84**: 185-218.

Oliveira, A. L., F. Hydling, E. Olsson, T. Shi, R. H. Edwards, F. Fujiyama, T. Kaneko, T. Hokfelt, S. Cullheim and B. Meister (2003). "Cellular localization of three vesicular glutamate transporter mRNAs and proteins in rat spinal cord and dorsal root ganglia." Synapse **50**(2): 117-129.

Olney, J. W. (1969). "Brain lesions, obesity, and other disturbances in mice treated with monosodium glutamate." Science **164**(880): 719-721.

Olney, J. W. (1971). "Glutamate-induced neuronal necrosis in the infant mouse hypothalamus. An electron microscopic study." J Neuropathol Exp Neurol **30**(1): 75-90.

Olson, L., A. Seiger and K. Fuxe (1972). "Heterogeneity of striatal and limbic dopamine innervation: highly fluorescent islands in developing and adult rats." Brain Res **44**(1): 283-288.

Ottem, E. N., J. G. Godwin, S. Krishnan and S. L. Petersen (2004). "Dual-phenotype GABA/glutamate neurons in adult preoptic area: sexual dimorphism and function." J Neurosci **24**(37): 8097-8105.

Ottersen, O. P. and J. Storm-Mathisen (1984). "Glutamate- and GABA-containing neurons in the mouse and rat brain, as demonstrated with a new immunocytochemical technique." J Comp Neurol **229**(3): 374-392.

Ozawa, S., H. Kamiya and K. Tsuzuki (1998). "Glutamate receptors in the mammalian central nervous system." Prog Neurobiol **54**(5): 581-618.

Parent, M. and A. Parent (2010). "Substantia nigra and Parkinson's disease: a brief history of their long and intimate relationship." Can J Neurol Sci **37**(3): 313-319.

Parsons, L. H. and J. B. Justice, Jr. (1992). "Extracellular concentration and in vivo recovery of dopamine in the nucleus accumbens using microdialysis." J Neurochem **58**(1): 212-218.

Patneau, D. K. and M. L. Mayer (1990). "Structure-activity relationships for amino acid transmitter candidates acting at N-methyl-D-aspartate and quisqualate receptors." J Neurosci **10**(7): 2385-2399.

Peng, S., Y. Zhang, J. Zhang, H. Wang and B. Ren (2011). "Glutamate receptors and signal transduction in learning and memory." Mol Biol Rep **38**(1): 453-460.

Perlow, M. J., W. J. Freed, B. J. Hoffer, A. Seiger, L. Olson and R. J. Wyatt (1979). "Brain grafts reduce motor abnormalities produced by destruction of nigrostriatal dopamine system." Science **204**(4393): 643-647.

Peter, D., Y. Liu, C. Sternini, R. de Giorgio, N. Brecha and R. H. Edwards (1995). "Differential expression of two vesicular monoamine transporters." J Neurosci **15**(9): 6179-6188.

Peters, A. and S. L. Palay (1996). "The morphology of synapses." J Neurocytol **25**(12): 687-700.

Pickel, V. M., T. H. Joh and D. J. Reis (1976). "Monoamine-synthesizing enzymes in central dopaminergic, noradrenergic and serotonergic neurons. Immunocytochemical localization by light and electron microscopy." J Histochem Cytochem **24**(7): 792-306.

Pickel, V. M., S. C. Beckley, T. H. Joh and D. J. Reis (1981). "Ultrastructural immunocytochemical localization of tyrosine hydroxylase in the neostriatum." Brain Res **225**(2): 373-385.

Plenz, D. and S. T. Kitai (1996). "Organotypic cortex-striatum-mesencephalon cultures: the nigrostriatal pathway." Neurosci Lett **209**(3): 177-180.

Prensa, L. and A. Parent (2001). "The nigrostriatal pathway in the rat: A single-axon study of the relationship between dorsal and ventral tier nigral neurons and the striosome/matrix striatal compartments." J Neurosci **21**(18): 7247-7260.

Ramamoorthy, S., T. S. Shippenberg and L. D. Jayanthi (2011). "Regulation of monoamine transporters: Role of transporter phosphorylation." Pharmacol Ther **129**(2): 220-238.

Reijnierse, G. L., H. Veldstra and C. J. Van den Berg (1975). "Subcellular localization of gamma-aminobutyrate transaminase and glutamate dehydrogenase in adult rat brain. Evidence for at least two small glutamate compartments in brain." Biochem J **152**(3): 469-475.

Ren, J., C. Qin, F. Hu, J. Tan, L. Qiu, S. Zhao, G. Feng and M. Luo (2011). "Habenula "cholinergic" neurons co-release glutamate and acetylcholine and activate postsynaptic neurons via distinct transmission modes." Neuron **69**(3): 445-452.

Riedel, G. and K. G. Reymann (1996). "Metabotropic glutamate receptors in hippocampal long-term potentiation and learning and memory." Acta Physiol Scand **157**(1): 1-19.

Ross, R. A., A. B. Judd, V. M. Pickel, T. H. Joh and D. J. Reis (1976). "Strain-dependent variations in number of midbrain dopaminergic neurones." Nature **264**(5587): 654-656.

Ruel, J., S. Emery, R. Nouvian, T. Bersot, B. Amilhon, J. M. Van Rybroek, G. Rebillard, M. Lenoir, M. Eybalin, B. Delprat, T. A. Sivakumaran, B. Giros, S. El Mestikawy, T. Moser, R. J. Smith, M. M. Lesperance and J. L. Puel (2008). "Impairment of SLC17A8 encoding vesicular glutamate transporter-3, VGLUT3, underlies nonsyndromic deafness DFNA25 and inner hair cell dysfunction in null mice." Am J Hum Genet **83**(2): 278-292.

Sabo, S. L., R. A. Gomes and A. K. McAllister (2006). "Formation of presynaptic terminals at predefined sites along axons." J Neurosci **26**(42): 10813-10825.

Sachs, C. and G. Jonsson (1975). "Mechanisms of action of 6-hydroxydopamine." Biochem Pharmacol **24**(1): 1-8.

Sam, P. M. and J. B. Justice, Jr. (1996). "Effect of general microdialysis-induced depletion on extracellular dopamine." Anal Chem **68**(5): 724-728.

Schafer, M. K., H. Varoqui, N. Defamie, E. Weihe and J. D. Erickson (2002). "Molecular cloning and functional identification of mouse vesicular glutamate transporter 3 and its expression in subsets of novel excitatory neurons." J Biol Chem **277**(52): 50734-50748.

Schoch, S. and E. D. Gundelfinger (2006). "Molecular organization of the presynaptic active zone." Cell Tissue Res **326**(2): 379-391.

Schoepfer, R., H. Monyer, B. Sommer, W. Wisden, R. Sprengel, T. Kuner, H. Lomeli, A. Herb, M. Kohler, N. Burnashev and et al. (1994). "Molecular biology of glutamate receptors." Prog Neurobiol **42**(2): 353-357.

Schousboe, A. (1981). "Transport and metabolism of glutamate and GABA in neurons are glial cells." Int Rev Neurobiol **22**: 1-45.

Schwarting, R. K. and J. P. Huston (1996a). "Unilateral 6-hydroxydopamine lesions of meso-striatal dopamine neurons and their physiological sequelae." Prog Neurobiol **49**(3): 215-266.

Schwarting, R. K. and J. P. Huston (1996b). "The unilateral 6-hydroxydopamine lesion model in behavioral brain research. Analysis of functional deficits, recovery and treatments." Prog Neurobiol **50**(2-3): 275-331.

Seal, R. P., O. Akil, E. Yi, C. M. Weber, L. Grant, J. Yoo, A. Clause, K. Kandler, J. L. Noebels, E. Glowatzki, L. R. Lustig and R. H. Edwards (2008). "Sensorineural deafness and seizures in mice lacking vesicular glutamate transporter 3." Neuron **57**(2): 263-275.

Seeman, P., T. Lee, M. Chau-Wong and K. Wong (1976). "Antipsychotic drug doses and neuroleptic/dopamine receptors." Nature **261**(5562): 717-719.

Shapira, M., R. G. Zhai, T. Dresbach, T. Bresler, V. I. Torres, E. D. Gundelfinger, N. E. Ziv and C. C. Garner (2003). "Unitary assembly of presynaptic active zones from Piccolo-Bassoon transport vesicles." Neuron **38**(2): 237-252.

Shepherd, G. (1994). The Synaptic Organization of the Brain. New York, Oxford Univ. Press.

Shutoh, F., A. Ina, S. Yoshida, J. Konno and S. Hisano (2008). "Two distinct subtypes of serotonergic fibers classified by co-expression with vesicular glutamate transporter 3 in rat forebrain." Neurosci Lett **432**(2): 132-136.

Sims, K. D. and M. B. Robinson (1999). "Expression patterns and regulation of glutamate transporters in the developing and adult nervous system." Crit Rev Neurobiol **13**(2): 169-197.

Smiley, J. F., A. I. Levey, B. J. Ciliax and P. S. Goldman-Rakic (1994). "D1 dopamine receptor immunoreactivity in human and monkey cerebral cortex: predominant and extrasynaptic localization in dendritic spines." Proc Natl Acad Sci U S A **91**(12): 5720-5724.

Smith, I. D. and A. A. Grace (1992). "Role of the subthalamic nucleus in the regulation of nigral dopamine neuron activity." Synapse **12**(4): 287-303.

Smith, Y., B. D. Bennett, J. P. Bolam, A. Parent and A. F. Sadikot (1994). "Synaptic relationships between dopaminergic afferents and cortical or thalamic input in the sensorimotor territory of the striatum in monkey." J Comp Neurol **344**(1): 1-19.

Soghomonian, J. J., G. Doucet and L. Descarries (1987). "Serotonin innervation in adult rat neostriatum. I. Quantified regional distribution." Brain research **425**(1): 85-100.

Somogyi, J., A. Baude, Y. Omori, H. Shimizu, S. El Mestikawy, M. Fukaya, R. Shigemoto, M. Watanabe and P. Somogyi (2004). "GABAergic basket cells expressing cholecystokinin contain vesicular glutamate transporter type 3 (VGLUT3) in their synaptic terminals in hippocampus and isocortex of the rat." Eur J Neurosci **19**(3): 552-569.

Soussi, R., N. Zhang, S. Tahtakran, C. R. Houser and M. Esclapez (2010). "Heterogeneity of the supramammillary-hippocampal pathways: evidence for a unique GABAergic neurotransmitter phenotype and regional differences." Eur J Neurosci **32**(5): 771-785.

Spillantini, M. G., M. L. Schmidt, V. M. Lee, J. Q. Trojanowski, R. Jakes and M. Goedert (1997). "Alpha-synuclein in Lewy bodies." Nature **388**(6645): 839-840.

Stachowiak, M. K., J. P. Bruno, A. M. Snyder, E. M. Stricker and M. J. Zigmond (1984). "Apparent sprouting of striatal serotonergic terminals after dopamine-depleting brain lesions in neonatal rats." Brain Res **291**(1): 164-167.

Stark, H., T. Rothe, T. Wagner and H. Scheich (2004). "Learning a new behavioral strategy in the shuttle-box increases prefrontal dopamine." Neuroscience **126**(1): 21-29.

Storm-Mathisen, J., A. K. Leknes, A. T. Bore, J. L. Vaaland, P. Edminson, F. M. Haug and O. P. Ottersen (1983). "First visualization of glutamate and GABA in neurones by immunocytochemistry." Nature **301**(5900): 517-520.

Storm-Mathisen, J. and O. P. Ottersen (1990). "Immunocytochemistry of glutamate at the synaptic level." J Histochem Cytochem **38**(12): 1733-1743.

Stornetta, R. L., C. P. Sevigny and P. G. Guyenet (2002a). "Vesicular glutamate transporter DNPI/VGLUT2 mRNA is present in C1 and several other groups of brainstem catecholaminergic neurons." J Comp Neurol **444**(3): 191-206.

Stornetta, R. L., C. P. Sevigny, A. M. Schreihofer, D. L. Rosin and P. G. Guyenet (2002b). "Vesicular glutamate transporter DNPI/VGLUT2 is expressed by both C1 adrenergic and nonaminergic presympathetic vasomotor neurons of the rat medulla." J Comp Neurol **444**(3): 207-220.

Strata, P. and R. Harvey (1999). "Dale's principle." Brain Res Bull **50**(5-6): 349-350.

Stuber, G. D., T. S. Hnasko, J. P. Britt, R. H. Edwards and A. Bonci (2010). "Dopaminergic terminals in the nucleus accumbens but not the dorsal striatum corelease glutamate." J Neurosci **30**(24): 8229-8233.

Suaud-Chagny, M. F., C. Dugast, K. Chergui, M. Msghina and F. Gonon (1995). "Uptake of dopamine released by impulse flow in the rat mesolimbic and striatal systems in vivo." J Neurochem **65**(6): 2603-2611.

Sulzer, D., M. P. Joyce, L. Lin, D. Geldwert, S. N. Haber, T. Hattori and S. Rayport (1998). "Dopamine neurons make glutamatergic synapses in vitro." J Neurosci **18**(12): 4588-4602.

Surmeier, D. J., J. N. Guzman, J. Sanchez-Padilla and J. A. Goldberg (2010). "What causes the death of dopaminergic neurons in Parkinson's disease?" Prog Brain Res **183**: 59-77.

Swanson, L. W. (1982). "The projections of the ventral tegmental area and adjacent regions: a combined fluorescent retrograde tracer and immunofluorescence study in the rat." Brain Res Bull **9**(1-6): 321-353.

Takamori, S., J. S. Rhee, C. Rosenmund and R. Jahn (2000). "Identification of a vesicular glutamate transporter that defines a glutamatergic phenotype in neurons." Nature **407**(6801): 189-194.

Takamori, S., J. S. Rhee, C. Rosenmund and R. Jahn (2001). "Identification of differentiation-associated brain-specific phosphate transporter as a second vesicular glutamate transporter (VGLUT2)." J Neurosci **21**(22): RC182.

Takamori, S., P. Malherbe, C. Broger and R. Jahn (2002). "Molecular cloning and functional characterization of human vesicular glutamate transporter 3." EMBO Rep **3**(8): 798-803.

Tanaka, K. (2000). "Functions of glutamate transporters in the brain." Neurosci Res **37**(1): 15-19.

Tang, C. M., M. Dichter and M. Morad (1989). "Quisqualate activates a rapidly inactivating high conductance ionic channel in hippocampal neurons." Science **243**(4897): 1474-1477.

Tashiro, A., A. Dunaevsky, R. Blazeski, C. A. Mason and R. Yuste (2003). "Bidirectional regulation of hippocampal mossy fiber filopodial motility by kainate receptors: a two-step model of synaptogenesis." Neuron **38**(5): 773-784.

Tecuapetla, F., J. C. Patel, H. Xenias, D. English, I. Tadros, F. Shah, J. Berlin, K. Deisseroth, M. E. Rice, J. M. Tepper and T. Koos (2010). "Glutamatergic signaling by mesolimbic dopamine neurons in the nucleus accumbens." J Neurosci **30**(20): 7105-7110.

Tennyson, V. M., R. E. Barrett, G. Cohen, L. Cote, R. Heikkila and C. Mytilineou (1972). "The developing neostriatum of the rabbit: correlation of fluorescence histochemistry, electron microscopy, endogenous dopamine levels, and (3 H)dopamine uptake." Brain Res **46**: 251-285.

Tennyson, V. M., R. Heikkila, C. Mytilineou, L. Cote and G. Cohen (1974). "5-Hydroxydopamine 'tagged' neuronal boutons in rabbit neostriatum: interrelationship between vesicles and axonal membrane." Brain Res **82**(2): 341-348.

Tiberi, M., S. R. Nash, L. Bertrand, R. J. Lefkowitz and M. G. Caron (1996). "Differential regulation of dopamine D1A receptor responsiveness by various G protein-coupled receptor kinases." J Biol Chem **271**(7): 3771-3778.

Triarhou, L. C., J. Norton and B. Ghetti (1988a). "Synaptic connectivity of tyrosine hydroxylase immunoreactive nerve terminals in the striatum of normal, heterozygous and homozygous weaver mutant mice." J Neurocytol **17**(2): 221-232.

Triarhou, L. C., W. C. Low, J. Norton and B. Ghetti (1988b). "Reinstatement of synaptic connectivity in the striatum of weaver mutant mice following transplantation of ventral mesencephalic anlagen." J Neurocytol **17**(2): 233-243.

Trudeau, L.-É. (2004). "Glutamate co-transmission as an emerging concept in monoamine neuron function." J Psychiatry Neurosci **29**(4): 296-310.

Trussell, L. O. and G. D. Fischbach (1989). "Glutamate receptor desensitization and its role in synaptic transmission." Neuron **3**(2): 209-218.

Tupala, E. and J. Tiihonen (2004). "Dopamine and alcoholism: neurobiological basis of ethanol abuse." Prog Neuropsychopharmacol Biol Psychiatry **28**(8): 1221-1247.

Umbriaco, D., K. C. Watkins, L. Descarries, C. Cozzari and B. K. Hartman (1994). "Ultrastructural and morphometric features of the acetylcholine innervation in adult rat parietal cortex: an electron microscopic study in serial sections." J Comp Neurol **348**(3): 351-373.

Ungerstedt, U. (1968). "6-Hydroxy-dopamine induced degeneration of central monoamine neurons." Eur J Pharmacol **5**(1): 107-110.

Ungerstedt, U. (1971a). "Stereotaxic mapping of the monoamine pathways in the rat brain." Acta Physiol Scand Suppl **367**: 1-48.

Ungerstedt, U. (1971b). "Stereotaxic mapping of the monoamine pathways in the rat brain." Acta Physiol. Scand. Suppl **367**: 1-48.

Ungerstedt, U. (1971c). "Adipsia and aphagia after 6-hydroxydopamine induced degeneration of the nigro-striatal dopamine system." Acta physiologica Scandinavica. Supplementum **367**: 95-122.

Usunoff, K. G., R. Hassler, K. Romansky, P. Usunova and A. Wagner (1976). "The nigrostriatal projection in the cat. Part 1. Silver impregnation study." J Neurol Sci **28**(3): 265-288.

Van der Zee, E. A., P. G. Luiten and J. F. Disterhoft (1997). "Learning-induced alterations in hippocampal PKC-immunoreactivity: a review and hypothesis of its functional significance." Prog Neuropsychopharmacol Biol Psychiatry **21**(3): 531-572.

Varga, V., A. Losonczy, B. V. Zemelman, Z. Borhegyi, G. Nyiri, A. Domonkos, B. Hangya, N. Holderith, J. C. Magee and T. F. Freund (2009). "Fast synaptic subcortical control of hippocampal circuits." Science **326**(5951): 449-453.

Varoqui, H., M. K. Schafer, H. Zhu, E. Weihe and J. D. Erickson (2002). "Identification of the differentiation-associated Na+/PI transporter as a novel vesicular glutamate transporter expressed in a distinct set of glutamatergic synapses." J Neurosci **22**(1): 142-155.

Venton, B. J., H. Zhang, P. A. Garris, P. E. Phillips, D. Sulzer and R. M. Wightman (2003). "Real-time decoding of dopamine concentration changes in the caudate-putamen during tonic and phasic firing." J Neurochem **87**(5): 1284-1295.

Voon, V., P. O. Fernagut, J. Wickens, C. Baunez, M. Rodriguez, N. Pavon, J. L. Juncos, J. A. Obeso and E. Bezard (2009). "Chronic dopaminergic stimulation in Parkinson's disease: from dyskinesias to impulse control disorders." Lancet Neurol **8**(12): 1140-1149.

Voorn, P., B. Jorritsma-Byham, C. Van Dijk and R. M. Buijs (1986). "The dopaminergic innervation of the ventral striatum in the rat: a light- and electron-microscopical study with antibodies against dopamine." J Comp Neurol **251**(1): 84-99.

Voorn, P., A. Kalsbeek, B. Jorritsma-Byham and H. J. Groenewegen (1988). "The pre- and postnatal development of the dopaminergic cell groups in the ventral mesencephalon and the dopaminergic innervation of the striatum of the rat." Neuroscience **25**(3): 857-887.

Wallén-Mackenzie, Å., H. Gezelius, M. Thoby-Brisson, A. Nygard, A. Enjin, F. Fujiyama, G. Fortin and K. Kullander (2006). "Vesicular glutamate transporter 2 is required for central respiratory rhythm generation but not for locomotor central pattern generation." J Neurosci **26**(47): 12294-12307.

Wassef, M., A. Berod and C. Sotelo (1981). "Dopaminergic dendrites in the pars reticulata of the rat substantia nigra and their striatal input. Combined immunocytochemical localization of tyrosine hydroxylase and anterograde degeneration." Neuroscience **6**(11): 2125-2139.

Watkins, J. C. (1986). Twenty-five yeahrs of excitatory amino acid research: The end of the beginning? Excitatory Amino Acid. P. J. Roberts, A. Storm-Mathisen and A. Bradford. Eds. London, Macmillan**:** 1-39.

Weihe, E., M. K. Schafer, J. D. Erickson and L. E. Eiden (1994). "Localization of vesicular monoamine transporter isoforms (VMAT1 and VMAT2) to endocrine cells and neurons in rat." J Mol Neurosci **5**(3): 149-164.

Weinberger, D. R. (1987). "Implications of normal brain development for the pathogenesis of schizophrenia." Arch Gen Psychiatry **44**(7): 660-669.

Westergaard, N., J. Drejer, A. Schousboe and U. Sonnewald (1996). "Evaluation of the importance of transamination versus deamination in astrocytic metabolism of [U-13C]glutamate." Glia **17**(2): 160-168.

Wightman, R. M. and J. B. Zimmerman (1990). "Control of dopamine extracellular concentration in rat striatum by impulse flow and uptake." Brain Res Brain Res Rev **15**(2): 135-144.

Wise, R. A. (1988). "The neurobiology of craving: implications for the understanding and treatment of addiction." J Abnorm Psychol **97**(2): 118-132.

Witkovsky, P., J. C. Patel, C. R. Lee and M. E. Rice (2009). "Immunocytochemical identification of proteins involved in dopamine release from the somatodendritic compartment of nigral dopaminergic neurons." Neuroscience **164**(2): 488-496.

Wojcik, S. M., J. S. Rhee, E. Herzog, A. Sigler, R. Jahn, S. Takamori, N. Brose and C. Rosenmund (2004). "An essential role for vesicular glutamate transporter 1 (VGLUT1) in postnatal development and control of quantal size." Proc Natl Acad Sci U S A **101**(18): 7158-7163.

Yamaguchi, T., W. Sheen and M. Morales (2007). "Glutamatergic neurons are present in the rat ventral tegmental area." Eur J Neurosci **25**(1): 106-118.

Yu, A. C., A. Schousboe and L. Hertz (1982). "Metabolic fate of 14C-labeled glutamate in astrocytes in primary cultures." J Neurochem **39**(4): 954-960.

Zahm, D. S. (1992). "An electron microscopic morphometric comparison of tyrosine hydroxylase immunoreactive innervation in the neostriatum and the nucleus accumbens core and shell." Brain Res **575**(2): 341-346.

Zander, J. F., A. Munster-Wandowski, I. Brunk, I. Pahner, G. Gomez-Lira, U. Heinemann, R. Gutierrez, G. Laube and G. Ahnert-Hilger (2010). "Synaptic and vesicular coexistence of VGLUT and VGAT in selected excitatory and inhibitory synapses." J Neurosci **30**(22): 7634-7645.

Zhai, R. G. and H. J. Bellen (2004). "The architecture of the active zone in the presynaptic nerve terminal." Physiology (Bethesda) **19**: 262-270.

Zhang, L., W. M. Doyon, J. J. Clark, P. E. Phillips and J. A. Dani (2009). "Controls of tonic and phasic dopamine transmission in the dorsal and ventral striatum." Mol Pharmacol **76**(2): 396-404.

Zhang, S. and M. Morales (2010). Serotonergic axons terminals with glutamatergic phenotype make synapses on both dopaminergic and nondopaminergic neurons in the ventral tegmental area. Neuroscience Meeting Planner, Society for Neuroscience, San Diego CA.

Zheng, J. Q., J. J. Wan and M. M. Poo (1996). "Essential role of filopodia in chemotropic turning of nerve growth cone induced by a glutamate gradient." J Neurosci **16**(3): 1140-1149.

Zigmond, M. J. and E. M. Stricker (1972). "Deficits in feeding behavior after intraventricular injection of 6-hydroxydopamine in rats." Science **177**(55): 1211-1214.

Annexe 1

Special issue : **Basal Ganglia**

GLUTAMATE IN DOPAMINE NEURONS:

SYNAPTIC VERSUS DIFFUSE TRANSMISSION

Laurent DESCARRIES [1,2,4], Noémie BÉRUBÉ-CARRIÈRE [1], Mustapha RIAD [1],

Grégory DAL BO [3], J. Alfredo MENDEZ [3] and Louis-Éric TRUDEAU [3,4]

Departments of [1] Pathology and Cell Biology, [2] Physiology, [3] Pharmacology,

and [4] GRSNC, Faculty of Medicine, Université de Montréal, Montreal, QC, Canada

Brain Res Rev. (2008) **58** : 290-302.

Abstract.- There is solid electron microscopic data demonstrating the existence of dopamine (DA) axon terminals (varicosities) with or without synaptic membrane specializations (junctional complexes) in many parts of the CNS, and notably in neostriatum and nucleus accumbens. The dual morphological character of these DA innervations has led to the suggestion that the meso-telencephalic DA system operates by diffuse (or volume) as well as by classical synaptic transmission. In the last decade, electrophysiological and neurochemical evidence has also accumulated indicating that monoamine neurons in various parts of the CNS, and particularly the mesencephalic DA neurons, might release glutamate as a co-transmitter. Following the identification of the vesicular transporters for glutamate (VGluT), *in situ* hybridization and RT-PCR studies carried out on isolated cell or standard tissue cultures, and more recently *in vivo*, have shown that VGluT2 mRNA may be expressed in a significant proportion of mesencephalic DA neurons, at least in the ventral tegmental area. A current study also suggests that the co-expression of tyrosine hydroxylase (TH) and VGluT2 by these neurons is regulated during embryonic development, and may be derepressed or reactivated postnatally following their partial destruction by neonatal administration of 6-hydroxydopamine (6-OHDA). In both 15 day-old and adult rats subjected or not to the neonatal 6-OHDA lesion, concurrent electron microscopic examination of the nucleus accumbens after dual immunocytochemical labeling for TH and VGluT2 reveals the co-existence of the two proteins in a significant proportion of these axon terminals. Moreover, all TH varicosities which co-localize VGluT2 are synaptic, as if there was a link between the potential of DA axon terminals to release glutamate and their establishment of synaptic junctions. Together with the RT-PCR and *in situ* hybridization data demonstrating the co-localization of TH and VGluT2 mRNA in mesencephalic neurons of the VTA, these observations raise a number of fundamental questions regarding the functioning of the meso-telencephalic DA system in healthy or diseased brain.

Section: 4. Structural Organization of the Brain

Keywords: dopamine, glutamate, VGluT2, co-localization, co-transmission, mesotelencephalic DA system

1. Introduction

The concept of diffuse or volume transmission was proposed in the nineteen seventies, on the basis of electron microscope autoradiographic observations on the serotonin and the noradrenaline innervations in adult rat cerebral cortex (Descarries et coll., 1975, 1977; Beaudet and Descarries, 1978). It was then demonstrated that many of these axon terminals or varicosities lacked the plasma membrane specializations that are the hallmark of morphologically defined synapses (Peters and Palay, 1996). These axonal boutons displayed the characteristic clusters of small vesicles implicated in the storage and release of transmitters, but often no junctional complex, that is, no small zone of plasma membrane thickening on either side of a slightly enlarged extracellular space, where receptors for transmitters were then assumed to be confined. It was inferred from these unexpected findings that the transmitter released from such non junctional or non synaptic terminals might diffuse in the extracellular space and reach remote targets, allowing for effects at a distance, on a variety of cellular elements in a relatively large tissue volume (reviewed in Descarries et coll., 1991).

This initial proposal had considerable merit. It provided an explanation for: i) some general, prolonged and/or indirect actions attributed to noradrenaline and serotonin in the cerebral cortex, and which came to be designated as «modulation» to distinguish them from classical, point-to-point, short-acting, excitatory or inhibitory synaptic transmission (Reader et coll., 1979); ii) the existence of so-called «pre-synaptic» effects of transmitters on their own release or that of other transmitters, which took place in the obvious absence of axo-axonic synapses (Vizi, 1984; Vizi and Labós, 1991); iii) the frequent mismatch between the regional distribution of many receptors for different transmitters and that of the corresponding innervations (Herkenham, 1987; Jansson et coll., 2001); iv) the extrasynaptic localization of many transmitter receptors, as visualized by immuno-electron microsopy (e.g. Pickel and Sesack 1995; Caillé et coll., 1996; Delle Donne et coll., 1997; Aoki et coll., 1998), and v) effects of monoamine and other transmitters on non neuronal targets, such as astrocytes and microvessels (e.g., Kalaria et coll., 1989; Hansson, 1991), endowed with receptors often remote from the corresponding release sites. The implications of

diffuse transmission for the understanding of normal and abnormal brain function as well as pharmacotherapeutics have since been the subject of extensive reviews (Agnati et coll., 1992, 1995; Zoli and Agnati, 1996; Zoli et coll., 1998, 1999).

The electron microscopic evidence that many axon terminals, boutons or varicosities issued from different kinds of transmitter-defined neurons in mammalian CNS do not form junctional complexes is now uncontrovertible (reviewed in Descarries and Mechawar, 2000). In recent years, this information has mostly been derived from immunocytochemical studies based on the use of specific antibodies against the neurotransmitters themselves or their biosynthetic enzymes, or else against the specific membrane transporters ensuring their reuptake. In some of these studies, the immunostained axon terminals have been examined in serial as well as single ultrathin sections, allowing scrutiny of their entire volume and direct determination of the frequency with which they made a synaptic junction (synaptic incidence). Most often, however, the frequency of junctions was extrapolated from observations in single ultrathin sections, by means of a stereological formula taking into account the average size of the sectional profiles, the average length of visible junctions and the thickness of the sections (Beaudet and Sotelo, 1981). The validity of this formula has since been verified experimentally in several studies where the same pool of axon varicosities was sampled in serial as well as single ultrathin sections (e.g., Umbriaco et coll., 1994).

The partly asynaptic nature of the three monoamine innervations (dopamine, noradrenaline, serotonin) in adult rat cerebral cortex was thus confirmed, and similar findings were made in other CNS regions and in different species, including monkey and human (reviewed in Descarries and Mechawar, 2000; see also Smiley, 1996). Other examples of largely asynaptic innervations include the histamine innervation of the rat cerebral cortex (Takagi et coll., 1986), as well as the cholinergic innervation of neocortex (Umbriaco et coll., 1994; Mechawar et coll., 2002), hippocampus (Umbriaco et coll., 1995; Aznavour et coll., 2005) and neostriatum (Contant et coll., 1996; Aznavour et coll., 2003). Of all transmitter-defined CNS systems thus far examined for the synaptic or asynaptic nature of their axon terminals or varicosities,

the mesencephalic dopamine (DA) neurons innervating the striatum are however the ones that have received the most attention.

2. Dual character, asynaptic and synaptic, of the dopamine innervation in striatum

Early electron microscopic descriptions after specific cytochemical and autoradiographic labeling have led to divergent conclusions about the synaptic features of neostriatal DA terminals. Early experiments on tissue slices fixed with potassium permanganate after preloading or not with false transmitter (Hökfelt, 1968; see also Tennyson et coll., 1974) gave no indication of the presence of junctional complexes on neostriatal boutons showing small granular vesicles and thus positively identified as containing dopamine or serotonin. A few years later, the first description by Pickel et coll. (1976) of neostriatal terminals immunostained with specific antibodies against the biosynthetic enzyme tyrosine hydroxylase (TH) seemed to confirm this finding in aldehyde-fixed tissue. In 1980, however, a preliminary report from our laboratory indicated that many single ultrathin sections from DA terminals of adult rat neostriatum labeled by uptake of [^{3}H]DA *in vivo* exhibited small, symmetrical, synaptic membrane specializations on dendritic branches or spines, suggesting a relatively high synaptic frequency (Descarries et coll., 1980). Another TH immunocytochemical study from Pickel's laboratory (1981), also carried out in single ultrathin sections, then suggested the existence of two categories of neostriatal DA terminals : a restricted one with larger varicosities that were deprived of synaptic membrane specializations, and a more abundant one with smaller varicosities exhibiting specializations that were indeed symmetrical and found occasionally on neuronal somata as well as on dendritic branches and spines (Pickel et coll., 1981; see also Kaiya and Namba, 1981; Arluison et coll., 1984; Triarhou et coll., 1988). In 1984, polyclonal antibodies directed against DA-glutaraldehyde-protein conjugate became available (Geffard et coll., 1984), followed by monoclonal antibodies against this same antigen (Chagnaud et coll. 1987). These allowed for a better morphological preservation of tissue processed for immunocytochemistry, as they were compatible with the use of higher concentrations of glutaraldehyde for primary fixation of the brain. Using these antibodies, Voorn et coll. (1986) described DA varicosities in the

ventral striatum of adult rat as making small symmetrical synaptic contacts with dendritic shafts and spines.

Meanwhile, in our laboratory, further autoradiographic experiments on neostriatal terminals labeled *in vivo* with [^{3}H]DA (**Fig. 1A**) revealed a synaptic incidence in the order of 30-40%, as extrapolated stereologically from single ultrathin sections (Descarries et coll., 1996). However, this sampling was limited to the paraventricular portion of neostriatum because of the restricted penetration of the tracer which had to be administered intraventricularly. For this reason, as soon as the DA antibodies became available, it was decided to pursue this study with immunocytochemistry (**Fig. 1B**) in a mediodorsal region of neostriatum. Moreover, an effort was made to obtain direct evidence by examining a great number of these DA terminals in long, uninterrupted, series of ultrathin sections (e.g. **Fig. 2**).

The results obtained through these various approaches are summarized in **Table 1**. They allowed us to conclude that, in adult rat, approximately 30-40% of DA terminals, in both a paraventricular and a more central zone of neostriatum were endowed with a synaptic membrane specialization (Descarries et coll., 1996). Similar values were later reported by Antonopoulos et coll. (2002), who showed that in 21 day-old rat, 63% of DA-immunolabeled varicosities from the striatal patches, but only 35% from the matrix, were synaptic. These authors also examined the ventral striatum in 21 day-old rat, and found that 47% and 71% of DA varicosities were synaptic in the core and the shell of nucleus accumbens (nAcb), respectively. As mentioned below, in our own material from the core of adult rat nAcb, we observed a junctional frequency of 11% in single thin sections, for a synaptic incidence of 34%, as extrapolated to the whole volume of these varicosities.

3. Dopamine-glutamate co-transmission by mesencephalic dopamine neurons

The observation that DA neurons establish both synaptic and non-synaptic junctions raises the question as to what distinguishes these two classes of terminals in terms of function. Although a definitive answer to this question is not presently available, the hypothesis has been raised that the synaptic junctions established by DA neurons are the sites at which these neurons release glutamate as a co-transmitter (Trudeau, 2004).

3.1 Converging evidence that CNS monoamine neurons use glutamate as a co-transmitter

The first indirect evidence that CNS monoamine neurons might release glutamate as a co-transmitter was the demonstration that a proportion of monoamine neurons, including DA, noradrenaline and serotonin neurons, were immunopositive for glutamate, in both rat and monkey (Ottersen et coll., 1984; Nicholas et coll., 1992; Fung et coll., 1994; Liu et coll., 1995; Sulzer et coll., 1998). These same cell populations were also shown to be immunopositive for phosphate-activated glutaminase, the glutamate biosynthetic enzyme (Kaneko et coll., 1990). Glutamate immunoreactivity was not sufficient evidence to prove that glutamate was being used as co-transmitter. However, electrophysiological data was then obtained demonstrating that rapid excitatory synaptic responses could be evoked in striatal neurons by extracellular stimulation in DA cell body areas or in the medial forebrain bundle (Hull et coll., 1970, 1973; Kitai et coll., 1975). Moreover, recent work has shown that local application of a D2 receptor agonist at the site of stimulation inhibits the generation of glutamatergic EPSPs in striatal neurons, suggesting that D2 responsive, putative DA neurons (and not fibres of passage), are indeed responsible for such EPSPs (Chuhma et coll., 2004). Similar responses in the anesthetized rat have also been reported to disappear after chemical ablation of the DA neurons, strongly arguing that they were indeed generated by these neurons (Lavin et coll., 2005). Rapid excitatory synaptic events sensitive to the AMPA/kainate glutamate receptor antagonist CNQX have also been shown to be evoked in spinal cord ventral horn motoneurons after extracellular stimulation of presumed noradrenergic neurons (Fung et coll., 1994; Liu et coll., 1995). Excitatory responses were also generated in striatal neurons and ventral horn motoneurons following extracellular stimulation of presumed serotonin neurons in raphe nuclei (Park et coll., 1982; Holtman et coll., 1986; Fung and Barnes, 1989).

A direct test for glutamate release by monoamine neurons *in vivo* would require paired recordings between, for example, a DA neuron and a target cell in a projection area such as the striatum. These experiments are hardly feasible, considering the low synaptic connectivity between these cells and the large distance between the cell

bodies of the pre- and post-synaptic neurons. Further evidence for the synaptic release of glutamate by monoamine neurons was therefore sought *in vitro*. Using a microculture system in which isolated postnatal serotonin neurons of the rat raphe nuclei develop on small (100-500 μm) micro droplets of substrate, Johnson (1994) studied the synaptic development of serotonin neurons. Under such conditions, isolated neurons establish synaptic contacts onto a limited subset of neighbouring neurons, or, if the neuron is alone, onto its own dendrites (i.e. "autapses"). Recordings from such isolated cells revealed that ~60% of serotonin neurons generate fast autaptic EPSPs that can be blocked by CNQX. This demonstrated clearly that these serotonin neurons indeed release glutamate as a co-transmitter (Johnson, 1994). Similar observations were then made by Sulzer et coll. (1998) in isolated rat DA neurons. A single action potential in a DA neuron evoked an EPSC that was blocked by AP5, an antagonist of NMDA glutamate receptors and by CNQX (Sulzer et coll., 1998; Bourque and Trudeau, 2000). Together with the results of glutamate and TH double-immunostaining experiments, these observations led Sulzer et coll. (1998) to propose that a proportion of axon terminals formed by DA neurons could be specialized for glutamate release (**Fig. 3**). Comparable results were also obtained in co-cultures of ventral tegmental area (VTA) DA neurons together with GABAergic medium spiny neurons of the nAcb (Joyce and Rayport, 2000), indicating that glutamate release by DA neurons was not restricted to isolated neuron cultures.

3.2 Vesicular glutamate transporters in transmitter-defined neurons of CNS

The physiological and immunocytochemical evidence of glutamate co-release by monoamine neurons implies that these neurons are able to package glutamate in synaptic vesicles. In the last few years, the identification of vesicular transporters for glutamate (VGluT) has provided new means to investigate the glutamatergic phenotype of neurons (Ni et coll., 1994; Takamori et coll., 2000). The first of these transporters to be identified, VGluT1 (BNPI) was shown to be present at high concentration in the synaptic vesicles of a subset of CNS glutamatergic neurons (Bellocchio et coll., 1998, 2000; Takamori et coll., 2000). Overexpression studies in cell lines proved that VGluT1 is a *bona fide* vesicular glutamate transporter that acts

to load synaptic vesicles with glutamate (Bellocchio et coll., 2000; Takamori et coll., 2000).

A close homologue of VGluT1, VGluT2, acts as another important vesicular glutamate transporter (Aihara et coll., 2000; Bai et coll., 2001; Fremeau et coll., 2001; Hayashi et coll., 2001; Herzog et coll., 2001; Takamori et coll., 2001; Varoqui et coll., 2002). Interestingly, the expression pattern of VGluT1 and VGluT2 in the brain are mostly complementary, with VGluT1 mRNA being widely expressed by pyramidal neurons of the neocortex and hippocampus, and in the cerebellar cortex, whereas VGluT2 mRNA is more abundantly produced in diencephalic and other subcortical nuclei, in deep cerebellar nuclei and in the brainstem (Ni et coll., 1995; Hisano et coll., 2000; Bai et coll., 2001; Fremeau et coll., 2001; Herzog et coll., 2001). Closer examination of VGluT2 mRNA in the brainstem showed that this transcript is present in most noradrenaline neurons of the A2 group in the nucleus tractus solitarii complex (Stornetta et coll., 2002a), and most adrenaline neurons of the C1, C2 and C3 groups in the medulla (Stornetta et coll., 2002b). It is noteworthy that overexpression of either VGluT1 or VGluT2 in cultured GABA neurons allowed these neurons to co-release glutamate, providing support for the idea that expression of a vesicular glutamate transporter is necessary and sufficient to permit vesicular glutamate release by neurons (Takamori et coll., 2000, 2001).

A third vesicular glutamate transporter (VGluT3) was also cloned more recently, showing a more restricted expression limited to a number of neurons not classically thought of as glutamatergic. In particular, VGluT3 mRNA and protein was found in most serotonin neurons of the raphe, as well as in cholinergic neurons of the striatum and forebrain (Gras et coll., 2002; Schafer et coll., 2002; Takamori et coll., 2002; Harkany et coll., 2003). Together with the work showing that monoamine neurons establish functional glutamate-releasing terminals in culture and contain glutamate immunoreactivity *in vivo*, these data support the view that glutamate co-transmission might be widespread in monoamine neurons of the CNS.

3.3 Expression of VGluT2 in DA neurons *in vitro* and *in vivo*

VGluT2 mRNA was first reported to be present in rat substantia nigra compacta (SNc) in a Northern blot experiment (Aihara et coll., 2000). However, initial *in situ*

hybridization studies at low resolution failed to detect significant amounts of VGluT2 mRNA in mesencephalic DA neurons from adult animals (Gras et coll., 2002). Considering the physiological evidence for glutamate release by DA neurons, we initiated efforts to better characterize the expression of VGluTs in DA neurons both *in vitro* and *in vivo*. We first evaluated the presence of VGluTs in postnatal rat mesencephalic neurons in primary culture. Using immunocytochemical labeling, we found that ~80% of isolated DA neurons were immunopositive for VGluT2 (Dal Bo et coll., 2004), while VGluT1 and 3 were not detected. The VGluT2 labeling was punctate in nature and particularly concentrated close to major dendrites and the cell body (**Fig. 4A**). Interestingly, although most VGluT2 positive varicosities were also TH positive, many neurons displayed long thin axonal-like segments bearing multiple TH positive/VGluT2-negative varicosities (**Fig. 4A**, lower right). In addition, in a triple-labeling experiment, it was apparent that a number of nerve terminals identified by the presence of the synaptic vesicle protein SV2 were VGluT2 negative (**Fig. 4B**). These findings were compatible with the hypothesis that DA neurons can establish distinct sets of terminals, a subset of which having the ability to co-release glutamate (Sulzer et coll., 1998).

The expression of VGluT2 mRNA in cultured mouse and rat DA neurons was then confirmed by single-cell RT-PCR (**Fig. 4C**). This expression of VGluT2 was specific for the DA neurons since GABA neurons in the same cultures did not express VGluT2. Another series of single-cell RT-PCR experiments was carried out on mesencephalic DA neurons acutely dissociated from mice at different ages. In these experiments, we took advantage of transgenic mice expressing GFP under the control of the TH promoter (Sawamoto et coll., 2001; Matsushita et coll., 2002; Jomphe et coll., 2005), thus allowing easy visual identification of DA neurons. Using this approach, we found that VGluT2 mRNA, but not VGluT1 nor VGluT3 mRNA, was present in 25% of GFP-expressing DA neurons acutely isolated from P0 pups (Mendez et coll., 2005, 2007 submitted). Interestingly, this proportion appeared to diminish with age, decreasing to 13% at P45.

To determine whether the dual dopamine-glutamate phenotype was also expressed by mesencephalic DA neurons *in vivo*, double *in situ* hybridization

experiments for TH and VGluT2 were performed on rat brain tissue obtained during embryonic development and at various postnatal ages, up to P15 (Dal Bo et coll., 2007 submitted). At embryonic days 14 and 15, there was a striking overlap in the labeling of TH and VGluT2 mRNA in the ventral mesencephalon, which was no longer found at late embryonic stages (E18-E21) and postnatally. In normal pups at P6-P15, only 1-2% of neurons containing TH mRNA in the ventral tegmental area (VTA) and SNc, also displayed VGluT2 mRNA. In a similar study carried out in adult rats, DA neurons co-expressing VGluT2 mRNA were reported to be rare (approximately 0.1%) in the VTA of adult rats (Yamaguchi et coll., 2007). However, another recent study combining *in situ* hybridization for VGluT2 with TH immunocytochemistry showed an expression of VGluT2 in as many as 19% of the DA neurons in the VTA (Kawano et coll., 2006). The much higher proportion of mesencephalic DA neurons expressing VGluT2 mRNA, as observed by single-cell RT-PCR (~25%) rather than *in situ* hybridization (1-2 %) in our own studies, supports the latter findings and presumably reflects the advantage of RT-PCR for detecting low abundance mRNAs.

In the objective of evaluating whether VGluT2 expression by DA neurons was regulated, we also examined tissue from postnatal rats cerebroventricularly injected with 6-hydroxydopamine (6-OHDA) at P4 to partially lesion DA neurons. Intraventricular infusion of 6-OHDA in neonatal rat destroys most of the DA neurons in SNc, but a significant proportion of the DA neurons in VTA are spared. In contrast to the low expression found in normal rodents, 25% of surviving DA neurons in the VTA of P6-P15 rats coexpressed VGluT2 after the administration of 6-OHDA at P4, suggesting an induction or derepression of the glutamatergic phenotype (Dal Bo et coll., submitted). Together with the enhanced expression of VGluT2 mRNA in cultured DA neurons (80% vs 25% in acutely dissociated neurons), these results support the exciting hypothesis that expression of the glutamatergic phenotype by mesencephalic DA neurons is a regulated phenomenon that might be induced or reactivated by injury. Additional studies are now required to directly address this possibility.

4. Co-localization of TH and VGluT2 in axon terminals of the nucleus accumbens

To seek *in vivo* evidence for the co-localization of TH and VGluT2 in axon terminals of DA neurons, the nAcb of P15 rats was examined by electron microscopy after double, pre-embedding immunolabeling for the two proteins (Bérubé-Carrière et coll., 2006). Knowing that the expression of VGluT2 was increased after the neonatal 6-OHDA lesion, this study was conducted in normal as well as 6-OHDA lesioned rats. In these experiments, VGluT2 was always labeled first with immunogold, and then TH, with the immunoperoxidase technique. Doubly as well as singly labeled axon terminals were readily identified in the nAcb of both normal and 6-OHDA-lesioned rats (**Fig. 5**). When determined in an equivalent surface of thin section surface in each rat, the mean number of axon varicosity profiles labeled for TH alone or for TH together with VGluT2 was markedly reduced after the 6-OHDA lesion (**Table 2**). In normal rat, VGluT2 was co-localized in 28% of all TH-labeled terminals. After the lesion, this proportion of dually labeled terminals was slightly but significantly increased (37%), in keeping with the hypothesis of an activation or reactivation of the glutamatergic phenotype of DA neurons following injury. An apparent decrease in the number of terminals labeled for VGluT2 alone was not statistically significant. Similar findings have recently been made in adult (P90) rats (Bérubé-Carrière et coll., 2007). In normal adults, the dually labeled terminals appeared to be less frequent than at P15 (12%), but again, after the 6-OHDA lesion, their percentage over all TH+ appears to be increased (**Table 2**).

In these studies, particular attention was also paid to the synaptic incidence of the singly and dually labeled terminals (**Fig. 6**). As extrapolated stereologically from the observations in single thin sections, in both normal and 6-OHDA-lesioned rats and at both ages, all terminals which co-localized TH and VGluT2 appeared to be synaptic, at variance with those labeled for TH alone or even for VGluT2 alone at P15, and for TH alone at P90. Moreover, at both ages, the proportion of axon terminals labeled for TH alone and displaying a synapse appears to be greater after the 6-OHDA lesion (Bérubé-Carrière et coll., 2007). Whether synaptic TH terminals

of the nAcb preferentially resist 6-OHDA lesioning or develop a synaptic phenotype as consequence of the lesion remains to be determined.

5. **Concluding remarks**

1) In adult as well as postnatal rat, a significant number of axon terminals in the nucleus accumbens co-localize TH and VGluT2 and should therefore be capable of releasing glutamate in addition to DA as neurotransmitter. Together with the single-cell RT-PCR and dual *in situ* hybridization data demonstrating the co-localization of TH and VGluT2 mRNA in mesencephalic neurons of the VTA, these ultrastructural observations raise a number of fundamental questions regarding the functioning of these neurons. Under what circumstances is glutamate released from DA terminals in the nAcb, and with what consequences on the functioning of this brain region? In this regard, it should be noted that the release of glutamate by DA neurons projecting to the prefrontal cortex has already been proposed to account for a rapid component in the response of pyramidal neurons and cortical interneurons to DA neuron activation (Lapish et coll., 2006, 2007).

2) It is also clear that all axon terminals endowed with the dual DA-glutamate phenotype are synaptic, at variance with the terminals containing TH only. This finding suggests a link between the potential of DA terminals to release glutamate and their establishment of synaptic junctions. Whether the presence of VGluT2 and the co-release of glutamate are one of the factors involved in the formation of synapses by axon varicosities is an open question. It should be interesting to determine if the proportion of DA varicosities colocalizing VGluT2 is higher in the shell as opposed to the core of nAcb, where the proportion of synaptic DA axon varicosities appears to be higher (Antonopoulos et coll., 2002), or in other parts of brain such as cerebral cortex, where the proportion of synaptic DA varicosities differs from one region to another (Séguéla et coll., 1988). It will also be interesting to evaluate whether the association of synaptic junctions to glutamate co-release applies to other monoamine neurons, and more generally to all those operating with both diffuse and synaptic transmission. Another key question is what distinguishes at the molecular level the synaptic and non-synaptic junctions established by DA neurons.

For example, whether the same complement of SNARE proteins involved in exocytosis will be found in both types of terminals needs to be determined.

3) Finally, it may be asked how and what regulates the dual DA-glutamate phenotype during development and in disease? And, more specifically, whether and how this dual transmitter phenotype might be implicated in pathological conditions affecting the DA neurons innervating the nAcb?

Further studies will obviously be needed answer these questions. Meanwhile, it should be feasible to determine whether similar characteristics and properties are shared by DA neurons innervating other brain regions, such as the neostriatum and the prefrontal cortex, and whether they prevail in higher species, including man!

5. Literature references

Aihara, Y., Mashima, H., Onda, H., Hisano, S., Kasuya, H., Hori, T., Yamada, S., Tomura, H., Yamada, Y., Inoue, I., Kojima, I., Takeda, J. 2000. Molecular cloning of a novel brain-type Na(+)-dependent inorganic phosphate co-transporter. J. Neurochem. 74, 2622-2625.

Agnati, L.F., Bjelke, B., Fuxe, K., 1992. Volume transmission in the brain. Do cells communicate solely through synapses? A new theory proposes that information also flows in the extracellular space. Am. Sci. 80, 362-374.

Agnati, L.F., Zoli, M., Strömberg, I., Fuxe, K. 1995. Intercellular communication in the brain: wiring versus volume transmission. Neuroscience 3, 711-726.

Antonopoulos, J., Dori, A., Dinopoulos, A., Chiotelli, M, Parnavelas, J.G. 2002. Postnatal development of the dopaminergic system of the striatum in the rat. Neuroscience 110, 245-256.

Aoki, C., Venkatesan, C., Go, C.G., Forman, R., Kurose, H. 1998. Cellular and subcellular sites for noradrenergic action in the monkey dorsolateral prefrontal cortex as revealed by the immunocytochemical localization of noradrenergic receptors and axons. Cerebral Cortex 8, 269-277.

Arluison , M., Dietl, D., Thibault, J. 1984. Ultrastructural morphology of dopaminergic nerve terminals and synapses in the striatum of the rat using tyrosine hydroxylase immunocytochemistry. A topographical study. Brain Res. Bull. 13, 269-285.

Aznavour, N., Mechawar, N., Watkins, K.C., Descarries, L. 2003. Fine structural features of the acetylcholine innervation in the developing neostriatum of rat. J. Comp. Neurol. 460, 280-291.

Aznavour, N., Watkins, K.C., Descarries, L. 2005. Postnatal development of the cholinergic innervation in the dorsal hippocampus of rat : A quantitative light and electron microscopic immunocytochemical description. J. Comp. Neurol. 486, 61-75.

Bai, L., Xu, H., Collin,s J.F., Ghishan, F.K. 2001. Molecular and functional analysis of a novel neuronal vesicular glutamate transporter. J. Biol. Chem. 276, 36764-36769.

Beaudet, A., Descarries, L. 1978. The monoamine innervation of rat cerebral cortex: synaptic and non synaptic relationships. Neuroscience 3, 851-860.

Beaudet, A., Sotelo, C. 1981. Synaptic remodeling of serotonin axon terminals in rat agranular cerebellum. Brain Res. 206, 305-329.

Bellocchio, E.E., Hu, H., Pohorille, A., Chan, J., Pickel, V.M., Edwards, R.H. 1998. The localization of the brain-specific inorganic phosphate transporter suggests a specific presynaptic role in glutamatergic transmission. J. Neurosci. 18, 8648-8659.

Bellocchio, E.E., Reimer, R.J., Fremeau, R.T. Jr, Edwards, R.H. 2000. Uptake of glutamate into synaptic vesicles by an inorganic phosphate transporter. Science 289, 957-960.

Bérubé-Carrière, N., Riad, M., Dal Bo, G., Trudeau, L.-É., Descarries, L. 2006. Co-localization of dopamine and glutamate in axon terminals of VTA neurons innervating the nucleus accumbens. Program No. 722.11. 2006. Abstract Viewer/Itinerary Planner. Washington, DC: Society for Neuroscience. Online.

Bérubé-Carrière, N., Riad, M., Dal Bo, G., Trudeau, L.-É., Descarries, L. 2007. Vesicular glutamate transporter 2 in dopamine axon terminals of the nucleus accumbens. Program No. 39.9. 2007. Abstract Viewer/Itinerary Planner. Washington, DC: Society for Neuroscience. Online.

Bourque, M.J., Trudeau, L.-E. 2000. GDNF enhances the synaptic efficacy of dopaminergic neurons in culture. Eur. J. Neurosci. 12, 3172-3180.

Caillé, I., Dumartin, B., Bloch, B. 1996. Ultrastructural localization of D1 dopamine receptor immunoreactivity in rat striatal neurons and its relation with dopaminergic innervation. Brain Res. 730, 17-31.

Chagnaud, J.L., Mons, N., Tuffet, S., Grandier-Vareilles, X., Geffard, M. 1987. Monoclonal antibodies against glutaraldehyde-conjugated dopamine. J. Neurochem. 49, 487-494.

Chuhma, N., Zhang, H., Masson, J., Zhuang, X., Sulzer, D., Hen, R., Rayport, S. 2004. Dopamine neurons mediate a fast excitatory signal via their glutamatergic synapses. J. Neurosci. 24, 972-981.

Contant, C., Umbriaco, D., Garcia, S., Watkins, K.C., Descarries L. 1996. Ultrastructural characterization of the acetylcholine innervation in adult rat neostriatum. Neuroscience 71, 937-947.

Dal Bo, G., St-Gelais, F., Danik, M., Williams, S., Cotton, M., Trudeau, L.-E. 2004. Dopamine neurons in culture express VGluT2 explaining their capacity to release glutamate at synapses in addition to dopamine. J. Neurochem. 88, 1398-1405.

Delle Donne, K.T., Sesack, S.R., Pickel, V.M. 1997. Ultrastructural immunocytochemical localization of the dopamine D2 receptor within GABAergic neurons of the rat striatum. Brain Res. 746, 239-255.

Descarries, L., Mechawar, N. 2000. Ultrastructural evidence for diffuse transmission by monoamine and acetylcholine neurons of the central nervous system. In Volume Transmission Revisited. Progress in Brain Research, Vol 125, L.F. Agnati, K. Fuxe, C. Nicholson, E. Siková, eds, Elsevier, Amsterdam, pp. 27-47.

Descarries, L., Beaudet, A., Watkins, K.C. 1975. Serotonin nerve terminals in adult rat neocortex. Brain Res. 100, 563-588.

Descarries, L., Watkins, K.C., Lapierre, Y. 1977. Noradrenergic axon terminals in the cerebral cortex of rat. III. Topometric ultrastructural analysis. Brain Res. 133, 197-222.

Descarries, L., Bosler, O., Berthelet, F., Des Rosiers, M.H. 1980. Dopaminergic nerve endings visualized by high-resolution autoradiography in adult rat neostriatum. Nature 284, 620-622.

Descarries, L., Séguéla, P., Watkins, K.C. 1991. Nonjunctional relationships of monoamine axon terminals in the cerebral cortex of adult rat. In Volume Transmission in the Brain: Novel Mechanisms for Neural Transmission. K. Fuxe , L.F. Agnati, eds, New York: Raven Press, pp. 53-62.

Descarries, L., Watkins, K.C., Garcia, S., Bosler, O., Doucet, G. 1996. Dual character, asynaptic and synaptic, of the dopamine innervation in adult rat neostriatum: a quantitative autoradiographic and immunocytochemical analysis. J. Comp. Neurol. 375, 167-186.

Fremeau, R.T. Jr, Troyer, M.D., Pahner, I., Nygaard, G.O., Tran, C.H., Reimer, R.J., Bellocchio, E.E., Fortin, D., Storm-Mathisen, J., Edwards, R.H. 2001. The expression of vesicular glutamate transporters defines two classes of excitatory synapse. Neuron 31, 247-260.

Fung, S.I., Chan, J.Y., Manzoni, D., White, S.R., Lai, Y.Y., Strahlendorf, H.K., Zhuo, H., Liu, R.H., Reddy, V.K., Barnes, C.D. 1994. Co-transmitter-mediated locus coeruleus action on motoneurons. Brain Res. Bull. 35, 423-432.

Fung, S.J., Barnes, C.D. 1989. Raphe-produced excitation of spinal cord motoneurons in the cat. Neurosci. Lett. 103, 185-190.

Fung, S.J., Reddy, V.K., Liu, R.H., Wang, Z., Barnes, C.D. 1994. Existence of glutamate in noradrenergic locus coeruleus neurons of rodents. Brain Res. Bull. 35, 505-512.

Geffard, M., Buijs, R.M., Séguéla, P., Pool, C.W., Le Moal, M. 1984. First demonstration of highly specific and sensitive antibodies against dopamine. Brain Res. 294, 161-165.

Gras, C., Herzog, E., Bellenchi, G.C., Bernard, V., Ravassard, P., Pohl, M., Gasnier, B., Giros, B., El Mestikawy, S. 2002. A third vesicular glutamate transporter expressed by cholinergic and serotoninergic neurons. J. Neurosci. 22, 5442-5451.

Hansson, E. 1991. Transmitter receptors on astroglial cells. In Volume Transmission in the Brain: Novel Mechanismx for Neural Transmission, K. Fuxe, L.F. Agnati, eds, New York: Raven Press, pp. 257-265.

Harkany, T., Hartig, W., Berghuis, P., Dobszay, M.B., Zilberter, Y., Edwards, R.H., Mackie, K., Ernfors, P. 2003. Complementary distribution of type 1 cannabinoid receptors and vesicular glutamate transporter 3 in basal forebrain suggests input-specific retrograde signalling by cholinergic neurons. Eur. J. Neurosci. 18, 1979-1992.

Hayashi, M., Otsuka, M., Morimoto, R., Hirota, S., Yatsushiro, S., Takeda, J., Yamamoto, A., Moriyama, Y. 2001. Differentiation-associated Na+-dependent inorganic phosphate co-transporter (DNPI) is a vesicular glutamate transporter in endocrine glutamatergic systems. J. Biol. Chem. 276, 43400-43406.

Herkenham, M. 1987. Mismatches between neurotransmitter and receptor localizations in brain: observations and implications. Neuroscience 23, 1-38.

Herzog, E., Bellenchi, G.C., Gras, C., Bernard, V., Ravassard, P., Bedet, C., Gasnier, B., Giros, B., El Mestikawy, S. 2001. The existence of a second vesicular glutamate transporter specifies subpopulations of glutamatergic neurons. J. Neurosci. 21, RC181.

Hisano, S., Hoshi, K., Ikeda, Y., Maruyama, D., Kanemoto, M., Ichijo, H., Kojima, I., Takeda, J., Nogami, H. 2000. Regional expression of a gene encoding a neuron-specific Na(+)- dependent inorganic phosphate co-transporter (DNPI) in the rat forebrain. Brain Res. Mol. Brain Res. 83, 34-43.

Hökfelt, T. 1968. *In vitro* studies on central and peripheral monoamine neurons at the ultrastructural level. Z. Zellforsch. 91, 1-74.

Holtman, J.R. Jr, Dick, T.E., Berger, A.J. 1986 Involvement of serotonin in the excitation of phrenic motoneurons evoked by stimulation of the raphe obscurus. J. Neurosci. 6, 1185-1193.

Hull, C.D., Bernardi, G., Buchwald, N.A. 1970. Intracellular responses of caudate neurons to brain stem stimulation. Brain Res. 22, 163-179.

Hull, C.D., Bernardi, G., Price, D.D., Buchwald, N.A. 1973. Intracellular responses of caudate neurons to temporally and spatially combined stimuli. Exp. Neurol. 38, 324-336.

Jansson, A., Descarries, L., Cornea-Hébert, V., Riad, M., Vergé, D., Bancila, M., Agnati, L.F., Fuxe, K. 2001. Transmitter-receptor mismatches in central dopamine, serotonin and neuropeptide systems. Further evidence for volume transmission. In The Neuronal Environment: Brain Homeostasis in Health and Disease, W. Walz, ed., Totowa: Humana Press, pp. 83-108.

Johnson, M.D. 1994. Synaptic glutamate release by postnatal rat serotonergic neurons in microculture. Neuron 12, 433-442.

Jomphe, C., Bourque, M.-J., Fortin, G.D., St-Gelais, F., Okano, H., Kobayashi, K., Trudeau, L.-E. 2005. Use of TH-EGFP transgenic mice as a source of identified dopaminergic neurons for physiological studies in postnatal cell culture. J. Neurosci. Methods 146, 1-12.

Joyce, M.P., Rayport, S. 2000. Mesoaccumbens dopamine neuron synapses reconstructed *in vitro* are glutamatergic. Neuroscience 99, 445-456.

Kaiya, H., Namba, M. 1981. Two types of dopaminergic nerve terminals in the rat neostriatum. An ultrastructural study. Neurosci. Lett. 25, 251-256.

Kalaria, R.N., Stockmeier, C.A., Harik, S.I. 1989. Brain microvessels are innervated by locus coeruleus noradrenergic neurons. Neurosci. Lett. 97, 203-208.

Kaneko, T., Akiyama, H., Nagatsu, I., Mizuno, N. 1990. Immunohistochemical demonstration of glutaminase in catecholaminergic and serotoninergic neurons of rat brain. Brain Res. 507, 151-154.

Kawano, M., Kawasaki, A., Sakata-Haga, H., Fukui, Y., Kawano, H., Nogami, H.,Hisano, S. 2006. Particular subpopulations of midbrain and hypothalamic dopamine neurons express vesicular glutamate transporter 2 in the rat brain. J. Comp. Neurol. 498, 581-592.

Kitai, S.T., Wagner, A., Precht, W., Ono, T. 1975. Nigro-caudate and caudato-nigral relationship: an electrophysiological study. Brain Res. 85, 44-48.

Lapish CC, Seamans JK, Judson Chandler L. 2006. Glutamate-dopamine co-transmission and reward processing in addiction. Alcohol Clin. Exp. Res. 30, 1451-1465.

Lapish CC, Kroener S, Durstewitz D, Lavin A, Seamans JK. 2007. The ability of the mesocortical dopamine system to operate in distinct temporal modes. Psychopharmacology (Berl) 191, 609-625.

Lavin, A., Nogueira, L., Lapish, C.C., Wightman, R.M., Phillips, P.E., Seamans, J.K. 2005. Mesocortical dopamine neurons operate in distinct temporal domains using multimodal signaling. J. Neurosci. 25, 5013-5023.

Liu, R.H., Fung, S.J., Reddy, V.K., Barnes, C.D. 1995. Localization of glutamatergic neurons in the dorsolateral pontine tegmentum projecting to the spinal cord of the cat with a proposed role of glutamate on lumbar motoneuron activity. Neuroscience 64, 193-208.

Matsushita, N., Okada, H., Yasoshima, Y., Takahashi, K., Kiuchi, K., Kobayashi, K. 2002. Dynamics of tyrosine hydroxylase promoter activity during midbrain dopaminergic neuron development. J. Neurochem. 82, 295-304.

Mechawar, N., Watkins, K.C., Descarries, L. 2002. Ultrastructural features of the acetylcholine innervation in the developing parietal cortex of rat. Neuroscience 111, 83-94.

Mendez, J.A., Bourque, M.-J., Trudeau, L.-E. 2005. Evidence for the expression of VGluT2 mRNA in acutely-dissociated TH-GFP mouse dopamine neurons. Program No. 155.3. 2005. Abstract Viewer/Itinerary Planner. Washington, DC: Society for Neuroscience. Online.

Ni, B., Rosteck, P.R. Jr, Nadi, N.S., Paul, S.M. 1994. Cloning and expression of a cDNA encoding a brain-specific Na(+)- dependent inorganic phosphate co-transporter. Proc. Natl. Acad. Sci. USA 91, 5607-5611.

Ni, B., Wu, X., Yan, G.M., Wang, J., Paul, S.M. 1995. Regional expression and cellular localization of the Na(+)-dependent inorganic phosphate co-transporter of rat brain. J. Neurosci. 15, 5789-5799.

Nicholas, A.P., Pieribone, V.A., Arvidsson, U., Hökfelt, T. 1992 Serotonin-, substance P- and glutamate/aspartate-like immunoreactivities in medullo-spinal pathways of rat and primate. Neuroscience 48, 545-559.

Ottersen O.P., Storm-Mathisen, J. 1984. Glutamate- and GABA-containing neurons in the mouse and rat brain, as demonstrated with a new immunocytochemical technique. J. Comp. Neurol. 229, 374-392.

Park, M.R., Gonzales-Vegas, J.A., Kitai, S.T. 1982. Serotonergic excitation from dorsal raphe stimulation recorded intracellularly from rat caudate-putamen. Brain Res. 243, 49-58.

Peters, A., Palay, S.L. 1996. The morphology of synapses. J. Neurocytol. 25, 687-700.

Pickel, V.M., Joh, T.H., Reis, D.J. 1976. Monoamine-synthesizing enzymes in central dopaminergic, noradrenergic and serotonergic neurons. Immunocytochemical localization by light and electron microscopy. J. Histochem. Cytochem. 24, 792-806.

Pickel, V.M., Beckley, S.C., Joh, T.H., Reis, D.J. 1981. Ultrastructural immunocytochemical localization of tyrosine hydroxylase in the neostriatum. Brain Res. 225, 373-385.

Pickel, V.M., Sesack, S.R. 1995. Electron microscopy of central dopamine systems. In Psychopharmacology. The Fourth Generation of Progress, F.E. Bloom and D.J. Kupfer, eds, New York, Raven Press, pp. 257-268.

Reader, T.A., Ferron, A., Descarries, L. Jasper, H.H. (1979) Modulatory role for biogenic amines in the cerebral cortex. Microiontophoretic studies. Brain Res. 160, 217-229.

Sawamoto, K., Nakao, N., Kobayashi, K., Matsushita, N., Takahashi, H., Kakishita, K., Yamamoto, A., Yoshizaki, T., Terashima, T., Murakami, F., Itakura, T., Okano, H. 2001. Visualization, direct isolation, and transplantation of midbrain dopaminergic neurons. Proc. Natl. Acad. Sci. USA 98, 6423-6428.

Schafer, M.K., Varoqui, H., Defamie, N., Weihe, E., Erickson, J.D. 2002. Molecular cloning and functional identification of mouse vesicular glutamate transporter 3 and its expression in subsets of novel excitatory neurons. J. Biol. Chem. 277, 50734-50748.

Séguéla, P., Watkins, K.C., Descarries, L. 1988. Ultrastructural features of dopamine axon terminals in the anteromedial and the suprarhinal cortex of adult rat. Brain Res. 442, 11-22.

Smiley, J.F. 1996. Monoamines and acetylcholine in primate cerebral cortex: what anatomy tells us about function. Rev. Brasil Biol. 56 (Suppl. 1), 153-164.

Stornetta, R.L., Sevigny, C.P., Guyenet, P.G. 2002a. Vesicular glutamate transporter DNPI/VGluT2 mRNA is present in C1 and several other groups of brainstem catecholaminergic neurons. J. Comp. Neurol. 444, 191-206.

Stornetta, R.L., Sevigny, C.P., Schreihofer, A.M., Rosin, D.L., Guyenet, P.G. 2002b. Vesicular glutamate transporter DNPI/VGluT2 is expressed by both C1 adrenergic and nonaminergic presympathetic vasomotor neurons of the rat medulla. J. Comp. Neurol. 444, 207-220.

Sulzer, D., Joyce, M..P, Lin, L., Geldwert, D., Haber, S.N., Hattori, T., Rayport, S. 1998. Dopamine neurons make glutamatergic synapses *in vitro*. J. Neurosci. 18, 4588-4602.

Takagi, H., Miroshima, Y., Matsuyama, T., Hayashi, H., Watanabe, T., Wada, H. 1986. Histaminergic axons in the neostriatum and cerebral cortex of the rat: a correlated light and electron microscopic immunocytochemical study using histidine decarboxylase as a marker. Brain Res. 364, 155-168.

Takamori, S., Rhee, J.S., Rosenmund, C., Jahn, R. 2000. Identification of a vesicular glutamate transporter that defines a glutamatergic phenotype in neurons. Nature 407, 189-194.

Takamori, S., Rhee, J.S., Rosenmund, C., Jahn, R. 2001. Identification of differentiation-associated brain-specific phosphate transporter as a second vesicular glutamate transporter (VGluT2). J. Neurosci. 21, RC182.

Takamori, S., Malherbe, P., Broger, C., Jahn, R. 2002. Molecular cloning and functional characterization of human vesicular glutamate transporter 3. EMBO Rep. 3, 798-803.

Tennyson, V.M., Heikkila, R., Mytilineou, C., Côté, L., Cohen, G. 1974. 5-Hydroxydopamine "tagged" neuronal boutons in rabbit neostriatum: Interrelationships between vesicles and axonal membrane. Brain Res. 82, 341-348.

Triarhou, L.C., Norton, J., Ghetti, B. 1988. Synaptic connectivity of tyrosine hydroxylase immunoreactive nerve terminals in the striatum of nomal, heterozygous and homozygous weaver mutant mice. J. Neurocytol. 17, 221-232.

Trudeau, L.-É. 2004. Glutamate co-transmission as an emerging concept in monoamine neuron function. J. Psychiat. Neurosci., 29, 296-310.

Trudeau, L.-E., Gutierrez, R. 2007. On co-transmission and neurotransmitter phenotype plasticity. Molecular Interventions 7, 138-146.

Umbriaco, D., Watkins, K.C., Descarries, L., Cozzari, C., Hartman, B.K. 1994. Ultrastructural and morphometric features of the acetylcholine innervation in adult rat parietal cortex : an electron microscopic study in serial sections. J. Comp. Neurol. 348, 351-373.

Umbriaco, D., Garcia, S., Beaulieu, C., Descarries, L. 1995. Relational features of acetylcholine, noradrenaline, serotonin and GABA axon terminals in the stratum radiatum of adult rat hippocampus (CA1). Hippocampus 5, 605-620.

Varoqui, H., Schafer, M.K., Zhu, H., Weihe, E., Erickson, J.D. 2002. Identification of the differentiation-associated Na+/PI transporter as a novel vesicular glutamate transporter expressed in a distinct set of glutamatergic synapses. J. Neurosci. 22, 142-155.

Vizi, E.S. 1984. Non-synaptic Interactions Between Neurons : Modulation of Neurochemical Transmission. Chichester: John Wiley.

Vizi, .ES., Labós, E. 1991. Non-synaptic interactions at presynaptic level. Progr. Neurobiol. 37, 145-163.

Voorn, P., Jorritsma-Byham, B., Van Dijk, C., Buijs, R.M. 1986. The dopaminergic innervation of the ventral striatum in the rat: a light- and electron-microscopical study with antibodies against dopamine. J. Comp. Neurol. 251, 84-99.

Yamaguchi, T., Sheen, W., Morales, M. 2007. Glutamatergic neurons are present in the rat ventral tegmental area. Eur. J. Neurosci. 25, 106-118.

Zoli, M., Agnati, L.F. 1996. Wiring and volume transmission in the central nervous system: the concept of closed and open synapses. Prog. Neurobiol. 49, 363-380.

Zoli, M., Torri, C., Ferrari, R., Jansson, A., Zini, I., Fuxe, K., Agnati, L.F. 1998. The emergence of the volume transmission concept. Brain Res. Rev. 26, 136-147.

Zoli, M., Jansson, A., Syková, E., Agnati, L.F., Fuxe, K. 1999. Volume transmission in the CNS and its relevance for neuropsychopharmacology. Trends Pharm. Sci. 20, 142-150.

Table 1

SYNAPTIC INCIDENCE OF DOPAMINE AXON TERMINALS IN ADULT RAT STRIATUM

		Showing a synapse (single sections)	Observed (serial sections)	Extrapolated
NEOSTRIATUM				
Descarries et coll. (1996)				
[^{3}H]DA autoradiography		9.6%		39%
DA immunocytochemistry		12.3%	35%	40%
Antonopoulos et coll. (20 02)				
DA immuno	pa tch	22%		63%
	matrix	11%		35%
NUCLEUS ACCUMBENS				
Antonopoulos et coll. (2002)				
DA immuno.	core	14%		47%
	Shell	2-%		71%
Bérubé-Carrière et coll. (2007)				
TH immuno.	core	11%		34%

Table 2

NUMBER OF SINGLY AND DOUBLY LABELED AXON TERMINALS (VARiCOSITIES) IN THE CORE OF NUCLEUS ACCUMBENS OF NORMAL OR 6-OHDA LESIONED RATS AT P15 AND P90

P15 (n = 7)	TH (total)	TH/VGluT2	TH	VGluT2
Normal	161 ± 12	45 ± 6 (28%)	115 ± 6	82 ± 21
6-OHDA	99 ± 7 ***	37 ± 4 (37%) *	63 ± 7 ***	46 ± 9
P90 (n = 3)	TH (total)	TH/VGluT2	TH	VGluT2
Normal	68 ± 4	8 ± 5 (12%)	60 ± 2	106 ± 11
6-OHDA	36 ± 11	14 ± 8 (39%)	22 ± 4	114 ± 4

Data for an equivalent ultrathin tissue section area of 1665 μm2 in each rat. * $P < 0.05$; *** $P < 0.001$ by unpaired Student's *t* test.

Figure legends

Figure 1: Electron micrographs of DA axon terminals (varicosities) in adult rat neostriatum, identified by high resolution autoradiography after *in vivo* uptake of tritiated DA (A), or by immunocytochemistry with primary antibodies against DA-glutaraldehyde-protein conjugate (B). In **A**, the elongated profile of the [^{3}H]DA-labeled varicosity displays the characteristic array of small vesicles associated with a mitochondrion, but no zone of plasma membrane differentiation suggestive of a synaptic contact. This varicosity is directly apposed to a neuronal cell body (N), a dendritic branch (db) and another axonal varicosity, unlabeled (av). In **B**, the DA-immunostained profile is one from a series of 10 thin sections across the same varicosity. In this and 2 adjacent sections, this DA varicosity is seen to make a small symmetrical synapse (between arrows) with the neck of a spine (sp) observed in continuity with its parent dendrite (db). Note that this spine also receives a relatively large asymmetrical synapse on its head from the unlabeled varicosity on its left (av). Scale bars: 0.5 μm. (Reproduced with permission from Wiley-Liss (J. Comp. Neurol., 1996, 375:167-186).

Figure 2: Series of 15 consecutive thin sections across the entire volume of a DA immunoreactive varicosity (V_{II} in B) from the neostriatum. Part of another DA varicosity (V_I) is also visible in **A** to **F**. Both the DA varicosities form small, symmetrical synaptic contacts (between arrows in **E** and **I**). In **E**, V_I is seen to make synapse with the dendritic branch (db) in **C**, whereas V_{II} displays a first synapse with a dendritic spine (sp). In **I** and **J**, V_{II} makes a second synapse with a dendritic spine (sp in **I**), which also receives a large asymmetrical synaptic contact from an adjacent unlabeled varicosity (av in **I**). Scale bar (in O): 1 μm. (Reproduced with permission from Wiley-Liss (J. Comp. Neurol., 1996, 375:167-186).

Figure 3: Schematic representation of the synaptic and non-synaptic axon terminals established by DA neurons. DA neurons are known to establish two morphologically distinguishable axon terminals: some that are non-synaptic and others that are synaptic. The non-synaptic terminals (varicose-like structures) display no obvious pre- and postsynaptic specialization (see lower right illustration showing a

magnified view of a single non-synaptic terminal), contain TH and could be specialized for the release of DA. The synaptic terminals, displaying a more classical active zone, postsynaptic density and synaptic cleft, could be the site of VGluT2 expression and of glutamate (Glu) release (see upper right illustration showing a magnified view of a synaptic axon terminal). Adapted from Trudeau and Gutierrez, 2007.

Figure 4: Confocal imaging (A,B) and RT-PCR detection (C) of the presence of VGluT2 in isolated DA neurons in culture. In **A**, the isolated neuron displays TH (green, upper left) as well as VGluT2 immunofluorescence (red, upper right). The merged image in the lower left panel demonstrates the co-localization of VGluT2 mainly in TH positive processes (yellow). In the enlarged view of the boxed area from this panel (lower right), it is apparent that there are varicose-like punctae immunopositive for both VGluT2 and TH (yellow) and others for TH only (green) along the same processes. In **B**, the upper panels illustrate the immunoreactivity to VGluT2 (green, upper left) and to the synaptic vesicle protein SV2 (red, upper right) in a subset of nerve terminals from the isolated TH positive neuron (lower left). The merged image (lower right) demonstrates the co-localization of VGluT2 and SV2 (yellow). The enlargement in inset shows that most VGluT2 positive structures are also SV2-positive (yellow), but that there are SV2 positive terminals which are VGluT2 negative (red). All scale bars: 15 μm. **C** represents the mRNA expression profile of an individual mesencephalic DA neuron in culture. Both TH and VGluT2 mRNA were found in this neuron. Expected size of PCR products in base pairs: TH (301), VGluT2 (315).

Figure 5: Electron micrographs of TH and VGluT2 immunoreactive axon terminals (varicosities) in the nAcb of normal (A,B) or 6-OHDA-lesioned (C) 15 day-old rats. TH and VGluT2 were respectively labeled with the immunoperoxidase technique (fine DAB precipitate) and the immunogold technique (silver-intensified, gold particles). In **A**, two doubly labeled varicosities (thick black arrows), as well as three varicosities labeled for TH only (thin black arrows) and two for VGluT2 only (empty arrows) are visible. The larger of these doubly labeled varicosities makes synapse (between small arrows) with a dendritic spine. In **B**, a doubly labeled

terminal lies between two other varicosities, one unlabeled, on its left, and the other labeled for VGluT2 only, on its right. Note the synaptic contact (between small arrows) made by the doubly labeled varicosity on a small dendritic spine. Scale bar (for A and B): 1 μm. In **C**, three doubly labeled terminals can be seen, two of which display a synaptic contact (between small arrows) with a dendritic spine. Scale bar: 0.5μm .

Figure 6: Frequency distribution histograms of the synaptic incidence of singly (TH or VGluT2) or doubly (TH/VGluT2) labeled axon varicosities in the nAcb of P15 and adult rats, normal or subjected to neonatal administration of 6-OHDA. Means ± sem from 7 rats in each group at P15. At P90, only 3 rats were examined. As stereologically extrapolated to the whole volume of varicosities, values above 100% suggest that some of the corresponding varicosities make more than one synaptic contact, which is indeed occasionally observed in single ultrathin sections for electron microscopy. ** $P < 0.01$; *** $P < 0.001$.

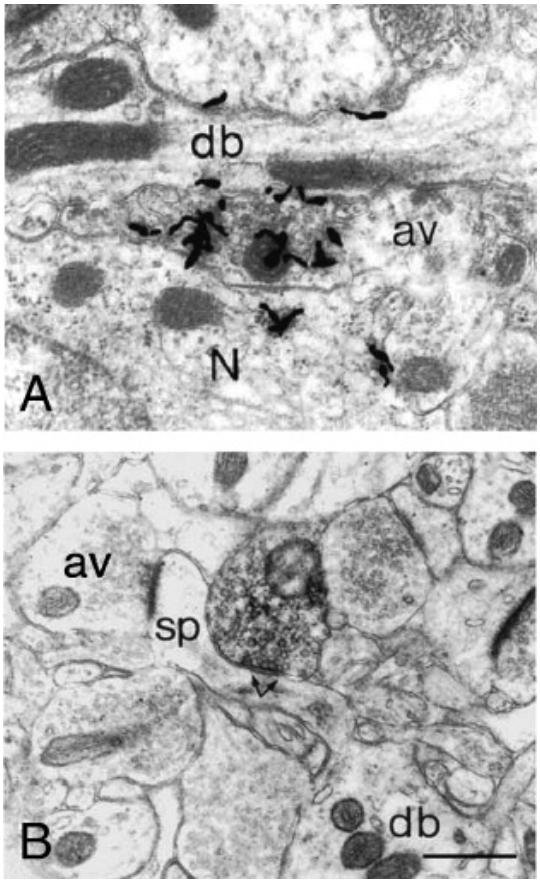

Figure 1: Electron micrographs of DA axon terminals (varicosities) in adult rat neostriatum, identified by high resolution autoradiography after *in vivo* uptake of tritiated DA (A), or by immunocytochemistry with primary antibodies against DA-glutaraldehyde-protein conjugate (B).

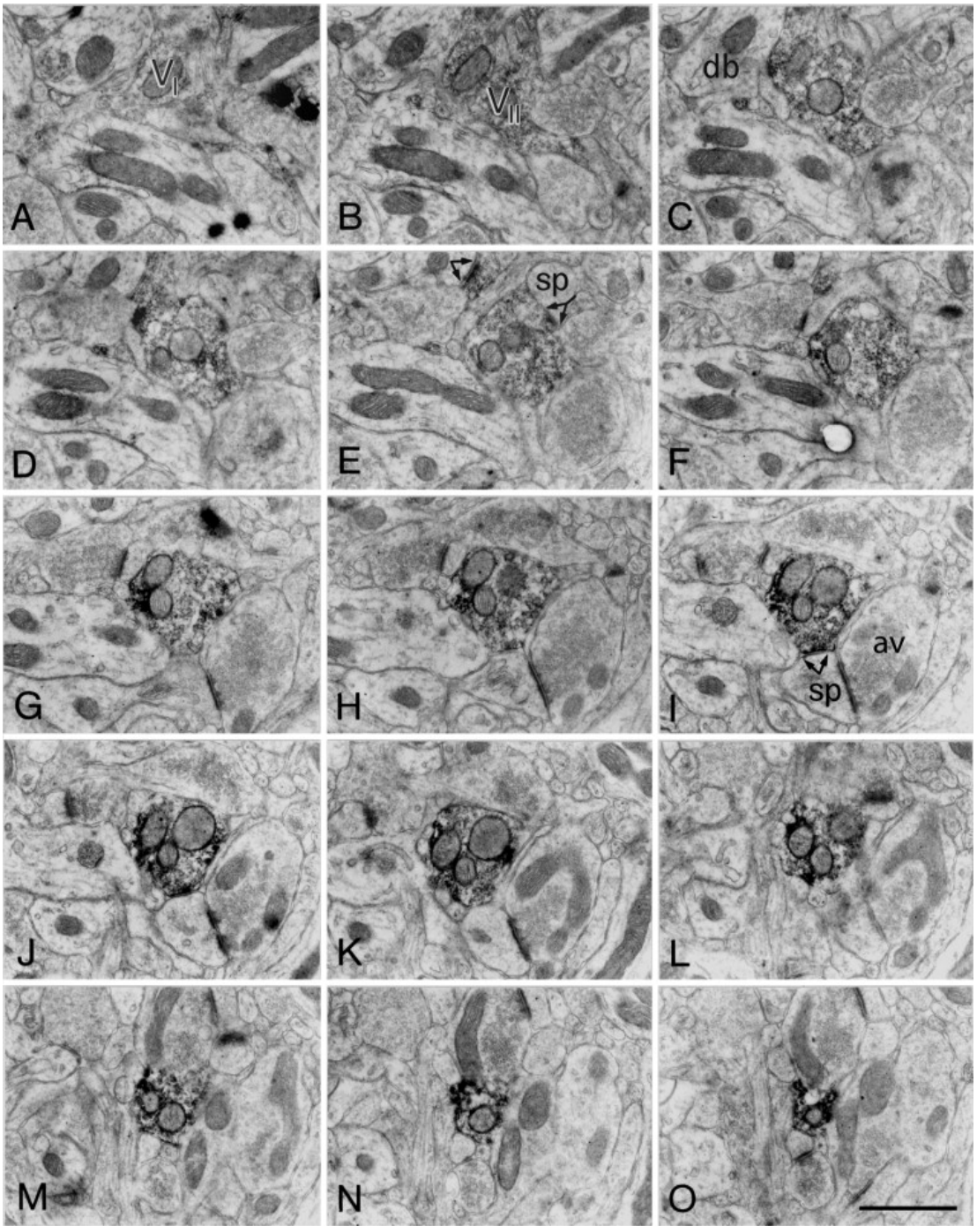

Figure 2: Series of 15 consecutive thin sections across the entire volume of a DA immunoreactive varicosity (V_{II} in B) from the neostriatum.

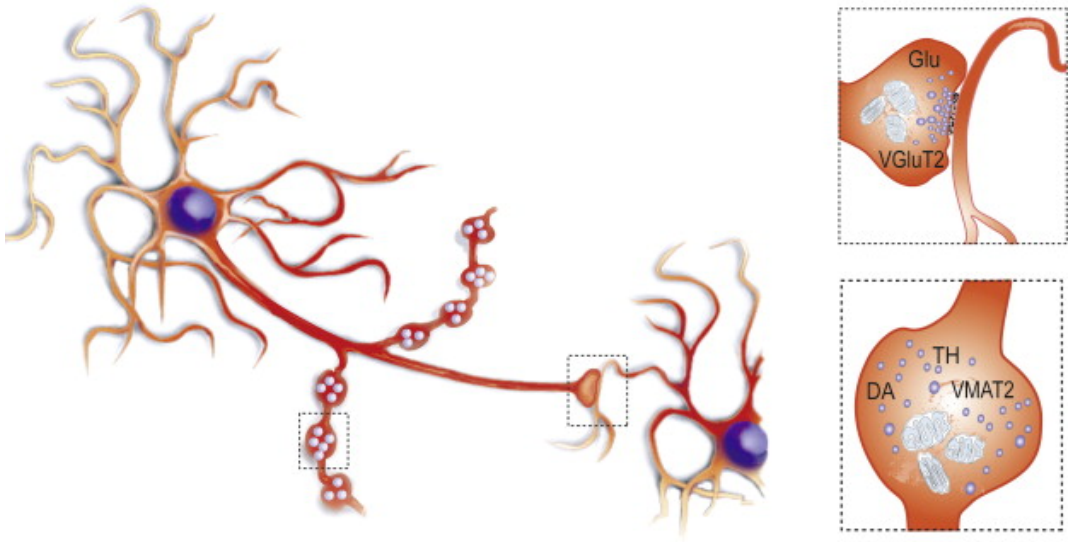

Figure 3: Schematic representation of the synaptic and non-synaptic axon terminals established by DA neurons.

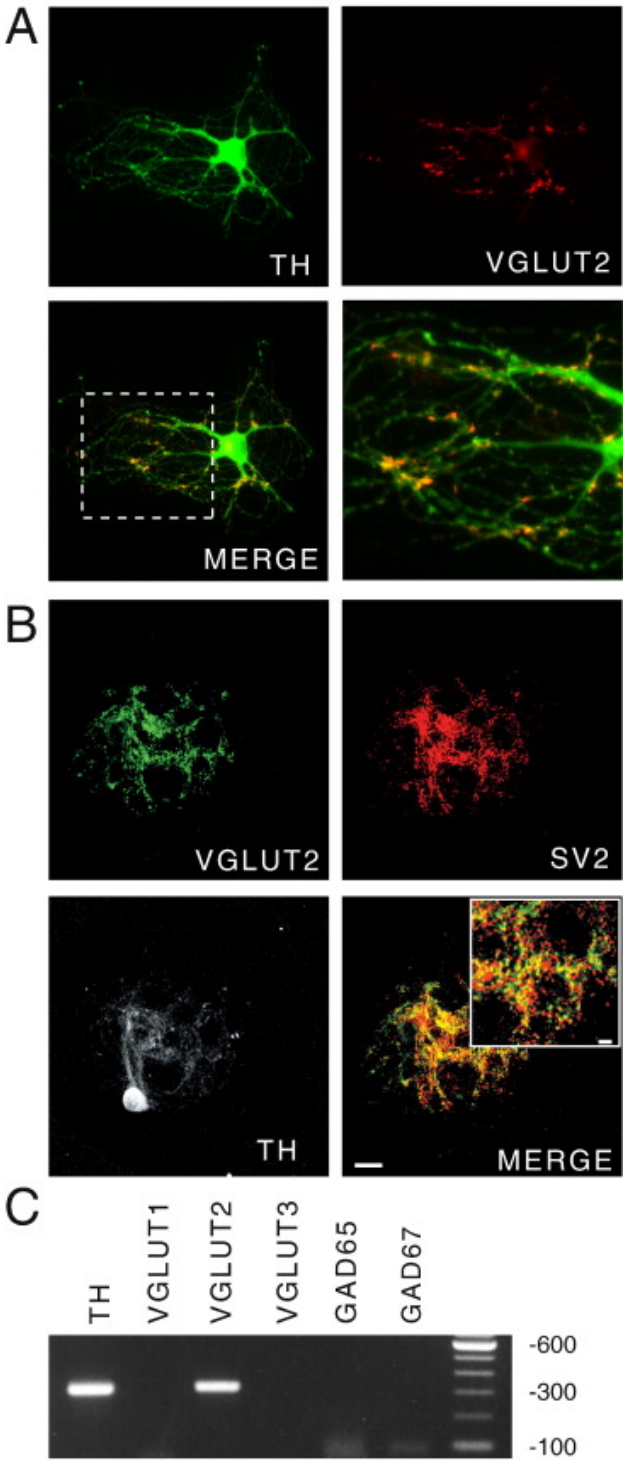

Figure 4: Confocal imaging (A,B) and RT-PCR detection (C) of the presence of VGluT2 in isolated DA neurons in culture.

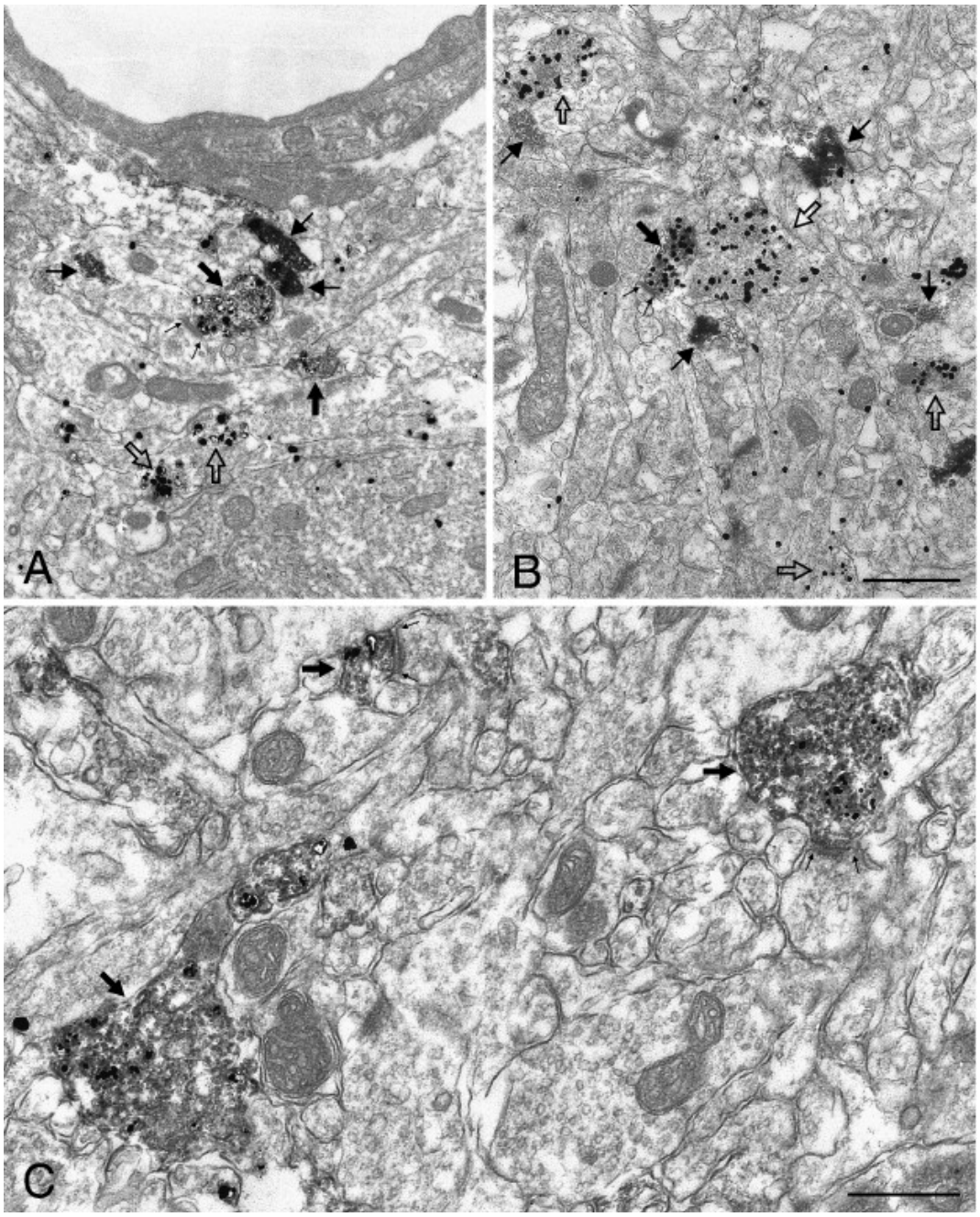

Figure 5: Electron micrographs of TH and VGluT2 immunoreactive axon terminals (varicosities) in the nAcb of normal (A,B) or 6-OHDA-lesioned (C) 15 day-old rats.

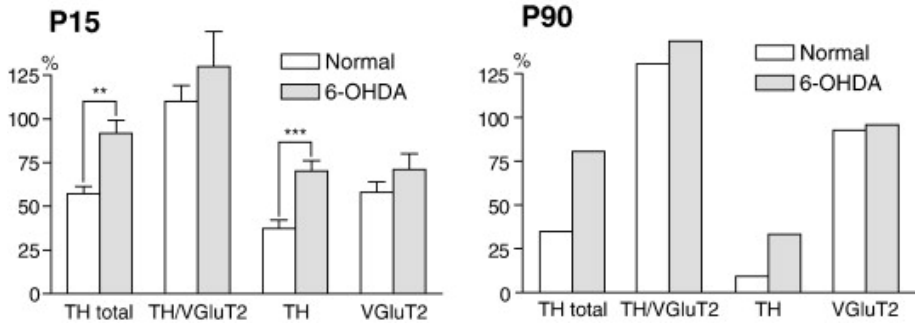

Figure 6: Frequency distribution histograms of the synaptic incidence of singly (TH or VGluT2) or doubly (TH/VGluT2) labeled axon varicosities in the nAcb of P15 and adult rats, normal or subjected to neonatal administration of 6-OHDA.

Annexe 2

ENHANCED GLUTAMATERGIC PHENOTYPE OF MESENCEPHALIC DOPAMINE NEURONS AFTER NEONATAL 6-HYDROXYDOPAMINE LESION

Grégory DAL BO [1], Noémie BÉRUBÉ-CARRIÈRE [2], Jose Alfredo MENDEZ [1], Damiana LEO[1], Mustapha RIAD [2], Laurent DESCARRIES [2,3,4], Daniel LÉVESQUE [5], Louis-Eric TRUDEAU [1,4]

Departments of [1] Pharmacology, [2] Pathology and Cell Biology, and [3] Physiology, Faculty of Medicine; [4] Groupe de Recherche sur le Système Nerveux Central; [5] Faculty of Pharmacy; Université de Montréal, Montréal, QC, Canada

Neuroscience (2008) **156** : 59-70.

Abbreviations: DA, dopamine; VGLUT, vesicular glutamate transporter; TH, tyrosine hydroxylase; 6-OHDA, 6-hydroxydopamine; RNA, ribonucleic acid; VTA, ventral tegmental area; i.c.v., intra-cerebroventricular; nAcb, nucleus accumbens; Dig , digoxigenin; SN, substantia nigra; RLi, rostral linear nucleus; DAB, 3,3'-diaminobenzidine tetrahydrochloride; GABA, gamma-aminobutyric acid; GDNF; glial cell derived neurotrophic factor.

ABSTRACT

There is increasing evidence that a subset of midbrain dopamine (DA) neurons uses glutamate as a co-transmitter and expresses VGLUT2, one of the three vesicular glutamate transporters. In the present study, double *in situ* hybridization was used to examine tyrosine hydroxylase (TH) and VGLUT2 mRNA expression during the embryonic development of these neurons, and postnatally, in normal rats and rats injected with 6-hydroxydopamine (6-OHDA) at P4 to destroy partially DA neurons. At embryonic days 15 and 16, there was a regional overlap in the labeling of TH and VGLUT2 mRNA in the ventral mesencephalon, which was no longer found at late embryonic stages (E18-E21) and postnatally. In normal pups from P5 to P15, only 1-2% of neurons containing TH mRNA in the ventral tegmental area (VTA) and substantia nigra, pars compacta, also displayed VGLUT2 mRNA. In contrast, after the cerebroventricular administration of 6-OHDA at P4, 26% of surviving DA neurons in the VTA of P15 rats expressed VGLUT2. To search for a colocalization of TH and VGLUT2 protein in axon terminals of these neurons, the nucleus accumbens of normal and 6-OHDA-lesioned P15 rats was examined by electron microscopy after dual immunocytochemical labeling. In normal rats, VGLUT2 protein was found in 28% of TH positive axon terminals in the core of nucleus accumbens. In 6-OHDA-lesioned rats, the total number of TH positive terminals was considerably reduced, and yet the proportion also displaying VGLUT2 immunoreactivity was modestly but significantly increased (37%). These results lead to the suggestion that the glutamatergic phenotype of VTA DA neurons is highly plastic, repressed toward the end of normal embryonic development, and derepressed postnatally following injury. They also support the hypothesis of co-release of glutamate and DA by mesencephalic neurons *in vivo*, at least in the developing brain.

Keywords: dopamine, glutamate, VGLUT2, 6-OHDA, mesencephalon, nucleus accumben

INTRODUCTION

The dopamine (DA) system is known to be critical for motor control and many aspects of cognition. It is implicated in Parkinson's disease and neuropsychiatric disorders, including schizophrenia and addiction. In the last 10 years, considerable evidence has accrued for glutamate co-transmission by central DA neurons. For example, release of glutamate was demonstrated to occur at autapses established by isolated DA neurons in culture (Sulzer et coll., 1998; Bourque and Trudeau, 2000; Joyce and Rayport, 2000) and stimulation of presumed DA neurons in the ventral tegmental area (VTA) was shown to evoke glutamatergic synaptic responses in neurons of the nucleus accumbens (nAcb) and prefrontal cortex (Chuhma et coll., 2004; Lavin et coll., 2005). In addition, mesencephalic DA neurons in culture were shown to express VGLUT2 (Dal Bo et coll., 2004), one of the three vesicular glutamate transporters (Ni et coll., 1995; Bellocchio et coll., 1998; Hisano et coll., 2000; Aihara et coll., 2000; Herzog et coll., 2001; Fremeau et coll., 2001; Varoqui et coll., 2002; Gras et coll., 2002).

In two recent *in situ* hybridization studies, expression of VGLUT2 mRNA by mesencephalic DA neurons has been demonstrated in intact tissue (Kawano et coll., 2006; Yamaguchi et coll., 2007). In the first study, the authors reported that as much as 19% of tyrosine hydroxylase (TH) immunopositive neurons of the VTA (A10 cell group) also expressed VGLUT2 mRNA (Kawano et coll., 2006). In the second study, the authors found that only 0.1% of neurons expressing TH mRNA in this region, also contained VGLUT2 mRNA (Yamaguchi et coll., 2007). This large difference in proportion remains to be explained, but could reflect technical differences in experimental approach. In any case, both studies indicated a striking difference between *in vivo* and *in vitro* data, since a majority (80%) of isolated mesencephalic DA neurons in culture have been shown to express VGLUT2 (Dal Bo et coll., 2004). In line with previous results demonstrating plasticity of the transmitter phenotype of neurons during development and in responses to changes in neuronal activity (Furshpan et coll., 1976; Borodinsky and Spitzer, 2007; Borodinsky et coll., 2004; Yang et coll., 2002; Gillespie et coll., 2005; Trevino and Gutierrez, 2005; Gutierrez and Heinemann, 2006; Gomez-Lira et coll., 2005), this discrepancy between the *in*

vivo and *in vitro* data is best resolved by hypothesizing that VGLUT2 expression in DA neurons is regulated during development, and may be up-regulated in response to trauma, such as tissue dissociation and culture or a partial lesion *in vivo*.

To investigate the glutamatergic phenotype of developing mesencephalic DA neurons *in vivo*, we used double *in situ* hybridization for tyrosine hydroxylase (TH) mRNA and each subtype of VGLUT transcripts in pre- and post-natal rats, as well as double labeling immuno-electron microscopy with specific antibodies against TH and VGLUT2 in 15 day-old pups. Intact rats as well as rats subjected to neonatal intra-cerebroventricular (i.c.v.) administration of the neurotoxin 6-hydroxydopamine (6-OHDA) were examined in order to evaluate the effects of an early injury on the transmitter phenotype of surviving DA neurons.

We confirm that a small subset of mesencephalic DA neurons selectively expresses VGLUT2 mRNA, but not VGLUT1 nor VGLUT3, and suggest that the glutamatergic phenotype of these neurons is repressed during late embryonic development and may be up-regulated in response to early postnatal injury. By visualizing both TH and VGLUT2 proteins in the same axon terminals of the nAcb, we also provide strong evidence for the capacity of mesencephalic DA neurons to release both DA and glutamate *in vivo,* at least in developing brain.

MATERIALS AND METHODS

Animals

All procedures involving animals and their care were conducted in strict accordance with the Guide to the Care and Use of Experimental Animals (Ed2) of the Canadian Council on Animal Care. The experimental protocols were approved by the animal ethics committee (CDEA) of the Université de Montréal. Sprague-Dawley male rats and pregnant dams were purchased from Charles River (Montreal, QC, Canada) and housed at a constant temperature (21°C) and humidity (60%), under a fixed 12 hours light/dark cycle, with free access to food and water.

Neonatal 6-hydroxydopamine lesions

Neonatal 6-OHDA lesions were produced as previously described (Stachowiak et coll., 1984; Jackson et coll., 1988; Fernandes Xavier et coll., 1994). Four day-old pups received a subcutaneous injection of desipramine (50 ml, 5.6 mg/ml in aCSF) (Sigma Chemical, St. Louis, MO) 45 min before toxin injection to protect noradrenergic neurons. The toxin (6-hydroxydopamine hydrochloride, Sigma), was dissolved (10 mg/ml) in aCSF containing 0.2% ascorbic acid to prevent oxidation. Pups were anesthetized on ice, immobilized on a cold body mould, and administered 5 µl of 6-OHDA solution in each lateral brain ventricle (stereotaxic coordinates: L ± 1.5 mm, AP 0 mm to Bregma, and V 3.3 mm below the dura), at a rate of approximately 1.5 µl /min. The intraventricular injections were made with a 30-gauge needle attached to a 10 µl Hamilton syringe. The syringe was left in place for 3 min after each injection. Sham controls were injected with vehicle under the same conditions. The pups were then warmed in a humidified box and returned to their mother two hours later. They were maintained with their mother until sacrifice, 11 days post-surgery (at P15).

Double *in situ* hybridization

The double *in situ* hybridization technique (Beaudry et coll., 2000) was used in rat embryos as well as in normal P5, P10 and P15 rat pups, and in 6-OHDA-lesioned P15 rats and their sham controls.(Cossette et coll., 2004; St-Hilaire et coll., 2005). The embryos were removed from gestating dams under isoflurane anesthesia (isoflurane 2%, O_2 1.8 l/min), on days 14, 15, 18 and 21 of gestation. They were immersed in frozen isopentane, and stored at - 80°C until used. The postnatal rats were anesthetized with halothane and their brain was quickly dissected out, immersed in cold phosphate-buffered saline (PBS, 50 mM, pH 7.4), and cut in two parts at the level of the median eminence. The rostral part containing the striatum was fixed by immersion in 4% paraformaldehyde (PFA) solution for 48 h and processed for TH immunohistochemistry as described below. The caudal part containing the mesencephalon was immersed in frozen isopentane and stored at - 80°C until used.

[^{35}S]UTP-labeled VGLUT1, 2 or 3 probes, and a nonradioactive digoxigenin (Dig)-labeled tyrosine hydroxylase probe were prepared as follows. Complementary

RNA (cRNA) probes for each VGLUT subtype were synthesized from pCRII-Topo plasmids containing a fragment of each VGLUT cDNA. cDNA fragment sizes were 519, 539 and 415 base pairs for VGLUT1, 2 and 3, respectively (Herzog et coll., 2001; Gras et coll., 2002). Antisense probes were produced by linearization of the plasmid using the *Not* I restriction enzyme and SP_6 polymerase, and synthesized with the Promega riboprobe kit (Promega, Madison, WI, USA) and [^{35}S]UTP (Perkin-Elmer, Missisauga, ON, Canada). For sense probes, the *Hind* III restriction enzyme was used to linearize the plasmid, and probes were synthesized with T_3 polymerase. Labeled probes were purified with mini QuickSpin RNA columns (Roche Diagnostics, Laval, QC, Canada). The Dig-labeled TH probe was generated as previously described (Cossette et coll., 2004). Both Dig-labeled TH (20 ng/ml) and specific radioactive-labeled VGLUT probes (2 x 10^6 CPM) were included simultaneously in the hybridization solution.

Transverse sections of the mesencephalon (12 µm-thick) were cut with a cryostat, mounted on Superfrost Plus slides (Fisher Scientific, Toronto, ON, Canada), and stored at - 80°C until used. Before hybridization, slides were fixed in 4% PFA for 20 min and rinsed 3 times in PBS. *In situ* hybridization was performed overnight at 58°C. To reduce non specific Dig labeling, an additional step was added to standard post hybridization treatments: immersion in a 50% formamide solution in 2x saline-sodium citrate buffer (SSC, 300 mM NaCl, 30 mM sodium citrate, pH 7 in DEPC water) for 30 min at 60°C. The slides were then immersed for 30 min in blocking solution containing 2% BSA and 0.3% Triton X-100 in buffer A solution (100 mM Tris–HCl, pH 7.5 and 150 mM NaCl), covered with 100 µl of an anti-Dig antibody conjugated to alkaline phosphatase (Roche Diagnostics) diluted 1/200 in buffer A, and placed at 4°C overnight. After 3 rinses (10 min) in buffer A, the Dig was revealed in buffer B (100 mM Tris–HCl, pH 9.5, 100 mM NaCl and 50 mM $MgCl_2$) containing 0.4 mM nitroblue tetrazolium chloride, 0.45 mM 5-bromo-4-chloro-3-indolyl phosphate (Dig detection kit, Roche Diagnostic) and 1mM levamisole, for 30 min at room temperature, in the dark. The Dig reaction was stopped by immersion in buffer C (100 mM Tris-HCl, pH 8 and 1 mM EDTA). After 3 additional washes with distilled water, slides were air-dried, and apposed against BiomaxMR

radioactive-sensitive film (Kodak, New Haven, CT, USA) for 3 days. Following film exposition, the slides were coated by dipping with LM-1 photographic emulsion (Amersham, ON, Canada), stored in the dark for 21 days at 4°C, developed in D-19 (Kodak) and coverslipped with a water-soluble mounting medium (Permafluor; Lipshaw Immunon, Pittsburgh, PA, USA). Slides used to compare the dual labeling at different ages and/or between experimental conditions were systematically processed together. All these sections were examined under bright-field illumination with an Olympus IX-50 microscope (Carsen Group, Markham, ON, Canada), at 400 X magnification.

In sections from embryos, the contour of individual neurons could not be distinguished after the above processing for dual *in situ* hybridization. To quantify *in situ* hybridization signals, counts of silver grains (VGLUT2 mRNA) were therefore obtained from tissue areas also displaying Dig positivity (TH mRNA). This was done with the aid of the public domain Image J software (NIH) in images captured with an ORCA-II cooled digital camera (Hamamatsu, NJ, USA). In each section, silver grain counts were obtained from 3 square areas (± 6000 μm^2 each) of the ventral mesencephalon displaying Dig positivity, and three 3 areas of the same sections (± 5600 μm^2 each) showing only weak, silver grain labeling (background). The counts from TH-Dig positive areas were then averaged at each embryonic age, and expressed in number of grains per 500 μm^2 (an area corresponding to a cluster of DA neurons cell bodies), after subtracting the background (0.9 -1.9 silver grains per 500 μm^2 of section). This analysis was performed in 3 or 4 sections per embryo, and 3 embryos each at E15 and E18, and 5 embryos each at E16 and E21.

In sections from postnatal rats, background labeling was similarly measured and found at 0.37 to 0.53 silver grains per 500 μm^2 of section. As in previous studies (Kawano et coll., 2006), TH-Dig positive cells (DA neurons) were considered to be labeled for VGLUT2 mRNA if displaying 3 times the background level, i.e., at least 6 silver grains per cell body (Gratto and Verge, 2003). In 4 rats of each experimental condition tested and 3 or 4 sections per rat, located between stereotaxic planes - 5.28 mm and - 6.24 mm from Bregma in adult rats (Paxinos, G. and Watson, C., 2005), singly and doubly labeled cells were then counted visually.

Tyrosine hydroxylase immunohistochemistry

TH immunohistochemistry was used to verify the extent of 6-OHDA lesions. After 48 h of fixation in PFA, 24 µm-thick transverse sections of the forebrain were cut with a VT1000s vibratome (Leica Microsystems, Nussloch, Germany), rinsed in PBS (3x10 min) and then incubated in 5% goat serum solution containing 10% BSA and 0.1% Triton X-100 for 1 h, in order to block non-specific labeling. Sections across the striatum were incubated overnight in mouse monoclonal TH antibody (Clone TH-2, Sigma) diluted 1/1000 in PBS. The signal was detected with biotinylated anti-mouse antibodies (Jackson Immunoresearch, West Grove, PA, USA) diluted 1/1000, followed by 1/1000 streptavidin-HRP (Jackson). After 3 x 10 min washes in PBS, followed by 2 x 10 min washes in Tris-HCl (50 mM, pH 7.4). The peroxidase reaction was revealed with 0.05% 3,3'-diaminobenzidine tetrahydrochloride (DAB; Sigma) and hydrogen peroxide (0.01%) in Tris-HCl. The DAB reaction was stopped by immersion in Tris-HCl.

RT-mPCR

Transverse slices (~1 mm thickness) of the mesencephalon, cut by hand at the level of the VTA and substantia nigra (SN), were isolated from the frozen brain of normal, sham-injected and 6-OHDA-lesioned, 15 day-old rats (n = 3 in each group). The slices were trimmed under the microscope to keep only the VTA and SN pars compacta (SNc). Total RNA was extracted from each individual sample using TRIzol® Reagent (Invitrogen, Burlington, ON, Canada), according to the manufacturer's instructions. All samples were stored at -80°C until used. Reverse transcription was performed on 2.5 mg of total RNA for 1 h at 37°C with 0.5 mM dNTPs mix (Qiagen), 2.5 µM random hexamers (RH) (Applied Biosystem, CA, USA) and 100 U M-MLV reverse transcriptase (Invitrogen). Reaction was stopped by heating at 70°C for 15 min., then multiplex-semiquantitative PCR amplification was performed using 10% of the RT reaction, 2.5 µl 10x PCR buffer, 0.5 µl of 100 mM dNTPs, 2.5 U of Taq polymerase (all from Quiagen, ON, Canada), 1.5 mM $MgCl_2$, and 10 pmol of each primer. Twenty-seven cycles were carried out as follows: denaturation at 94°C for 60 s, annealing at 55°C for 30 s and extension at 72°C for 30

s. Amplification products were analyzed by 1.6% agarose gel electrophoresis. Band intensities were evaluated with Kodak ID v3.6.0 software.

Multiplex single-cell RT-PCR.

Cells dissociation was performed following a protocol modified from (Puma et coll., 2001). Briefly, the ventral mesencephalon was dissected from E15 embryos and collected in ice-cold PBS supplemented with 6 mg/ml glucose. The tissue was treated with papaïn (Worthington Biochemical Corp., Lakewood, NJ) for 20 min at 37°C in dissociation solution (in mM: 90 Na_2SO_4, 30 K_2SO_4, 5.8 $MgCl_2$, 0.25 $CaCl_2$, 10 HEPES, 20 glucose, 0.001% phenol red, pH 7.4), and then triturated to obtain a cell suspension (Bourque and Trudeau, 2000), that was subjected to a differential gradient centrifugation to eliminate dead cells and debris. Cells were plated on Polyethyleneimine-coated (PEI) coverslips mounted into an electrophysiology recording chamber and were left to adhere at room temperature for 15 minutes, then washed under perfusion with physiological saline solution (in mM: 140 NaCl, 5 KCl, 2 $MgCl_2$, 2 $CaCl_2$, 10 HEPES, 10 glucose, 6 sucrose, pH 7.35 and 305 mOsm) to remove non-attached cells.

Cells were collected individually under RNAse-free conditions by using sterile borosilicate patch pipettes. No intracellular pipette solution was used. Each cell was collected by applying light negative pressure to the pipette. The recording chamber was fixed to the stage of an inverted Nikon Eclipse TE-200 microscope. Coverslips were kept under perfusion of physiological saline solution using a gravity flow system (1 ml/min). Once samples were collected, the content of the pipette was transferred immediately into a pre-chilled 200-µl tube containing 6 µl of a freshly prepared solution of 20 U of RNaseOUT and 8.3 mM of DTT (Invitrogen) and then frozen immediately until use. Frozen samples were thawed on ice and subjected to the RT reaction as describe for total RNA but using 1.25 µM RH, 100 units M-MLV RT and 20 additional units of RNaseOUT. A first round of PCR was done as mentioned above but using the half of the RT reaction and 27 cycles. A second round of PCR was done using 10% of first PCR reaction and 28 cycles.

Primers

All primers were designed according to the NCBI GenBank sequence database using Primer3 (http://frodo.wi.mit.edu/cgi-bin/primer3/primer3_www.cgi) as well as Vector NTI software, and synthesized by AlphaDNA (Montreal, QC, Canada). All primers were tested using the appropriate positive and negative controls. For β-actin, the forward and reverse primers were 5'-CTCTTTTCCAGCCTTCCTTCTT-3' and 5'-AGTAATCTCCTTCTGCATCCTGTC-3', respectively (product size 175 pb). For TH, the primers were 5'-GTTCTCAACCTGCTCTTCTCCTT-3' and 5'-GGTAGCAATTTCCTCCTTTGTGT-3'; TH-nested, 5'-GTACAAAACCCTCCTCACTGTCTC-3' and 5'-CTTGTATTGGAAGGCAATCTCTG-3' (product size 375 pb). For VGLUT2, the primers were 5'-GGGGAAAGAGGGGATAAAGAA-3' and 5'-TGGCTTTCTCCTTGATAACTTTG-3; VGLUT2-nested 5'-ATCTACAGGGTGCTGGAGAAGAA-3' and 5'-GATAGTGCTGTTGTTGACCATGT-3' (product size 230 pb). Nested primers are the ones used in the RT-mPCR experiments.

Double immunolabeling for electron microscopy

Fifteen day-old pups were deeply anesthetized with sodium pentobarbital (80 mg/kg, i.p.) and fixed by intra-cardiac perfusion of a solution of 3% acrolein in 0.1 M phosphate buffer (PB, pH 7.4), followed by 4% PFA in the same buffer. The brain was removed, post-fixed by immersion in the PFA solution at 4°C for 2 h, and washed in PBS. Fifty μm-thick transverse sections across the nAcb were cut in PBS with a vibratome, immersed in 0.1% sodium borohydride in PBS for 30 min at room temperature, and washed in this buffer before further processing. After preincubation for 1 h at room temperature in a blocking solution containing 5% normal goat serum and 0.5% gelatin in PBS, sections were incubated for 48 h at room temperature with both mouse monoclonal anti-TH (Sigma) (1:500) and rabbit polyclonal anti-VGLUT2 antiserum (Synaptic Systems, Goettingen, Germany) (1:500) (Anlauf and Derouiche, 2005) antibodies in blocking solution. The monoclonal anti-TH antibody recognizes an epitope present in the N-terminal region of both rodent and human tyrosine hydroxylase (Haycock, 1993), while the polyclonal anti-VGLUT2 antibody was

raised against a C-terminal segment of mammalian VGLUT2 (Fujiyama et coll., 2001). The VGLUT2 and TH antibodies were then sequentially labeled in this order with the immunogold and the immunoperoxidase technique, respectively. Sections were rinsed in PBS, incubated overnight at room temperature in goat anti-rabbit IgGs conjugated to 1 nm colloidal gold particles (AuroProbe One, Amersham, Oakville, ON, Canada), diluted 1:50 in blocking solution, and the size of immunogold particles was increased by silver enhancement for 15 min with IntenSE kit (Amersham). Sections were then rinsed in PBS, incubated for 1.5 h at room temperature with biotinylated goat anti-mouse IgGs (Jackson) diluted 1:1000 in blocking solution, rinsed in PBS, incubated for 1 h in a 1:1000 solution of streptavidin-HRP (Jackson), washed in PBS and then in 0.05 M Tris-saline buffer (TBS; pH 7.4), incubated for 2-5 min in TBS containing 0.05% DAB and hydrogen peroxide (0.02%), and washed again in TBS to stop the reaction.

Further processing for electron microscopy was as previously described in detail (Riad et coll., 2000). In brief, sections were osmicated, dehydrated and flat-embedded in resin between a glass slide and a plastic coverslip (Rinzl, Thomas Scientific, Swedesboro, NJ, USA). After 48 h of polymerization at 60°C, the coverslips were removed, and the region of interest (nAcb), identified by light microscopy, was excised from the slides and glued at the tip of resin blocks. Ultrathin sections were then cut with an ultramicrotome (Reichert Ultracut S, Leica Canada, St-Laurent, QC, Canada), collected on bare square-meshed copper grids, stained with lead citrate and examined with an electron microscope (Philips CM100, Philips Electronics, St-Laurent, QC, Canada). Immunocytochemical controls included processing as above but without either one or both primary antibodies. Only the expected single labeling was observed when omitting one or the other primary antibody, and no labeling whatsoever in the absence of both of them.

The electron microscopic analysis focused on the core of the nAcb, at transverse levels that correspond to between A 10.8 and 11.28 mm in the stereotaxic atlas of Paxinos and Watson (Paxinos, G. and Watson, C., 2005). Material from seven normal and seven 6-OHDA-lesioned rats, aged 15 days, was examined. In both normal and 6-OHDA-lesioned rats, a minimum of 50 electron micrographs per rat

were obtained from a narrow area of thin sections less than 10 µm away from the tissue-resin border at working magnifications ranging from 3,000 to 15,000 X. The film negatives were scanned (Epson Perfection 3200), converted into a positive picture, adjusted for brightness and contrast with Photoshop (Adobe), and printed at a final magnification ranging from 7,500 to 37,500 X.

Most immunolabeled profiles could then be positively identified as axon varicosities, i.e. axon dilations (> 0.25 µm in transverse diameter) containing aggregated small vesicles and often one or more mitochondria, and displaying or not a synaptic membrane specialization (junctional complex). Smaller immunolabeled profiles were assumed to represent intervaricose segments of unmyelinated axons. Only profiles decorated with 3 or more immunogold particles were considered as immunogold-labeled. The immunoperoxidase labeling was readily identified as a more or less dense precipitate, often outlining the small vesicles or mitochondria and the membrane of varicosities. In 30 micrographs per rat, printed at a uniform magnification of 30,000 X and showing the best morphological preservation, all singly or dually immunolabeled profiles of axon varicosities were counted and categorized as immunopositive for TH alone, for VGLUT2 alone or for both TH and VGLUT2 (TH/VGLUT2). As an equivalent ultrathin section surface (± 1665 μm^2) was being examined in every rat, the total number of varicosities in the different categories could be merely divided by the number of rats (n = 7) for the comparison between normal and 6-OHDA-lesioned rats.

Statistical analyses

All data were expressed as group mean ± SEM. Statistical analyses were performed with SigmaStat (Systat Software) or GraphPad Prism 4. T-tests, analyses of variance (one-way ANOVA) and Tukey post-hoc tests were used to determine statistical significance. *P* values below 0.05 were considered statistically significant.

RESULTS

Expression of VGLUT2 mRNA in pre- and post-natal ventral mesencephalon

Double *in situ* hybridization against TH and the three VGLUT subtypes was performed in order to detect VGLUT1-3 mRNAs in developing DA neurons *in vivo*. The selectivity of the [^{35}S]VGLUT mRNA probes was validated by evaluating their distribution in autoradiographs from the brain of normal 15 day-old rats. In keeping with previous observations (Boulland et coll., 2004; Fremeau et coll., 2002; Gras et coll., 2002; Herzog et coll., 2004b), VGLUT1 mRNA was abundant in the pyramidal cell layer of hippocampus and in cerebral cortex; VGLUT2 mRNA in the red nucleus and the medial geniculate nucleus, and VGLUT3 mRNA in the dorsal and median raphe nuclei (Supplementary online Material) (Herzog et coll., 2004a). No signal was observed with sense probes (data not shown).

Inspection of these autoradiographs did not show abundant VGLUT2 labeling in the ventral mesencephalon, including the VTA and SN, which could be due to a low sensitivity of detection of our *in situ* hybridization technique, but could also reflect a truly low level of VGLUT2 mRNA at that age (Boulland et coll., 2004). However, this did not exclude co-expression by a sub-population of these neurons, nor the repression of a broader co-expression at earlier stages of development.

The expression of each VGLUT subtype was therefore examined from E14 to E21 as well as in neonatal rats, using double *in situ* hybridization with Dig-TH and [^{35}S]VGLUT probes. No labeling for VGLUT1 and VGLUT3 mRNA was detected in the mesencephalic region of embryonic or neonatal rats (data not shown). In contrast, at E14-E15 and E16, strong labeling for VGLUT2 mRNA was observed in the region displaying TH mRNA labeling (Fig. 1A,A1), i.e., in the ventral and paramedial zone of the mesencephalon where developing DA neurons are found (Smits et coll., 2006). At later embryonic ages (E18-21), TH mRNA labeling remained abundant, but the overlap with VGLUT2 labeling was lost, suggesting a lowering of VGLUT2 expression in dopaminergic nuclei (Fig. 1B,B1). Quantification of the VGLUT2 mRNA labeling in TH-Dig-positive regions of embryonic ventral mesencephalon showed averages of 7.9 ± 0.9 and 7.3 ± 0.6 silver grains per 500 μm^2 of section at E15 (N=3) and E16 (N=5), respectively, and significant decreases to 2.3 ± 0.4 and 1.9

± 0.2 per 500 μm^2 at E18 (N=3) and E21 (N=5), respectively ($P < 0.001$ by one way ANOVA and Tukey's multiple comparison post-hoc test) (Fig. 1C). To confirm the presence of VGLUT2 mRNA in embryonic DA neurons, single-cell RT-PCR was used in individual E15 DA neurons. After acute dissociation of the ventral mesencephalon from E15 embryos, 54 cells were collected. Of these 54 cells, 13 were found to contain VGLUT2 mRNA and 4 to contain TH mRNA. Out of these 4 DA neurons, 3 were found to contain VGLUT2 mRNA (Fig. 1D), thus confirming the apparent frequent expression of this transcript in embryonic DA neurons.

In postnatal rats, numerous neurons dually-labeled for TH and VGLUT2 mRNAs were visible in the rostral linear raphe (RLi) nucleus (Fig. 2A,B), while only small numbers were observed in the VTA and SNc (Fig. 2C,D). The percentage of DA (TH mRNA) neurons co-expressing VGLUT2 mRNA in the VTA and SN of normal neonatal rats is given in Table 1. In P5, P10 and P15 pups (N=4 for each age), we counted a total of 5382 neurons containing TH mRNA in the SN, and 4656 in the VTA. Out of these, only a small subset showed dual labeling (33 in the SN, and 120 in the VTA). There was no statistically significant change in the percentage of dually labeled neurons in the VTA or the SN between these ages (Table 1). At each age, the percentage of co-expression was significantly higher in the VTA (parabrachial and paranigral subdivisions) than the SN (2.6 ± 0.5 % versus 0.6 ± 0.1 % in average; $p < 0.001$, t-test). The highest ratio was observed in the RLi (24.1 ± 6.4 %; N=3), in which DA neurons are less numerous and dispersed along the midline (Fig. 2A,B). Some neurons expressing VGLUT2 only were also seen in the VTA, suggesting the presence of primarily glutamatergic neurons in this mesencephalic region (e.g., Fig. 4A).

Co-expression of VGLUT2 by DA neurons after neonatal 6-OHDA lesion

The neonatal administration of 6-OHDA allowed to evaluate the effects of an early injury on the transmitter phenotype of surviving DA neurons. As expected from earlier studies (Fernandes Xavier et coll., 1994), eleven days after 6-OHDA (P15), TH immunoreactivity was almost abolished in the dorsal striatum of 6-OHDA rats, but residual labeling persisted in the ventral striatum, and notably in the nAcb (Figs 3A,B). The consequences of the 6-OHDA lesion on VGLUT2 expression were first

investigated by measuring TH, VGLUT2 and β-actin mRNAs in tissue blocks of the VTA and SN of normal, sham and 6-OHDA-lesioned 15 day-old rats (N=3), using semi-quantitative RT-PCR. As shown in Figs 3C and D, TH mRNA was markedly decreased after 6-OHDA compared to normal or sham controls (optical density 0.41 ± 0.04 vs. 1.1 ± 0.04 and 0.87 ± 0.16 for normal and sham respectively; one way ANOVA, $F(2,8) = 12,1$, $p < 0.05$). In contrast, there were no significant differences in VGLUT2 mRNA levels between either group (Fig. 3C,D; OD 0.94 ± 0.03 for 6-OHDA rats vs. 0.88 ± 0.03 and 0.82 ± 0.1 for normal and sham rats, respectively; one way ANOVA, $F(2,8) = 0,9$, $p > 0.05$).

In view of the major decrease in the number of DA neurons, the lack of a parallel decrease in VGLUT2 mRNA was compatible with either one of two possibilities. The proportion of surviving DA neurons expressing VGLUT2 could be increased following the 6-OHDA lesion, thus compensating for the decrease in DA neuron number, or else, most of the VGLUT2 mRNA that was measured originated from non-DA neurons that were not affected by the lesion. To distinguish between these possibilities, the number and proportion of DA neurons that expressed VGLUT2 mRNA were determined by double *in situ* hybridization in sham-operated compared to 6-OHDA-lesioned rats. As shown in Table 2, 11 days after the lesion, there was a modest but non significant increase in the number and proportion of dually labeled neurons in the VTA of sham operated (N=4) compared to control rats (N=4) (56 TH+/VGLUT2+ over 1124 TH+, i.e. 7.1 ± 1.5% *versus* 19 TH+/VGLUT2+ over 1116 TH+, i.e., 1.8 ±0.3%), and no change in the SN. As also shown in Table 2, the total number of neurons displaying TH mRNA was considerably reduced in the VTA of the lesioned rats (N=4), while such neurons had almost totally disappeared from the SN. Yet, the number of VTA neurons co-expressing TH and VGLUT2 mRNA after 6-OHDA (142 TH+/VGLUT2+ over 530 TH+ neurons) was higher than in control and sham-operated animals (Fig. 4), whereas none were observed in the SN. As the number of VTA DA neurons was markedly reduced by the lesion, this resulted in a highly significant increase in the proportion of dually labeled VTA neurons (26.3 ± 2.5%; Table 2). An analysis of variance confirmed the statistical significance of this difference ($p < 0.001$ for 6-

OHDA versus each other group), in the absence of a significant difference between the sham and control rats.

TH and VGLUT2 containing axon terminals in the nAcb of normal and 6-OHDA-lesioned 15 day-old rats

In every specimen from both normal and 6-OHDA-treated rats examined by electron microscopy after dual immunolabeling for TH and VGLUT2, axon terminals (varicosities) labeled for TH only (DAB), VGLUT2 only (gold particles) and both TH and VGLUT2 could be observed (Fig. 5). A quantification of these results revealed a considerable reduction (38%) in the number of TH positive singly-labeled varicosities after the 6-OHDA lesion compared to normal (Table 3). An apparent reduction in the number of singly labeled, VGLUT2 positive terminals was also measured, but did not reach statistical significance because of the considerable variability between rats. Surprisingly, there was no significant decrease in the number of dually labeled terminals estimated as a proportion of the total number of TH positive terminals after 6-OHDA (Table 3). To the contrary, 37% of residual TH positive terminals in the nAcb of 6-OHDA-lesioned rats were dually labeled, a value which was significantly higher than the 28% measured in normal rats ($p < 0.05$). Interestingly, even in single thin sections, the dually labeled terminals frequently showed a synaptic membrane specialization (junctional complex), either asymmetrical or symmetrical (Figs. 5C and 5F). However, a larger sample will be required to determine the relationship between synaptic specializations and transmitter status.

DISCUSSION

While confirming that, in normal rats, a subset of VTA DA neurons expresses VGLUT2 mRNA, this study suggests that this dual transmitter phenotype is more broadly expressed during early than late embryonic development, and reveals that it may be activated in VTA DA neurons surviving a neonatal 6-OHDA lesion. It also provides the first demonstration of the presence of VGLUT2 protein in TH-immunopositive axon varicosities of the nAcb, reinforcing the possibility of a dual release of glutamate and dopamine by these nerve terminals *in vivo*.

VGLUT2 expression in mesencephalic DA neurons *in vivo*

The initial goal of the present study was to characterize the glutamatergic phenotype of mesencephalic DA neurons, and to determine whether, as in culture (Dal Bo et coll., 2004), these neurons co-express vesicular glutamate transporters *in vivo*. In agreement with two recent reports (Kawano et coll., 2006; Yamaguchi et coll., 2007), in normal postnatal rat, only VGLUT2 mRNA was detected in a small sub-population of ventral mesencephalic neurons containing TH mRNA. Therefore, alike other monoaminergic neuronal populations expressing a glutamatergic phenotype, such as C1 adrenergic neurons expressing VGLUT2 (Stornetta et coll., 2002) and raphe serotonin neurons expressing VGLUT3 (Gras et coll., 2002), mesencephalic DA neurons co-express only one VGLUT subtype. Albeit low, the proportion of DA neurons co-expressing VGLUT2 in normal postnatal rat was significantly higher in the VTA than in the SNc. This was in keeping with the recent observations of Kawano et coll. (2006) in adult animals, and further highlights phenotypic differences between DA neurons in these two nuclei, as already shown for the levels of expression of TH, DA transporter and calbindin (Rogers, 1992; Blanchard et coll., 1994; Korotkova et coll., 2005; Korotkova et coll., 2004). The small subset of DA neurons expressing VGLUT2 mRNA in normal postnatal rat contrasted with the high proportion of isolated DA neurons in culture known to release glutamate synaptically (~60%) (Sulzer et coll., 1998) or to express VGLUT2 protein (~80%) (Dal Bo et coll., 2004), suggesting that VGLUT2 expression might be enhanced in isolated DA neurons *in vitro*.

In vivo, VGLUT2 expression may be abundant and widespread during development but repressed in mature DA neurons. Indeed, at 14 to 16 embryonic days, VGLUT2 mRNA was strongly and broadly co-expressed with TH mRNA in the region of ventral mesencephalon where DA neurons first develop (Kalsbeek et coll., 1988), and no longer detectable at later embryonic stages (E18 and E21). Single-cell RT PCR confirmed the frequent co-expression of VGLUT2 in E15 DA neurons. In rat ventral midbrain at E18, DA neurons are found in the same relative location that they will occupy in the adult brain, and their projections begin to reach the ventro-lateral part of the neostriatum (Specht et coll., 1981; Voorn et coll., 1988) in which neurogenesis begins (Bayer, 1984). Future work will be needed to verify that the

rapid change in regional overlap of TH and VGLUT2 expression in embryonic ventral midbrain does represent a reduced number of DA neurons expressing VGLUT2 mRNA, and to determine the specific role of this dual phenotype during the growth of these neurons. Rapid declines in VGLUT2 expression have been described previously in postnatal rat brain (Boulland et coll., 2004) (see also Danik et coll., 2005). They are likely to reflect the repression of a glutamatergic phenotype transiently expressed during critical periods of development.

VGLUT2 expression in DA neurons surviving a neonatal 6-OHDA lesion

Neonatal i.c.v. administration of 6-OHDA is a well-established model to study adaptive and plastic properties of central DA neurons *in vivo* (Fernandes Xavier et coll., 1994; Joyce et coll., 1996; Penit-Soria et coll., 1997; Neal-Beliveau and Joyce, 1999). This lesion destroys most DA in the SNc and decreases the number of DA neurons in the VTA, but, as previously shown, many DA neurons of this latter region survive. The present study revealed that the percentage of VTA DA neurons expressing VGLUT2 mRNA was markedly increased in 15 day-old 6-OHDA lesioned rats compared to normal or sham controls. This increase in number of VTA DA neurons containing VGLUT2mRNA was far greater than could be explained by a preferential survival of those VTA neurons normally expressing the dual phenotype. Interestingly, an increase in the number and in the proportion of dually labeled DA neurons was already observed 2 days after the surgery, at P6 (96 VGLUT2+/TH+ over 561 TH+ counted in 3 animals; 17.1 ± 4.4), indicating an early and rapid activation of VGLUT2 expression in surviving DA neurons (data not shown). These data argue in favor of the hypothesis of an induction or derepression of VGLUT2 expression in many of the surviving DA neurons.

The proportion of VTA DA neurons expressing VGLUT2 appeared to be also slightly increased in sham-injected rats that were pre-treated with desipramine to prevent degeneration of noradrenergic neurons. Although this trend did not reach statistical significance, it may have been due to an elevation of extracellular norepinephrine. Interestingly, in adult rat, chronic desipramine treatment has been shown to increase VGLUT1 mRNA in the cerebral cortex and hippocampus (Moutsimilli et coll., 2005; Tordera et coll., 2005), and VGLUT2 mRNA in the

thalamus (Tordera et coll., 2005). Preliminary data suggests that a modest increase of VGLUT2 mRNA in the ventral mesencephalon may indeed result from a single injection of desipramine in normal neonatal rats (not shown).

On the other hand, there was no detectable increase in VGLUT2 mRNA expression in the SNc DA neurons having survived the 6-OHDA lesion. This perhaps reflected a further difference between VTA and SNc DA neurons, not only in their ability to express VGLUT2 under normal conditions, but also in their potential to up-regulate its co-expression after trauma. Experiments in progress should tell whether VTA DA neurons of adult rats retain the potential to express VGLUT2 after partial 6-OHDA lesion. Interestingly, a number of recent reports have described an enhanced expression of VGLUT2 by mature neurons in response to various stimuli (Kawasaki et coll., 2006; Kawasaki et coll., 2005; Hrabovszky et coll., 2006; Aymerich et coll., 2006). These findings illustrate the remarkable plasticity of the glutamate transmitter phenotype of neurons. The recent demonstration that hippocampal granule cells begin to express glutamic acid decarboxylase and to release GABA in addition to glutamate after a kindling protocol (Gutierrez, 2000; Gutierrez and Heinemann, 2006) or in response to GDNF (Gomez-Lira et coll., 2005) also favors this view. These latter results have been interpreted as the reactivation of a normally repressed developmental program (Seal and Edwards, 2006), which might also be the case for VGLUT2 expression by neonatally-lesioned DA neurons.

Presence of VGLUT2 protein in DA terminals

Considering that mesencephalic DA neurons of the VTA densely innervate the nAcb (Oades and Halliday, 1987), this small nucleus was the ideal anatomical area to search for a colocalization of TH and VGLUT2 protein in axon terminals. After dual immunolabeling for electron microscopy, 28% of TH positive terminals in the core of nAcb could be distinctly visualized as also containing VGLUT2 protein. Such a proportion of axon terminals containing both TH and VGLUT2 protein was much higher than the observed proportion of DA neurons expressing VGLUT2 mRNA, a discrepancy for which several possible explanations could be advanced, in addition to limitations in sensitivity of the dual *in situ* hybridization technique. VGLUT2 positive DA neurons could have established a higher density of axon terminals at this stage of

development than DA neurons which do not express VGLUT2. It is also possible that the half-life of the VGLUT2 protein is relatively long, accounting for its persistence many days after interruption of its synthesis and export to axon terminals.

As expected, the 6-OHDA lesion caused a substantial decrease in the number of TH-immunopositive terminals in the nAcb, as evaluated either by dual immunofluorescence or by double labeling immuno-electron microscopy. In the latter material, the 38% decrease in axon terminals labeled for TH was considerably less than the 60% reduction in number of VTA neurons displaying TH mRNA, perhaps reflecting, at least in part, the survival of DA neurons which no longer expressed detectable amounts of TH mRNA. Interestingly, this diminished number of TH terminals was not accompanied by a statistically significant reduction in the number of dually TH and VGLUT2 positive axon terminals (decrease of less than 20%). On the contrary, there was a small but significant increase in the percentage of all TH terminals which exhibited the dual phenotype (from 28% to 37%; $p < 0.05$). This finding is in line with the increase in the proportion of VTA DA neurons that co-expressed VGLUT2 mRNA after the lesion. Alternatively, it could indicate that axon terminals arising from DA neurons that also contain VGLUT2 were less sensitive to the 6-OHDA-induced degeneration. Because, in many brain regions, central DA neurons are endowed with non-synaptic as well as synaptic axon varicosities (Hattori et coll., 1991; Descarries et coll., 1996; Ingham et coll., 1998), it will be of interest to explore the possible relationship between the glutamatergic phenotype of TH positive terminals and their synaptic versus non-synaptic differentiation.

Conclusion

Although the specific role of glutamate in mesencephalic DA neurons remains undetermined, the early developmental expression of VGLUT2 in these neurons suggests an implication of glutamate release in the establishment or fine-tuning of their projections. Further experiments will be required to test this hypothesis more directly and to investigate which signals activate or derepress VGLUT2 expression in lesioned VTA neurons. It will also be of major interest to determine whether such a phenotypic switch may occur in adult animals, as well as the possible role of the dual DA-glutamate phenotype (and its regulation) within the context of pathological states.

Acknowledgments: This work was funded in part by a grant from NARSAD to L.-E. T and by CIHR grant MOP-3544 to L.D., and also supported by an infrastructure grant from the FRSQ to the GRSNC (Groupe de Recherche sur le Système Nerveux Central). N. B.-C. was recipient of a studentship from the GRSNC. The plasmids used to prepare VGLUT probes were kindly provided by Dr. S. El Mestikawy. The authors wish to thank François Gilbert, Brigitte Paquet and Geneviève Beaudry for their help with the *in situ* hybridization experiments.

REFERENCES

Aihara Y., Mashima H., Onda H., Hisano S., Kasuya H., Hori T., Yamada S., Tomura H., Yamada Y., Inoue I., Kojima I., and Takeda J. (2000) Molecular cloning of a novel brain-type Na(+)-dependent inorganic phosphate cotransporter. *J Neurochem* 74, 2622-5.

Anlauf E. and Derouiche A. (2005) Astrocytic exocytosis vesicles and glutamate: a high-resolution immunofluorescence study. *Glia* 49, 96-106.

Aymerich M.S., Barroso-Chinea P., Perez-Manso M., Munoz-Patino A.M., Moreno-Igoa M., Gonzalez-Hernandez T., and Lanciego J.L. (2006) Consequences of unilateral nigrostriatal denervation on the thalamostriatal pathway in rats. *Eur J Neurosci* 23, 2099-108.

Bayer S.A. (1984) Neurogenesis in the rat striatum. *Internat J Dev Neurosci* 2, 163-175.

Beaudry G., Langlois M.C., Weppe I., Rouillard C., and Lévesque D. (2000) Contrasting patterns and cellular specificity of transcriptional regulation of the nuclear receptor nerve growth factor-inducible B by haloperidol and clozapine in the rat forebrain. *J Neurochem* 75, 1694-702.

Bellocchio E.E., Hu H., Pohorille A., Chan J., Pickel V.M., and Edwards R.H. (1998) The localization of the brain-specific inorganic phosphate transporter suggests a specific presynaptic role in glutamatergic transmission. *J Neurosci* 18, 8648-59.

Blanchard V., Raisman-Vozari R., Vyas S., Michel P.P., Javoy-Agid F., Uhl G., and Agid Y. (1994) Differential expression of tyrosine hydroxylase and membrane dopamine transporter genes in subpopulations of dopaminergic neurons of the rat mesencephalon. *Brain Res Mol Brain Res* 22, 29-38.

Borodinsky L.N., Root C.M., Cronin J.A., Sann S.B., Gu X., and Spitzer N.C. (2004) Activity-dependent homeostatic specification of transmitter expression in embryonic neurons. *Nature* 429, 523-30.

Borodinsky L.N. and Spitzer N.C. (2007) Activity-dependent neurotransmitter-receptor matching at the neuromuscular junction. *Proc Natl Acad Sci U S A* 104, 335-40.

Boulland J.L., Qureshi T., Seal R.P., Rafiki A., Gundersen V., Bergersen L.H., Fremeau R.T. Jr, Edwards R.H., Storm-Mathisen J., and Chaudhry F.A. (2004)

Expression of the vesicular glutamate transporters during development indicates the widespread corelease of multiple neurotransmitters. *J Comp Neurol* 480, 264-80.

Bourque M.-J. and Trudeau L.-E. (2000) GDNF enhances the synaptic efficacy of dopaminergic neurons in culture. *Eur J Neurosci* 12 , 3172-80.

Chuhma N., Zhang H., Masson J., Zhuang X., Sulzer D., Hen R., and Rayport S. (2004) Dopamine neurons mediate a fast excitatory signal via their glutamatergic synapses. *J Neurosci* 24, 972-81.

Cossette M., Parent A., and Lévesque D. (2004) Tyrosine hydroxylase-positive neurons intrinsic to the human striatum express the transcription factor Nurr1. *Eur J Neurosci* 20, 2089-95.

Dal Bo G., St-Gelais F., Danik M., Williams S., Cotton M., and Trudeau L.-E. (2004) Dopamine neurons in culture express VGLUT2 explaining their capacity to release glutamate at synapses in addition to dopamine . *J Neurochem* 88, 1398-405.

Danik M., Cassoly E., Manseau F., Sotty F., Mouginot D., and Williams S. (2005) Frequent coexpression of the vesicular glutamate transporter 1 and 2 genes, as well as coexpression with genes for choine acetyltransferase or glutamic acid decarboxylase in neurones of rat brain. *J Neurosci Res* 81, 506-21.

Descarries L., Watkins K.C., Garcia S., Bosler O., and Doucet G. (1996) Dual character, asynaptic and synaptic, of the dopamine innervation in adult rat neostriatum: a quantitative autoradiographic and immunocytochemical analysis. *J Comp Neurol* 375, 167-86.

Fernandes Xavier F.G., Doucet G., Geffard M., and Descarries L. (1994) Dopamine neoinnervation in the substantia nigra and hyperinnervation in the interpeduncular nucleus of adult rat following neonatal cerebroventricular administration of 6-hydroxydopamine. *Neuroscience* 59, 77-87.

Fremeau R.T. Jr, Burman J., Qureshi T., Tran C.H., Proctor J., Johnson J., Zhang H., Sulzer D., Copenhagen D.R., Storm-Mathisen J., Reimer R.J., Chaudhry F.A., and Edwards R.H. (2002) The identification of vesicular glutamate transporter 3 suggests novel modes of signaling by glutamate. *Proc Natl Acad Sci U S A* 99, 14488-93.

Fremeau R.T. Jr, Troyer M.D., Pahner I., Nygaard G.O., Tran C.H., Reimer R.J., Bellocchio E.E., Fortin D., Storm-Mathisen J., and Edwards R.H. (2001) The expression of vesicular glutamate transporters defines two classes of excitatory synapse. *Neuron* 31, 247-60.

Fujiyama F., Furuta T., and Kaneko T. (2001) Immunocytochemical localization of candidates for vesicular glutamate transporters in the rat cerebral cortex. *J Comp Neurol* 435, 379-87.

Furshpan E.J., MacLeish P.R., O'Lague P.H., and Potter D.D. (1976) Chemical transmission between rat sympathetic neurons and cardiac myocytes developing in microcultures: evidence for cholinergic, adrenergic, and dual-function neurons. *Proc Natl Acad Sci U S A* 73, 4225-9.

Gillespie D.C., Kim G., and Kandler K. (2005) Inhibitory synapses in the developing auditory system are glutamatergic. *Nat Neurosci* 8, 332-8.

Gomez-Lira G., Lamas M., Romo-Parra H., and Gutierrez R. (2005) Programmed and induced phenotype of the hippocampal granule cells. *J Neurosci* 25, 6939-46.

Gras C., Herzog E., Bellenchi G.C., Bernard V., Ravassard P., Pohl M., Gasnier B., Giros B., and El Mestikawy S. (2002) A third vesicular glutamate transporter expressed by cholinergic and serotoninergic neurons. *J Neurosci* 22, 5442-51.

Gratto K.A. and Verge V.M. (2003) Neurotrophin-3 down-regulates trkA mRNA, NGF high-affinity binding sites, and associated phenotype in adult DRG neurons. *Eur J Neurosci* 18, 1535-48.

Gutierrez R. (2000) Seizures induce simultaneous GABAergic and glutamatergic transmission in the dentate gyrus-CA3 system. *J Neurophysiol* 84, 3088-90.

Gutierrez R. and Heinemann U. (2006) Co-existence of GABA and Glu in the hippocampal granule cells: implications for epilepsy. *Curr Top Med Chem* 6, 975-8.

Hattori T., Takada M., Moriizumi T., and Van der Kooy D. (1991) Single dopaminergic nigrostriatal neurons form two chemically distinct synaptic types: possible transmitter segregation within neurons. *J Comp Neurol* 309, 391-401.

Haycock J.W. (1993) Multiple forms of tyrosine hydroxylase in human neuroblastoma cells: quantitation with isoform-specific antibodies. *J Neurochem* 60, 493-502.

Herzog E., Bellenchi G.C., Gras C., Bernard V., Ravassard P., Bedet C., Gasnier B., Giros B., and El Mestikawy S. (2001) The existence of a second vesicular glutamate transporter specifies subpopulations of glutamatergic neurons. *J Neurosci* 21, RC181.

Herzog E., Gilchrist J., Gras C., Muzerelle A., Ravassard P., Giros B., Gaspar P., and El Mestikawy S. (2004a) Localization of VGLUT3, the vesicular glutamate transporter type 3, in the rat brain. *Neuroscience* 123, 983-1002.

Herzog E., Landry M., Buhler E., Bouali-Benazzouz R., Legay C., Henderson C.E., Nagy F., Dreyfus P., Giros B., and El Mestikawy S. (2004b) Expression of vesicular glutamate transporters, VGLUT1 and VGLUT2, in cholinergic spinal motoneurons. *Eur J Neurosci* 20, 1752-60.

Hisano S., Hoshi K., Ikeda Y., Maruyama D., Kanemoto M., Ichijo H., Kojima I., Takeda J., and Nogami H. (2000) Regional expression of a gene encoding a neuron-specific Na(+)- dependent inorganic phosphate cotransporter (DNPI) in the rat forebrain. *Brain Res Mol Brain Res* 83, 34-43.

Hrabovszky E., Kallo I., Turi G.F., May K., Wittmann G., Fekete C., and Liposits Z. (2006) Expression of vesicular glutamate transporter-2 in gonadotrope and thyrotrope cells of the rat pituitary. Regulation by estrogen and thyroid hormone status. *Endocrinology* 147, 3818-25.

Ingham C.A., Hood S.H., Taggart P., and Arbuthnott G.W. (1998) Plasticity of synapses in the rat neostriatum after unilateral lesion of the nigrostriatal dopaminergic pathway. *J Neurosci* 18, 4732-43.

Jackson D., Bruno J.P., Stachowiak M.K., and Zigmond M.J. (1988) Inhibition of striatal acetylcholine release by serotonin and dopamine after the intracerebral administration of 6-hydroxydopamine to neonatal rats. *Brain Res* 457, 267-73.

Joyce J.N., Frohna P.A., and Neal-Beliveau B.S. (1996) Functional and molecular differentiation of the dopamine system induced by neonatal denervation. *Neurosci Biobehav Rev* 20, 453-86.

Joyce M.P. and Rayport S. (2000) Mesoaccumbens dopamine neuron synapses reconstructed *in vitro* are glutamatergic. *Neuroscience* 99, 445-456.

Kalsbeek A., Voorn P., Buijs R.M., Pool C.W., and Uylings H.B. (1988) Development of the dopaminergic innervation in the prefrontal cortex of the rat. *J Comp Neurol* 269, 58-72.

Kawano M., Kawasaki A., Sakata-Haga H., Fukui Y., Kawano H., Nogami H., and Hisano S. (2006) Particular subpopulations of midbrain and hypothalamic dopamine neurons express vesicular glutamate transporter 2 in the rat brain. *J Comp Neurol* 498, 581-92.

Kawasaki A., Hoshi K., Kawano M., Nogami H., Yoshikawa H., and Hisano S. (2005) Up-regulation of VGLUT2 expression in hypothalamic-neurohypophysial neurons of the rat following osmotic challenge. *Eur J Neurosci* 22, 672-80.

Kawasaki A., Shutoh F., Nogami H., and Hisano S. (2006) VGLUT2 expression is up-regulated in neurohypophysial vasopressin neurons of the rat after osmotic stimulation. *Neurosci Res* 56, 124-127.

Korotkova T.M., Ponomarenko A.A., Brown R.E., and Haas H.L. (2004) Functional diversity of ventral midbrain dopamine and GABAergic neurons. *Mol Neurobiol* 29, 243-59.

Korotkova T.M., Ponomarenko A.A., Haas H.L., and Sergeeva O.A. (2005) Differential expression of the homeobox gene Pitx3 in midbrain dopaminergic neurons. *Eur J Neurosci* 22, 1287-93.

Lavin A., Nogueira L., Lapish C.C., Wightman R.M., Phillips P.E., and Seamans J.K. (2005) Mesocortical dopamine neurons operate in distinct temporal domains using multimodal signaling. *J Neurosci* 25, 5013-23.

Moutsimilli L., Farley S., Dumas S., El Mestikawy S., Giros B., and Tzavara E.T. (2005) Selective cortical VGLUT1 increase as a marker for antidepressant activity. *Neuropharmacology* 49, 890-900.

Neal-Beliveau B.S. and Joyce J.N. (1999) Timing: A critical determinant of the functional consequences of neonatal 6-OHDA lesions. *Neurotoxicol Teratol* 21, 129-40.

Ni B., Wu X., Yan G.M., Wang J., and Paul S.M. (1995) Regional expression and cellular localization of the Na(+)-dependent inorganic phosphate cotransporter of rat brain. *J Neurosci* 15, 5789-99.

Oades R.D. and Halliday G.M. (1987) Ventral tegmental (A10) system: neurobiology. 1. Anatomy and connectivity. *Brain Res* 434, 117-65.

Paxinos G. and Watson C. (2005) The rat brain in stereotaxic coordinates. Academic Press, San Diego.

Penit-Soria J., Durand C., Hervé D., and Besson M.J. (1997) Morphological and biochemical adaptations to unilateral dopamine denervation of the neostriatum in newborn rats. *Neuroscience* 77, 753-66.

Puma C., Danik M., Quirion R., Ramon F., and Williams S. (2001) The chemokine interleukin-8 acutely reduces Ca(2+) currents in identified cholinergic septal neurons expressing CXCR1 and CXCR2 receptor mRNAs. *J Neurochem* 78, 960-71.

Riad M., Garcia S., Watkins K.C., Jodoin N., Doucet E., Langlois X., El Mestikawy S., Hamon M., and Descarries L. (2000) Somatodendritic localization of

5-HT1A and preterminal axonal localization of 5-HT1B serotonin receptors in adult rat brain. *J Comp Neurol* 417, 181-94.

Rogers J.H. (1992) Immunohistochemical markers in rat brain: colocalization of calretinin and calbindin-D28k with tyrosine hydroxylase. *Brain Res* 587, 203-10.

Seal R.P. and Edwards R.H. (2006) Functional implications of neurotransmitter co-release: glutamate and GABA share the load. *Curr Opin Pharmacol* 6, 114-9.

Smits S.M., Burbach J.P., and Smidt M.P. (2006) Developmental origin and fate of meso-diencephalic dopamine neurons. *Prog Neurobiol* 78, 1-16.

Specht L.A., Pickel V.M., Joh T.H., and Reis D.J. (1981) Fine structure of the nigrostriatal anlage in fetal rat brain by immunocytochemical localization of tyrosine hydroxylase. *Brain Res* 218, 49-65.

St-Hilaire M., Landry E., Lévesque D., and Rouillard C. (2005) Denervation and repeated L-DOPA induce complex regulatory changes in neurochemical phenotypes of striatal neurons: implication of a dopamine D1-dependent mechanism. *Neurobiol Dis* 20, 450-60.

Stachowiak M.K., Bruno J.P., Snyder A.M., Stricker E.M., and Zigmond M.J. (1984) Apparent sprouting of striatal serotonergic terminals after dopamine-depleting brain lesions in neonatal rats. *Brain Res* 291, 164-7.

Stornetta R.L., Sevigny C.P., and Guyenet P.G. (2002) Vesicular glutamate transporter DNPI/VGLUT2 mRNA is present in C1 and several other groups of brainstem catecholaminergic neurons. *J Comp Neurol* 444, 191-206.

Sulzer D., Joyce M.P., Lin L., Geldwert D., Haber S.N., Hattori T., and Rayport S. (1998) Dopamine neurons make glutamatergic synapses *in vitro*. *J Neurosci* 18, 4588-4602.

Tordera R.M., Pei Q., and Sharp T. (2005) Evidence for increased expression of the vesicular glutamate transporter, VGLUT1, by a course of antidepressant treatment. *J Neurochem* 94, 875-83.

Trevino M. and Gutierrez R. (2005) The GABAergic projection of the dentate gyrus to hippocampal area CA3 of the rat: pre- and postsynaptic actions after seizures. *J Physiol* 567, 939-49.

Varoqui H., Schafer M.K., Zhu H., Weihe E., and Erickson J.D. (2002) Identification of the differentiation-associated Na+/PI transporter as a novel vesicular glutamate transporter expressed in a distinct set of glutamatergic synapses. *J Neurosci* 22, 142-55.

Voorn P., Kalsbeek A., Jorritsma-Byham B., and Groenewegen H.J. (1988) The pre- and postnatal development of the dopaminergic cell groups in the ventral mesencephalon and the dopaminergic innervation of the striatum of the rat. *Neuroscience* 25, 857-87.

Yamaguchi T., Sheen W., and Morales M. (2007) Glutamatergic neurons are present in the rat ventral tegmental area. *Eur J Neurosci* 25, 106-118.

Yang B., Slonimsky J.D., and Birren S.J. (2002) A rapid switch in sympathetic neurotransmitter release properties mediated by the p75 receptor. *Nat Neurosci* 5, 539-45.

Table 1

NUMBER AND PROPORTION OF VTA AND SN NEURONS CO-EXPRESSING TH AND VGLUT2 mRNA IN POSTNATAL CONTROL RATS

Control Rats		TH+ cells per section	TH+/VGLUT2+ cells per section	TH+/VGLUT2+ / TH+
P5 (N=4)	VTA	121 ± 14	4.1 ± 1.2	3.4 ± 0.8 %
	SN	131 ± 10	0.9 ± 0.2	0.7 ± 0.1 %
P10 (N=4)	VTA	158 ± 18	3.8 ± 1	2.4 ± 0.4 %
	SN	167 ± 19	1.3 ± 0.6	0.8 ± 0.3 %
P15 (N=4)	VTA	102 ± 7	1.8 ± 0.3	1.8 ± 0.3 %
	SN	152 ± 12	0.7 ± 0.4	0.4 ± 0.2 %

Means ± SEM for the number of neurons counted per section in 4 rats at each age (3 or 4 sections per rat). On the right, the number of dually labeled neurons (TH+/VGLUT2+) is expressed as a percentage of all neurons containing TH mRNA (TH+).

Table 2

NUMBER AND PROPORTION OF VTA AND SNC NEURONS CO-EXPRESSING TH AND VGLUT2 mRNA IN SHAM AND 6-OHDA LESIONED RATS

P15		TH+ cells per section	TH+/VGLUT2+ cells per section	TH+/VGLUT2+ / TH+
Shams (N=4)	VTA	98 ± 7	6.9 ± 2.7	7.1 ± 1.5 %
	SN	126 ± 13	0.9 ± 0.4	0.7 ± 0.3 %
6-OHDA (N=4)	VTA	39 ± 5	10.3 ± 1	26.3 ± 2.5 %***
	SN	4.6 ± 2.6	0	0

Data from P15 rats subjected to vehicle (sham) or 6-OHDA injection at P4. As in Table 1, means ± SEM for the number of neurons counted per section in 4 rats of each group. The proportion of dually labeled neurons (TH+/VGLUT2+ over all TH+) is significantly greater in 6-OHDA-lesioned than sham rats. *** $p < 0.001$ by ANOVA and Tuckey Test post-hoc.

Table 3

NUMBER OF TH, VGLUT2, AND TH/VGLUT2 IMMUNOPOSITIVE AXON TERMINALS IN THE nAcb OF 15 DAY-OLD NORMAL VERSUS 6-OHDA-LESIONED RATS

P15		TH+ terminals	VGLUT2+ terminals	TH+/VGLUT2+ terminals	TH+/VGLUT2+ / TH+
Normal (N=7)	N varicosities	1125	892	318	28 ± 2 %
	Mean ± SEM	161 ± 8	127 ± 32	45 ± 6	
6-OHDA (N=7)	N varicosities	696	581	256	37 ± 4 % *
	Mean ± SEM	99 ± 11 ***	88 ± 16	37 ± 4	

N varicosities is the total number of immunopositive axon varicosities in each category, counted over an equivalent total surface of 11 655 μm^2 of thin section (1665 μm^2 per rat) in each group, as explained in Materials and Methods. The percentage of all TH-labeled axon terminals dually immunolabeled for VGLUT2 is given on the right. *** $p < 0.001$ and * $p < 0.05$ by unpaired Student's *t*-test.

FIGURE LEGENDS

Figure 1: Selectivity and evaluation of co-expression of TH and VGLUT2 mRNA in prenatal ventral mesencephalon. A-B1 Double *in situ* hybridization with DIG-labeled probes to detect TH mRNA (purple) and radiolabeled probes to detect VGLUT2 mRNA (silver grains). **A-A1**: TH and VGLUT2 mRNAs in the ventral mesencephalon of an E15 rat. Note the strong overlap in regional co-localization of both mRNAs. **B-B1**: At E18, there is little overlap in the regional distribution of the two mRNAs. **A1** and **B1** are enlargements of the areas outlined in dashed line in **A** and **B**. **C**: Density of VGLUT2 mRNA labeling (number of silver grains per 500 μm^2 of section) in TH-Dig positive areas of mesencephalic sections from embryos at different ages. Both E18 and E21 values are significantly lower than E15 and E16 values (means ± SEM from 3 embryos at E15 and E18 and 5 embryos at E16 and E21). *** $p < 0.001$ by ANOVA and Tuckey post-hoc test. **D**: Presence of VGLUT2 mRNA in freshly dissociated mesencephalic DA neurons (cells 1-3) identified by the presence of TH mRNA. Cell 4 only expresses TH mRNA, while cell 5 only expresses VGLUT2. MS, mesencephalon plus striatum used as positive control; m, muscle, used as negative control.

Figure 2: Co-expression of TH and VGLUT2 mRNA in RLi, VTA or SNc neurons of 15 day-old normal rats. Double *in situ* hybridization with DIG-labeled and radiolabeled probes as in Fig. 1 (TH mRNA in purple, and silver grains for VGLUT2 mRNA). **A** and **B**: Co-expression of VGLUT2 and TH mRNA is observed in a subset of DA neurons (black arrows) in the rostral linear nucleus of the raphe (RLi). Many other neurons displayed only TH mRNA (red arrows). **C** and **D**: A few neurons in the SNc (**C**) and VTA (**D**) of normal rats display both mRNAs (black arrows). Red arrows designate neurons containing TH mRNA only. Outlines of VTA, SNc and RLi drawn from Paxinos & Watson (2005).

Figure 3: Effect of the neonatal 6-OHDA lesion on TH and VGLUT2 mRNA levels in the ventral mesencephalon of 15 day-old rats. A and **B**: TH immunoreactivity in the P15 rat striatum after i.c.v. injection of aCSF (sham) (**A**) or 6-OHDA (**B**). Note that the 6-OHDA lesion induced an almost complete loss of TH

levels, confirming the success of the lesion. **C**: Expression profile of relative TH, VGLUT2 and β-actin mRNA levels in the mesencephalon of P15 rats. Measurements were made by multiplex semi-quantitative RT-PCR from control, sham-operated and 6-OHDA-lesioned rats (3 animals per condition). **D**: Histogram representing the relative levels of TH and VGLUT2 mRNA measured from control, sham or lesioned tissue. The data represents the average ± SEM from 3 rats per condition. Values were normalized to the signal obtained for β-actin mRNA levels. * <0.05 when compared to control or sham groups by ANOVA and Tuckey post-hoc test.

Figure 4: Co-expression of TH and VGLUT2 mRNA in VTA neurons of 15 day-old sham control (A) or 6-OHDA-lesioned (B) rats. A and **B**: Compared to normal (**Fig. 2D**) and sham control (**A**), a greater number of VTA neurons co-expressed TH and VGLUT2 mRNA (black arrows) in 6-OHDA lesioned rats (**B**). Red arrows designate neurons containing TH mRNA only, and double arrows neurons with VGLUT2 mRNA only.

Figure 5: Electron microscopic visualization of singly (TH or VGLUT2) and doubly (TH/VGLUT2) immunopositive axon terminals (varicosities) in the nAcb of normal (A-C) or 6-OHDA-lesioned (D-F) 15-day old rats. TH and VGLUT2 were respectively labeled with the immunoperoxidase (fine DAB precipitate) and the immunogold technique (dense, silver-intensified, gold particles). At the relatively low magnification of **A** and **D**, varicosities labeled for TH only (thin black arrows), VGLUT2 only (empty arrows) or TH and VGLUT2 (thick black arrows) may be observed in the same field. In **D**, note the presence of two doubly labeled varicosities closely apposed to a neuronal cell body (N in cytoplasm). In **B**, a triad is formed by three juxtaposed axon varicosities, one of which shows TH labeling only (thin black arrow) and the two others VGLUT2 labeling only (empty arrows). In **C**, the thick black arrows designate two varicosities along the same axon, which display both TH and VGLUT2 labeling. Both of these varicosities make an asymmetrical synaptic contact (between small arrows) with a dendritic spine (asterisks). In **E**, a doubly labeled varicosity (thick black arrow) is seen emerging from its parent unmyelinated axon. To its right, a small profile (presumably axonal) is labeled for TH only (thin black arrow). In **F**, underneath a small profile singly labeled for VGLUT2, a larger,

doubly labeled axon varicosity (thick black arrow) forms a symmetrical synaptic contact (between small arrows) with a dendritic spine (asterisk). Scale bars: 1 μm (**A and D**); 0.5μm (**B, C, E** and **F**).

Supplementary figure 1: Distribution of VGLUT1, VGLUT2 and VGLUT3 mRNA labeling in P15 rats. A-C are representative pictures of autoradiographs obtained by single-probe *in situ* hybridization with [^{35}S]UTP-labeled VGLUT mRNA probes. VGLUT1 mRNA is abundant in the hippocampus (Hipp) (**A**), VGLUT2 mRNA in the red nucleus (RN) and the medial geniculate nucleus (MGN) (**B**), and VGLUT3 mRNA in the dorsal (DR) and median raphe (MR) nuclei (**C**).

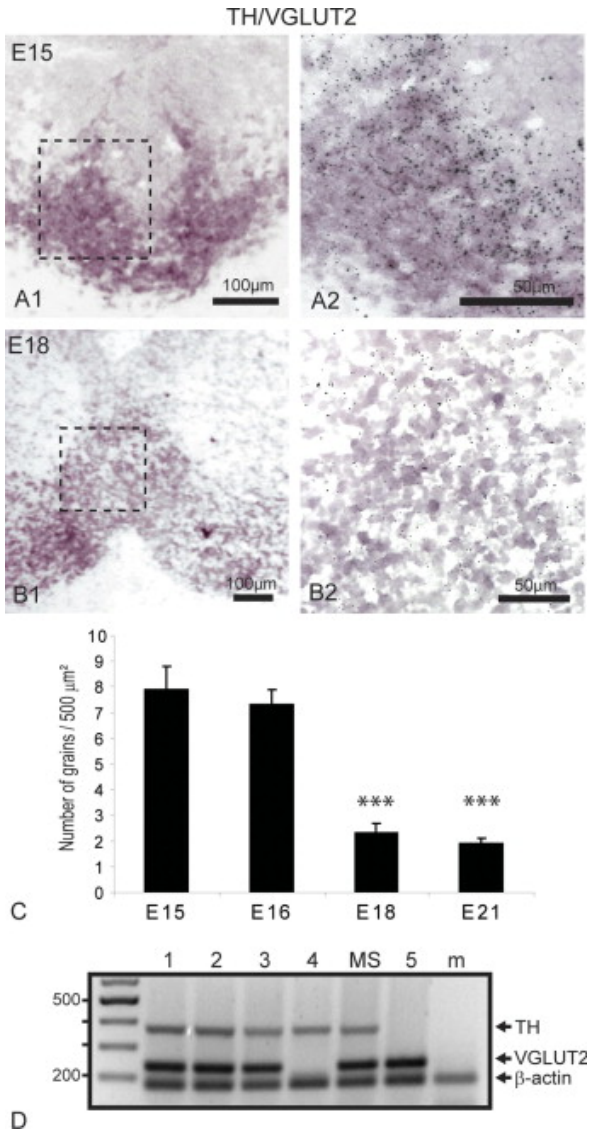

Figure 1: Selectivity and evaluation of co-expression of TH and VGLUT2 mRNA in prenatal ventral mesencephalon.

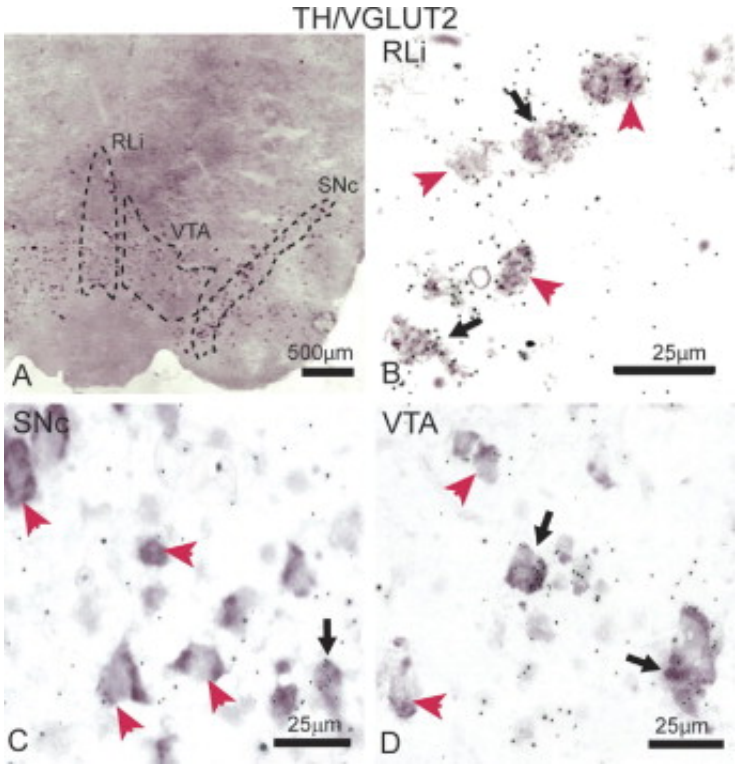

Figure 2: Co-expression of TH and VGLUT2 mRNA in RLi, VTA or SNc neurons of 15 day-old normal rats.

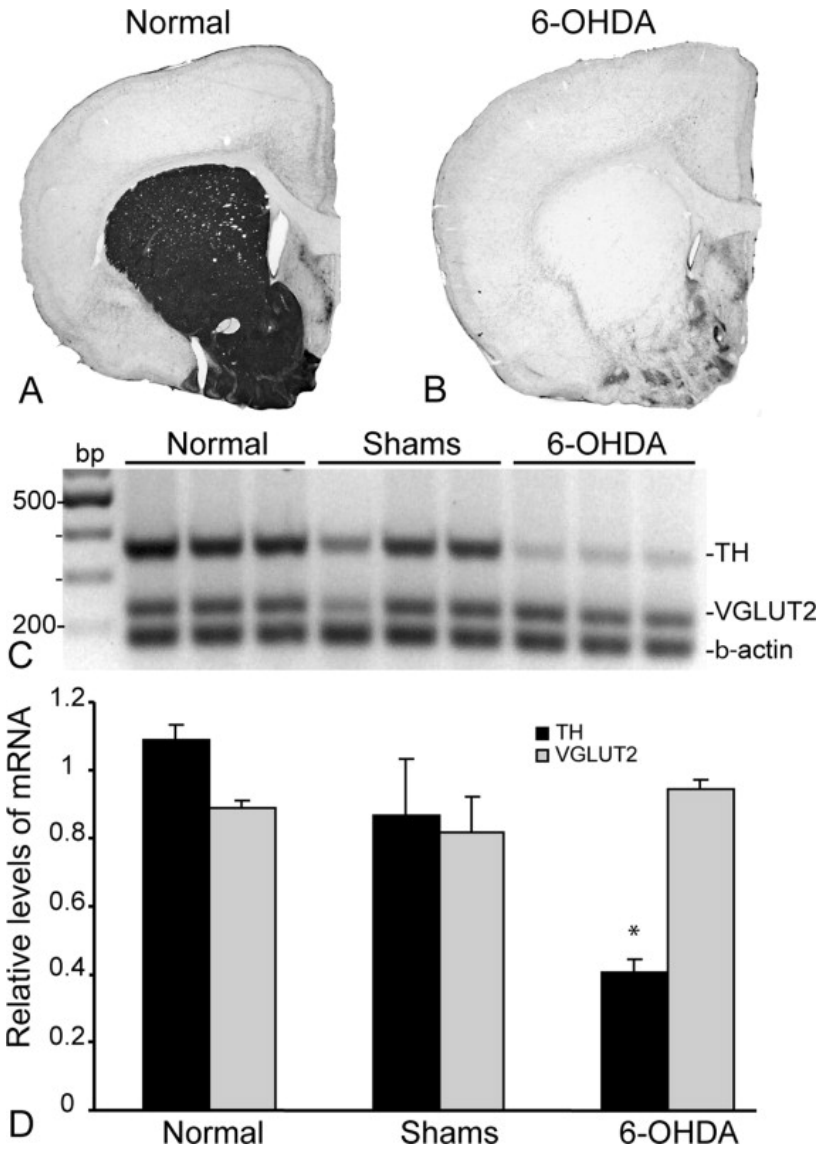

Figure 3: Effect of the neonatal 6-OHDA lesion on TH and VGLUT2 mRNA levels in the ventral mesencephalon of 15 day-old rats.

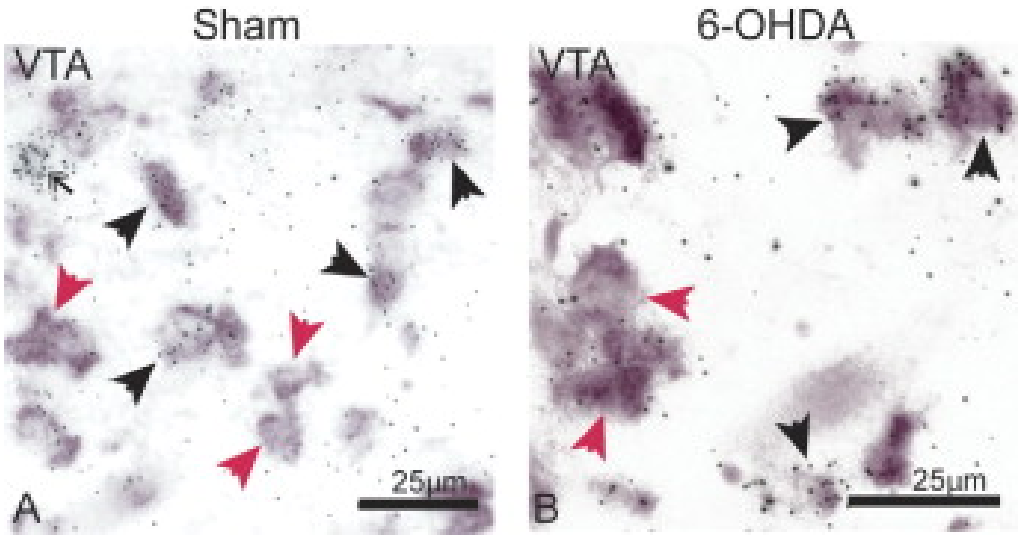

Figure 4: Co-expression of TH and VGLUT2 mRNA in VTA neurons of 15 day-old sham control (A) or 6-OHDA-lesioned (B) rats.

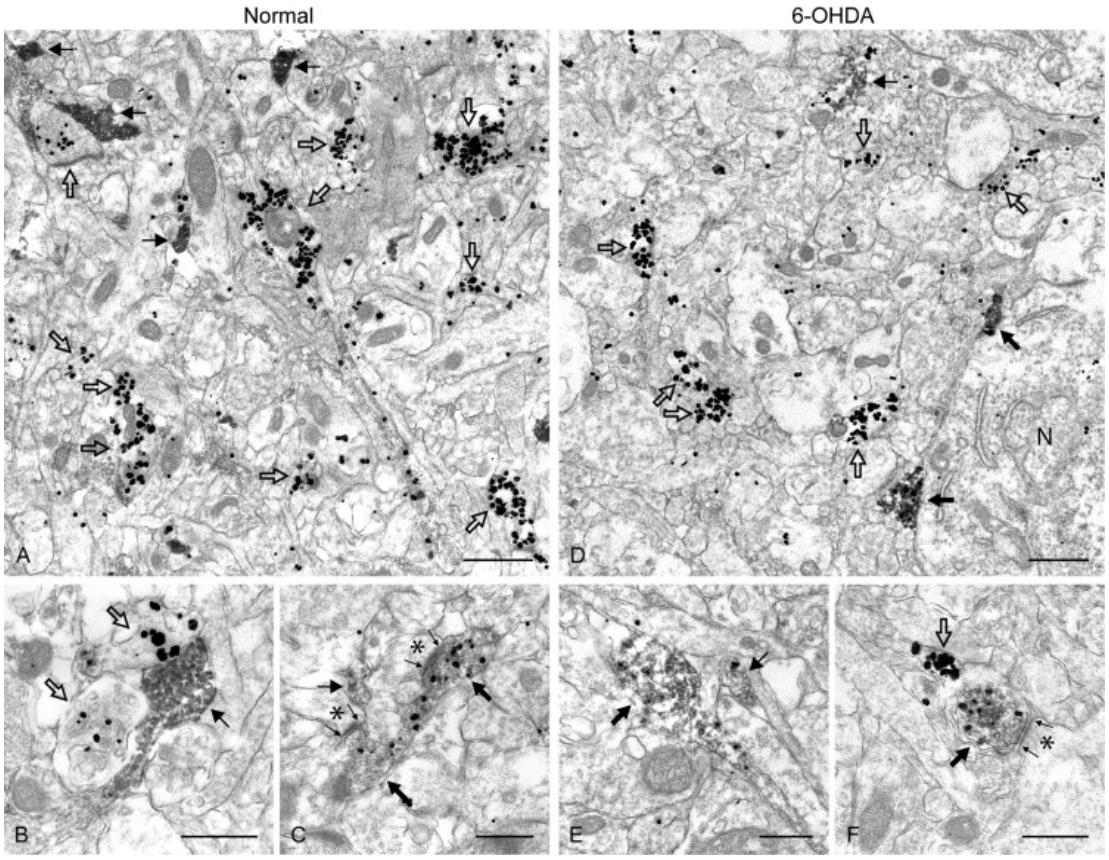

Figure 5: Electron microscopic visualization of singly (TH or VGLUT2) and doubly (TH/VGLUT2) immunopositive axon terminals (varicosities) in the nAcb of normal (A-C) or 6-OHDA-lesioned (D-F) 15-day old rats.

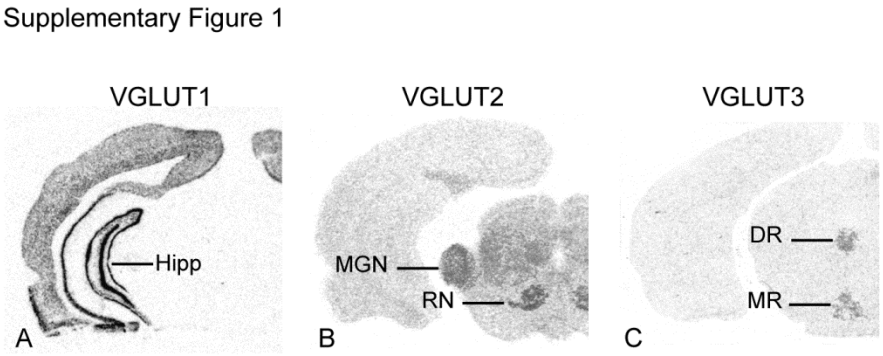

Supplementary figure 1: Distribution of VGLUT1, VGLUT2 and VGLUT3 mRNA labeling in P15 rats.